# Assessing the storm inundation hazard for coastal margins around the Wellington region

Prepared for Greater Wellington Regional Council, Kapiti Coast District Council and Wellington City Council
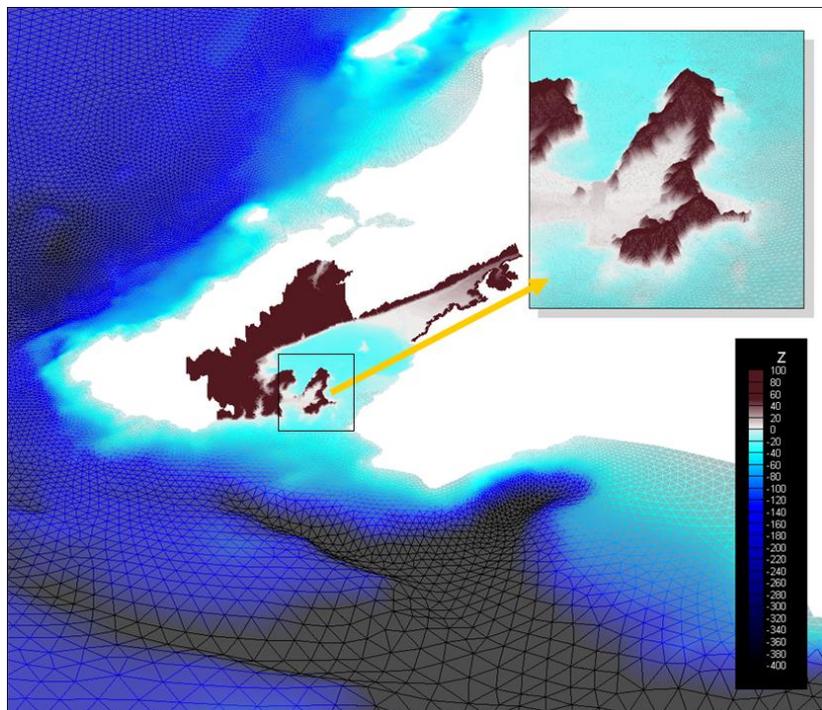
Authors/Contributors:
Emily Lane
Richard Gorman
David Plew
Scott Stephens

For any information regarding this report please contact:

Emily Lane
Scientist
Hydrodynamics Group
+64-3-343 7856
Emily.Lane@niwa.co.nz

National Institute of Water & Atmospheric Research Ltd
10 Kyle Street
Riccarton
Christchurch 8011
PO Box 8602, Riccarton
Christchurch 8440
New Zealand

Phone +64-3-348 8987
Fax +64-3-348 5548

Contents

Tables

Figures

Reviewed by

Approved for release by

Dr R.G. Bell

Dr G.M. Smart

Executive summary

This report has been prepared by NIWA for the Greater Wellington Regional Council (GWRC), Kapiti Coast District Council (KCDC) and Wellington City Council (WCC) to provide an assessment of the exposure to inundation from storm-tide and wave hazards for coastal margins in the Wellington Region. It follows previous reports for GWRC describing Joint Probability Analysis of Storm-tide and Wave Heights (Stephens et al. 2011 and minor edits 2012), and Sea-level Variability and Trends: Wellington Region (Bell and Hannah 2012). In this final report, we present coastal inundation depths and levels in the form of maps, based on numerical modelling of waves and storm-tides around the Greater Wellington Region coast.

This report assesses total storm inundation along the Wellington region's shoreline from storm-tide (a combination of high tide plus storm surge) and wave setup inside the wave-breaking zone. The assessment is based on modelling the combined effects of storm-tides and waves for selected storm events with a joint annual exceedance probability (AEP) of 1%.[1] The inundation levels and maps in this report do not include tsunami, wave runup or river or stormwater flooding, which may need to be taken into account in more detailed assessments for specific projects.

The historic storm events assessed cover a range of scenarios from large storm-tides with low wave heights, moderate storm-tides and wave heights, and comparatively small storm-tides with large wave heights. Wave modelling was conducted to predict significant wave heights along the coast of the Greater Wellington Region for each of 8 storm events (four covering the Kapiti coast and four events for the South Wellington and Wairarapa coasts). The wave modelling also provides input to the storm-tide modelling.

Sea level and inundation modelling used atmospheric wind and pressure data, along with wave-induced stresses and tidal water levels, to simulate the storm-tide along the Greater Wellington Region coast line. Detailed sea level and inundation modelling was conducted separately for the Wellington Harbour area and the Kapiti Coast area, where accurate LiDAR topography data was available. The Wellington Harbour model includes land areas around the Wellington Harbour including Lyall Bay, Evans Bay, Central Wellington, Petone and Seaview. The Kapiti Coast model grid includes land areas concentrated around Porirua Harbour, Waikanae, and Otaki Beach. Inundation by storm-tides was modelled for present day sea levels, and for sea-level rise increments of 0.5 m, 1.0 m, and 1.5 m (with no specific timeframe for when these rises would be reached).

The model simulations show that the coastline south and east of the Wellington Harbour (particularly the Wairarapa Coast) is exposed to the largest waves, with significant wave heights of over 6 m in places during some of the storm events simulated. The southern part of Cape Terawhiti is also exposed to large waves. In contrast, the Kapiti Coast receives smaller waves with significant wave heights less than 3 m in the storm events analysed.

In New Zealand, storm-tides are generally dominated by the contribution from astronomical tides rather than the smaller storm-surge heights we receive (in comparison to areas

---

[1] The combined storm inundation level that is likely to be reached or exceeded with a probability of 1% in any year. Over a design or planning timeframe of say 50 years, the probability of such an event exceeding this level is 39% (or 63% probability in a 100-year period).

elsewhere in the world that are subject to tropical cyclones or hurricanes). The tidal range near Wellington, however, is relatively small and so the storm surge contribution is similar to the tides in parts of the region (with Oteranga Bay on the south-west Wellington coast having the smallest tide range in New Zealand). Simulated storm-surge for the historic events modelled contributed up to 0.33 m in Wellington Harbour, and 0.65-0.71 m along the Kapiti Coast.

Wave setup is also a major contributor to the total storm inundation levels in exposed open-coast regions.

Two representative historic scenarios, one for the Kapiti coast, the other for the south Wellington and Wairarapa coasts, were adjusted to yield a 1% AEP total inundation level (to Wellington Vertical Datum-1953) above land for a combined storm-tide and wave event relevant to the present-day. This relatively infrequent event (for the present time) would also only cause inundation in low-lying areas over a period of 1–3 hours straddling the high tide associated with such a coastal storm event.

Flooding maps of total storm inundation for the environs of Wellington harbour and parts of Kapiti coast were produced for these representative historic scenarios displaying both total inundation level (to Wellington Vertical Datum-1953) and depths above land for the combined 1% AEP storm-tide and wave event relevant to the present-day. Only minor localised coastal inundation is apparent in the areas mapped for the present-day exposure to coastal inundation at the 1% joint AEP level.

These same scenarios were repeated for the 3 increments in sea-level rise and further inundation maps produced to illustrate the future exposure to coastal inundation. However, in future, the likelihood of present-day inundation (i.e., AEP) will escalate as sea-level rise accelerates. Alternatively, the frequency of the present-day coastal inundation events considered will increase, from an average recurrence interval of 100 years (or 1% AEP) now to occurring around once a year on average for sea-level rises of only 0.2 to 0.3 m, depending on the tide range. As sea levels rise, total storm inundation levels will threaten low-lying areas of Wellington Central City, potentially large areas of Petone and Seaview, and to a limited extent Evans Bay and smaller areas of Miramar Peninsula. Along the Kapiti Coast, total storm inundation levels elevated by sea-level rise will begin to threaten Otaki Beach, low lying areas of Waikanae, and narrow margins of the Porirua Harbour.

1   Introduction and report outline

This report has been prepared for the Greater Wellington Regional Council (GWRC), Kapiti Coast District Council (KCDC) and Wellington City Council (WCC) to provide an assessment of the exposure to inundation from storm-tide and wave hazards for coastal margins in the Wellington Region. It follows previous reports describing Joint Probability Analysis of Storm-tide and Wave Heights (Stephens et al. 2011 and minor edits 2012), and Sea-level Variability and Trends: Wellington Region (Bell and Hannah 2012). In this final report, we present coastal inundation depths and levels in the form of maps, based on numerical modelling of waves and storm-tides around the Greater Wellington Region coast.

The report presents plots of extreme inundation levels around the greater Wellington coastline, resulting from storm tides and wave setup (but excludes storm wave runup, tsunami and river floods). A series of maps show the areas of low-lying land that are expected to be inundated during more extreme storm and sea conditions for those areas where accurate topography data was available on the Kapiti coast and around Wellington Harbour (Wellington and Lower Hutt). Combined wave and storm-tide inundation levels at the shoreline are also provided for the south Wellington coast and the Wairarapa coast, but not overland inundation maps as high-resolution topography was not available for these areas.

Eight storm events (four for the west coast and four for the south and east coasts) were initially simulated, each with different combinations of wave height and storm-tide offshore from the coast, but adjusted to have the same joint-probability of 1% annual exceedance probability (AEP). From these four historical storm events in each sub-region, a single scenario for the Kapiti coast and another for Wellington Harbour and the South Wellington and Wairarapa coasts were selected as representative of the upper range of total storm inundation levels for a 1% joint AEP event. These scenarios were then used for modelling and mapping combined wave and storm-tide inundation for both present and future climate-change conditions.

Present-day sea-level for the region was assumed to be represented by a 7-year average mean sea level at Port of Wellington from 2005 to 2011 inclusive. Inundation levels and maps were also created for future increments in sea-level rise of 0.5 m, 1.0 m and 1.5 m, relative to present-day sea level.

The report is structured as follows:

- A description of the methods used to model the combined inundation levels and maps is presented in Section 2. This section presents enough information to understand the important concepts and interpret the results that follow. More detailed explanation of the modelling is included later in Appendices A and B.

- The results section includes figures and tables containing inundation levels around the coast of the Wellington region. Aerial photographs are also presented, with expected areas of coastal inundation overlaid.

2   Methods

This methods section provides the key information required to understand how the inundation levels and inundation maps were derived. More detail on the storm-tide, wave and wave setup modelling methods is provided in Appendices A and B.

Several steps were required to determine coastal inundation levels, and map inundation:

1. As part of the recent Waves And Storm-tides Predictions (WASP)[2] project (previously funded by the Ministry of Business, Innovation & Employment), separate hindcasts of storm-surge and waves were simulated for the 45-year period 1957-2002. This provided time series of storm-surge heights and wave statistics for offshore locations around the coast of New Zealand.

2. A joint-probability analysis (Stephens et al. 2011 and minor edits 2012) was conducted using the time-series produced in the WASP project to determine large wave and storm-tide conditions with equal probability of occurring together, offshore around the Wellington Region.

3. Several storm events were selected from the joint probability analysis to model in more detail. The storm events were chosen because they had large storm-tides and/or large waves. For each selected storm event, the joint annual exceedance probability (AEP) of the storm-tide and wave heights was around 1%.[3] Since our aim was to simulate events with exactly 1% AEP, adjustments where applied to the mean level of the sea for the modelled events, thus "sliding" the event along the storm-tide axis of the joint-probability curve to meet the 1% AEP contour.

4. Maximum tidal water heights (high tides) at the coast on the day of the selected storm events were calculated using NIWA's tide model TIDE2D.

5. The RiCOM hydrodynamic model was used to simulate the storm-surge component and land inundation for the selected storm events. The effects of tides, mean level of the sea and sea-level rise were incorporated by including them as the base level sea level for the storm surge simulations. Thus the peak of the simulated storm surge always coincides with high-tide peak in the inundation simulations, and so the simulations are conservative (i.e., storm-surge may not always peak at high tide for any given 1% AEP event, but it will on some occasions). The maximum sea level obtained during the simulation is the storm-tide level. The RiCOM model simulates overland flow across the schematized low-lying land, representing the flow paths of the storm surge along rivers, roads and drains.

6. A wave model was run to simulate wave conditions for these selected events.

7. Wave setup at the coast for these events was calculated using a 1−dimensional wave transformation model.

8. Wave setup was added to the simulated storm-tide level at the coast, and the associated land inundation calculated.

---

[2] http://wrenz.niwa.co.nz/webmodel/coastal
[3] The level that is likely to be reached or exceeded with a probability of 1% in any year. Over a design or planning timeframe of say 50 years, the probability of such an event exceeding this level is 39% (or 63% probability in a 100-year period).

The remainder of the methods section addresses the following topics:

2.1   Sea-level datum and long-term sea-level change including a description of the vertical datum and sea-level reference timeframe for this study.

2.2   Outline of processes contributing to coastal inundation. If we understand and can quantify the important drivers of inundation, then we can include them in the inundation modelling.

2.3   The WASP models – how waves and storm-tides were simulated offshore from the New Zealand coastline. The present coastal inundation study relied on output from the WASP project.

2.4   Introduction to probability analysis – how big will the inundation levels be, and how likely are they to occur? Which events will cause the most inundation and which events should we model in greater detail?

2.5   Modelling storm-tides and waves. We describe the transformation of storm tides and waves from offshore into the coast, and the resulting coastal inundation during large storm events. Verification is also provided matching simulated wave height and storm-tide levels against available measurements.

2.6   Inundation mapping – how the coastal inundation maps were derived.

2.7   Sea-level rise scenarios – constant increments of sea-level rise of +0.5, 1.0 and 1.5 m were applied to create inundation maps covering a range of possible future coastal scenarios.

2.1   Vertical datum

This report presents coastal inundation maps from simulated storm events. The simulated scenarios include present-day sea level, plus increments of sea-level rise of 0.5, 1.0, and 1.5 m relative to present day. As mean sea levels are constantly changing, we need to define the timeframe to which our simulations are referenced.

Present-day sea-level for the region was assumed to be represented by a 7-year average mean sea level at Port of Wellington (Queens Wharf) from 2005 to 2011 inclusive described in this report as MSL05–11. The levels of the storm tide, alone and in combination with wave setup, were specified relative to Wellington Vertical Datum 1953 (WVD-53)[4]. Unless otherwise stated, all plotted and tabulated data in this report are given relative to WVD-53 based on MSL05-11, i.e. present mean sea level is 0.196 m above WVD-53. This is similar to the mean sea level over the longer nodal-tide period of 1993 to 2011 of 0.18 m above WVD-53 (1.09 m above Chart Datum) calculated by Land Information NZ (2012).

The present-day mean level of the sea (MLOS) as measured in Wellington Harbour was uniformly applied to the Greater Wellington Region. The justification for this is that MLOS tends to vary slowly around the New Zealand coastline, and is regionally quite consistent (Bell & Hannah 2012). At any given time, differences in MLOS will therefore be small (< ~10 cm) around the Wellington region.

---

[4] WVD-53 was based on sea-level measurements over 14 years in the period 1909 to 1942 (Bell & Hannah 2012)

The process of determining MLOS to add to the modelled tide and storm surge events was:

1.   Obtain measured monthly MLOS at Wellington 1944–2011 (blue line Figure 2-1).

1.   Fit linear trend in MLOS at Wellington for 1944–2011 = 2.46 mm/yr (black upward sloping line Figure 2-1).

2.   Determine the mean sea level for 2005–2011 (MSL05–11) = 0.196 m WVD-53 (green line Figure 2-1).

3.   Adjusted detrended MLOS time series to have a base sea level set at MSL05–11 (red line Figure 2-1).

4.   Add adjusted, detrended MLOS to modelled tide and storm surge to get total storm tide. The adjusted, detrended MLOS was added for the month for any particular historical event modelled, so that each event was modelled based on mean sea level 2005–11.

Note that the International Panel for Climate Change (IPCC) provides long-term sea-level rise scenarios relative to a base sea level for 1980–1999, centred on 1990. Wellington mean sea-level 1980–1999 was 0.14 m (WVD-53). Thus 0.056 m should be subtracted from the values in this report (which are specified based on MSL05–11), in order to adjust them to the slightly lower 1980–1999 base sea level.
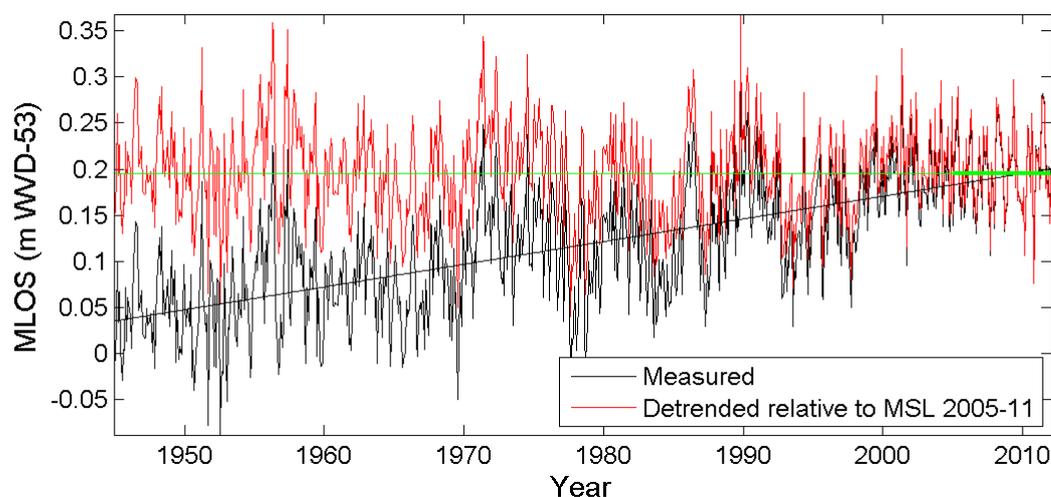
Figure 2-1: Monthly mean level of the sea (MLOS) from 1944-2011 at Queen's Wharf Wellington.

2.2   An overview of the processes contributing to coastal inundation

There are a number of meteorological and astronomical phenomena involved in the development of a combined extreme sea level and wave event. These processes can combine in a number of ways to inundate low-lying coastal margins with seawater. The processes involved are:

- Mean level of the sea (MLOS).

- Astronomical tides.

- Storm surge (winds and low barometric pressure).

- Wave setup (and runup).

- Climate-change effects including sea-level rise.

The **mean level of the sea (MLOS)** describes the variation of the non-tidal sea level on longer time scales ranging from monthly up to decades due to climate variability, including seasonal effects and the effects of El Niño–Southern Oscillation (ENSO) and the Interdecadal Pacific Oscillation (IPO) on sea level through changes or climate-regime shifts in wind patterns and sea temperatures.

The astronomical tides are caused by the gravitational attraction of solar-system bodies, primarily the Sun and the Earth's moon. In New Zealand the astronomical tides have by far the largest influence on sea level, followed by storm surge (in most locations).

Low-pressure weather systems and/or adverse winds cause a rise in water level known as **storm surge**. Storm surge results from two processes: 1) low-atmospheric pressure causes the sea-level to rise, and 2) wind stress on the ocean surface pushes water down-wind and to the left (in the Southern Hemisphere) of a persistent wind field, piling up against any adjacent coast.

Storm-tide is defined as the sea-level peak reached during a storm event, from a combination of MLOS + tide + storm surge. It is the storm-tide that is measured by sea-level gauges such as in Wellington Harbour. Large storm-tide events cause coastal inundation.

Waves also raise the sea level at the coastline higher above the offshore storm-tide levels. **Wave setup** is the increase in mean sea level at the coast, pushed up inside the surf zone from the release of wave energy as waves break in shallow water (Figure 2-2). The term wave setup describes an average raised elevation of sea level at the shore when breaking waves are present. Thus wave setup also contributes to coastal inundation during a storm event. **Wave runup** is the maximum vertical extent of wave "up-rush" on a beach or structure above the still water level (that would occur without waves). Consequently runup constitutes only a short-term fluctuation in water level (and hence water volume) compared with wave setup and storm surge, which generate more sustained water levels and inundating volumes at the coast (Figure 2-2). Wave runup does not contribute significantly to coastal inundation except in circumstances where the flowing "green water" in wave runup overtops a barrier and cannot readily exit back to the sea.

Where waters are sufficiently deep adjacent to the shoreline, waves may break right at the shoreline, causing wave overtopping e.g., at rock revetments and seawalls. Wave-overtopping volumes in this situation comprise green water (flowing seawater), wave splash and wind drift.

Climate change also is projected to produce increasing acceleration in long-term sea-level rise (i.e. an increase in MLOS) but at this stage, only minor increases are projected for the drivers (winds, barometric pressure) that produce storm surges. The WASP project has shown that storm surges and significant wave heights are each only likely to increase by up to 3-5 centimetres by the latter part of this century, which means councils can focus mostly on the effects of sea-level rise.

Flooding, from rivers, streams and stormwater, is another contributor to coastal inundation when the flood discharge is constrained inside narrower sections of estuaries. Neither riverine flooding nor tsunami inundation is considered in this report, which focuses solely on the joint effects of waves and storm-tides.
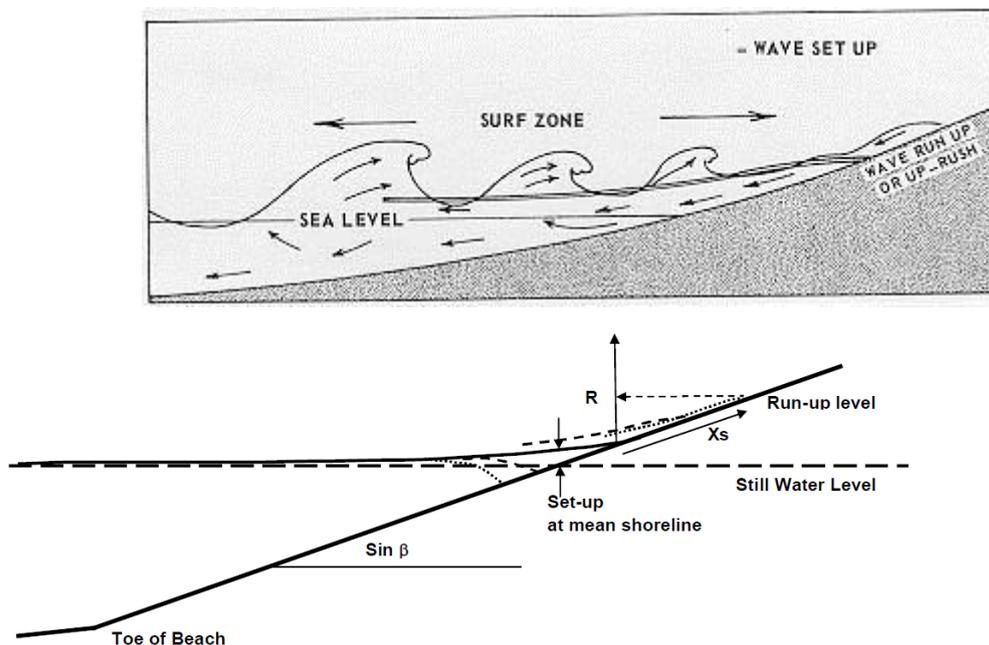
Figure 2-2: Illustration of wave setup and runup.

In this report, we present maps of **total storm inundation** that include the effects of MLOS, astronomical tides, storm surge, and wave setup. We also conduct simulations that include increments in sea-level rise of 0.5 m, 1.0 m and 1.5 m. Wave runup does not significantly contribute to coastal inundation in most coastal situations and so is not included, however estimates of wave runup at certain locations are given in Table B-2 and Figure B-9.

In summary, in this study we modelled the following processes and their contribution to coastal inundation:

- Mean level of the sea (MLOS05–11) relative to WVD-53.

- Astronomical tide.

- Storm surge.

- Wave setup.

- Mean-sea-level rise increments of 0.5, 1.0 and 1.5 m.

2.3   The WASP models – simulating waves and storm-tides offshore from the New Zealand coastline.

The present study is based on 45-year-long wave and storm-tide hindcast simulations around the coast of New Zealand, produced during the Waves And Storm surge Predictions (WASP) project.

The WASP hindcasts provide the following information that was used for the present coastal inundation study:

- 45-year-long hindcast wave and storm-tide conditions for the present-day climate.

- The 45-year-long time-series enable us to undertake extreme-value and joint-probability analyses, to determine frequency–magnitude relationships for wave heights and storm tides, and the likelihood of large waves and storm tides occurring at the same time (see Stephens et al. 2011 and minor edits 2012).

- The offshore WASP simulations were used as boundary conditions to drive detailed coastal simulations for the Wellington region to predict inundation for specific large storm events.

For the WASP project, NIWA carried out a hindcast of wave and storm tide conditions for the period September 1957 through August 2002, forced by inputs from the ERA-40 reanalysis data set. ERA-40 is a global re-analysis of the weather spanning the period mid-1957 to mid-2002 produced by the European Centre for Medium-Range Weather Forecasts (ECMWF), which provides global six-hourly wind and barometric pressure fields at $1.125^\circ \times 1.125^\circ$ resolution (Uppala et al. 2005).

A global wave model grid was established at the same resolution, along with a nested New Zealand regional grid covering longitudes 162.000°E to 185.625°E (174.375°W) at 0.125° resolution, and latitudes 51.750°S to 32.625°S at 0.09375° resolution. The latter New Zealand regional grid was used to provide more accurate representation of nearshore wave conditions, but both models were forced with the same ERA-40 wind fields in hindcasts from October 1957 to September 2002. Outputs of wave statistics computed at each model grid cell, including significant wave height, peak and mean wave period, peak and mean wave direction, directional spread and wave energy transport were archived at 3 hour intervals from the global model, and hourly intervals from the New Zealand regional wave model.

Similarly to the wave modelling, hindcasts of storm surge were calculated using wind and barometric pressure fields based on the ERA-40 Reanalysis data set. The ERA-40 Reanalysis provides atmospheric forcing fields (surface winds and sea-level pressure for this study) at $1.125^\circ \times 1.125^\circ$ resolution for the whole world. To drive the New Zealand-scale storm surge model, these wind fields were dynamically downscaled to around 30 km resolution around New Zealand using a Regional Climate Model (Ackerley et al. 2012). Wind and pressure fields from the regional climate model were then interpolated onto RiCOM model grids (Appendix A), providing spatially explicit time-series of surface boundary conditions.

2.4 Defining the frequency and magnitude of extreme storm-tides and waves

This study aims to produce coastal inundation maps for combined storm-tide and wave events with a joint Annual Exceedance Probability of 1%. To assess the magnitude of these events, Stephens et al. (2011 and minor edits 2012) combined wave and storm-tide information in a **joint-probability** analysis, calculating the likelihoods of high storm-tides and large waves coinciding. In this section we first define some important concepts needed to

understand extreme event analysis and then we detail the process of quantifying the joint probabilities of the waves and the storm-tide.

2.4.1 Some extreme-value terms and concepts

The likelihoods associated with extreme storm-tides and/or waves, are reported in terms of their probability of occurrence. The **annual exceedance probability** (AEP) describes the chance of an event reaching or exceeding a certain water level in any given year. For example, if a storm-tide of 1.26 m (WVD-53) has a 5% AEP, then there is a 5% chance of a storm-tide this high, or higher, occurring in any 1-year period. So it is unlikely, but could still happen and should be planned for. Furthermore, although the occurrence probability is only 5%, more than one storm-tide this high or higher could occur in any given year.

Alongside AEP, the likelihood of extreme events can also be described in terms of their more familiar **average recurrence interval** (ARI), which is the average time interval between events of a specified magnitude (or larger), when averaged over <u>many</u> occurrences. Table 2-1 shows the relationship between AEP and ARI; small relatively common events have a high annual exceedance probability and a low average recurrence interval, and *vice versa* for large, rare events.

Table 2-1: **Relationship between annual exceedance probability (AEP) and average recurrence interval (ARI) for peaks over a threshold.** $AEP = 1 - e^{(-1/ARI)}$.

AEP (%)	99%	86%	63%	39%	18%	10%	5%	2%	1%	0.5%
ARI (years)	0.2	0.5	1	2	5	10	20	50	100	200

ARI (or its often used surrogate "return period") is an easily misinterpreted term, with people often assuming that because one large event has just occurred, then the average recurrence interval will pass before another such event. It is also prone to confusion with planning lifetimes, which, like ARI, are also expressed in years. We therefore prefer the term AEP, because it conveys the continuous probability that large events could occur at any time.

Occurrence likelihoods for extreme storm-tide and wave height magnitudes are only one aspect of the planning process. Another essential component is to consider the planning timeframe, or design lifetime, of interest. This is particularly relevant in the context of rising sea levels, which will change the base level for future storm-tide inundation (Bell and Hannah 2012). For example, a typical planning lifetime for residential housing is about 100 years. Table 2-2 presents the likelihood that events with various occurrence probabilities will occur within a specified planning lifetime. The likelihoods can be shaded according to their chance of occurring in the specified timeframe, for example:

▪	> 85%	Almost certain
▪	60%–85%	Likely
▪	35%–60%	Possible
▪	16%–35%	Unlikely
▪	< 15%	Rare

For example, a relatively common (smaller) event with a 39% AEP, is *almost certain* to occur over a 20-year lifetime. However, a rare (larger) 2% AEP event is *unlikely* to occur over the same 20-year lifetime. A 1% AEP is a commonly used planning or design event magnitude, and 100-year planning lifetimes are commonly used for assessing risk for infrastructure (e.g., bridges) or the requirement in the NZ Coastal Policy Statement[5] (DOC, 2010) to consider "at least 100 years" when assessing coastal hazard risks (Policy 24). Table 2-2 shows that a 1% AEP event is *likely* to occur or be exceeded over a 100-year planning lifetime with a probability of 63%.

Table 2-2: **Likelihood of an event with a specified probability of occurrence (AEP / ARI), occurring within planning or design lifetimes for peaks over a threshold.** $P = 1 - e^{-L / ARI}$, where L = planning lifetime and P = probability of occurrence within planning lifetime.

AEP (%)	ARI (years)	Planning or design lifetime (years)						
		2	5	10	20	50	100	200
39%	2	63%	92%	99%	100%	100%	100%	100%
18%	5	33%	63%	86%	98%	100%	100%	100%
10%	10	18%	39%	63%	86%	99%	100%	100%
5%	20	10%	22%	39%	63%	92%	99%	100%
2%	50	4%	10%	18%	33%	63%	86%	98%
1%	100	2%	5%	10%	18%	39%	63%	86%
0.5%	200	1%	2%	5%	10%	22%	39%	63%

2.4.2 Joint-probability analysis for storm-tide and waves

Joint probability analyses identify the probability of a storm-tide height and significant wave height coinciding. For this report we conducted analyses at nine sites around the greater Wellington coastline (shown in Figure 2-3) using joint-probability software (Hawkes et al. 2002; HR Wallingford 2000; HR Wallingford and Lancaster University 2000) to fit the joint probability dependence to the largest 5% of the wave heights and storm tides at these locations.

An example of the joint probability analysis for site 4 offshore from Wellington Harbour entrance is shown in Figure 2-4 and Figure 2-5. Figure 2-6 shows the joint probability analysis for site 3 offshore of Waikanae. Joint probability analyses for the other sites are given in Appendix C These plots illustrate how a storm with a small storm-tide but large significant wave height can have a similar joint annual exceedance probability to a storm with a larger storm-tide but smaller significant wave heights.

Figure 2-4 plots the raw data output from the WASP model. However the WASP wave hindcast under-predicts extreme significant wave height and needs to be adjusted by a factor of 1.5 in the Wellington region before use in the joint probability analysis (as determined through comparisons with wave records from Baring Head and Maui-A platform

---

[5] http://www.doc.govt.nz/publications/conservation/marine-and-coastal/new-zealand-coastal-policy-statement/new-zealand-coastal-policy-statement-2010/

(Stephens et al. 2011, minor edits 2012). Figure 2-5 shows the same data as Figure 2-4 after applying the H_s ×1.5 scaling, and re-calculating the joint-probability contours. The cause of the WASP wave model under-prediction is the spatial resolution of the ERA-40 wind fields that don't fully resolve storm systems adequately to impart sufficient energy to the waves. Conversely, storm surges operate over wider spatial scales, so the hindcast results were used directly. The problem of wave height under-prediction was overcome by using a trained interpolation technique for the present study (Appendix D). The joint-probability analysis and selection of events for detailed inundation modelling was based on the WASP H_s ×1.5.
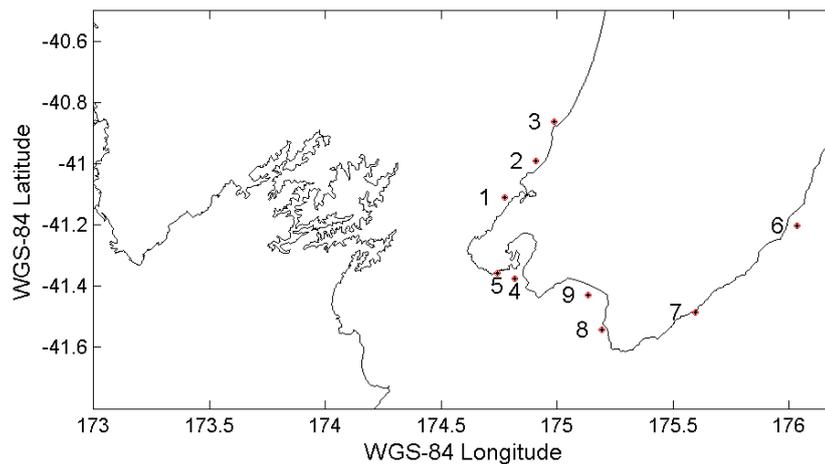
Figure 2-3: Locations where joint-probability analyses for storm-tide and wave heights were carried out.
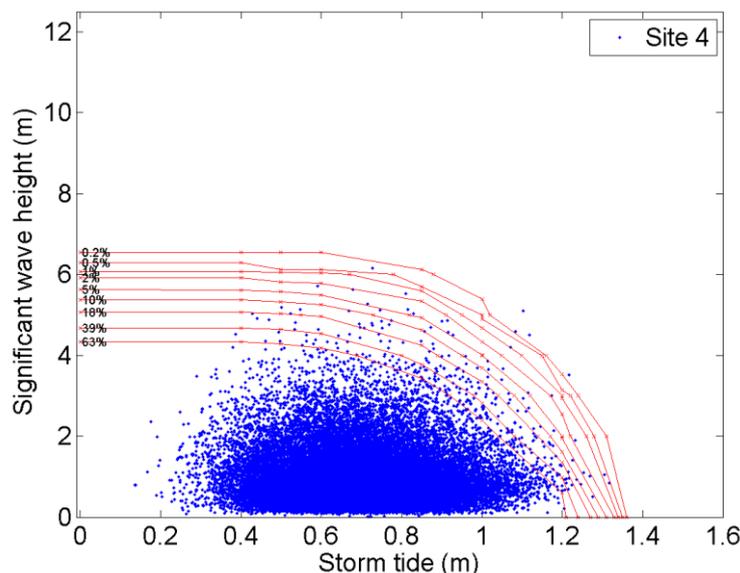
Figure 2-4: Joint probability of storm-tide and un-scaled significant wave height at site 4, (Figure 2-3) offshore from Wellington Harbour entrance. The blue dots show individual observations of storm-tide and wave height simulated by the WASP models. The red contours indicate the joint annual exceedance probability (%) for this combination of storm-tide and wave height. The plotted significant wave heights (and associated joint-probability contours) are raw wave heights from the WASP model.
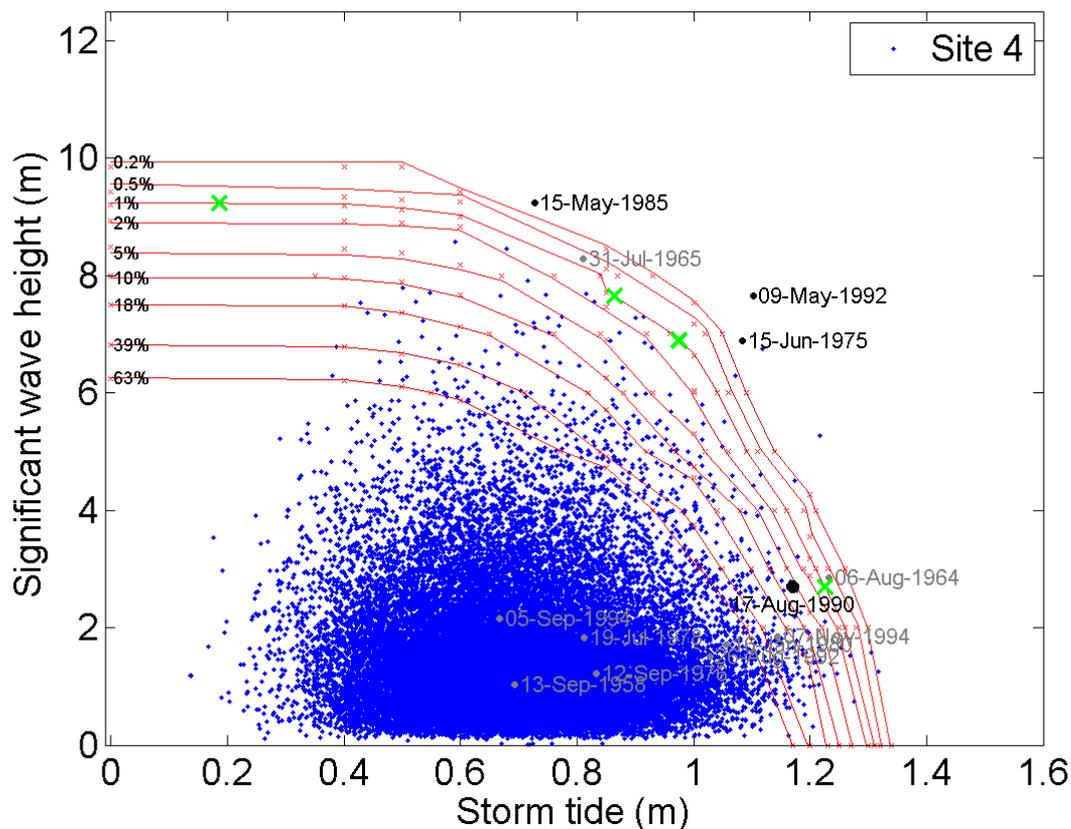
Figure 2-5: Joint probability of storm-tide and significant wave height scaled up by ×1.5, at site 4 (Figure 2-3) offshore from Wellington Harbour entrance.   The blue dots show individual observations of storm-tide and wave height simulated by the WASP models, and red contours indicate the joint annual exceedance probability (%) for this combination of storm-tide and wave height. Significant wave heights have been scaled up by ×1.5, based on model–buoy comparisons in Stephens et al. (2011, minor edits 2012). Individual storm events selected for further analysis (Table 2-3) are marked. Events selected for inundation modelling on the Wellington coast are marked in bold (Table 2-3), and green crosses mark the intersection of bolded events with the 1% AEP contour, after "sliding" the events along the horizontal storm-tide axis.

 On the western Kapiti coast of the Wellington region, hazardous events are most likely to involve a combination of large waves coinciding with a high storm tide, because storm tide and waves are highly correlated (Stephens et al. 2011, minor edits 2012; Figure 2-6 and figures in Appendix C). The exposure increases toward the north along this coast, due to increasing tidal range and exposure to larger waves from the west. On the Wellington and Wairarapa coasts to the south and east, large waves and swell are more likely to occur in isolation from large storm tides (Stephens et al. 2011, minor edits 2012; Figure 2-5 and Figures in Appendix C). The wave climate is also considerably more energetic than on the west coast, with larger extreme significant wave heights.

For each of the nine analysis sites, three to five storm events with AEP close to 1% were identified. These events covered a range of storm-tide/significant wave height combinations. Figure 2-5 and Figure 2-6 show that the Wellington and Kapiti coasts have different dependence between wave height and storm tide. Furthermore, storm events that are more extreme on one coast may be less extreme on the other. A total of thirteen events were identified across the nine sites, and these are marked on Figure 2-5 and Figure 2-6. Eight of

these events were identified as having AEP close to 1% across a range of sites. On the Wellington and Wairarapa coast, events occurring on 15 June 1975, 15 May 1985, 17 August 1990 and 9 May 1992 were selected for detailed hazard exposure and inundation modelling (Figure 2-5). On the Kapiti coast, events occurring on 12 September 1976, 16 January 1980, 6 September 1994 and 7 November 1994 were selected for detailed hazard exposure and inundation modelling (Figure 2-6).
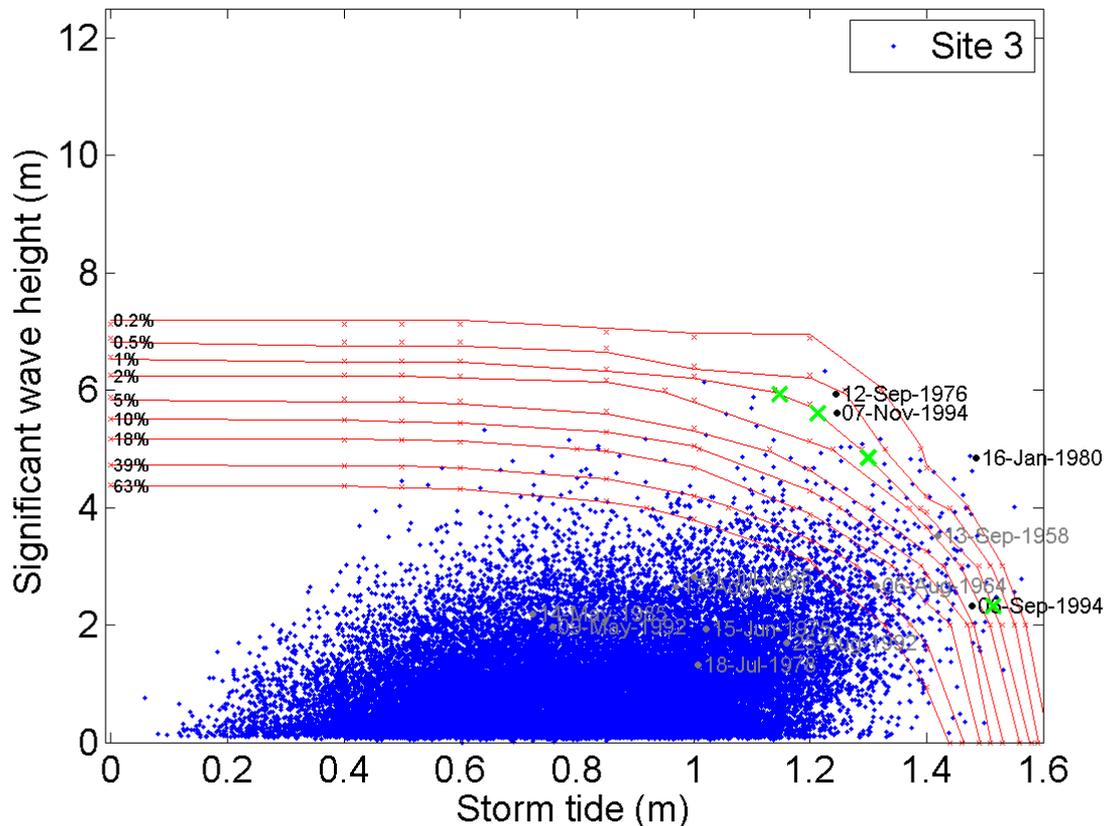
Figure 2-6: Joint probability of storm-tide and significant wave height scaled up by ×1.5, at site 3 (Figure 2-3) offshore from Waikanae. The blue dots show individual observations of storm-tide and wave height simulated by the WASP models, and red contours indicate the joint annual exceedance probability (%) for this combination of storm-tide and wave height. Significant wave heights have been scaled up by ×1.5, based on model–buoy comparisons in Stephens et al. (2011, minor edits 2012). Events selected for inundation modelling on the Kapiti coast are marked in bold (Table 2-3, and green crosses mark the intersection of bolded events with the 1% AEP contour, after "sliding" the events along the horizontal storm-tide axis.

An objective of the study was to simulate combined wave and storm-tide events with a joint annual exceedance probability of 1% (or 100-year average recurrence interval). To produce inundation levels and maps, detailed simulations of storm tide, waves and wave setup were undertaken for each of the 8 storm events in Table 2-3. Each storm event was applied to all coasts, even though the sub-groups of events affected the east and west coasts differently. However, it is seen from Figure 2-5 and Figure 2-6 that these events do not exactly match the 1% joint AEP contour. To assign each event a joint probability of 1% AEP, the mean level of the sea was adjusted to shift the storm event along the storm-tide axis onto the 1% AEP contour. The adjusted event storm-tide levels are marked by the green crosses in Figure 2-5 and Figure 2-6, and the average MLOS adjustments are given in the 3rd column

of Table 2-3. For example, the event occurring on the 17 August 1990 (Figure 2-5) has a joint AEP of approximately 6%. To shift the joint probability to an AEP of 1%, an MLOS of +0.06m is required, corresponding to the distance along the storm-tide axis required to shift the event to the 1% AEP contour. This adjustment varied slightly between sites, so we used the average adjustment across the nine sites where the joint probability analyses were conducted. The sea-level adjustments contribute (with the high tide) to a net water level relative to WVD-53, but equilibrate events to a 1% AEP relative to the present day (2005-2011) base sea level. The net water level offset is given in column 4 of Table 2-3 as the sum of the values in columns 2 and 3, and MSL05–11 (rounded to two significant figures). A relative ranking of storm-tide (first letter) and significant wave height (second letter) are given in the 5th column of Table 2-3.

Table 2-3: **Historical storm event adjustments for simulations of inundation.** Column two gives the high tide (astronomical) on the day of the event, column three gives the mean level of sea adjustment relative to MLOS used to assign the storm a 1% joint AEP, column 4 the net water offset used in the simulation, consistent with the present day (2005-2011) mean sea level relative to (WVD-53). The fifth column gives an indicator of the relative size of the storm-tide (first letter) and wave height (second letter). S = small, M = moderate and L = large.

Storm Date	Highest astronomical tide on day of storm (MLOS, m)	MLOS adjustment for 1% joint storm-tide and wave height AEP (m)	Net water level offset relative to WVD-53 (m)	Storm-tide/wave height indicator
Wellington Harbour and Hutt Valley Region				
15 June 1975	0.64	0.14	0.98	MM
15 May 1985	0.43	-0.01	0.62	SL
17 August 1990	0.61	0.27	1.08	LS
9 May 1992	0.66	0.07	0.93	MM
Kapiti Coast Region				
12 September 1976	0.84	0.02	1.06	MM
16 January 1980	0.83	0.04	1.07	MM
6 September 1994	1.05	0.20	1.45	LS
7 November 1994	0.88	-0.03	1.05	SL

The sites closest to Wellington Harbour (4 and 5 in Figure 2-3) were used to identify significant storms for the Wellington Harbour area. As these two points are near each other similar storm-tides and wave heights were observed at both sites. Plotting the significant wave height against MLOS-adjusted storm-tide (Figure 2-7) shows that the 15 May 1985 storm had small storm-tide and large waves (SL), the 17 August 1990 event had large storm-tide and small waves (LS), while the 15 June 1975 and 9 May 1992 had moderate storm-tide and moderate wave heights (MM).

Both storm-tide and significant wave heights increase in magnitude northward along the Kapiti Coast. Figure 2-8 shows the significant wave heights and storm-tides for the four modelled events at analysis sites 1 (southernmost), 2 and 3 (northernmost) (Figure 2-3). Storm-tides were larger on the Kapiti coast than in Wellington Harbour, but significant wave heights were smaller, in open water offshore from the coast. As a relative classification, the 6

September 1994 event was considered to have large storm-tide and low wave heights (LS), the 7 November 1994 event had small storm-tide and large waves (SL), and the 16 January 1980 and 12 September 1976 events had moderate storm-tides and wave heights (MM).
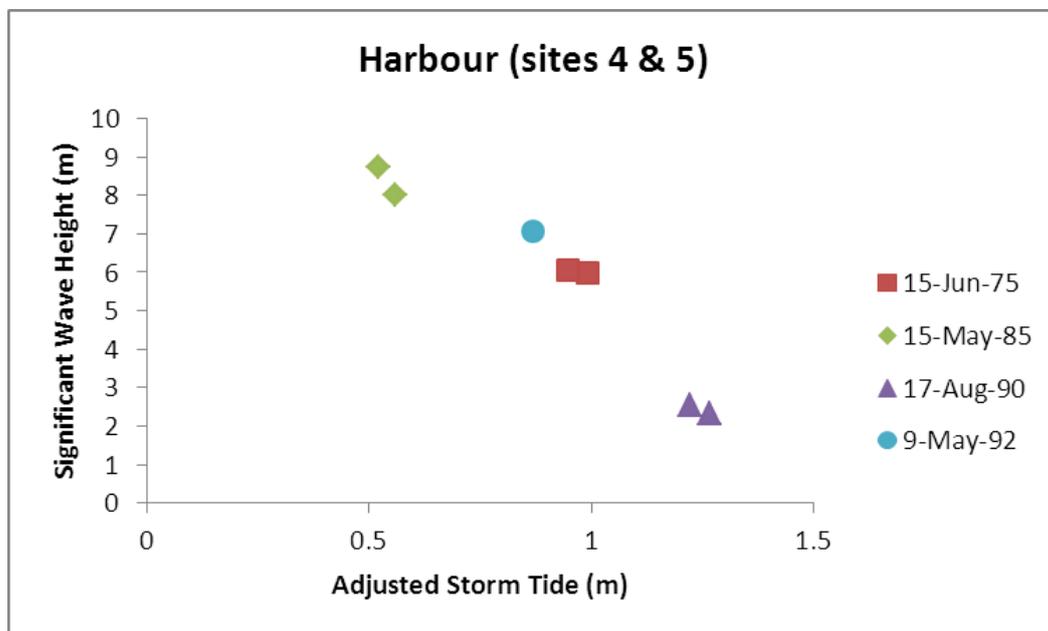
Figure 2-7: Storm-tide and significant wave height for the four storm events modelled on the Wellington Harbour inundation grid. The storm-tide includes an MLOS adjustment to assign the storm events a common joint AEP of 1% as explained above. The locations of the points where the wave heights and storm-tides were calculated are shown in Figure 2-3.
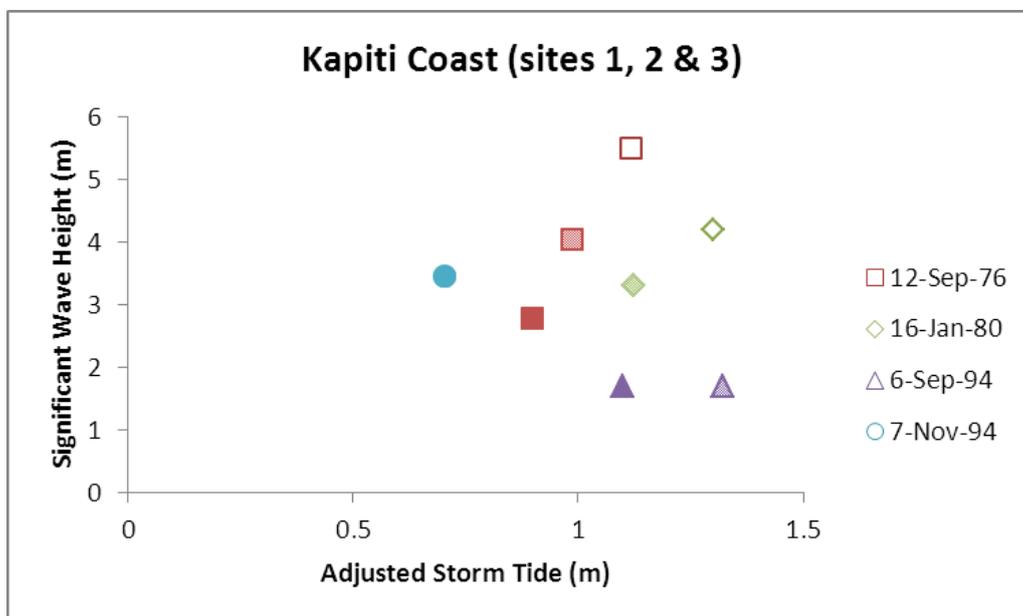
Figure 2-8: Storm-tide and significant wave height for the four storm events modelled on the Kapiti Coast inundation grid. The storm-tide includes an MLOS adjustment to assign the storm events a joint AEP of 1% as explained above. The locations of the points where the wave heights and storm-tides were calculated are shown in Figure 2-3. Solid symbols are site 1, shaded symbols site 2, and open symbols site 3.

For a more comprehensive explanation about the joint-probability analyses using storm tides and waves from the WASP wave hindcasts, see Stephens et al. (2011, minor edits 2012).

2.5   Modelling storm-tides, waves and wave setup, and inundation

The WASP project provided 45-year-long (1957–2002) simulations of storm tide levels and wave statistics, at offshore (outside the surf zone) locations around the coast of New Zealand.

The joint-probability analysis put the simulated WASP storm tide and wave events into context of their joint likelihood of occurrence. This allowed us to select a few events with rare combinations of large storm tides and/or waves (Table 2-3). These events were then modelled in more detail near the coast to map the resulting coastal inundation.

In this section we describe the detailed inundation modelling process.

The following numerical models were used to simulate inundation during the 8 selected storm events (Table 2-3):

- Tide2D – This is NIWA's New Zealand tidal model which predicts tidal amplitudes and timing at any open coast location around New Zealand. The model uses 12 tidal constituents to construct a time series of water elevations Walters et al. (2001). Tide2D was used to predict the tides during each of the 8 simulated storms.

- RiCOM – is a general purpose 3-D coastal model that is used routinely by NIWA to forecast storm surge around New Zealand (Walters and Casulli 1998; Walters 2005a; 2005b; Walters et al. 2007; Walters et al. 2010; Gillibrand et al. 2011). The model is driven by time- and spatially-varying wind stress and atmospheric pressure data. In this study, an existing grid covering the entire NZ region was modified to produce two different grids in which the resolution was increased in the Wellington and Hutt Valley region and the Kapiti Coast region. Simulations were run separately for each of the two grids. Land topography around Wellington, the Hutt Valley, and the Kapiti Coast was incorporated in the grids using LiDAR data supplied by GWRC and WCC so inundation could also be modelled.

- SWAN –Wave conditions in the Wellington region were simulated using the SWAN model (Booij et al. 1999; Ris et al. 1999). This spectral model describes the sea state in terms of the amount of energy in each band of wave frequency and propagation direction. The model computes the evolution of this wave spectrum by accounting for the input, transfer and loss of energy through the various physical processes. The model accommodates the processes of generation by wind stress, propagation with refraction by the seabed and/or currents, transfer of energy between interacting waves of different frequencies and directions (a nonlinear effect), and dissipation by white-capping, bottom friction and depth-induced breaking. The model can incorporate boundary conditions representing waves arriving from outside the model domain.

In theory, it is possible to model the tides, storm surge and wave setup simultaneously using RiCOM coupled with the SWAN wave model to simulate inundation due to storm-tides and

wave setup. This process would accurately represent the physics of all processes (tide, storm surge and waves), and account for the interactions that occur between them. For example, at high tide, the storm surge will propagate further inland, but the extent of inundation will be limited by the ~3-hour duration of the tide peak. Likewise, wave setup will be influenced by the depth of the storm tide at the coast. In reality, the high modelling detail (small grid size), the associated numerical expense (model takes too long to run), and the large area (entire Wellington region) being simulated, meant that the various models had to be de-coupled and run separately. The method used was:

1. Identify the mean level of the sea offset required so that the offshore storm-tide and waves had a joint 1% annual exceedance probability relative to mean level of the sea. These MLOS adjustments are given in the 3rd column of Table 2-3.

2. Use Tide2D to predict the tide during the storm event. Extract the level of the high-tide peak closest to the storm-surge peak. These tide height offsets are given in the 2nd column of Table 2-3. Add the MLOS adjustments to the tide height offsets, to the 2005–11 mean sea level at the Port of Wellington. These net water level offsets are given in the 4th column of Table 2-3, and provide the base sea level for the storm-surge simulations.

3. Use RiCOM to simulate storm surge for each of the 8 events, using the net offsets as a constant base sea level for the storm surge simulations. RiCOM included bathymetric data and topographic data from LiDAR. The grid cell size was approximately 20 m near the coast and over the land (and larger out to sea), so the storm surge inundation modelling resolves land-based flow paths such as drains and low-lying roads that are > 20 m across, and inundation of the grid is physically realistic. Thus the RiCOM model produced the initial inundation maps due to storm tide. The storm surge simulations were modelled over the entire New Zealand continental shelf regions and forced by the same barometric pressure and wind stress taken from the WASP hindcast. The use of a fixed high-tide base level (net water level offset in Table 2-3) for the storm surge simulations adds conservatism to the inundation modelling, because in reality the peak inundation levels would be maintained for only about 1–1.5 hours either side of the high-tide peak. By maintaining them for the whole storm-surge simulation, more inundation occurs above the high-tide level, than may actually occur, because the elevated water levels have longer to overcome friction and continue flowing overland until the low-lying depressions or areas are filled up to the storm-tide level. However, as the tide is generally the largest component of sea-level variability in New Zealand, the highest inundation levels are likely to occur at high tide. This was the case for the 8 simulated events.

4. The SWAN wave model was run for each of the 8 storm events, to simulate wave conditions offshore and at the coast. The method to interpolate the wave setup onto the inundation grids is given in Section 2.6.

5. An analysis was undertaken of the storm-tide and wave set-up combinations for these 8 adjusted historic scenarios that have a common 1% joint AEP. Even though these scenarios have the same likelihood (based on offshore storm-tide levels and offshore significant wave height), different combinations along a common joint AEP contour will produce different total inundation levels due to wave set-up being a non-linear function of offshore significant wave height (Appendix B) and also water depth at the shore

(that is increased during high storm tides). A representative combination that produced total inundation levels towards the upper end of the range was selected for each coast from the 4 events in each sub-region (Table 2-3) to undertake the coastal inundation mapping. For the Kapiti Coast down to Oteranga Bay, an adjusted 6 Sept 1994 event was used to represent a 1% joint AEP event, while a representative 1% AEP combination chosen for the South Wellington and Wairarapa Coast was an adjusted 17 Aug 1990 event. Note: this does not mean that the actual events on those dates yielded the highest historical inundation levels recorded as they have had the actual MLOS adjusted upwards in these two cases to produce a common 1% joint AEP (Table 2-3).

A detailed explanation of the storm surge model and its verification is presented in Appendix A. Details of the wave modelling and verification are presented in Appendix B, along with the wave setup calculation method.

2.5.1 Caveats

The inundation modelling is based on events that have been identified (and adjusted) to have an offshore storm-tide – wave joint probability of 1% AEP. This does not mean that the overland inundation caused by each event necessarily has an annual exceedance probability of 1%. The probability reflects the likelihood of the storm conditions offshore in deep water and not the inundation hazard per se.

A fixed high-tide water level was used in the inundation modelling rather than modelling tides and storm-surge together. The effect of this approach is that it is implicitly assumed that the maximum storm-surge coincides with high tide. Therefore storm-tide levels predicted in the modelling may be higher than would have actually occurred if maximum storm-surge actually occurred at a time other than high tide. This may lead to conservative estimates of the inundation hazard. However, we note that the joint probability analysis is based on storm-tide, which are the combination of tide and storm-surge, and that tides are significantly larger than storm-surge. Thus the events on which the model scenarios are based on will have had maximum storm-tide levels at or near high tide, and the error from using a fixed tidal water level is expected to be small.

Wave runup is a transient process, so it does not cause large volumes of water to inundate low-lying land. Therefore, the inundation modelling does not include wave runup. Exposed areas beyond the regions simulated to be inundated by storm-tide may still be at risk of temporary wetting from wave runup, and minor inundation could occur if wave runup overtopped dunes or sea walls. Estimates of wave runup at specific locations are, however, given in Appendix B.

As stated previously, the model grids are based on LIDAR data but our model grid scale reaches 20 m resolution. Smaller waterways are not resolved at this model scale, so it is possible that storm-tides may cause water to travel inland along unresolved waterways. Stop banks and sea walls in the Hutt Valley have been resolved in the model. We note that although storm surge overtopping these structures is considered, wave overtopping is not modelled but may also occur. It is also important to note that river flows are not included in the modelling. This is particularly important where storms coincide with high rainfall, increasing river flows. This could be incorporated in future modelling.

Simulations with sea level rise increments are modelled using the current coastal topography. This does not take into account coastal changes in response to the sea level rise (e.g. erosion, deposition and changes to the beach orientation) which could also affect the inundation hazard.

2.6   Inundation mapping including wave setup

The RICOM modelling incorporates inundation due to storm-tide for all the land areas included in the local grids. The wave setup was included in the inundation maps as follows:

1.   For each of the 8 storm events, the storm-surge model RiCOM was used to simulate inundation of low-lying coastal land due to storm-tide only. The maximum inundation levels during the simulation were saved.

2.   For each of the 8 storm events, the wave model SWAN was used to simulate waves near the coast. Wave setup at the coast was calculated using a 1–dimensional wave-transformation model.

3.   An approximation was made that wave setup increases from zero at the depth that waves break (80% of the wave height) to the full value at the maximum inundation extent where depth is zero.

4.   To identify extra land that may be inundated by the additional wave setup we used a "bath-tub" approach flooding all areas below the combined storm-tide and wave setup water level.

5.   A "de-puddling" algorithm was run to ensure that only areas with a direct flowpath to the sea would be shown as inundated.

2.7   Future relative sea-level rise

In agreement with the Greater Wellington Regional Council, Wellington City Council and Kapiti Coast District Council, we reran the selected present day inundation scenarios for each grid (17 August 1990 for Wellington Harbour and surrounds and 6 September 1994 for Kapiti Coast) with three different increments in sea-level to quantify the effects of relative sea-level rise on inundation. As discussed in Appendix E, direct changes in storm-tide level due to climate-induced changes in storm intensity are projected to be small compared to sea-level rise and are thus not included in these simulations.

The average rise in relative sea-level for the Wellington region over the last 100 years has been 2.05 ± 0.15 mm yr^{-1} according to a recent report by Bell and Hannah (2012). This is an increase from earlier assessments of 1.73 mm yr^{-1} up to 1988 and 1.78 mm yr^{-1} up to 2001 (Hannah 1990, 2004). Much of this apparent recent acceleration, however, is due to slow slip tectonic events in the Wellington region that have been occurring since possibly 1997. These slow slip events have caused an average land subsidence of 1.7 mm yr^{-1} in Wellington City over the last 10 years (which is commensurate with the rate of absolute rise in ocean levels over the past 100 years). Although this subsidence is not climate-induced, it increases the relative sea-level rise and therefore will exacerbate the inundation hazard posed by storm-tide to the Wellington region, particularly if it persists. Climate-induced (absolute) sea-level rise for the region is projected to reach around 1 m by 2115 (Bell and Hannah 2012), covering the "at least 100 year" period from the present required by the New Zealand Coastal Policy Statement, without including an allowance for ongoing subsidence

Based on the report by Bell and Hannah (2012) and in consultation with the client three constant increments in sea-level rise of +0.5 m, +1.0 m and +1.5 m were modelled to cover a range of future magnitudes in relative sea-level rise. Note that in this report there is no time frame associated with these increases. This report merely shows the increase in storm-tide and wave setup inundation hazard that would occur given any of the three increments in relative sea-level rise.

The storm events producing the highest coastal water levels were 17 August 1990 for Wellington Harbour, and 6 September 1994 for the Kapiti Coast. The sea-level rise increments were added to the net water level offsets in Table 2-3.

3 Results

3.1 Inundation levels along the Greater Wellington coastline

Figure 3-1 shows the storm-tide levels above WVD-53 for the entire coast of the Greater Wellington Region for the 4 adjusted events in each coastal sub-region (Table 2-3) representing a 1% joint AEP likelihood, While not strictly comparable, the horizontal lines mark the 1% AEP storm-tide only level at the Port of Wellington (lower line) and Kapiti Island sea-level gauges respectively, to provide a context for the storm-tide component of the combined storm-tide and wave inundation scenarios modelled. The storm-tide levels plotted in Figure 3-1 are listed in Table 3-1. The highest simulated storm-tide level in the Wellington Harbour was for an adjusted 17 August 1990 event at approximately 1.35 m (WVD-53), which closely matches the 1% AEP storm-tide only line on Figure 3-1 from Port of Wellington gauge analysis, given there is minimal wave set-up inside the Harbour. In Porirua Harbour, the highest storm-tide for the adjusted 6 September 1994 event was 1.6–1.7 m above WVD-53, which is somewhat higher than the 1% storm-tide only AEP level from an analysis of Kapiti Island sea level measurements – although it is expected that offshore storm-tide levels may be slightly lower than inshore.

Figure 3-2 shows the simulated wave setup height for the entire coast of the Greater Wellington Region, for the 4 adjusted events in each coastal sub-region (Table 2-3) representing a 1% joint AEP likelihood. Wave setup depends on the depth of water near the coast, which controls wave breaking and energy dissipation and also the nearshore seabed slope. This meant that relatively small waves sometimes resulted in relatively large wave setup when coinciding with a high storm tide. For example, the 17 August 1990 event, selected as a representative event for the south and east coasts, comprised a high inundation water level which included a significant wave setup contribution along these coasts, even though the significant wave heights were relatively small offshore (Figure 2-5, Table 2-3). The nearshore depth and sea-bed slope factors explain why there is more local variability in wave setup around the coast than for the smoothly varying changes in storm-tide levels shown in Figure 3-1.Wave setup was small inside Porirua and Wellington Harbours, as expected due to the short wind fetches. The wave setup heights plotted in Figure 3-2 are listed in Table 3-2.

Figure 3-3 shows the total sea-level at the shoreline simulated from the sum of storm tide and wave setup for the entire coast of the Greater Wellington Region, for the representative 17 Aug 1990 event selected for the south and east coasts, and the representative 6 September 1994 event selected for the Kapiti coast. For comparison, the same horizontal lines used in Figure 3-1 mark the 1% AEP storm-tide only levels at the Port of Wellington and Kapiti Island sea-level gauges respectively. The combined effect of wave setup and storm-tide elevates the simulated sea-levels well above local 1% AEP storm-tide only levels at all wave-exposed locations. When wave setup was also included the 6 September 1994 event was still one of the largest simulated events on the Kapiti coast and was the largest event in Porirua Harbour where wave setup effects are negligible. The total sea-level, including wave setup, for the modelled scenario increased in a northerly direction from 1.5 m up to 2.4 m above WVD-53 along the Kapiti coast. For Wellington and the southern coast, the representative 17 August 1990 simulation produced total shoreline sea-levels including wave setup ranging from values around 1.5 m above WVD−53 in Wellington Harbour up to around 2.4 to 2.5 m above WVD-53 on the southern coast and the Wairarapa coast. The total shoreline water levels plotted in Figure 3-3 are listed in Table 3-3.
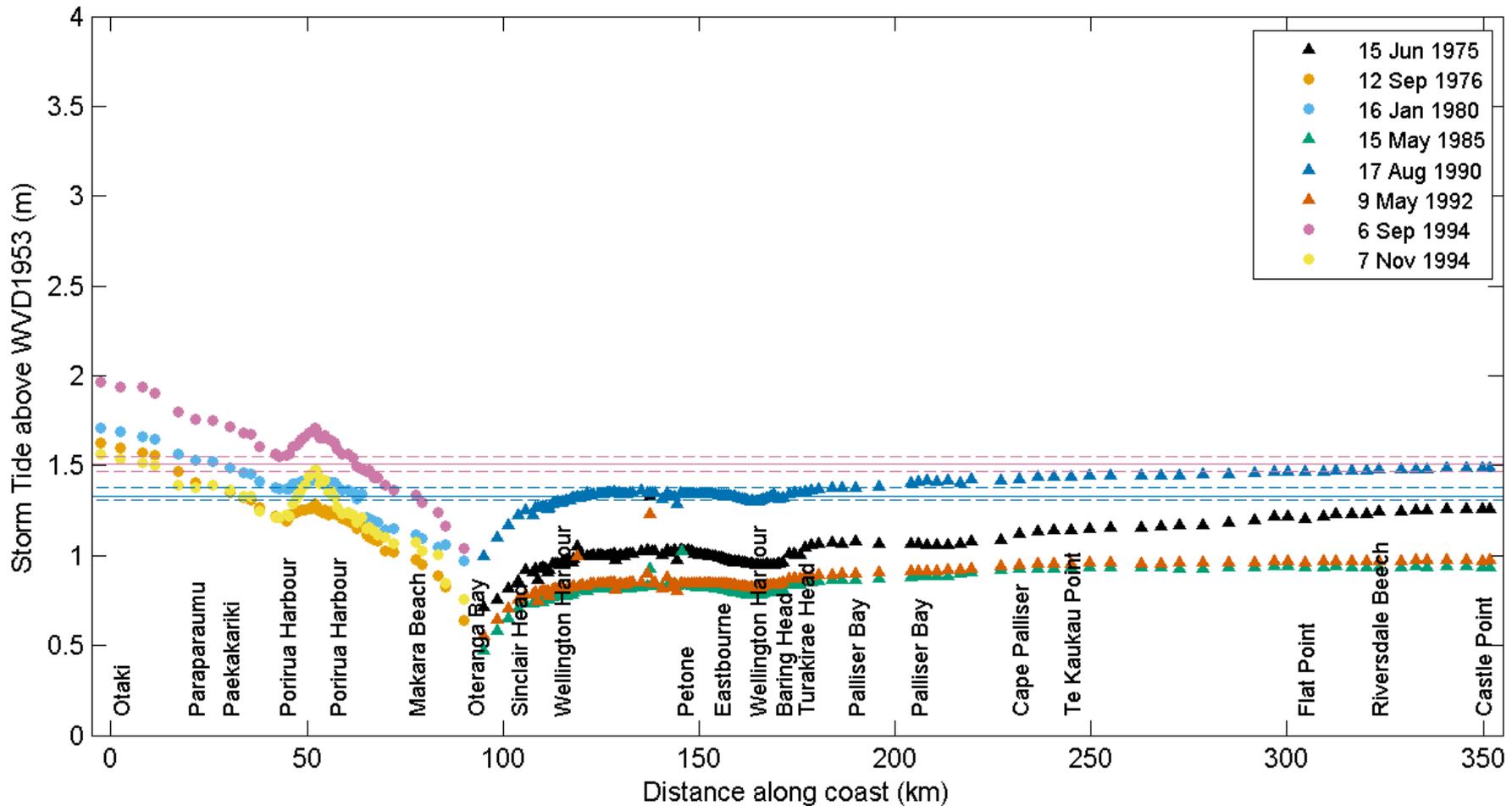
Figure 3-1: Storm-tide levels along Greater Wellington Region coastline for the selected 1% joint AEP storm scenarios. Distances are measured along the coastline from Otaki (left) to Castle Point (right). Various locations along the coast are labelled. The two labels for Porirua Harbour and Wellington Harbour and Palliser Bay mark the opposite sides of harbour entrances or embayment. Triangles are for the representative 17 Aug 1990 event selected for the south and east coasts, and circles are for the representative 6 September 1994 event selected for the Kapiti Coast. Horizontal magenta lines mark 1% AEP (100-year ARI) storm tide level at Kapiti Island (with dashed 95% confidence intervals) and the lower light-blue horizontal lines mark 1% AEP (100-year ARI) storm tide level Port of Wellington (with dashed 95% confidence intervals).
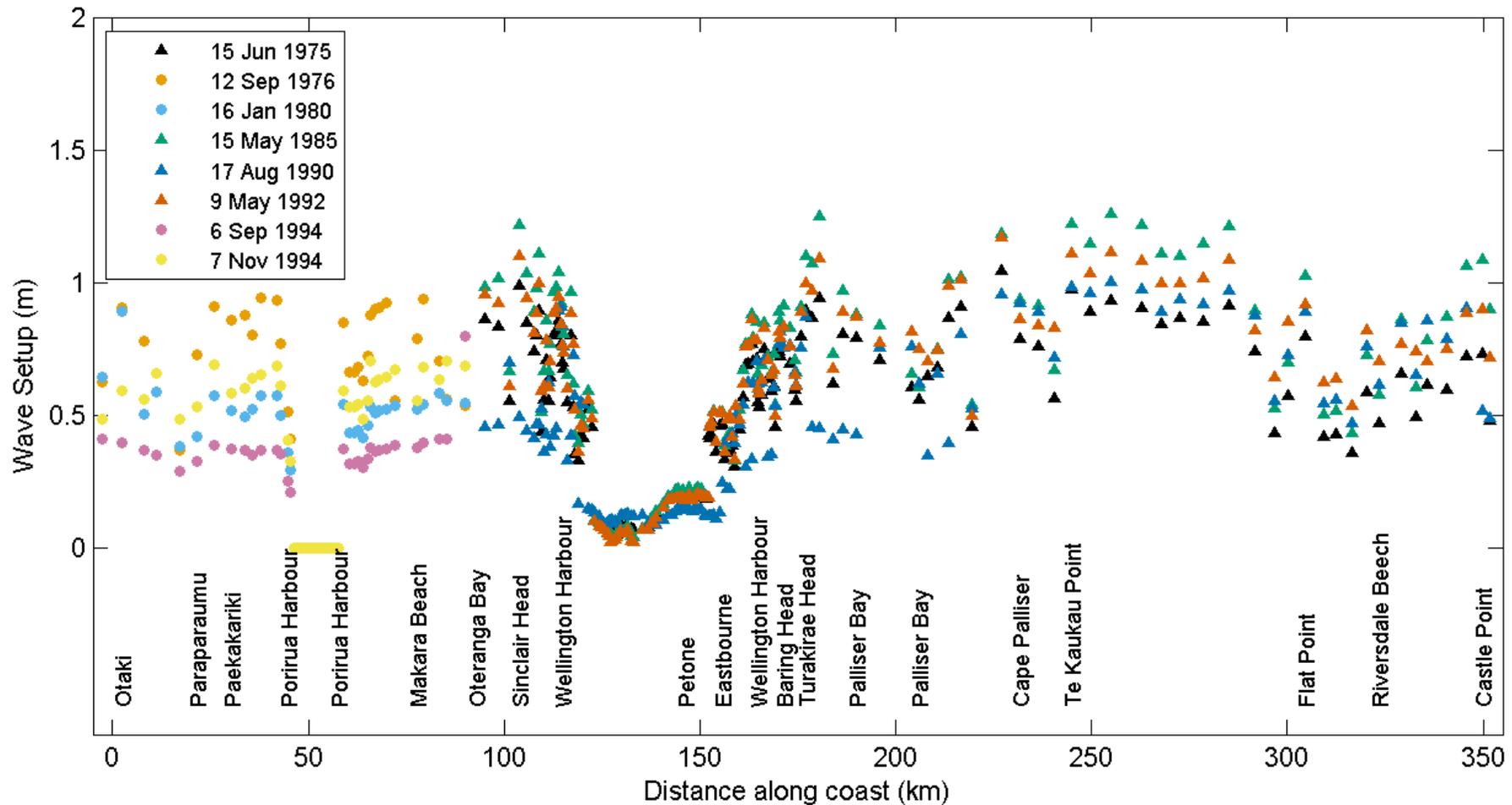
Figure 3-2: Wave setup heights along Greater Wellington Region coastline for the selected 1% joint AEP storm scenarios. Distances are measured along the coastline from Otaki (left) to Castle Point (right). Various locations along the coast are labelled. The two labels for Porirua Harbour, Wellington Harbour and Palliser Bay mark opposite sides of the harbour entrances or embayment. Triangles are for the representative 17 Aug 1990 event selected for the south and east coasts, and circles are for the representative 6 September 1994 event selected for the Kapiti coast.
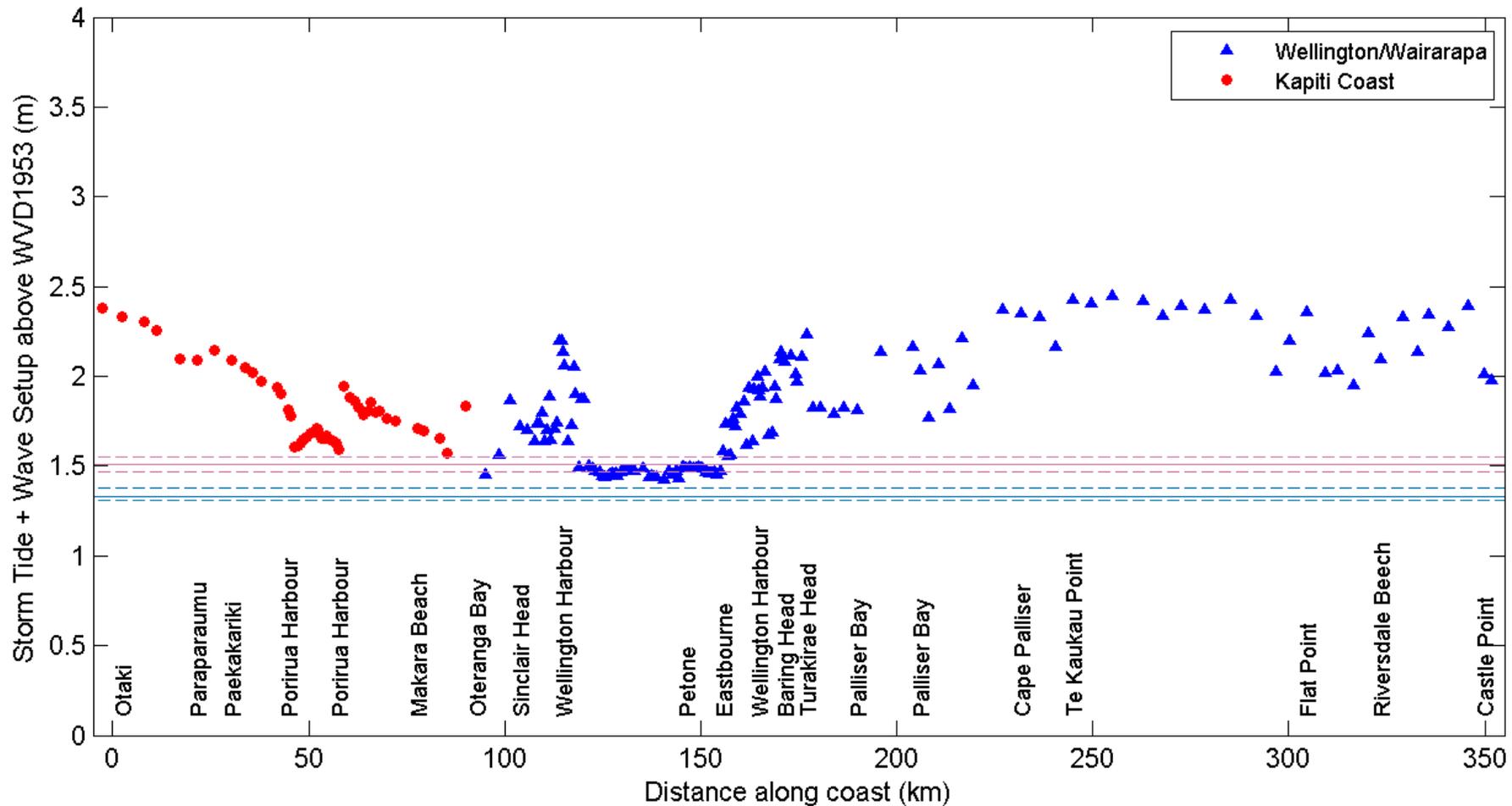
Figure 3-3: Storm-tide including wave setup levels along Greater Wellington Region coastline for the selected 1% joint AEP storm scenarios. Distances are measured along the coastline from Otaki (left) to Castle Point (right). Various locations along the coast are labelled. The two labels for Porirua Harbour, Wellington Harbour and Palliser Bay mark opposite sides of the harbour entrances or embayment. Triangles are for the representative 17 Aug 1990 event selected for the south and east coasts, and circles are for the representative 6 September 1994 event selected for the Kapiti coast. Horizontal magenta lines (same as in Figure 3-1) mark 1% AEP storm-tide only level at Kapiti Island (with dashed 95% confidence intervals) and the lower light-blue horizontal lines mark 1% AEP storm-tide only level Port of Wellington (with dashed 95% confidence intervals).

Table 3-1: **Simulated storm-tide levels for the four 1% joint AEP events along each sub-region of the coastline (m WVD-53).** Values correspond to Figure 3-1.

Location	Longitude	Latitude	15-Jun-75	12-Sep-76	16-Jan-80	15-May-85	17-Aug-90	9-May-92	6-Sep-94	7-Nov-94
Otaki North	175.11	-40.73		1.63	1.71				1.96	1.56
Waikanae Beach	175.04	-40.85		1.56	1.64				1.90	1.50
Paraparaumu Beach	174.98	-40.88		1.47	1.57				1.80	1.39
Raumati Beach	174.97	-40.92		1.41	1.53				1.76	1.38
Paekakariki	174.94	-41.00		1.35	1.49				1.72	1.36
Pukerua Bay	174.90	-41.03		1.31	1.45				1.67	1.33
Porirua Harbour Entrance	174.85	-41.09		1.23	1.38				1.59	1.27
Porirua City	174.84	-41.13		1.26	1.42				1.70	1.47
Titahi Bay	174.83	-41.11		1.19	1.36				1.56	1.24
Makara Beach	174.71	-41.22		0.98	1.12				1.33	1.07
Oteranga Bay	174.63	-41.32	0.71			0.47	1.00	0.56		
Owhiro Bay	174.77	-41.35	0.87			0.75	1.27	0.75		
Island Bay	174.77	-41.34	0.93			0.75	1.27	0.80		
Lyall Bay	174.80	-41.34	0.96			0.77	1.29	0.81		
Breaker Bay	174.84	-41.33	0.97			0.79	1.31	0.83		
Evans Bay	174.80	-41.30	1.00			0.82	1.35	0.84		
Oriental Bay	174.79	-41.29	1.01			0.82	1.35	0.86		
Wellington Motorway	174.83	-41.24	1.03			0.83	1.35	0.88		
Petone	174.88	-41.23	1.03			0.84	1.35	0.85		
Hutt River	174.90	-41.24	1.01			0.83	1.34	0.85		
Lowry Bay	174.91	-41.26	1.00			0.82	1.34	0.84		
Eastbourne	174.87	-41.32	0.97			0.80	1.33	0.84		
Baring Head	174.87	-41.41	0.96			0.81	1.32	0.85		
Palliser Bay	175.12	-41.39	1.07			0.87	1.38	0.91		
Cape Palliser	175.29	-41.60	1.12			0.93	1.43	0.95		
Glendhu	175.74	-41.39	1.17			0.93	1.45	0.96		
Riversdale Beach	176.07	-41.10	1.24			0.94	1.48	0.97		
Castlepoint	176.23	-40.90	1.26			0.94	1.49	0.97		

Table 3-2: Simulated wave setup heights (m) for the four 1% joint AEP events along each sub-region of the coastline.   Values correspond to Figure 3-2.

Location	Longitude	Latitude	15-Jun-75	12-Sep-76	16-Jan-80	15-May-85	17-Aug-90	9-May-92	6-Sep-94	7-Nov-94
Otaki North	175.11	-40.73		0.63	0.65				0.41	0.49
Waikanae Beach	175.04	-40.85		1.03	0.59				0.35	0.66
Paraparaumu Beach	174.98	-40.88		0.37	0.39				0.29	0.49
Raumati Beach	174.97	-40.92		0.73	0.42				0.33	0.53
Paekakariki	174.94	-41.00		0.86	0.52				0.37	0.59
Pukerua Bay	174.90	-41.03		0.80	0.53				0.35	0.64
Porirua Harbour Entrance	174.85	-41.09		0.00	0.00				0.00	0.00
Porirua City	174.84	-41.13		0.00	0.00				0.00	0.00
Titahi Bay	174.83	-41.11		0.66	0.43				0.32	0.53
Makara Beach	174.71	-41.22		0.79	0.52				0.38	0.55
Oteranga Bay	174.63	-41.32	0.86			0.99	0.46	0.96		
Owhiro Bay	174.77	-41.35	0.90			1.11	0.47	1.00		
Island Bay	174.77	-41.34	0.44			0.52	0.53	0.59		
Lyall Bay	174.80	-41.34	0.80			0.97	0.42	0.89		
Breaker Bay	174.84	-41.33	0.80			0.97	0.43	0.89		
Evans Bay	174.80	-41.30	0.07			0.08	0.12	0.07		
Oriental Bay	174.79	-41.29	0.08			0.05	0.12	0.03		
Wellington Motorway	174.83	-41.24	0.19			0.20	0.13	0.19		
Petone	174.88	-41.23	0.18			0.20	0.14	0.18		
Hutt River	174.90	-41.24	0.20			0.22	0.15	0.20		
Lowry Bay	174.91	-41.26	0.19			0.20	0.13	0.20		
Eastbourne	174.87	-41.32	0.50			0.54	0.50	0.54		
Baring Head	174.87	-41.41	0.76			0.92	0.76	0.84		
Palliser Bay	175.12	-41.39	0.71			0.84	0.76	0.77		
Cape Palliser	175.29	-41.60	0.79			0.94	0.92	0.86		
Glendhu	175.74	-41.39	0.85			1.15	0.92	1.02		
Riversdale Beach	176.07	-41.10	0.47			0.58	0.62	0.70		
Castlepoint	176.23	-40.90	0.73			1.09	0.52	0.90		

Table 3-3: **Simulated storm tide + wave setup (m WVD-53) for the representative 1% joint AEP events along the region's coastline.** Values correspond to Figure 3-3.

Location	Longitude	Latitude	17-Aug-90	6-Sep-94
Otaki North	175.11	-40.73		2.38
Waikanae Beach	175.04	-40.85		2.26
Paraparaumu Beach	174.98	-40.88		2.09
Raumati Beach	174.97	-40.92		2.09
Paekakariki	174.94	-41.00		2.09
Pukerua Bay	174.90	-41.03		2.02
Porirua Harbour Entrance	174.85	-41.09		1.59
Porirua City	174.84	-41.13		1.70
Titahi Bay	174.83	-41.11		1.88
Makara Beach	174.71	-41.22		1.71
Oteranga Bay	174.63	-41.32	1.45	
Owhiro Bay	174.77	-41.35	1.74	
Island Bay	174.77	-41.34	1.80	
Lyall Bay	174.80	-41.34	1.71	
Breaker Bay	174.84	-41.33	1.73	
Evans Bay	174.80	-41.30	1.47	
Oriental Bay	174.79	-41.29	1.47	
Wellington Motorway	174.83	-41.24	1.48	
Petone	174.88	-41.23	1.49	
Hutt River	174.90	-41.24	1.49	
Lowry Bay	174.91	-41.26	1.47	
Eastbourne	174.87	-41.32	1.83	
Baring Head	174.87	-41.41	2.08	
Palliser Bay	175.12	-41.39	2.14	
Cape Palliser	175.29	-41.60	2.35	
Glendhu	175.74	-41.39	2.37	
Riversdale Beach	176.07	-41.10	2.10	
Castle Point	176.23	-40.90	2.01	

3.2   Inundation maps

3.2.1   Present-day total inundation (storm-tide plus wave setup)

Inundation maps for joint 1% storm-tide and wave AEP events are shown only for the representative storm scenarios. These scenarios comprise an adjusted 17 August 1990 event for Wellington Harbour (Wellington City and Lower Hutt) and an adjusted 6 September 1994 event for the Kapiti Coast. Both these events generally had smaller offshore significant wave heights than some of the other simulated storm events, but had a large storm-tide component, which in some areas also exacerbated the wave setup heights at the coastline (Table 2-3, Figure 2-5, Figure 2-6, Table 3-2). Wave runup is not included in the inundation modelling, but wave setup generated inside the breaker zone is included in the inundation maps as described in Section 2.6.

The maps in this section of the report show the maximum depth of inundation (in metres) over the land, sea-bed or river-bed for the representative 1% joint AEP event. Total inundation water levels relative to WVD-53 for the same mapped areas can be found in Appendix H.

### Wellington Harbour present day inundation maps

Essentially no inundation was observed for the present-day 17 August 1990 simulation (with MLOS adjusted to have an offshore storm-tide and wave height joint annual exceedance probability of 1%, Figure 3-4). Simulated water levels in the harbour reached ~1.35 m above WVD-53. This is higher than highest astronomical tide (which is 0.985m above WVD-53), but not sufficiently high to cause significant inundation; 1.35 m storm-tides are rare, having a 1% annual probability of occurrence at Queen's Wharf (Stephens et al. 2009). Further details of the Hutt Valley are shown in Figure 3-5. Water is confined to the Hutt River and tributary streams. There is a slight mismatch between the plotted and actual coastline in the Seaview Marina which gives the appearance of inundation, however water is confined to the marina. Water levels relative to WVD-53 can be found in Appendix H. Figure H-1 shows the harbour area and the Petone/Seaview area is shown in more detail in Figure H-5.

Kapiti Coast present day inundation maps

The simulated depth of total inundation for the Otaki area, based on an adjusted 6 September 1994 event, is shown in Figure 3-6. Water levels relative to WVD-53 are shown in the Appendix H (Figure H-17). Simulated inundation occurs in the Otaki River lagoon and near the mouth of the Waitohu stream. Inundation extends north from the Otaki River into low-lying areas between Rangiuru Road and Tasman Road. There is a low lying area between the northern end of the Otaki Beach Township and the Waitohu Stream which has elevations lower than the sea level at the coast. These regions are shown as white areas in Figure 3-6. While not shown as inundated in the modelling, this may be due to streams connecting these areas not being resolved within the 20 m resolution grid.

Total inundation maps for the area around Waikanae show inundation of land near the lower reaches of the Waikanae River, coming close to roads around Otaihanga (Figure 3-7). Highest astronomical tide at the Waikanae coast (relative to the present day MLOS of 0.195m) is 1.28 m above WVD-53. Total inundation water levels at the coast (shown in

Figure H-21) of 1.90-1.95 m exceed this level and inland total inundations levels exceed 2.3 m in places.
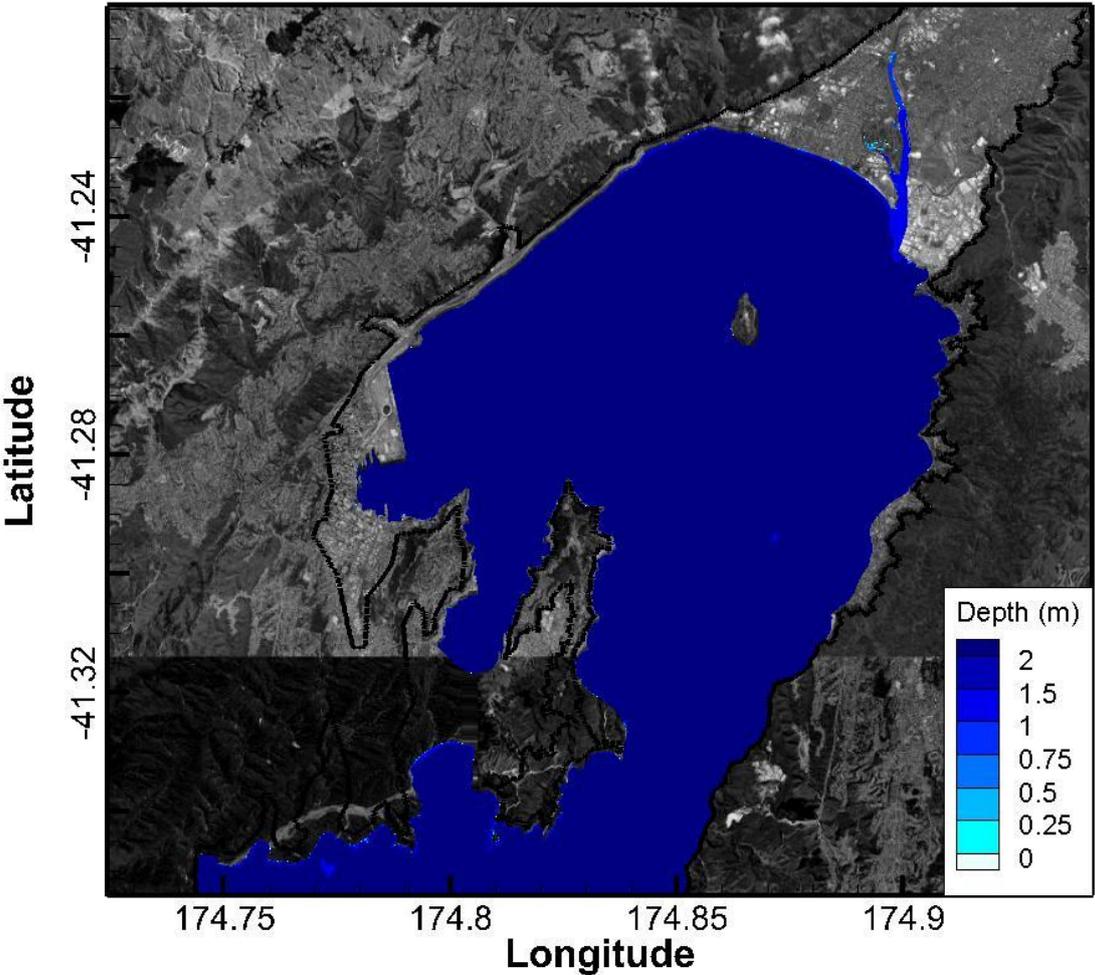
Figure 3-4: Total inundation map for the 17 August 1990 event adjusted to present day sea level and 1% joint Annual Exceedance Probability (AEP). The colours show water depth overlaid on images from Google Earth (2012). The solid line shows the extent of the model grid.
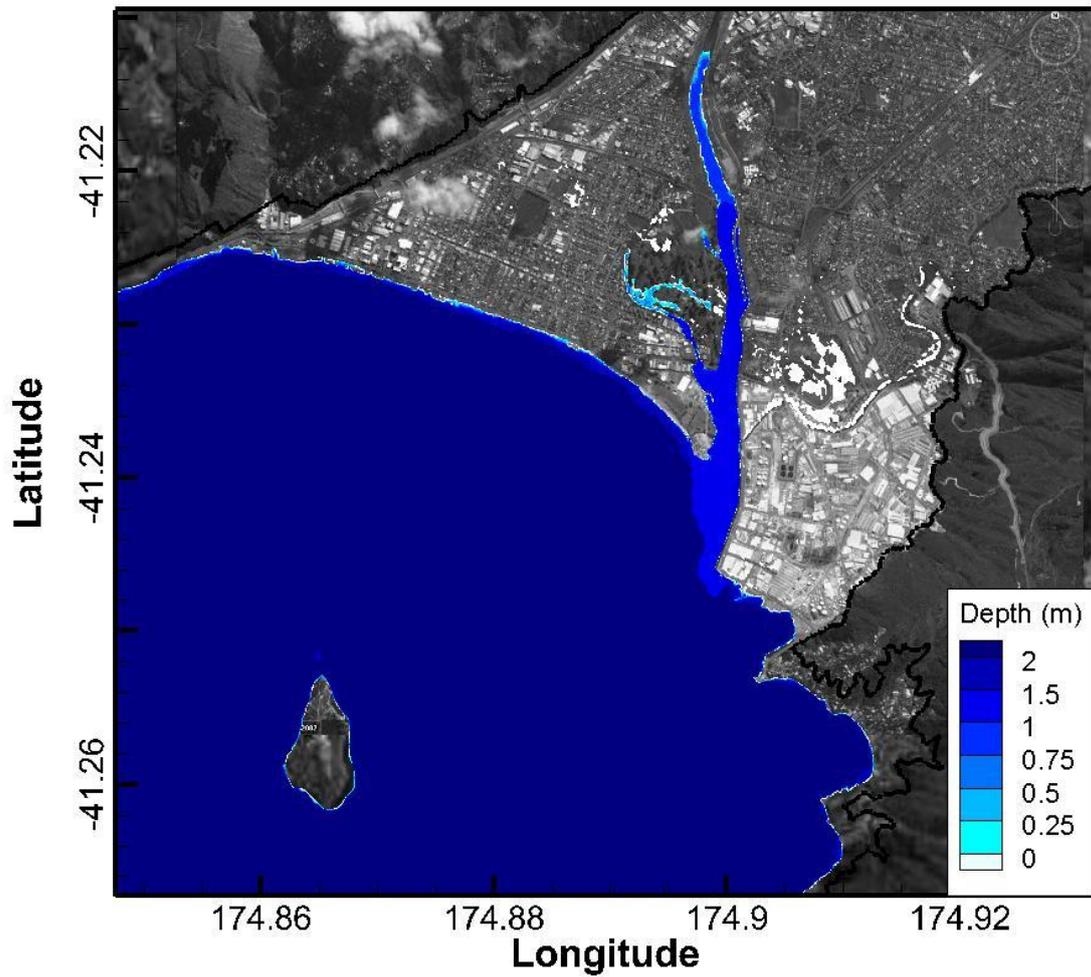
Figure 3-5: Total inundation depths for Seaview and Petone for the 17 August 1990 event adjusted to present day sea level and 1% joint AEP. The colours show water inundation depth overlaid on images from Google Earth (2012). The black line shows the edge of the model domain.
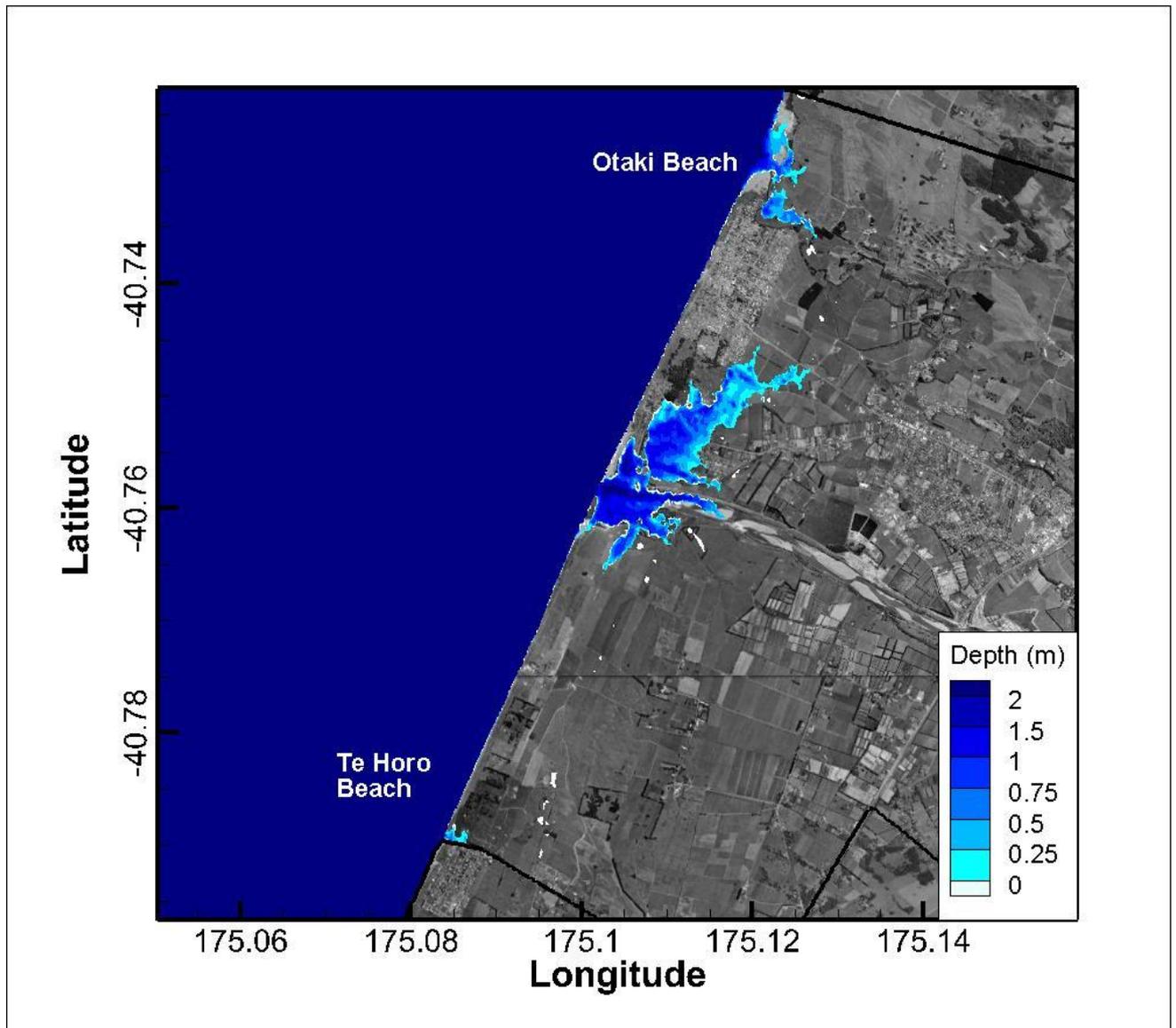
Figure 3-6: Total inundation map for the area near Otaki for the September 1994 event adjusted to present day sea level and 1% joint AEP. The colours show the maximum water depth over-laid on images from Google Earth (2012). The solid black line shows the extent of the land inundation grid. White regions show where land elevations are lower than sea level at the coast but not inundated in the model.
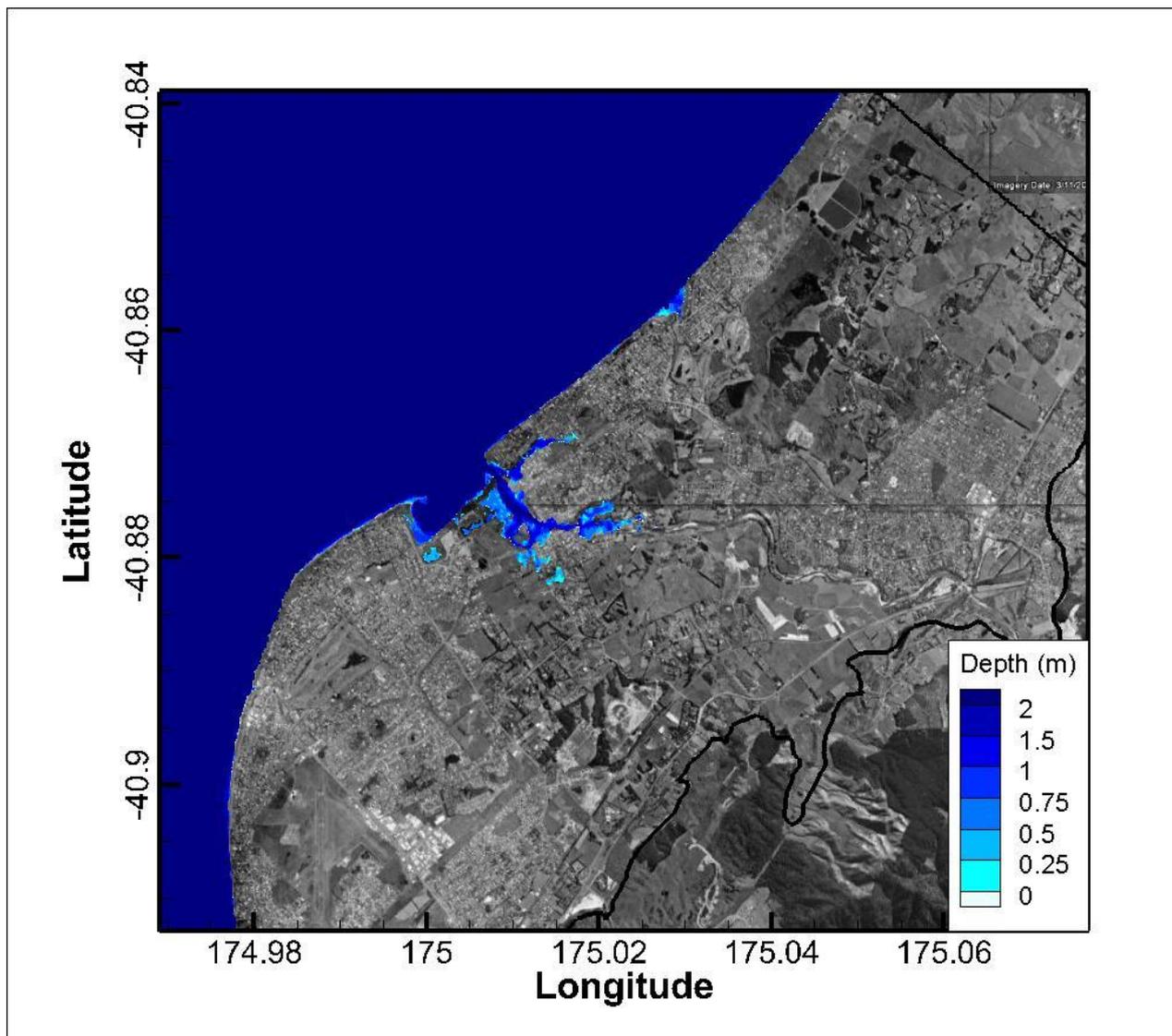
Figure 3-7: Total inundation map for Waikanae for the September 1994 event adjusted to present day sea level and 1% joint AEP. The colours show maximum depth overlaid on images from Google Earth. The solid black line shows the extents of the land inundation grid. White regions show where land elevations are lower than the sea level at the coast but are not inundated in the model.

While total inundation level in the Porirua Harbour extends beyond the formed coastline (Figure 3-8), there does not appear to be significant flooding of land with most of the inundated area being wetlands. Water levels (plotted in Figure H-25) exceed 1.7 m in the entire harbour and are almost 2 m above WVD-53 in the upper reaches. This is considerably higher than highest astronomical tide of 0.95m (relative to WVD-53).

3.2.2 Future Scenarios

Climate change and storm intensity

The most well-known effect of climate change is sea-level rise. However, climate change could also influence storm intensity and storm tracks. This would in turn affect storm-tides and waves. An analysis of climate change induced effects on storm intensity is presented in

Appendix E. In summary, the expected change in storm surge heights is small for the Wellington region by the end of this century, although an increase of around 6% at the 99th percentile exceedance level is expected for the Kapiti region. The latter is equivalent to around 3 cm of additional storm surge height, which is small compared to projected sea-level rises (MfE 2008; Bell and Hannah 2012). Due to the small increase in storm surge relative to sea-level rise, and because we are not forecasting storm-tides at particular future dates, rather at increments of sea-level increase, we have not included the 3 cm additional storm-surge component in our analyses.
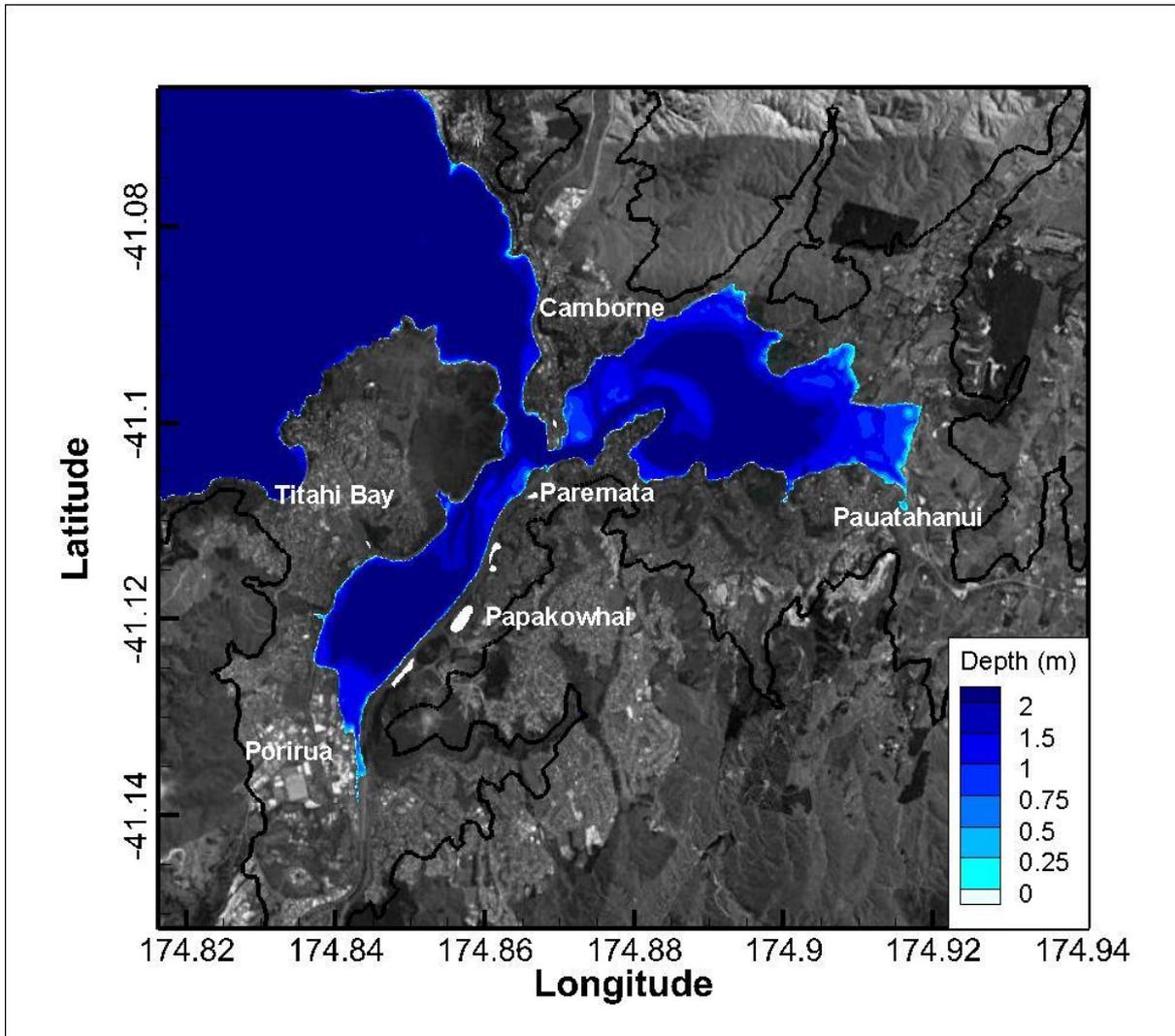
Figure 3-8: Total inundation map for Porirua Harbour for the 9 September 1994 event adjusted to present day sea level and 1% joint AEP. The colours show the maximum water depth overlaid on images from Google Earth. White regions are areas with elevations lower than the sea level at the coast.

Simulations of total storm inundation for sea-level rise increments of 0.5 m, 1.0 m and 1.5 m are based on the same representative 1% joint AEP storm events used for the present-day inundation mapping in the previous section. These are the adjusted 17 August 1990 event for the Wellington Harbour Grid and the adjusted 6 September 1994 event for the Kapiti Coast Grid. The simulations were run as described previously but with the additional sea-level rise increment added to the net water level offset (Table 2-3)..

Coastal water levels

The effects of sea-level rise on predicted storm-tide only levels around the Greater Wellington Region coast are shown in Figure 3-9 for the representative inundation scenarios in each coastal sub-region (hence break in curves north of Oteranga Bay). The representative storm-tide scenarios for the Harbour Grid (adjusted 17 August 1990 event) and Kapiti Grid (adjusted 6 September 1994 event) are shown with 0.5 m, 1.0 m, and 1.5 m sea-level rise increments. With a 1.5 m sea-level rise, total inundation water levels would reach around 3 m above WVD-53 in Wellington Harbour and eastward from the Harbour to Castlepoint. At Otaki, storm-tide levels would reach around 3.4 m above WVD-53.

The same data but with wave setup added to yield total storm inundation levels are plotted in Figure 3-10. Wave setup increases water levels at the coast, particularly along the exposed southern and eastern coastlines, up to total inundation levels of 3.9 m above WVD-53 around Otaki and the Wairarapa coast.

Inundation with sea-level rise – Wellington Harbour

Figure 3-11 to Figure 3-13 give overviews of maximum storm inundation levels based on the 17 August 1990 scenario with sea-level rise increments of 0.5 m, 1.0 m and 1.5 m. Note that these mapped areas of inundation depth will only apply for 1-3 hours straddling high tide associated with a 1% joint AEP event in combination with the applied sea-level rise increment. More detailed maps of particular areas are given in Figure 3-14 to Figure 3-22. The modelling suggests that as sea levels incrementally rise in 0.5 m steps, areas most at risk from inundation during storm events are as follows. Appendix H gives equivalent figures which show total inundation levels relative to WVD-53.

0.5 m rise:

- **Hutt Valley**: (Figure 3-14). Marchbank St and Port Rd in Seaview near the mouth of the Hutt River are inundated. Areas in the vicinity of the Hutt Valley Golf Centre and Raceway have land elevations below the total storm inundation level, as do areas around North Park, Petone. While these were not inundated in the modelling, they may be at risk of flooding through drains and small streams or channels not resolved in the model. The Hutt River flood banks are likely to provide protection to these low lying areas. Total storm inundation levels relative to WVD-53 are shown in Figure H-6.

- **Central Wellington**: (Figure 3-17). Inundation is predicted near where Jervois Quay intersects Victoria Street and also Willis St. Total storm inundation levels relative to WVD-53 are shown in Figure H-14.

- **Evans Bay**: (Figure 3-20).Essentially no inundation is predicted other than to areas currently used to park boats at the Evans Bay Yacht Club. Parts of Rongotai Rd between Troy St and Evans Bay Parade have land elevations below the total storm inundation level at the coast, and may be at risk of flooding if seawater travels up through drains. Total storm inundation levels relative to WVD-53 are shown in Figure H-10.
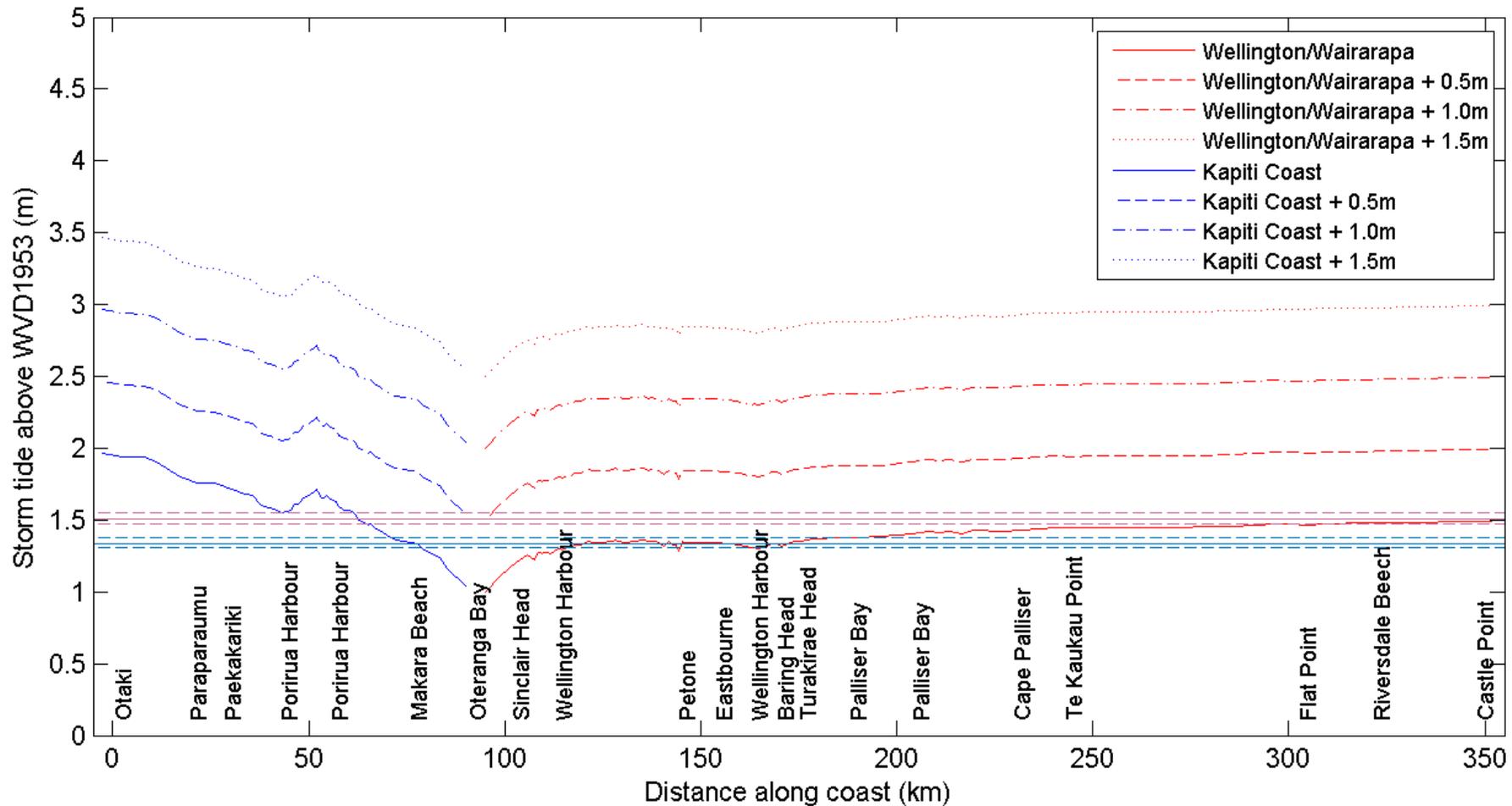
Figure 3-9: Effect of sea-level rise on total inundation water levels along the Greater Wellington Regional coastline. Sea-level rises of 0.5m, 1.0m, and 1.5m have been added to the storm-tide predictions from the worst case scenarios with storm-tide and wave joint probability AEP of 1% for the Wellington Harbour (blue) and Kapiti (red) regions. Distances along the coast are measured from Otaki. Various locations are listed to assist with interpretation. Depths are relative to WVD-53. Present day 1% AEP levels (and 95% confidence levels in dashed lines) for Kapiti Island (red) and Port of Wellington (blue) are also shown for comparison.
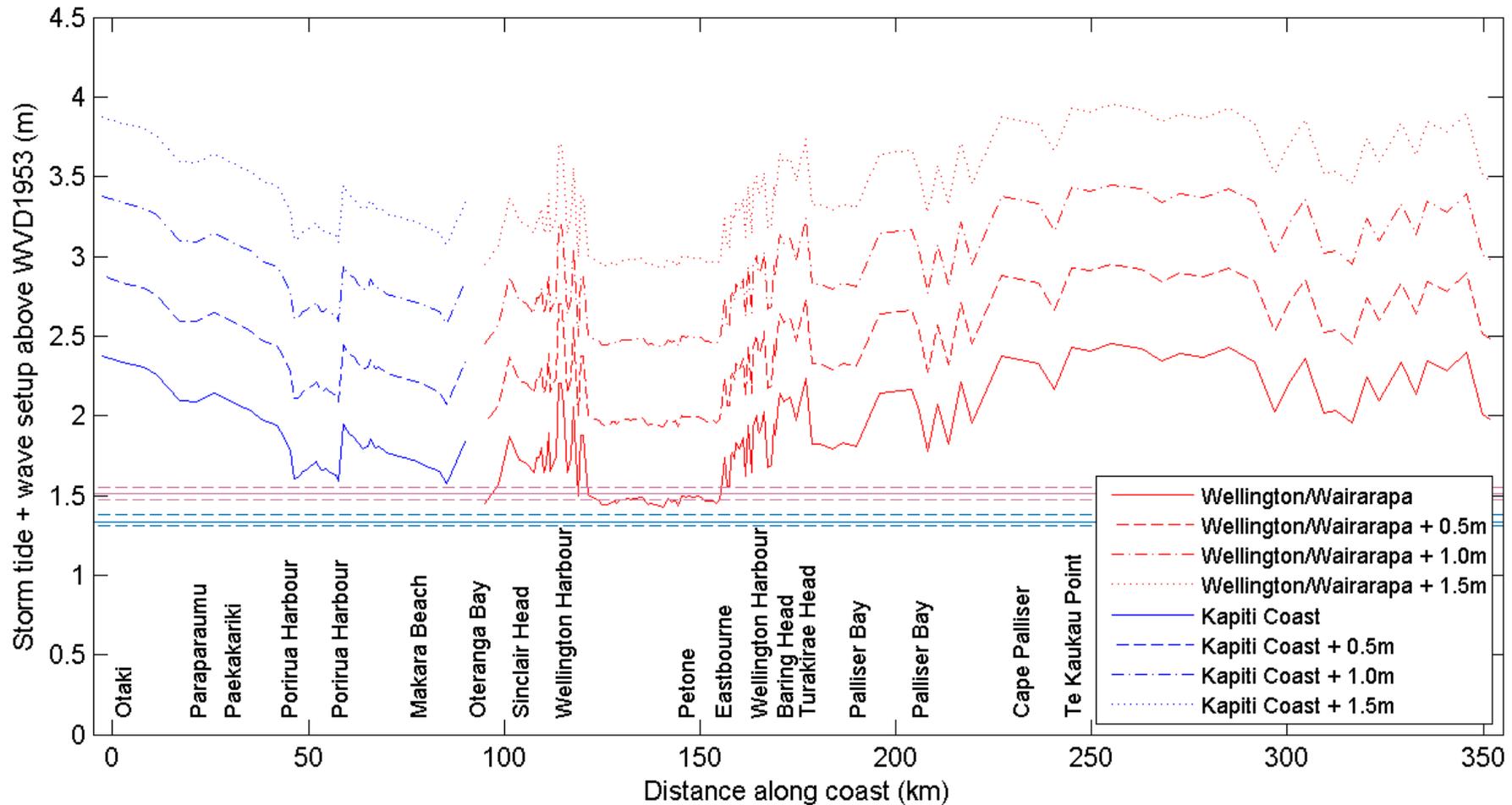
Figure 3-10:Effect of sea-level rise on total inundation water levels with wave setup along the Greater Wellington Regional coastline. Sea-level rises of 0.5m, 1.0m, and 1.5m have been added to the storm-tide predictions from the worst case scenarios with storm-tide and wave joint probability AEP of 1% for the Wellington Harbour (blue) and Kapiti (red) regions. Distances along the coast are measured from Otaki. Various locations are listed to assist with interpretation. Depths are relative to WVD-53.

1.0 m rise:

- **Hutt Valley**: (Figure 3-15).Much of Seaview near the mouth of the Hutt River is inundated. Inundation also occurs in Moera in the vicinity of the Hutt Valley Golf Centre and Raceway. On the western side of the Hutt River, the Shandon Golf Club is inundated, and inundation extends in Petone around the North Park area as far to the west as the Hutt Rd, and to the north as far as Kiwi, Moa and Tui Streets. Total storm inundation levels relative to WVD-53 are shown in Figure H-7.

- **Central Wellington**: (Figure 3-18). Inundation is predicted on Wakefield St, Jervois Quay, Customhouse Quay, reaching as far north as the Wellington Railway Station. Depths of up to 0.6 m are predicted. Total storm inundation levels relative to WVD-53 are shown in Figure H-15.

- **Evans Bay**: (Figure 3-21) Parts of Cobham Drive are predicted to be inundated. It is not clear if Evans Bay Parade is inundated due to the resolution of the model grid, although it appears to be at risk. Much of the land seaward of Evans Bay Parade is inundated. An area along Rongotai Rd is below the total storm inundation level and may be a risk of flooding if seawater is able to enter through drains. Total storm inundation levels relative to WVD-53 are shown in Figure H-11.

1.5 m rise:

- **Hutt Valley**: (Figure 3-16) Large areas of Seaview, Moera, Waiwhetu, Petone and Alicetown are predicted to be inundated. Total storm inundation levels relative to WVD-53 are shown in Figure H-8.

- **Central Wellington**: (Figure 3-19) Large areas of the central city are predicted to be inundated, including the railway station and lines alongside and north of the Westpac Stadium, Waterloo Quay, most of Featherston Street, Jervois Quay, and areas south of Te Papa including Wakefield Street. Total storm inundation levels relative to WVD-53 are shown in Figure H-16.

- **Evans Bay**: (Figure 3-22) A significant part of Kilbirnie is inundated with water depths of typically 0.4-0.6 m. An area of Miramar in the vicinity of the intersections of Ellesmere Ave and Chelsea St has land elevations below the total storm inundation level at the coast and may be at risk of flooding from seawater flowing up drains. Total storm inundation levels relative to WVD-53 are shown in Figure H-12.

- **Miramar Peninsula**: (Figure 3-22) Inundation occurs at Churchill.
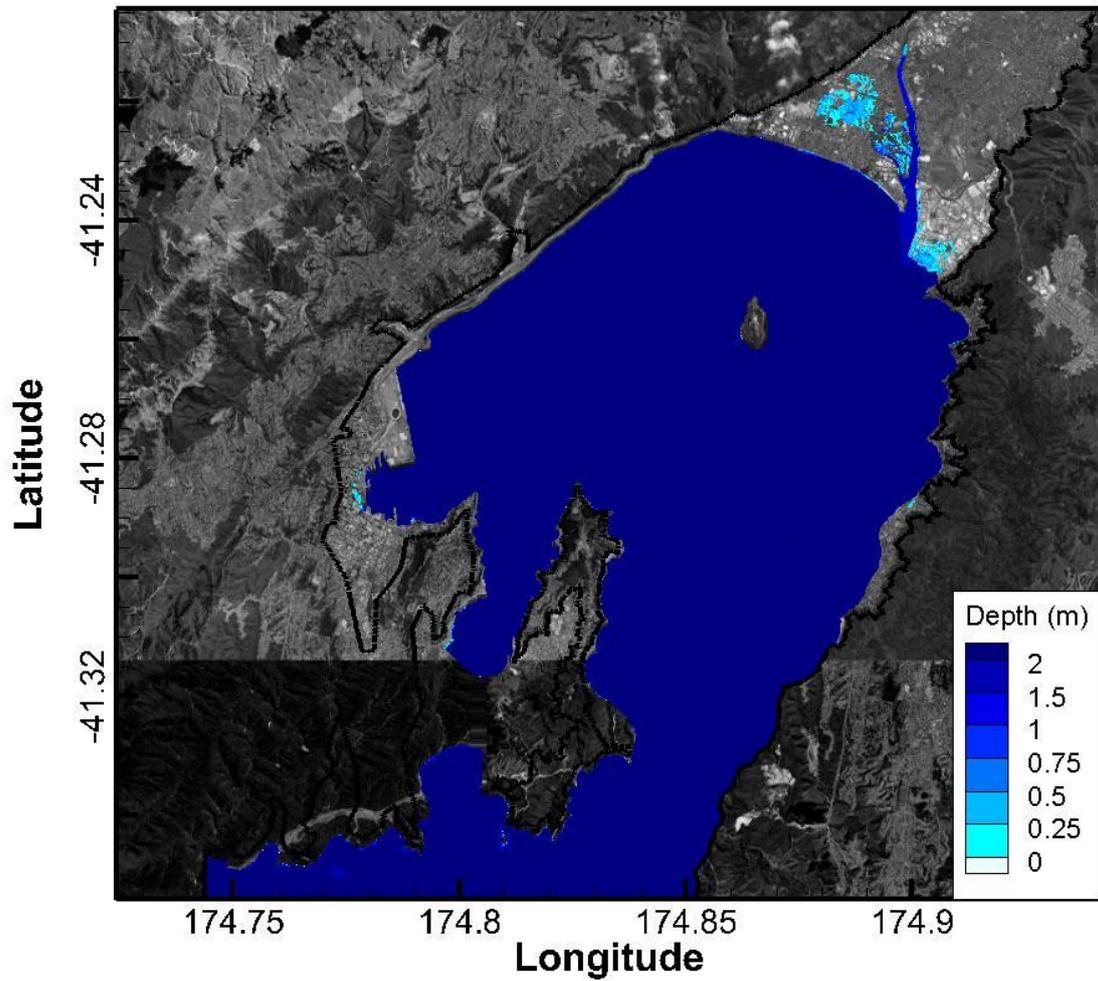
Figure 3-11:Total storm inundation map of Wellington Harbour with 0.5 m sea-level rise.
Simulations are based on the 17 August 1990 event and represent a 1% AEP joint probability wave
and storm-tide producing the largest coastal water depths. Total storm inundation levels relative to
WVD-53 are shown in Figure H-2.
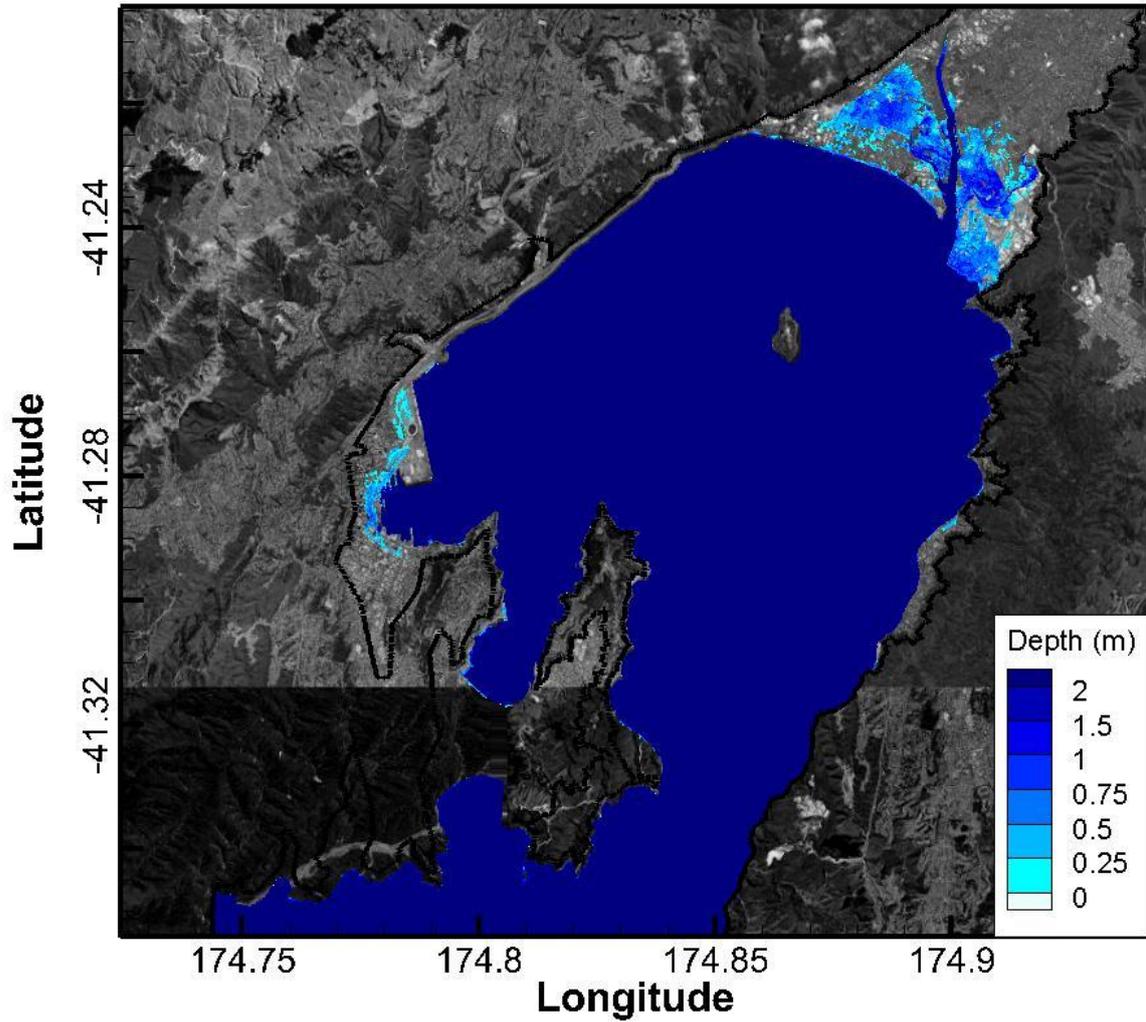
Figure 3-12:Total storm inundation map of Wellington Harbour with 1.0 m sea-level rise.
Simulations are based on the 17 August 1990 event and represent a 1% AEP joint probability wave and storm-tide producing the largest coastal water depths. Total storm inundation levels relative to WVD-53 are shown in Figure H-3.
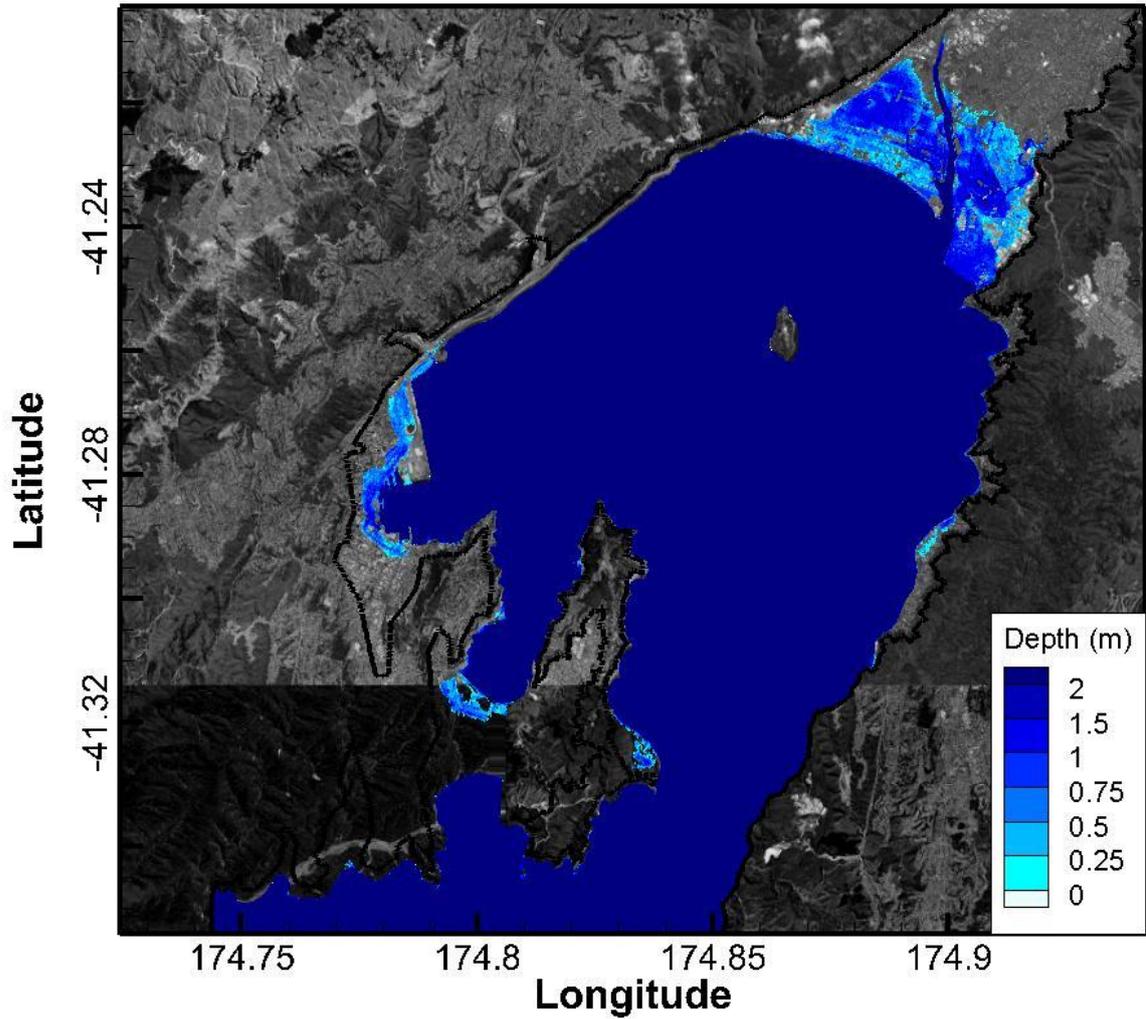
Figure 3-13:Total storm inundation map of Wellington Harbour with 1.5 m sea-level rise.
Simulations are based on the 17 August 1990 event and represent a 1% AEP joint probability wave and storm-tide producing the largest coastal water depths. Total storm inundation levels relative to WVD-53 are shown in Figure H-4.
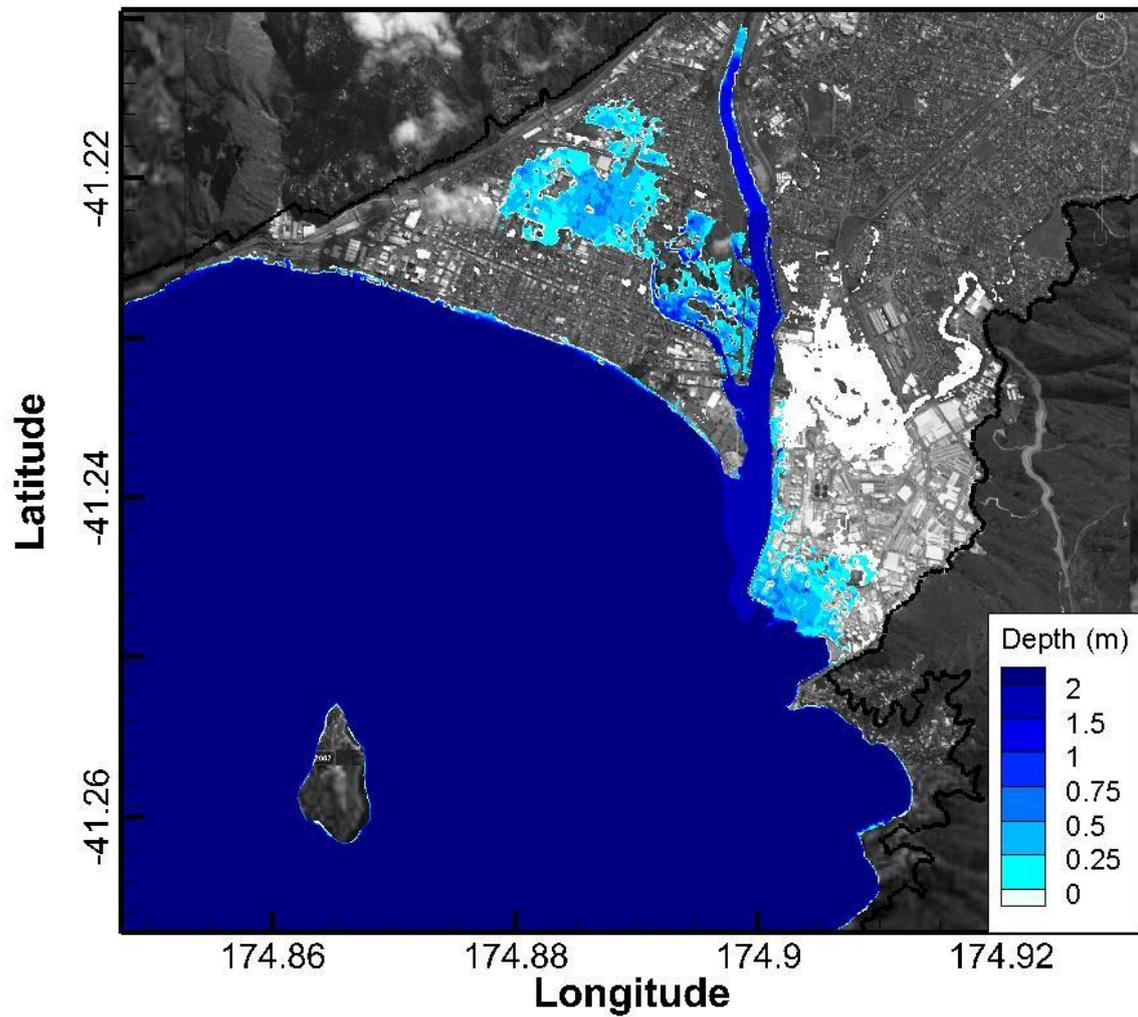
Figure 3-14:Total storm inundation map for Petone and Seaview with 0.5 m sea-level rise.
Simulations are based on the 17 August 1990 event and represent a 1% AEP joint probability wave and storm-tide producing the largest coastal water depths.
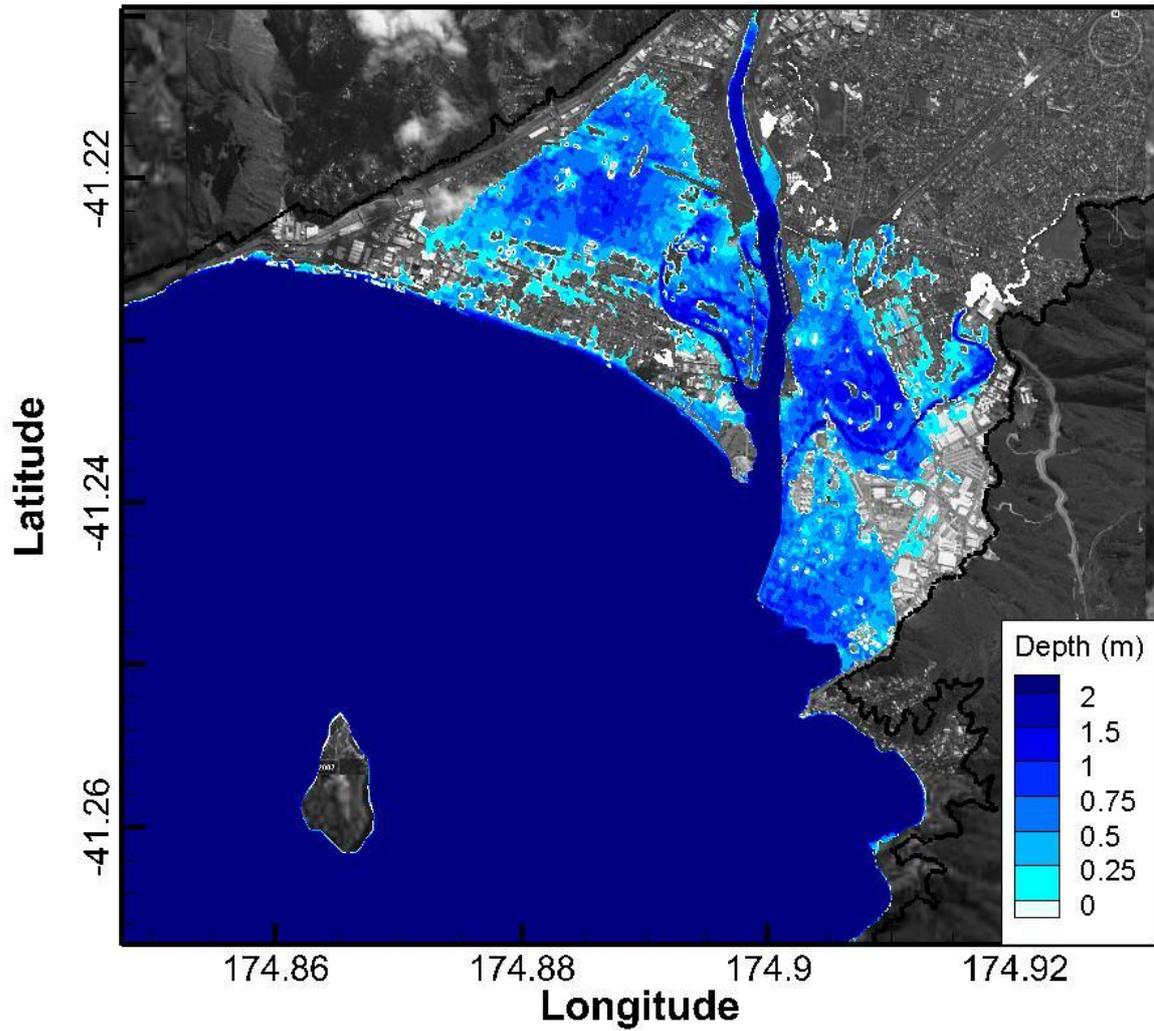
Figure 3-15:Total storm inundation map for Petone and Seaview with 1.0 m sea-level rise.
Simulations are based on the 17 August 1990 event and represent a 1% AEP joint probability wave and storm-tide producing the largest coastal water depths.
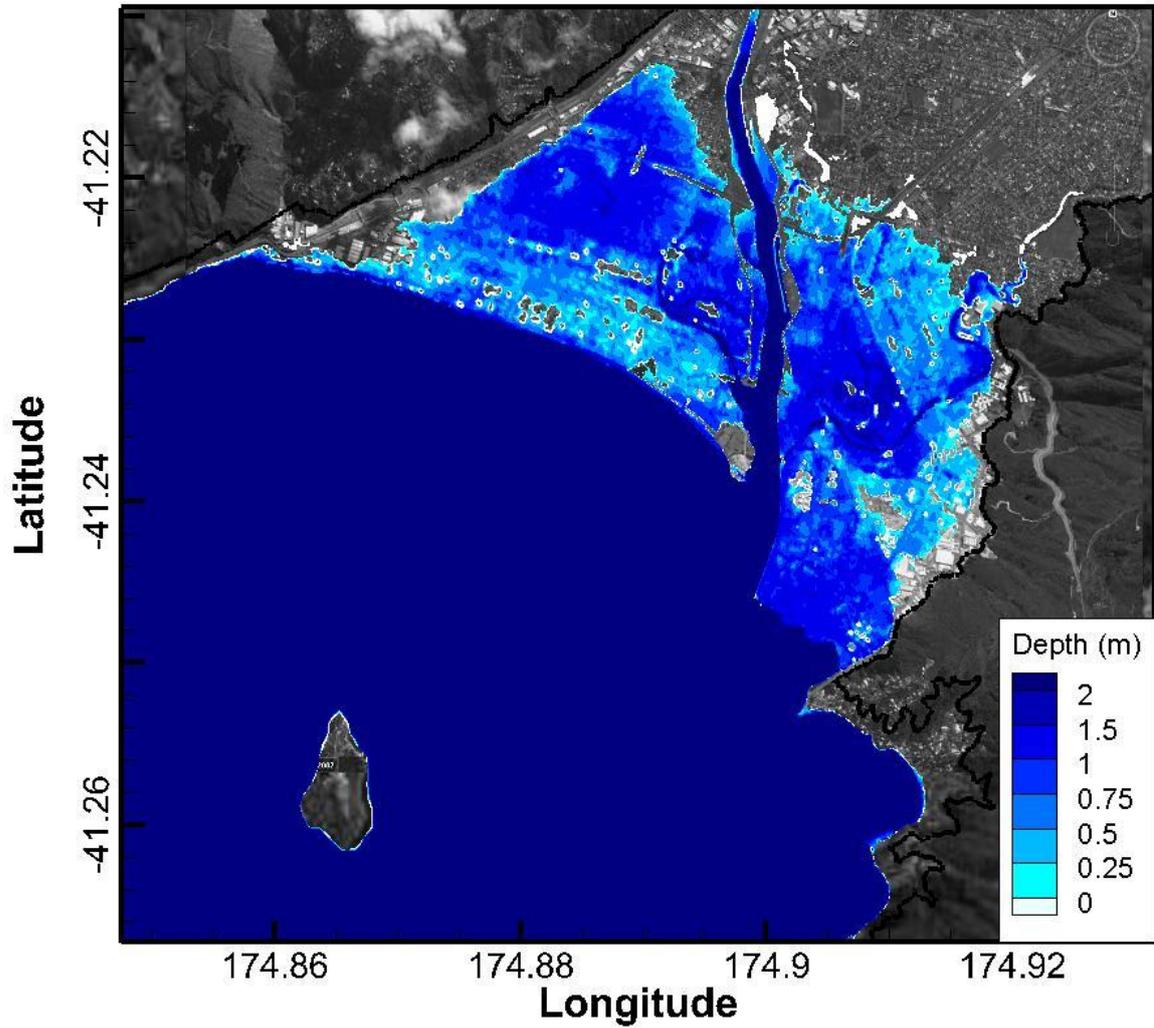
Figure 3-16:Total storm inundation map for Petone and Seaview with 1.5 m sea-level rise.
Simulations are based on the 17 August 1990 event and represent a 1% AEP joint probability wave and storm-tide producing the largest coastal water depths.
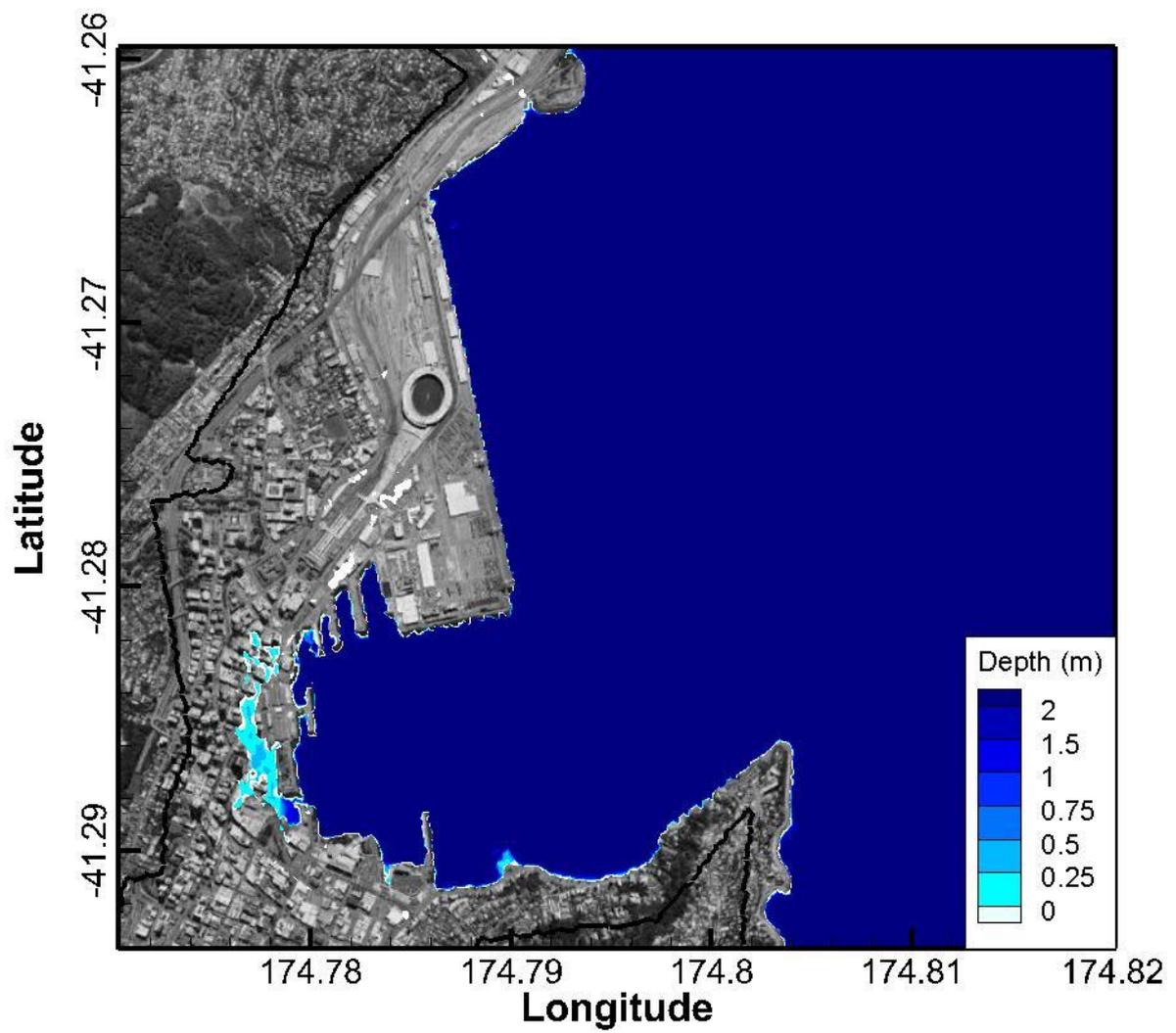
Figure 3-17: Total storm inundation map of Wellington central city with 0.5 m sea-level rise.
Simulations are based on the 17 August 1990 event and represent a 1% AEP joint probability wave and storm-tide producing the largest coastal water depths.
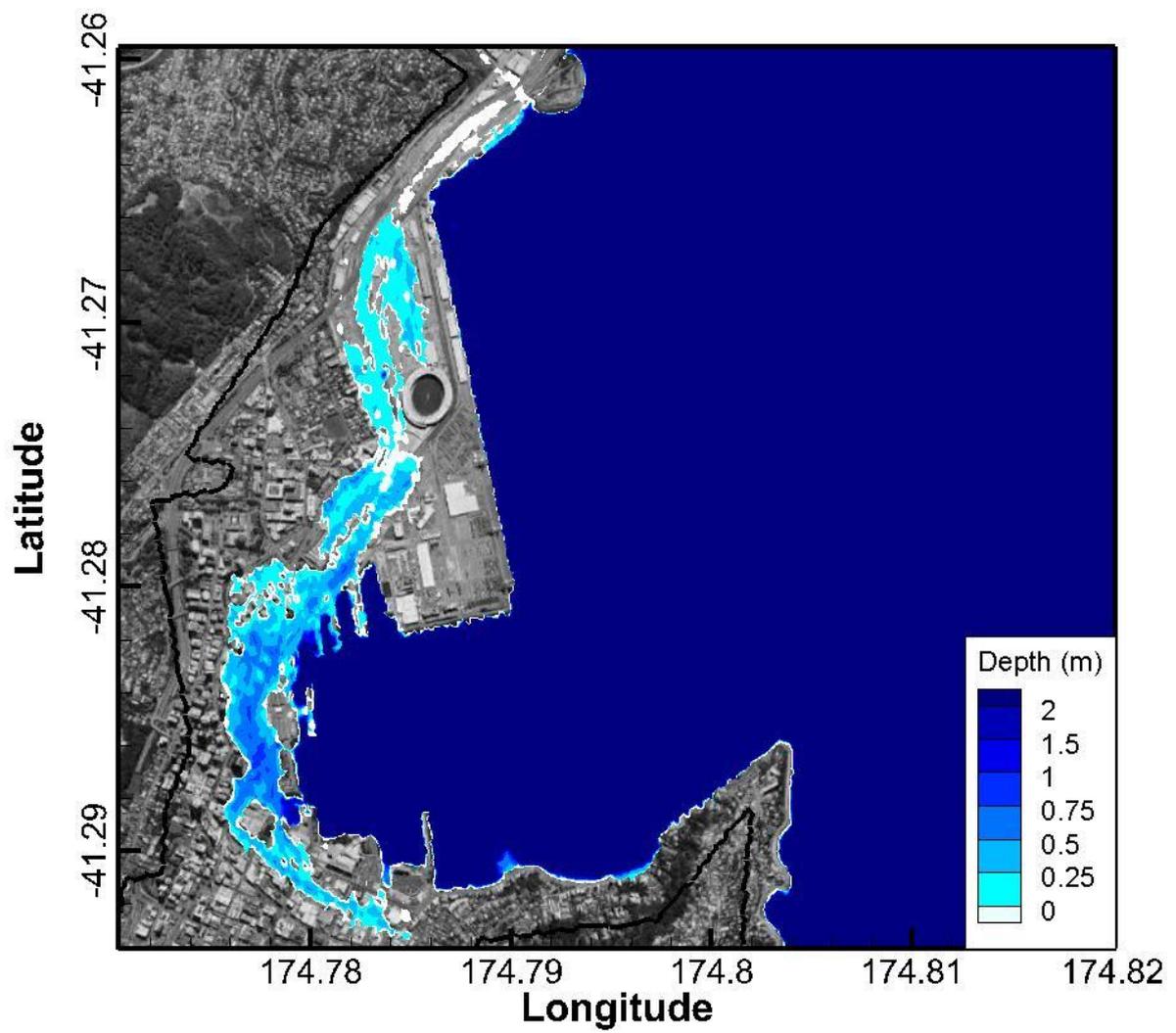
Figure 3-18: Total storm inundation map of Wellington central city with 1.0 m sea-level rise.
Simulations are based on the 17 August 1990 event and represent a 1% AEP joint probability wave and storm-tide producing the largest coastal water depths.
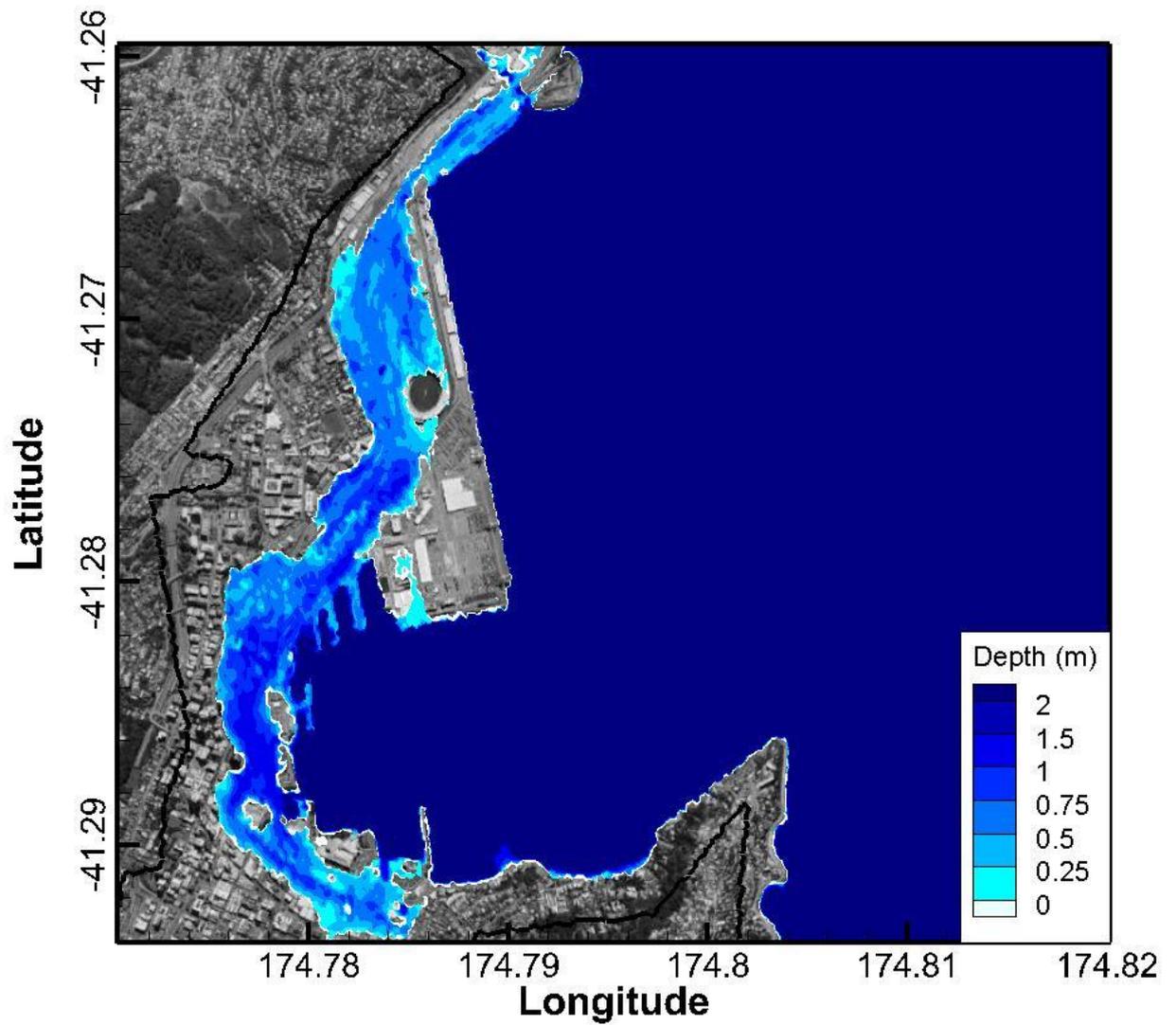
Figure 3-19: Total storm inundation map of Wellington central city with 1.5 m sea-level rise.
Simulations are based on the 17 August 1990 event and represent a 1% AEP joint probability wave and storm-tide producing the largest coastal water depths.
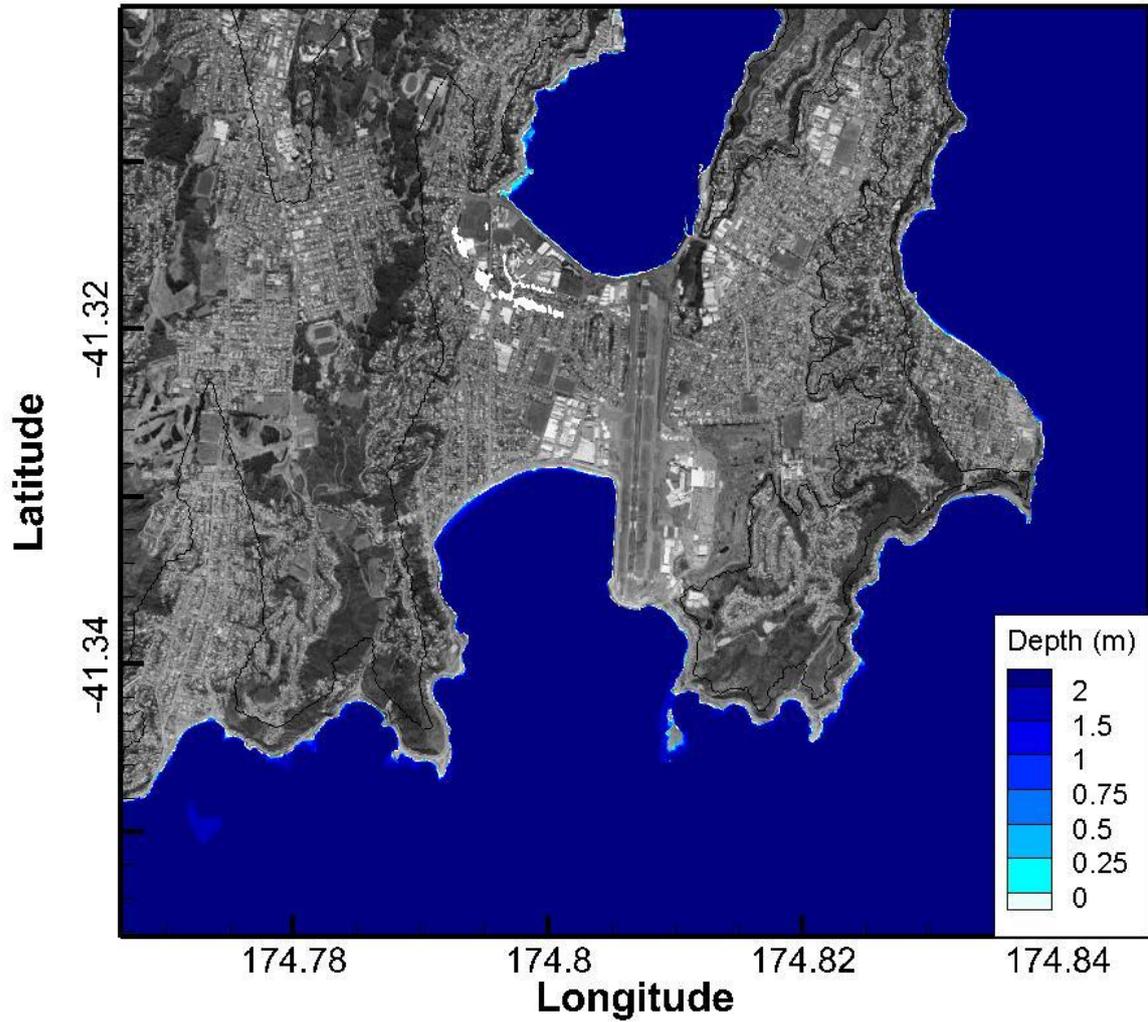
Figure 3-20:Total storm inundation map of Evans Bay and Lyall Bay with 0.5 m sea-level rise.
Simulations are based on the 17 August 1990 event and represent a 1% AEP joint probability wave
and storm-tide producing the largest coastal water depths. White regions indicate areas that are
below sea level at high tide but not inundated in the modelling.
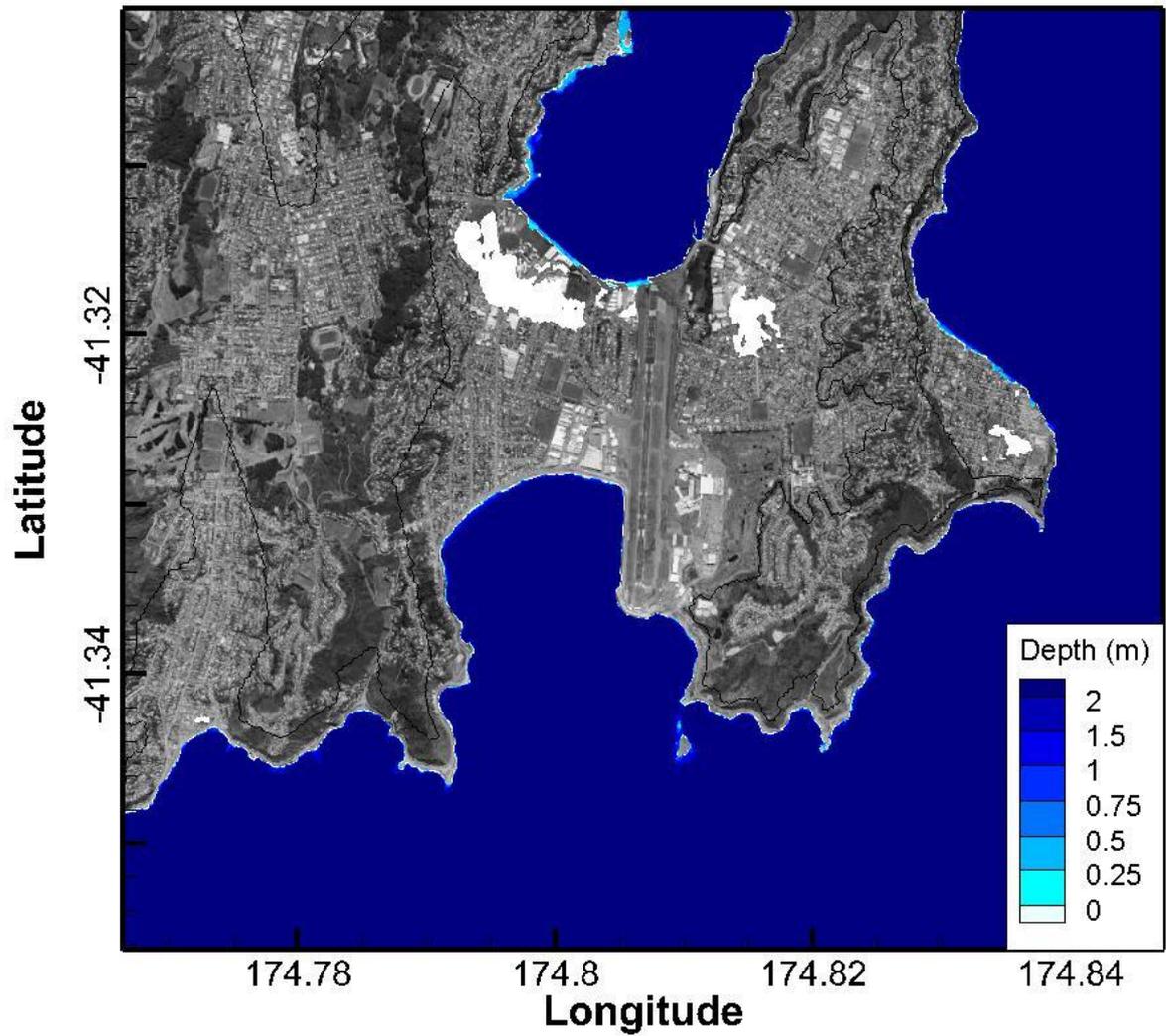
Figure 3-21:Total storm inundation map of Evans Bay and Lyall Bay with 1.0 m sea-level rise.
Simulations are based on the 17 August 1990 event and represent a 1% AEP joint probability wave and storm-tide producing the largest coastal water depths. White regions indicate areas that are below sea level at high tide but not inundated in the modelling.
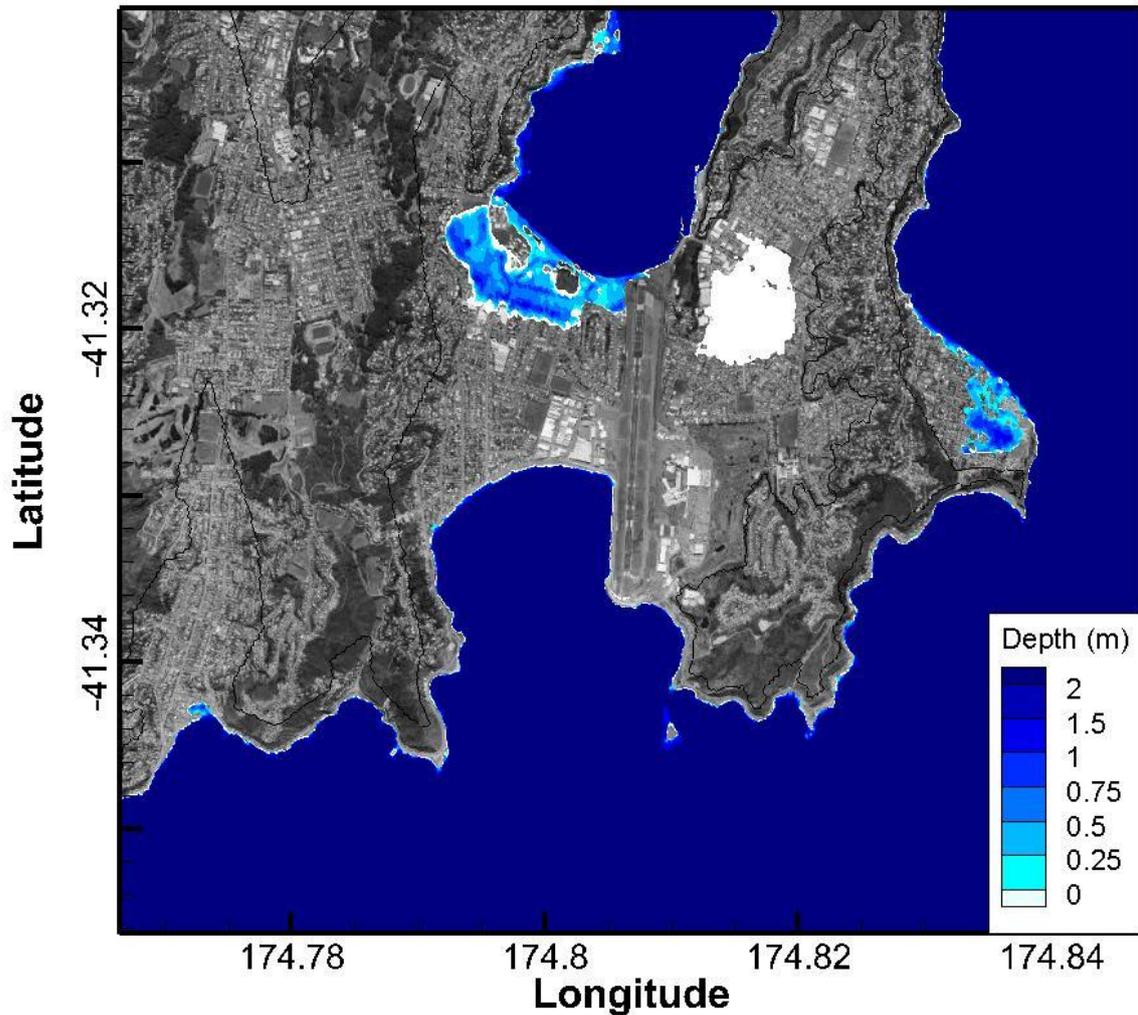
Figure 3-22:Total storm inundation map of Evans Bay and Lyall Bay with 1.5 m sea-level rise.
Simulations are based on the 17 August 1990 event and represent a 1% AEP joint probability wave
and storm-tide producing the largest coastal water depths. White regions indicate areas that are
below sea level at high tide but are not inundated in the model.

Inundation with sea-level rise – Kapiti Coast

Total storm inundation maps for areas surrounding Otaki, Waikanae and Porirua are
presented in the following sections. The local-area model grids for these areas contain land
that is below the total storm inundation level when sea-level rise increments are included. In
some model simulations these particular low-lying areas were not inundated, generally
where there was no direct flowpath from the sea. These low lying areas may either be an
artefact from the LiDAR data, or more probably low areas with narrow streams draining to
rivers or the sea directly. Small/narrow streams may not be resolved at the 20 m model grid
resolution. These low lying areas are coloured white in the following figures and indicate
areas where the possibility of coastal flooding during combined storm-tides and wave set-up
may occur and further investigation may be considered.

Otaki

As sea levels rise from present day to 0.5 m, 1.0 m and 1.5 m, progressively more land around Otaki Beach is inundated.

0.5 m rise (Figure 3-23):

- Water levels in the lower Otaki River rise and the lagoon to the north of the river mouth floods land towards the south of Otaki Beach Township. There is also flooding of land to the south of the river mouth. Areas shown inundated north of Otaki Beach are currently sand and lagoon areas near the mouth of the Waitohu Stream. The southern extent of the inundation model grid stops at the Manganoe Stream, where it is possible that some inundation occurs near the stream mouth. Total storm inundation levels relative to WVD-53 are shown in Figure H-18.

1.0 m rise (Figure 3-24):

- Inundation extends north and south of the Otaki River mouth. Satellite images indicate that the inundated areas are mostly farmland, although properties on Atkinson Avenue are exposed to inundation. Inundation from the Waitohu Stream spreads further inland, extending behind Otaki Beach. Maximum storm inundation levels relative to WVD-53 are shown in Figure H-19.

1.5 m rise (Figure 3-25):

- Otaki Beach is surrounded by storm-tide inundation that travels inland from the Otaki River to the south and Waitohu Stream to the north. There are regions between To Horo Beach and the Otaki River which are inundated. The grid does not include the Manganoe Stream which will provide an additional pathway for sea water to intrude inland and may further increase inundation. Maximum total inundation water levels relative to WVD-53 are shown in Figure H-20.
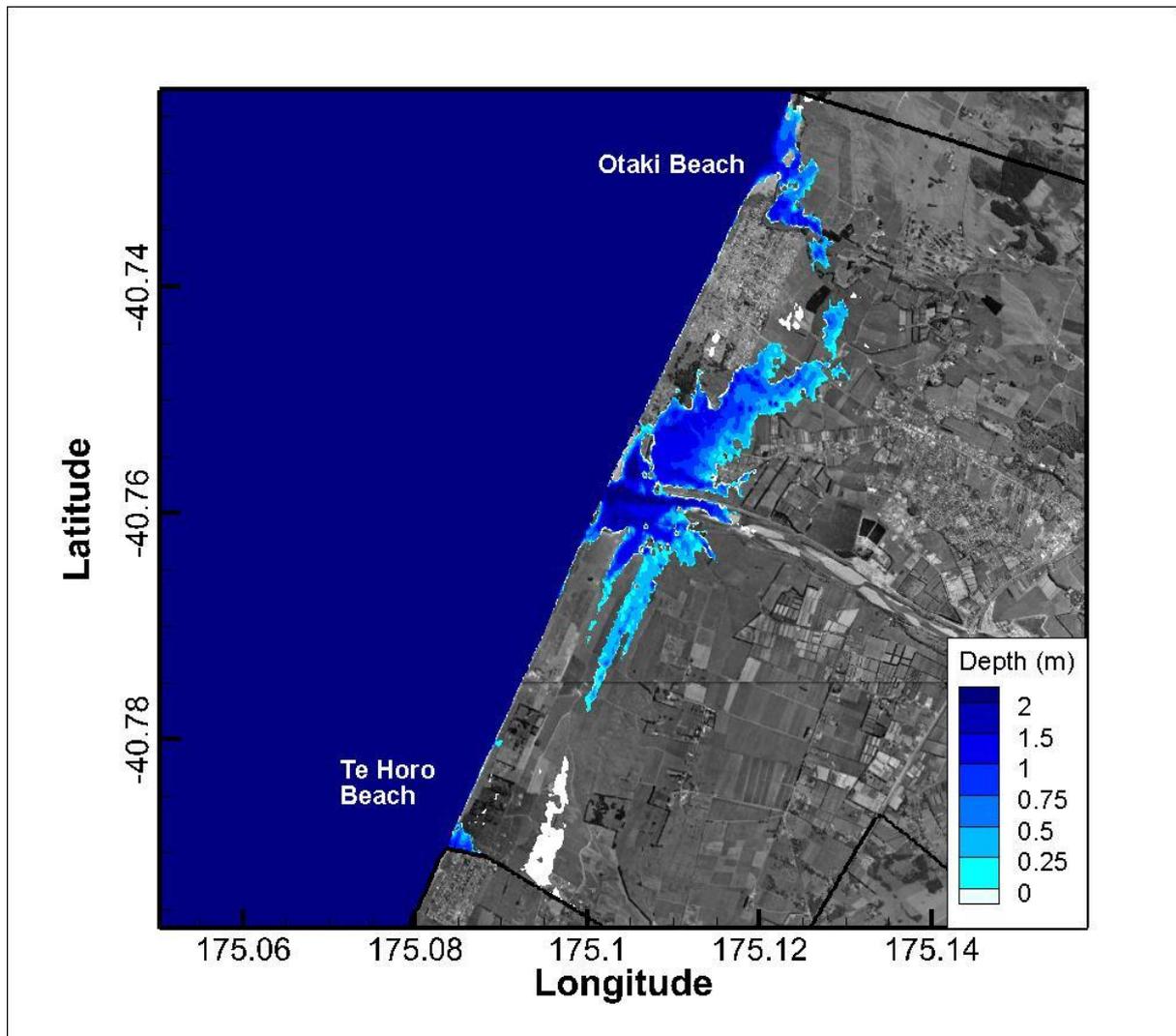
Figure 3-23:Total storm inundation map at Otaki with 0.5 m sea-level rise. The simulation is based on the 6 September 1994 event. The coast line and extent of the land grid are indicated by the black lines. White regions indicate areas with topography below storm-tide level at the coast but not inundated in the simulation.
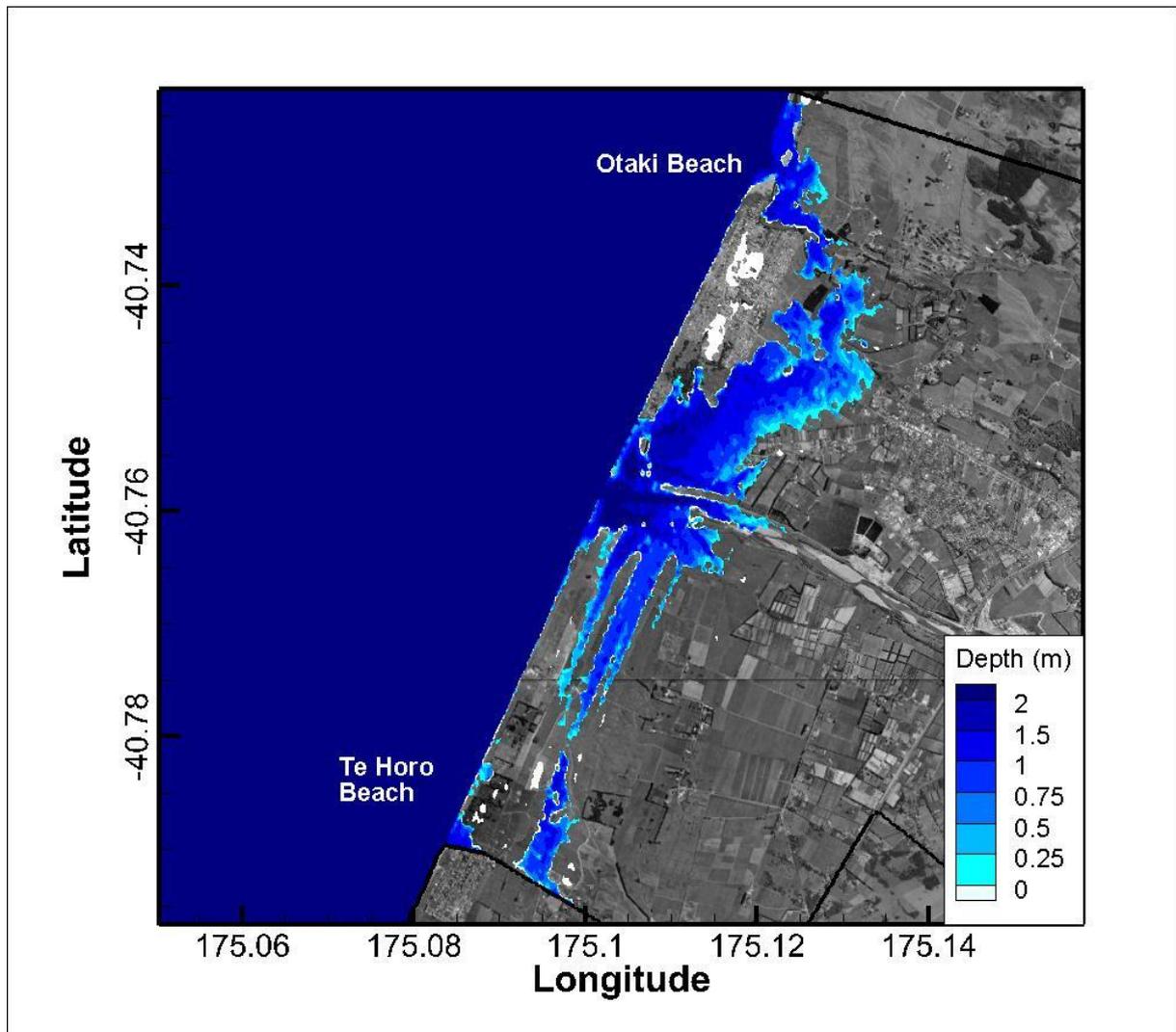
Figure 3-24:Total storm inundation at Otaki with 1.0 m sea-level rise. The simulation is based on the 6 September 1994 event. The coast line and extent of the land grid are indicated by the black lines. White regions indicate areas with topography below storm-tide level at the coast but not inundated in the simulation.
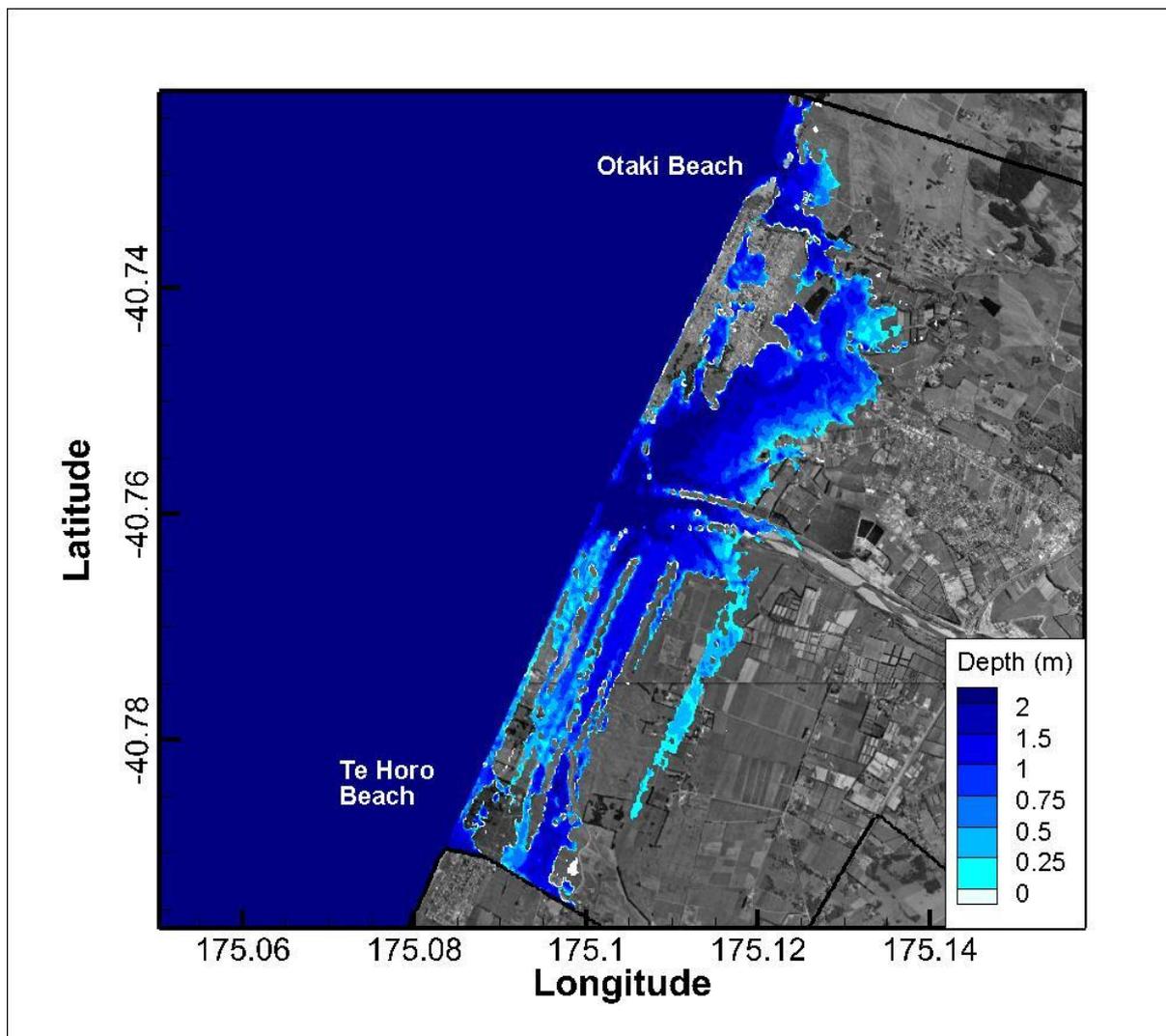
Figure 3-25:Total storm inundation map for Otaki with 1.5 m sea-level rise. The simulation is based on the 6 September 1994 event. The coast line and extent of the land grid are indicated by the black lines. White regions indicate areas with topography below storm-tide level at the coast but not inundated in the simulation.

Waikanae

As sea levels rise from present day to 0.5 m, 1.0 m and 1.5 m, progressively more land around Waikanae is inundated. Note that these mapped areas of inundation depth will only apply for 1-3 hours straddling high tide associated with a 1% joint AEP event in combination with the applied sea-level rise increment.

0.5 m rise (Figure 3-26):

- Water levels rise in the lower Waikanae River and Waimeha Lagoon. Parts of the Otaihanga Domain and Wildlife Refuge are likely to be inundated. There are also low-lying areas including parts of the Waikanae Golf Course, Te Kupe Rd and Te Atiwawa Park which have land elevations below the total storm inundation level (indicated as white regions in Figure 3-26). If there is a connection to the sea or river via streams or storm water drains, it is likely that

these areas will also be inundated. Maximum water elevations relative to WVD-53 are shown in Figure H-22.

1.0 m rise (Figure 3-27):

- Low lying areas to the north and south of the Waikanae River mouth are inundated. These include residential areas near Te Atiawa Park and Kena Kena Park to the south of the Waikanae River. North of the Waikanae River water levels rise in the Waimeha Lagoon causing inundation in the Otaihanga Domain and Wildlife Refuge. The model indicates residential areas surrounding these locations will also be inundated. Further residential areas between the Otaihanga Domain and the Waimeha/Ngarara Stream have land elevations lower than the total storm inundation level and may be flooded via streams or storm drains. Parts of the Waikanae Golf Course and Totara Lagoon are inundated. Inland, the river is likely to rise as far as the camp ground at the end of Kauri Road with flooding both north and south of the river at this point. Maximum water levels relative to WVD-53 are shown in Figure H-23.

1.5 m rise (Figure 3-28):

- Further flooding occurs to low-lying areas to the north and south of the Waikanae River mouth. These include residential areas near Te Atiawa Park and Kena Kena Park to the south of the Waikanae River. Farm land south east of The Drive is inundated, and the river expands almost as far as the subdivision on Kotuku Drive. Water levels rise in the Waikanae causing inundation as far inland as Kauri Rd, and to low-lying land in the areas roughly bounded by Toroa Rd, Otaihanga Rd and Tieko St. There is considerable inundation to the north of the Waikanae River, extending through residential areas as far as the Waimeha Stream. Inundation also extends from the Ngarara Stream through the Totara Lagoon. Maximum water levels relative to WVD-53 are shown in Figure H-24.
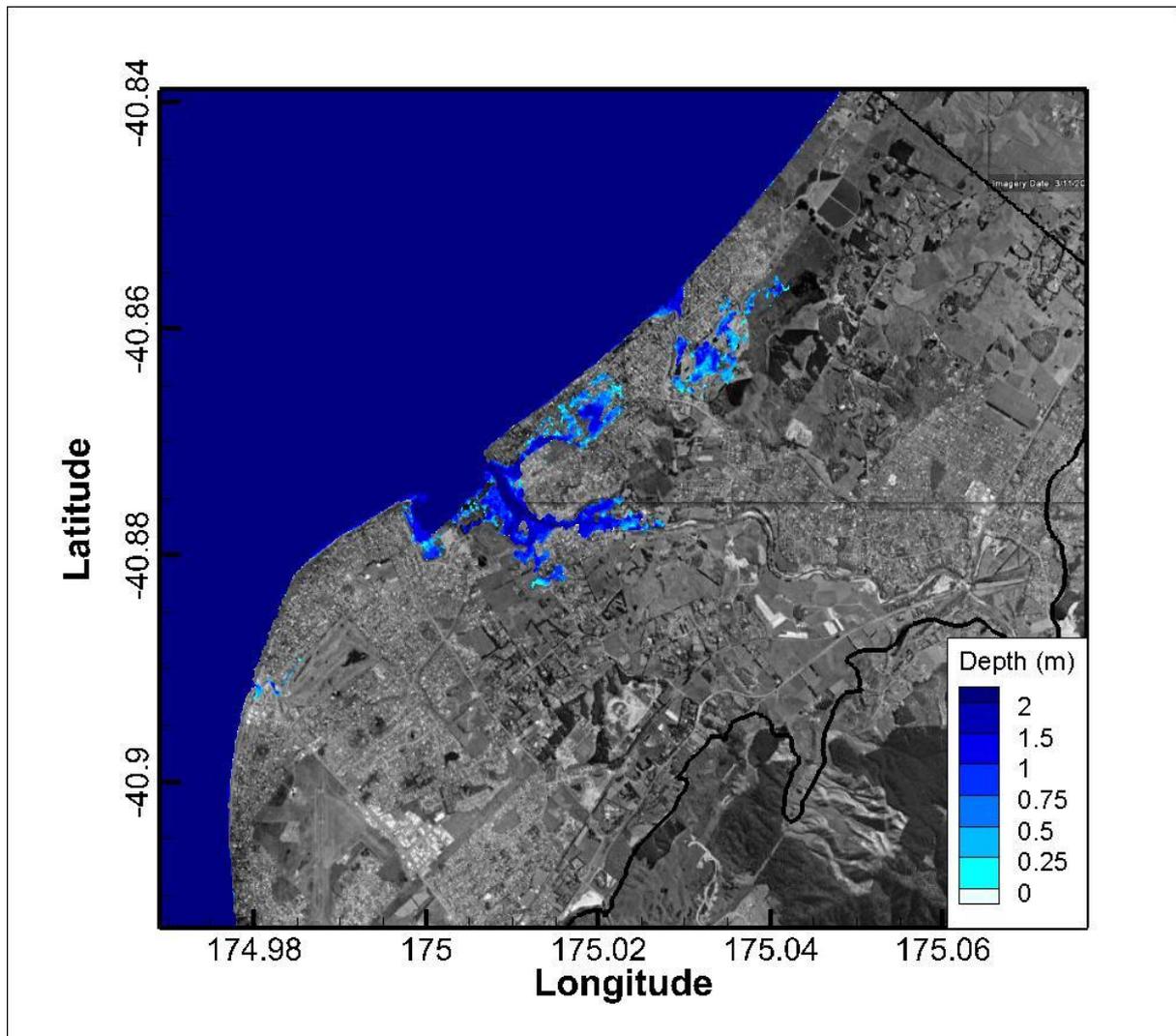
Figure 3-26:Total storm inundation at Waikanae with 0.5 m sea-level rise. The simulation is based on the 6 September 1994 event. . The coast line and extent of the land grid are indicated by the black lines. White regions show areas where the topography is below storm-tide sea level, but not inundated in the modelling.
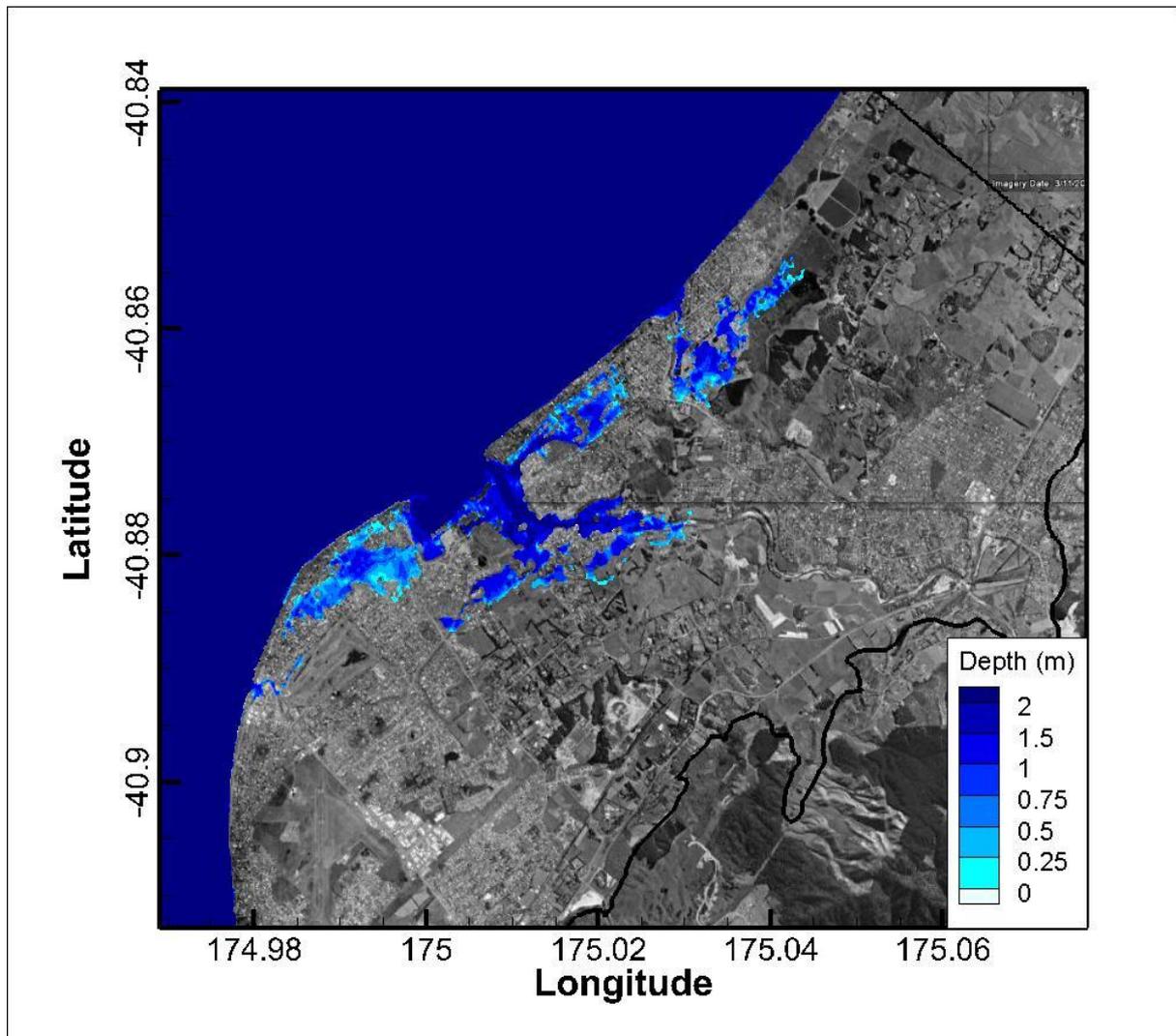
Figure 3-27:Total storm inundation at Waikanae with 1.0 m sea-level rise. The simulation is based on the 5 September 1994 event. The coast line and extent of the land grid are indicated by the black lines. White regions show areas where the topography is below storm-tide sea level, but not inundated in the modelling.
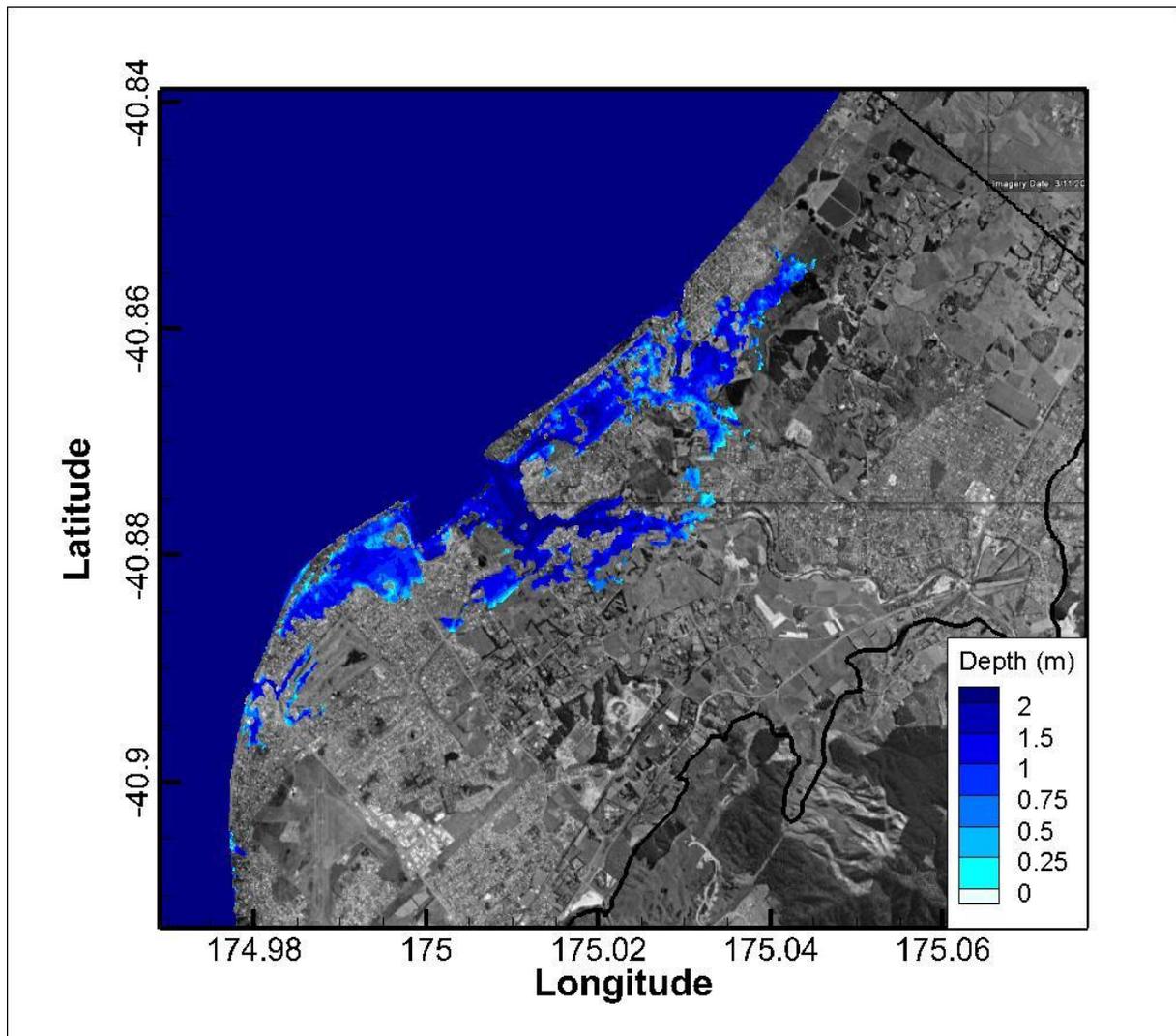
Figure 3-28:Total storm inundation at Waikanae with 1.5 m sea-level rise. The simulation is based on the 6 September 1994 event. The coast line and extent of the land grid are indicated by the black lines. White regions show areas where the topography is below storm-tide sea level, but not inundated in the modelling.

Porirua

Due to the steep topography surrounding Porirua Harbour, changes in storm-tide inundation from rising sea levels are most obvious at the head of the Porirua Harbour and Pauatahanui Arm where land is flatter. Note that these areas of mapped inundation depth on land will only apply for 1-3 hours straddling high tide associated with a 1% joint AEP event in combination with the applied sea-level rise increment.

**0.5 m rise (Figure 3-29):**

- The Ngatitoa Domain (Mana) is shown to be inundated. Water levels come close to buildings on Paekakariki Hill Road at the head of the Pauatahanui Arm. Storm inundation may also reach the commercial area at the southern end of Porirua Harbour. The white areas to the east of Porirua Harbour are lagoons separated from the harbour by the Johnsonville Porirua Motorway. These are

not connected to the Harbour in the model. Maximum water levels relative to WVD-53 are shown in Figure H-26.

1.0 m rise (Error! Reference source not found.**):**

- Coastal storm inundation spreads further inland in the areas described above. At the southern end of the harbour, Titahi Bay Road is flooded. Water crosses the motorway near Papakowhai and Paremata. Flooding extends further up the Pauatahanui Stream and at the head of the Pauatahanui arm. Maximum water levels relative to WVD-53 are shown in Figure H-27.
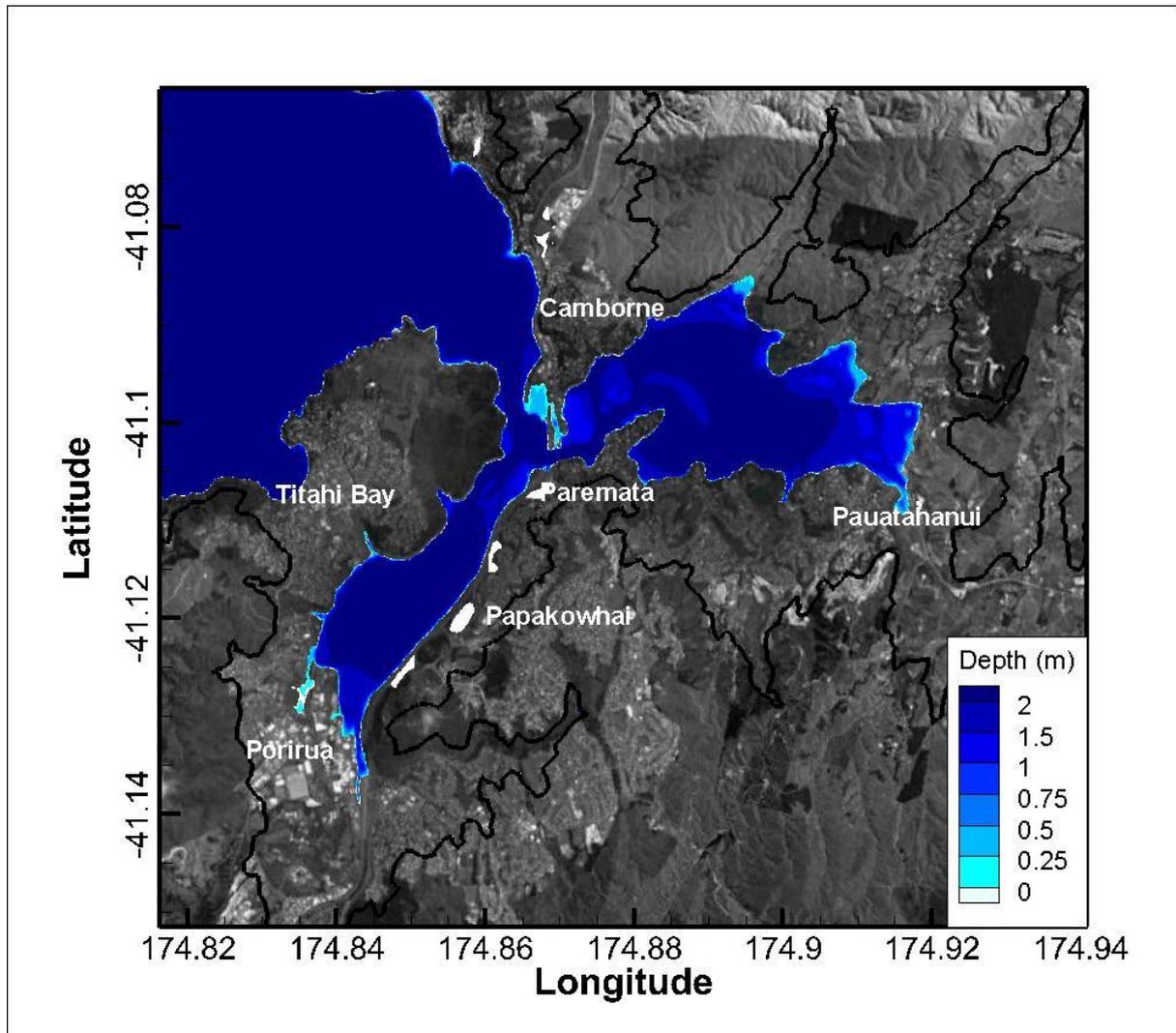
Figure 3-29:Total storm inundation at Porirua with 0.5 m sea-level rise. The simulation is based on the 6 September 1994 event. The coast line and extent of the land grid are indicated by the black lines. White regions show areas with elevations below storm-tide sea level but not inundated in the model.

1.5 m rise (Figure 3-31):

- Much of the low-lying commercial area at the southern end of Porirua Harbour is inundated. The motorway is shown to be inundated at a number of points along the side of the harbour. Low lying areas around Mana are flooded. The eastern margins of the Pauatahanui arm are also inundated. The Plimmerton

Domain has land elevations lower than the total storm inundation level and while not inundated in the model due to higher land separating this area from the sea, may be at risk through drain connections unresolved in the model grid. Maximum water levels relative to WVD-53 are shown in Figure H-28.
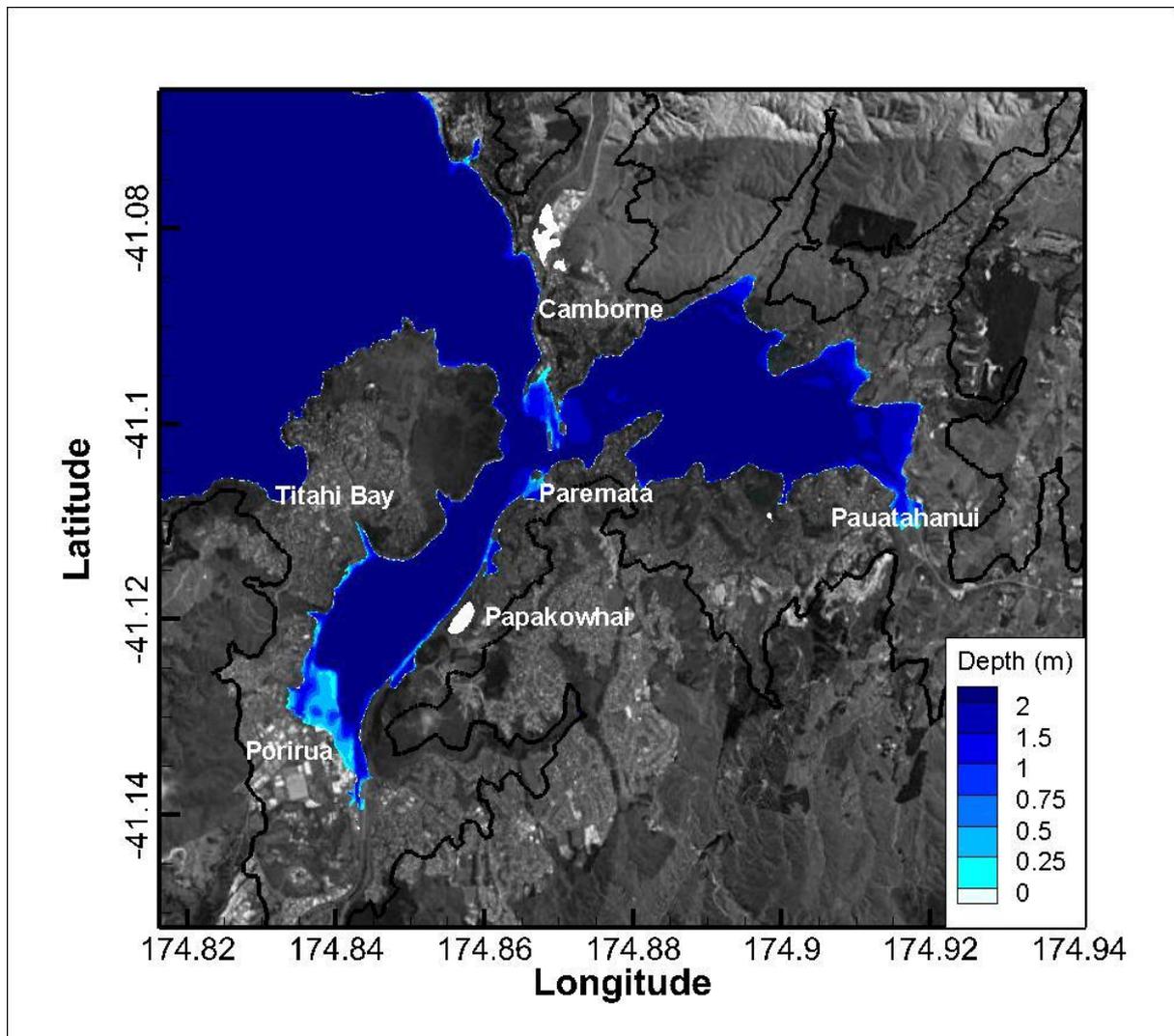

Figure 3-30:Total storm inundation at Porirua with 1.0 m sea-level rise. The simulation is based on the 6 September 1994 event. The coast line and extent of the land grid are indicated by the black lines. White regions show areas with elevations below storm-tide sea level but not inundated in the model.
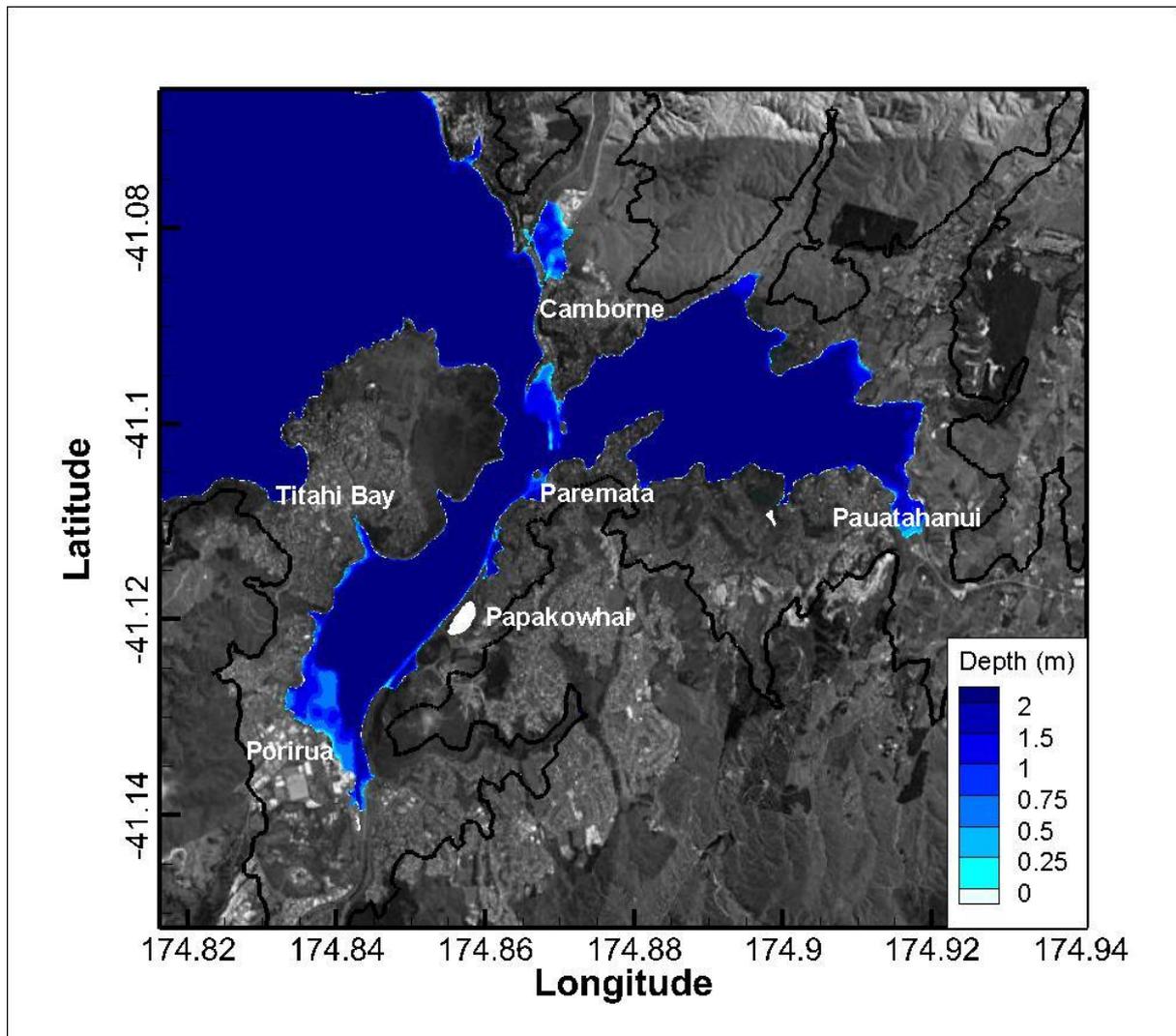
Figure 3-31:Total storm inundation at Porirua with 1.5 m sea-level rise. The simulation is based on the 6 September 1994 event. The coast line and extent of the land grid are indicated by the black lines. White regions show areas with elevations below storm-tide sea level but not inundated in the model.

4   Conclusions

This study shows that the largest coastal inundation levels in the Greater Wellington Region result from high storm tides (MLOS + tide + storm surge), compounded by additional wave setup. We mapped total storm inundation from simulations of two representative storm-tide events that, combined with the coincident offshore wave heights, had a 1% joint-probability of occurrence in any given year. Mapped inundation areas however, will only apply for relatively short periods of 1–3 hours straddling high tide associated with a 1% joint AEP event, or further compounded by a sea-level rise increment in the future.

Simulated total storm inundation levels (storm-tide plus wave setup) for the present-day 1% joint AEP events varied around the coast of the Wellington region, but were up to 2.4 m above WVD-53 on the exposed north-western and southern/eastern coasts. In Porirua and Wellington Harbours the 1% AEP (100-year ARI) storm-tide plus wave setup ranged from 1.5–1.7 m above WVD-53, with the higher end of this range applying to Porirua Harbour.

Sea-level rise increments of 0.5 m, 1.0 m and 1.5 m were applied to the present-day representative storm-tide and wave inundation events applied respectively to the Kapiti coast and the south Wellington and Wairarapa coast. Sea-level rise greatly increases the simulated inundation from storm-tides and wave setup, with flooding of the Hutt Valley, Central Wellington, Otaki, Waikanae and to a lesser extent Porirua, Evans Bay and Churchill (Miramar Peninsula).

The storm events modelled for this study have joint storm-tide and wave height annual exceedance probabilities of 1% offshore from the coast, which may be considered to be rare and severe events. However, a 1% AEP is a commonly used planning or design event magnitude, and 100-year planning lifetimes are commonly used for assessing risk for infrastructure (e.g., bridges) or the requirement in the NZ Coastal Policy Statement to consider "at least 100 years" when assessing coastal hazard risks (Policy 24). Also a 1% AEP event is *likely* to occur or be exceeded over a 100-year planning lifetime with a probability of 63%.

A further factor to consider with sea-level rise is that more frequent but less severe storm-inundation events are likely to become more problematic as they occur with increasing frequency relative to present coastal land elevations. For example, an event with 25% AEP at present-day sea levels may not presently cause any concern for a locality, but may cause inundation in the future when say a sea-level rise exceeds 0.5 m. By the same reasoning, coastal inundation is expected to be more frequent with rising sea level as the storm-tide required to inundate low-lying coastal land will progressively become smaller. Alternatively, the frequency of the present-day coastal inundation events considered in this study will increase, from an average recurrence interval of 100 years (or 1% AEP) now to occurring around once a year on average for sea-level rises of 0.3 to 0.5 m, depending on the tide range.

The inundation simulations with sea-level rise increments were modelled assuming the present-day coastal topography. This does not take into account future coastal changes in response to sea-level rise, climate change or even climate variability that may result in regional or localised erosion, aggradation and changes to shoreline orientation. Such changes could alter somewhat the future exposure to coastal inundation hazards, than those modelled in this report using the present-day topography.

5   Glossary of abbreviations and terms

Annual exceedance probability (AEP)
The probability of a given (usually high) sea level being equalled or exceeded in elevation, in any given calendar year. AEP can be specified as a fraction (e.g., 0.01) or a percentage (e.g., 1%).

Average recurrence interval (ARI)
The average time interval (averaged over a long time period and many "events") that is expected to elapse between recurrences of an infrequent event of a given large magnitude (or larger). A large infrequent event would be expected to be equalled or exceeded in elevation, once, on average, every "ARI" years.

Future cast
A numerical simulation (representation) of *future* conditions. Differs from a *forecast*; whereas a forecast aims to predict the exact time-dependent conditions in the immediate future, such as a weather forecast a *future cast* aims to simulate a time-series of conditions that would be typical of the future (from which statistical properties can be calculated) but does not predict an exact time-sequence.

Hindcast
A numerical simulation (representation) of *past* conditions. As opposed to a forecast or future cast that simulates the future.

Joint-probability
The probability of two separate processes occurring together (e.g., large waves and high storm-tide).

Marginal variable
Refers to a single variable (e.g., wave height, or storm-tide) representing one axis, or "margin", of a joint-probability plot.

Mean level of the sea (MLOS)
The variation of the non-tidal sea level on time scales ranging from a monthly basis to decades, due to climate variability. This includes seasonal effects and the effects of El Niño–Southern Oscillation (ENSO) and the Interdecadal Pacific Oscillation (IPO) on sea level through winds and sea temperatures.

Storm surge
The rise in sea level due to storm meteorological effects. Low-atmospheric pressure causes the sea-level to rise, and wind stress on the ocean surface pushes water down-wind and to the left up against any adjacent coast.

Storm-tide
Storm-tide is defined as the sea-level peak resulting from a combination of MLOS + tide + storm surge. (In New Zealand this generally occurs at high tide)

Total storm inundation level
The water level at the shoreline comprising storm-tide and wave setup (plus a sea-level rise increment for future scenarios)

Wave runup
The maximum vertical extent of wave "up-rush" on a beach or structure above the still water level and thus constitutes only a short-term upper-bound fluctuation in water level relative to wave setup.

Wave setup
The increase in mean still-water sea level at the coast, resulting from the release of wave energy in the surf zone as waves break.

6   References

Ackerley, D.; Dean, S.; Sood, A.; Mullan,B. (2012). Regional climate modelling in NZ: Comparison to observations. *Weather and Climate 32(1)*: 3-23*.*

Amante, C.; Eakins, B.W. (2009). ETOPO1 1 Arc-Minute Global Relief Model: Procedures, Data Sources and Analysis. NOAA Technical Memorandum NESDIS NGDC-24, NOAA: 19.

Bell, R.G.; Hannah, J. (2012). Sea-level variability and trends: Wellington Region. NIWA Client Report HAM2012-043 prepared for Greater Wellington Regional Council, NIWA and Vision NZ Ltd. 74 p.

Booij, N.; Ris, R.C.; Holthuijsen, L.H. (1999). A third-generation wave model for coastal regions 1. Model description and validation. *Journal of Geophysical Research 104(C4)*: 7649-7666.

DOC (2010). New Zealand Coastal Policy Statement 2010. New Zealand Department of Conservation.

Gillibrand, P.A.; Lane, E.M.; Walters, R.A.; Gorman, R.M. (2011). Forecasting extreme sea level events and coastal inundation from tides, surge and wave setup. *Australian Journal of Civil Engineering 9(1).*

Google Earth (2012). from http://www.google.com/earth/index.html

Goring, D.G.; Stephens, S.A.; Bell, R.G.; Pearson, C.P. (2010). Estimation of extreme sea levels in a tide-dominated environment using short data records. *Journal of Waterway, Port, Coastal and Ocean Engineering (ASCE) 137(3)*: 150-159.

Gringorten, I.I. (1963). A plotting rule for extreme probability paper. *Journal of Geophysical Research 68*: 813-814.

Hannah, J. (1990). Analysis of mean sea-level data from New Zealand for the period 1899-1988. *Journal of Geophysical Research-Solid Earth and Planets 95(B8)*: 12399-12405.

Hannah, J. (2004). An updated analysis of long-term sea level change in New Zealand. *Geophysical Research Letters 31(3).*

Hawkes, P.J.; Gouldby, BR.; Tawn, J.S.; Owen, M.W. (2002). The joint probability of waves and water levels in coastal engineering design. *Journal of Hydraulic Research 40(3)*: 241-251.

Wallingford, H.R. (2000). The joint probability of waves and water levels: JOIN-SEA. Version 1.0. User Manual No. TR 71. 12 p.

Wallingford, H.R.; Lancaster University (2000). The joint probability of waves and water levels: JOIN-SEA, a rigorous but practical new approach. No. SR 537. 47 p.

Kidson J.W. (2000). An analysis of New Zealand synoptic types and their use in defining weather regimes. *International Journal of Climatology 20(3)*: 299-316.

Lane, E.M.; Walters, R.A.; Gillibrand, P.A.; Uddstrom, M. (2009a). Operational forecasting of sea level height using an unstructured grid ocean model. *Ocean Modelling 28(1-3)*: 88-96.

Lane, E.M.; Walters, R.A. (2009b). Verification of RiCOM for storm surge forecasting. *Marine Geodesy 32(2):* 118-132.

Lane, E M.; Gillibrand, P.A.; Arnold, J.R.; Walters, R.A. (2011). Tsunami inundation modelling using RiCOM. *Australian Journal of Civil Engineering 9(1).*

Land Information NZ (2012). The New Zealand Nautical Almanac, 2012/2013 edition, NZ204, page 36-37.

Mullins, B.; Carey-Smith, T.; Griffiths, G.; Sood, A. (2011). Scenarios of storminess and regional wind extremes under climate change. Prepared for Ministry of Agriculture and Forestry, Wellington, National Institute of Water & Atmospheric Research Ltd: NIWA Client Report WLG2010-31.

Nakicenovic, N.; Swart, R. (Eds.) (2000). IPCC Special Report on Emissions Scenarios. Cambridge University Press.

Ris, R.C.; Holthuijsen, L.H.; Booij, N. (1999). A third-generation wave model for coastal regions 2. Verification. *Journal of Geophysical Research 104(C4)*: 7667-7681.

Senechal, N.; Coco, G.; Bryan, K.R.; Holman, R.A. (2011). Wave runup during extreme storm conditions. *Journal of Geophysical Research-Oceans 116(C7)*: C07032.

Stephens, S.; Reeve, G.; Bell, R. (2009). Modelling of the 2 February 1936 storm tide in Wellington Harbour. NIWA Client Report HAM2009-014 prepared for Greater Wellington Regional Council. 33 p.

Stephens, S.; Gorman, R.; Lane, E.M. (2011, minor edits 2012). Joint-probability of storm-tide and waves on the open coast of Wellington. Prepared for Greater Wellington Regional Council. Hamilton, National Institute of Water & Atmospheric Research Ltd: 43 p.

Stockdon, H.F.; Holman, R.A.; Howd, P.A.; Sallenger, A.H. (2006). Empirical parameterization of setup, swash, and runup. *Coastal Engineering 53(7)*: 573-588.

Tolman, H.L. (2009). User manual and system documentation of WAVEWATCH-III, version 3.14, NOAA / NWS / NCEP / OMB: 194.

Uppala, S.M.; KÅllberg, P.W.; Simmons, A.J.; Andrae, U.; Bechtold, V.D.; Fiorino, M.; Gibson, J.K.; Haseler, K.; Hernandez, A.; Kelly, G.A.; Li, X.; Onogi, K.; Saarinen, S.; Sokka, N.; Allan, R.P.; Andersson, E.; Arpe, K.; Balmaseda, A.C.M.; Beljaars, M.A.M.; Van De Berg, L.; Bidlot, J.; Bormann, N.; Caires, S.; Chevallier, F.; Dethof, A.; Dragosavac, M.; Fisher, M.; Fuentes, M.; Hagemann, S.; Hólm, E.; Hoskins, B.J.; Isaksen, L.; Janssen, P.; Jenne, R.; McNally, A.P.; Mahfouf, J.F.; Morcrette, J.J.; Rayner, N.A.; Saunders, R.W.; Simon, P.; Sterl,

A.; Trenberth, K.E.; Untch, D.; Vasiljevic, D.; Viterbo, P.; Woollen, J. (2005). The ERA-40 reanalysis. *Quarterly Journal of the Royal Meteorological Society, 131(612)*: 2961-3012.

Walters, R.A.; Goring. D.G.; Bell, R.G. (2001). Ocean tides around New Zealand. *New Zealand Journal of Marine and Freshwater Research 35*: 567-579.

Walters, R.A. (2005a). Coastal ocean models: two useful finite element methods. *Continental Shelf Research 25*: 775-793.

Walters, R.A. (2005b). A semi-implicit finite element model for non-hydrostatic (dispersive) surface waves. *International Journal for Numerical Methods in Fluids 49(7)*: 721-737.

Walters, R.A.; Casulli, V. (1998). A robust, finite element model for hydrostatic surface water flows. *Communications in Numerical Methods in Engineering 14*: 931-940.

Walters, R.A.; Barnes, P.; Goff, J.R. (2006). Locally generated tsunami along the Kaikoura coastal margin: Part 1. Fault ruptures. *New Zealand Journal of Marine and Freshwater Research 40(1)*: 1-16.

Walters, R.A.; Gillibrand, P.A.; Bell, R.G.; Lane, E.M. (2010). A study of tides and currents in Cook Strait, New Zealand. *Ocean Dynamics 60(6)*: 1559-1580.

Walters, R.A.; Lane, E.M.; Henry, R.F. (2007). Semi-Lagrangian methods for a finite element coastal ocean model. *Ocean Modelling 19*: 112-124.

Zijlema, M. (2010). Computation of wind-wave spectra in coastal waters with SWAN on unstructured grids. *Coastal Engineering 57(3)*: 267-277.

Appendix A Storm surge model description

The general purpose 3-D coastal model (RiCOM), developed by Dr Roy Walters, was used to model the inundation resulting from storm-tide. RiCOM is used routinely by NIWA to forecast storm surge around New Zealand, and is also used in studies of general coastal hydrodynamics and for studies of tsunami inundation for local government agencies (Gillibrand et al. 2011; Lane et al. 2009a & b, 2011; Walters et al. 2006, 2010) The model is driven by time- and spatially-varying wind stress and atmospheric pressure data, derived from either meteorological models or observed data. Recent developments of RiCOM have incorporated wave-induced stress into the forcing of the model. However because the wave model in this study did not fully resolve the wave breaking we could not directly calculate the wave setup in the RiCOM calculations. Thus, the wave setup component of the inundation is added separately according to the procedure described in Section 2.6. We do include wave stresses (obtained from the wave model) off-shore as they have a small effect on currents and sea-level in addition to the setup occurring at the coast. As described elsewhere, wave runup is not included in the inundation modelling.

RiCOM is capable of simulating 3-dimensional flows, but was run in the vertically well-mixed (2-D) mode for the work here, which is suitable for storm-tide modelling. Simulations were started 5 days before the date of the peak of the simulated storm events, and run for eight days with a time step of 3.6 seconds. Details of, and studies using the model, have been published in a number of peer-reviewed scientific journals (e.g. Walters and Casulli 1998; Walters 2005a; 2005b; Walters et al. 2007; Walters et al. 2010; Gillibrand et al. 2011)

RiCOM storm surge model grids

RiCOM simulations are run on flexible triangular mesh grids, which allow variable spatial resolution across the modelling domain. In general, shallower areas are modelled at higher resolution than deeper areas. In this study, an existing grid covering the entire NZ region (Figure A-1) was modified to produce two different grids in which the resolution was increased in the Wellington and Hutt Valley region and the Kapiti Coast region (Figure A-2 and Figure A-3). The reason for using such a large grid spanning the NZ region was to better include the atmospheric forcing of wind and pressure, which are large scale processes affecting storm surge generation. High-resolution land topography around Wellington, the Hutt Valley, and the Kapiti Coast was incorporated in the grid using LiDAR data supplied by GWRC and WCC (Figure A-2, A & B). The Hutt River stop banks and the Petone sea wall were resolved in the model grid by aligning grid nodes along these features and fixing their elevation to the crest of the stop bank or sea wall (Figure A-2, C). The model grid resolution over the land areas and near the coast is approximately 20 m.

Forcing and boundary conditions

As part of the WASP project, NIWA carried out a hindcast of storm surge conditions for the period September 1957 through August 2002, forced by inputs from the ERA-40 reanalysis data set (A global re-analysis of the weather spanning the period mid-1957 to mid-2002 produced by the European Centre for Medium-Range Weather Forecasts (ECMWF), Uppala et al. 2005), which provides global six-hourly wind fields at 1.125º×1.125º resolution. The global wind fields were dynamically downscaled to around 30 km resolution around New Zealand using a Regional Climate Model (Ackerley et al. 2012). Wind and pressure fields from the regional climate model were then interpolated onto the RiCOM model grids, providing spatially explicit time-series of surface boundary conditions.
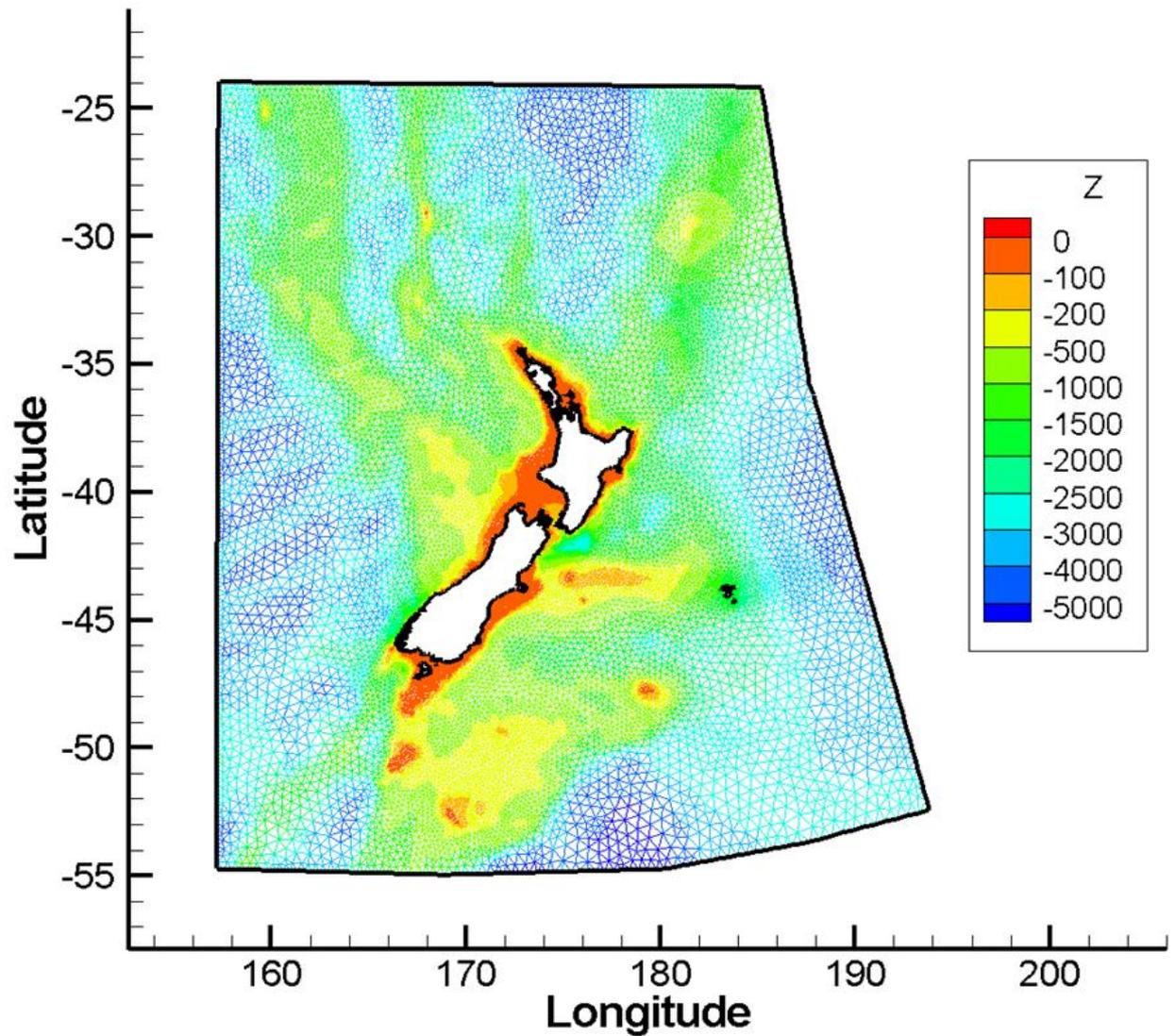
Figure A-1: Extent of the grid used for RiCOM modelling of storm-tides. The flexible-mesh triangular grid has a resolution that is proportional to the depth (Z) measured in metres to MSL. Additional refinement of the grid is used in areas were inundation is to be simulated.

A

B

C
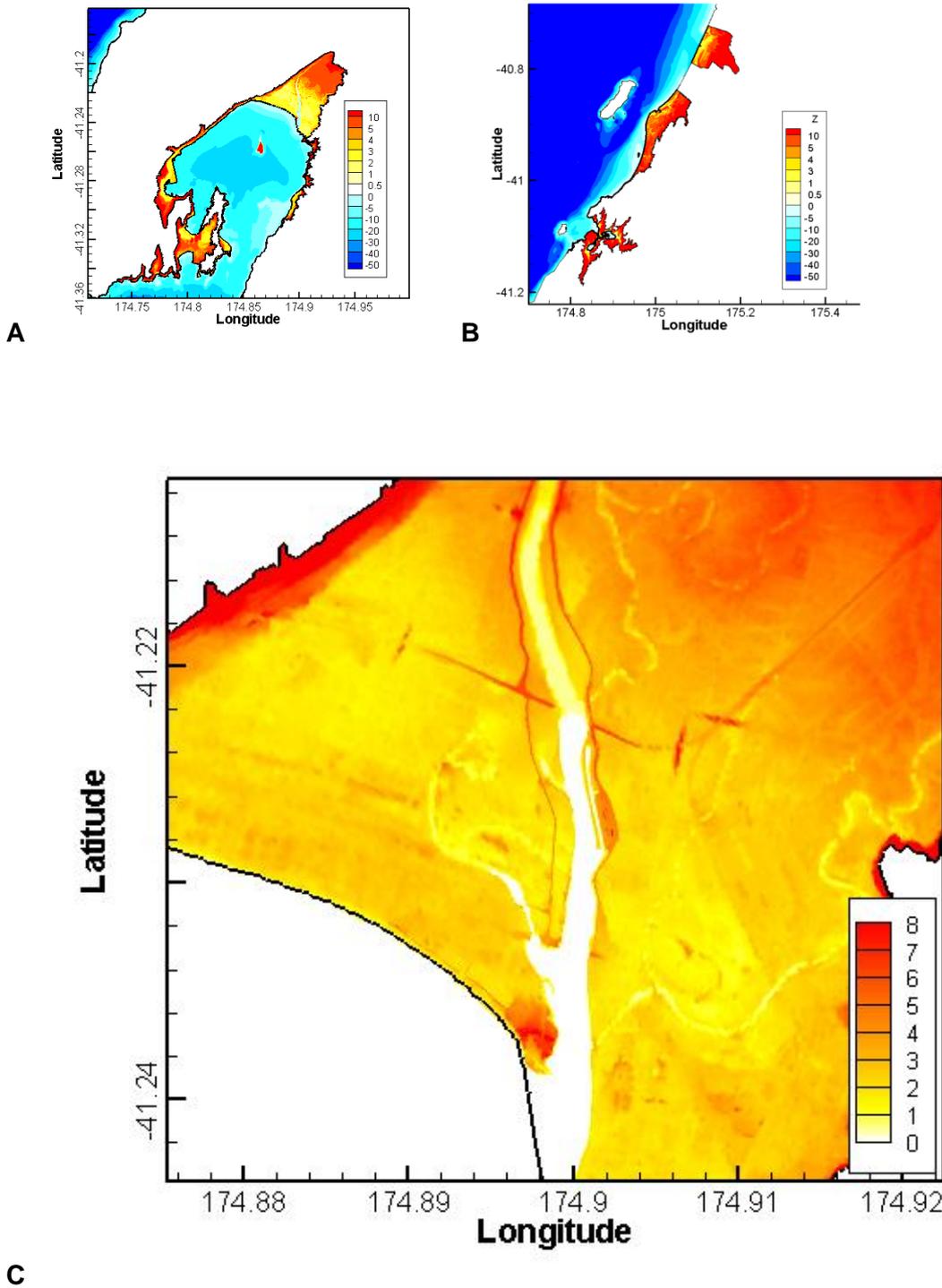
Figure A-2: Water depths and land elevations showing the areas where land topography is included at around 20m resolution. (A) the Wellington Harbour grid, (B) Kapiti Coast grid and (C) close up view of the Hutt River area showing sea wall and stream channels resolved in the model taken from the Wellington Harbour Grid.
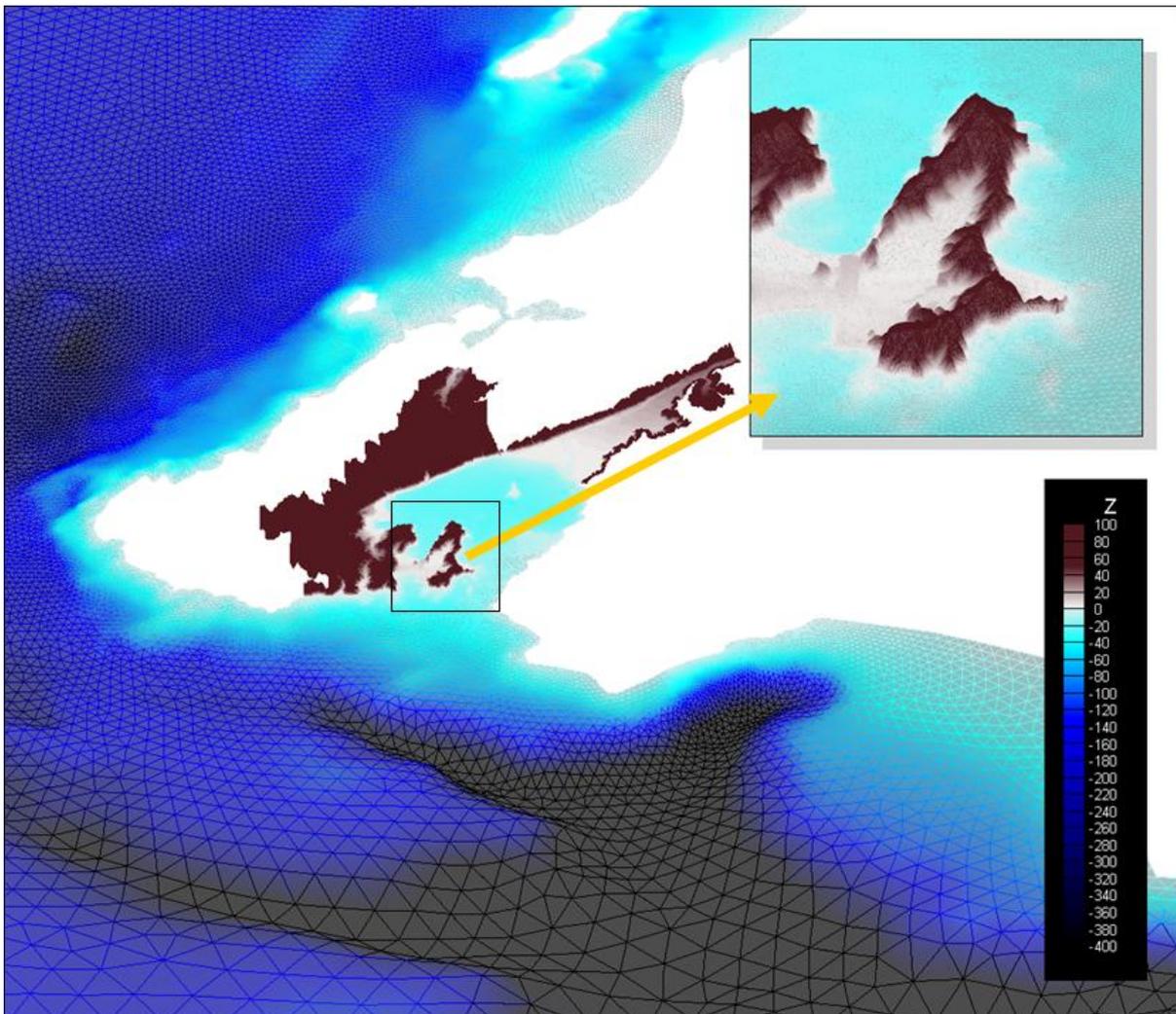
Figure A-3: Perspective view of the bathymetry and topography in and around Wellington Harbour in the existing model grid. The larger image depicts the model grid and bathymetry in Cook Strait, south of Greater Wellington region, and illustrates the extent of the incorporated LiDAR topography around Wellington and the Hutt Valley. The inset illustrates the enhanced grid resolution and seamless transition from sea to land in the Harbour region.

While it is technically possible to simulate tides and storm-surge concurrently, we have found that more reliable simulations of storm surge can be obtained by simulating each separately. This is because different types of boundary conditions are required around the edge of the model domain. Tidal boundary conditions require the water surface elevations around the edge of the model domain to be specified. However, these boundary conditions tend to reflect long-waves, such as those generated by storm surge, back into the domain. Radiation boundary conditions are used for storm surge modelling. This allows energy to radiate out of the model domain. Because tides and storm-surge are generally long-wave phenomena they do not interact significantly. Hence, the error from adding them linearly is generally small.

Storm surge model verification

In this section we compare the storm surge simulations against sea-level measurements made at the Port of Wellington gauge. We also compare the simulated storm surges to extreme-sea-level analyses of the Port of Wellington and Kapiti Island sea-level records, to put the simulated storm-tide levels in context with large historical measurements.

Figure A-4 shows the extreme storm-tide analysis of Stephens et al. (2009) and the corresponding data are shown in Table A-1. The extreme-value analysis suggests that a 1% AEP storm-tide lies

between 1.32–1.35 m (WVD-53) at the Port of Wellington. An extreme-value analysis was undertaken for the Kapiti Island sea-level record (Table A-2), using an extreme-sea-level analysis technique designed for use with short sea-level records (Goring et al. 2010). The Kapiti sea-level recorded was not surveyed to a known datum, so Wellington MSL05–11 = 0.196 m (WVD-53) was assumed to apply, and was added to the extreme sea-levels in Table A-2 before comparing with simulations.
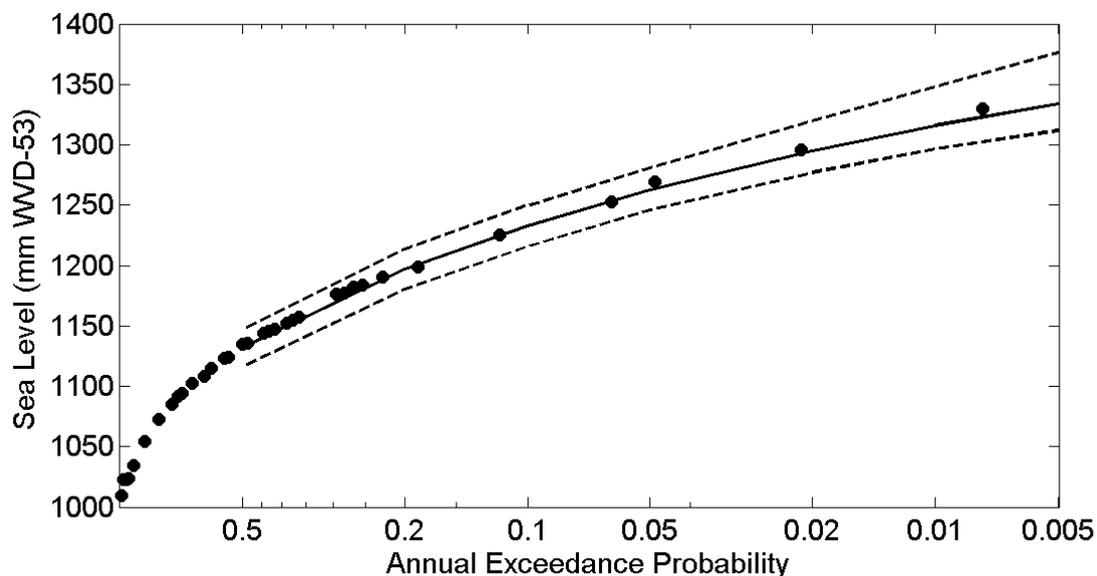
Figure A-4: GEV fit to measured annual maxima sea levels and also including a simulated storm tide of 1.33 m for Queens Wharf on 2 February 1936. From Stephens et al. (2009). The dots mark the annual maxima plotted in their Gringorten (1963) plotting positions. The solid line marks the best-fit of the GEV model to the data. The dashed lines show the 95% confidence intervals for the GEV model.

Table A-1: Extreme storm-tide calculations from analysis of Queens Wharf measurements (Stephens et al. 2009). Results are in m WVD-53 relative to the MLOS over the 1975–2008 period. ARI = average recurrence interval. AEP = annual exceedance probability. C.I. = confidence intervals of GEV fit.

AEP (%)	39	18	10	5	2	1	0.5
ARI (years)	2	5	10	20	50	100	200
Median	1.13	1.20	1.23	1.26	1.30	1.32	1.33
2.5% C.I.	1.12	1.18	1.22	1.25	1.28	1.30	1.31
97.5% C.I.	1.15	1.21	1.25	1.28	1.32	1.35	1.38

Table A-2: Extreme storm-tide calculations from analysis of Kapiti Island sea-level measurements. The Kapiti Island sea-level recorder has not been surveyed to a known datum, so results are relative to the MLOS over the August 1999 – July 2012 period. Add MSL05–11 = 0.196 m (WVD-53) to compare with Figure 6-4. ARI = average recurrence interval. AEP = annual exceedance probability. C.I. = confidence intervals of Monte Carlo Joint Probability fit (Goring et al. 2010).

| AEP (%)	63	39	18	10	5	2	1
ARI (years)	1	2	5	10	20	50	100
Median	1.23	1.29	1.33	1.37	1.41	1.47	1.51
2.5% C.I.	1.22	1.28	1.33	1.36	1.40	1.44	1.47
97.5% C.I.	1.23	1.29	1.34	1.39	1.43	1.49	1.55

Figure A-5: Verification of storm-tide simulations against Port of Wellington tide gauge records. compares the raw simulated storm-tide levels with sea-level gauge data and extreme storm-tide levels, at Port of Wellington. It is seen that measured sea levels were not particularly extreme on any of the days chosen for the inundation level simulations. Measured storm tides approached the 39% AEP level corresponding with the 1975 and 1992 simulations. The extreme storm-tide comparisons agree with joint-probability analyses (e.g., Figure 2-5), which show low joint probability for the simulated events, but higher marginal (storm-tide and wave height) probability (the effects of wave setup are yet to be included in the model–data comparisons, although the Port of Wellington is relatively wave-sheltered, with little wave setup).
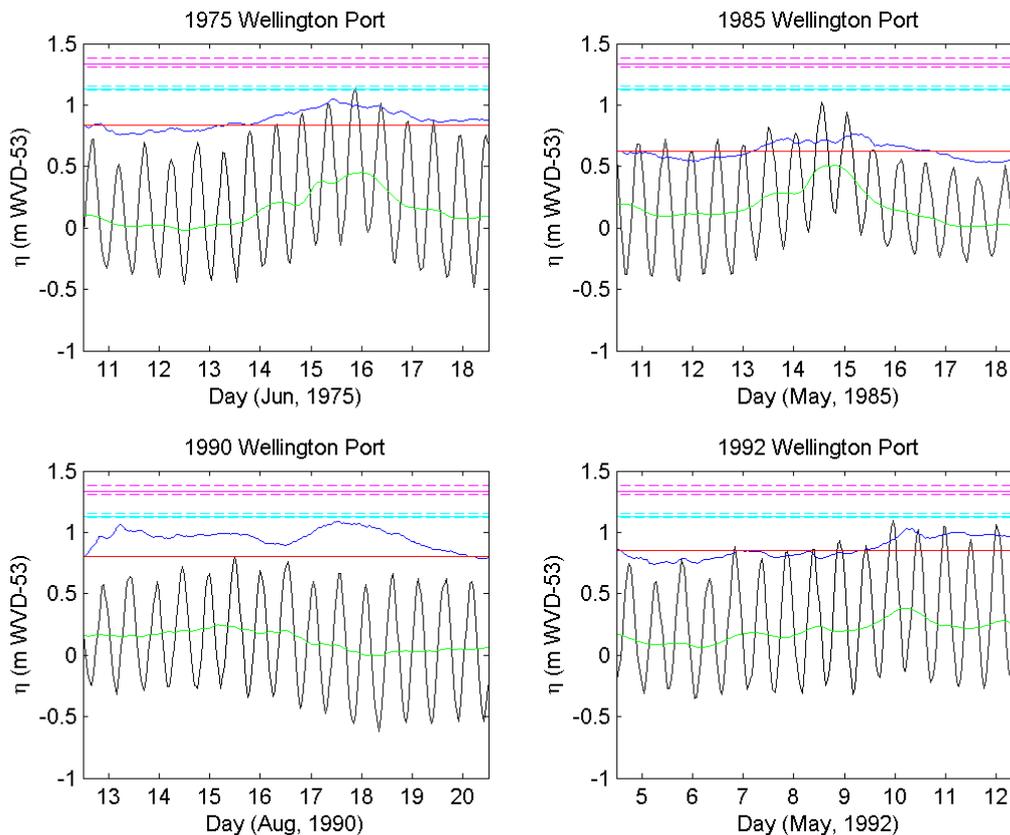
Figure A-5: Verification of storm-tide simulations against Port of Wellington tide gauge records.
Black = Half-hourly tide gauge record; green = storm surge component of measured sea-level; magenta = 1% AEP (100-year ARI) storm tide level (with dashed 95% confidence intervals); light blue = 39% AEP (2-year ARI) storm tide level (with dashed 95% confidence intervals); red = high-tide offset for storm-tide simulation; blue = simulated storm-tide. Wave setup has not been added to the plotted simulated storm tide.

The net water level offsets for the storm-tide simulations were adjusted so that the joint-probability of the waves and storm tides had a 1% joint AEP (Table 2-3). Figure A-6: Verification of storm-tide simulations against Port of Wellington tide gauge records, after scaling MLOS to give a joint wave and storm-tide 1% AEP. compares the simulated storm-tide levels with sea-level gauge data, after the MLOS adjustments to alter the occurrence probability of the simulated events (Figure A-5 differs from Figure A-6: Verification of storm-tide simulations against Port of Wellington tide gauge records, after scaling MLOS to give a joint wave and storm-tide 1% AEP. in that the simulated storm tides do not include the MLOS adjustments). The MLOS adjustments raised the simulated storm-tide levels toward more extreme AEP events, with the simulated storm-tides on 15 June 1975 and 10 May 1992 reaching or exceeding the 39% AEP storm-tide level, and the event on 17 August 1990 reaching the 1% AEP storm-tide level.
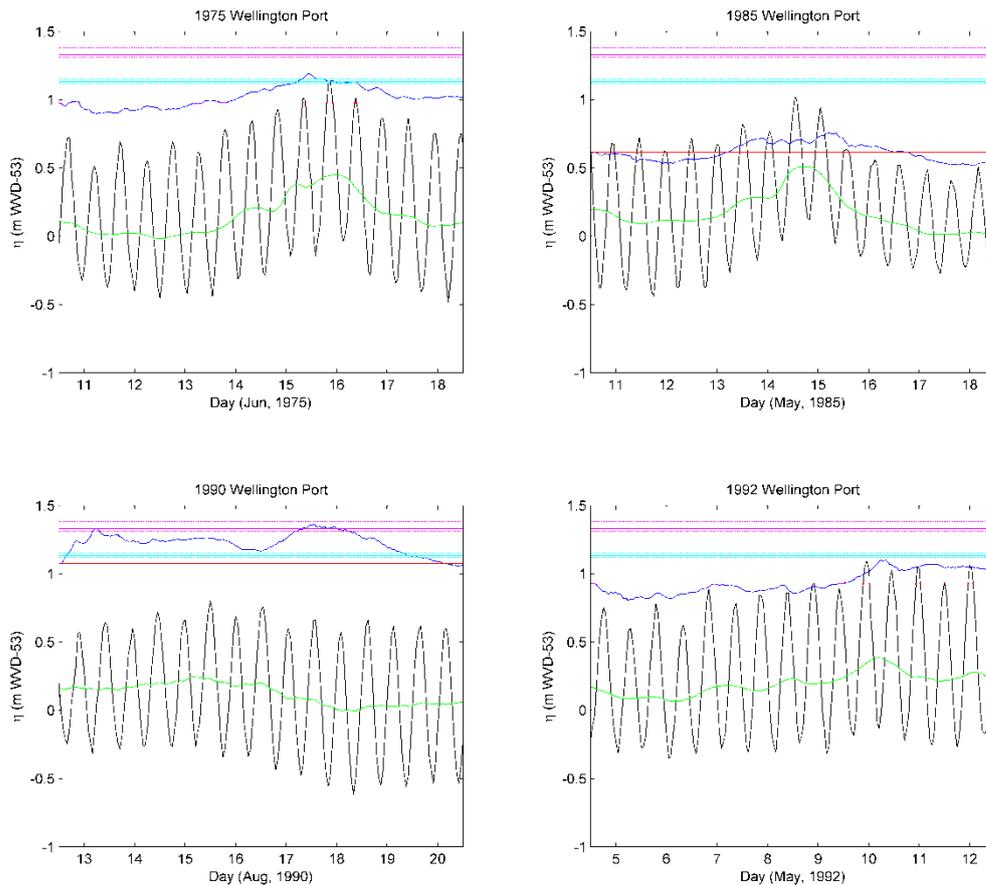
Figure A-6: Verification of storm-tide simulations against Port of Wellington tide gauge records, after scaling MLOS to give a joint wave and storm-tide 1% AEP. The net water level offset for the simulation was adjusted so that the joint-probability of the offshore storm-tide and wave height had a 1% annual exceedance probability (100-year ARI), as explained in Section 2.4.2 and Table 2-3. Black = Half-hourly tide gauge record; green = storm surge component of measured sea-level; magenta = 1% AEP (100-year ARI) storm tide level (with dashed 95% confidence intervals); light blue = 39% AEP (2-year ARI) storm tide level (with dashed 95% confidence intervals); red = high-tide offset for storm-tide simulation; blue = simulated storm-tide. Wave setup has not been added to the plotted simulated storm tide.

None of the historical events simulated for the Kapiti coast overlapped with the Kapiti Island sea-level record (1999–2012), so time-series comparisons cannot be made. However, Figure A-7: Comparison of storm-tide simulations at Otaki against extreme-value analysis of Kapiti Island sea-level records. compares the simulated storm-tides at Otaki with extreme storm-tide levels calculated from the Kapiti sea-level recorder (Table A-2). All of the simulated events on the Kapiti coast had relatively large storm tides, in excess of the 63% AEP (1-year ARI) level. Two of the simulated storm tides reached the 1% AEP (100-year ARI) level, on 12 September 1994 and 12 November 1994, which seems unusual. The September 1994 simulation used a very high net water level offset that was higher than the 63% AEP (1-year ARI) storm-tide level. This occurred because the MLOS offsets were averaged for the Kapiti coast, and because the tide range changes rapidly along this coast, the average between sites 1–3 has resulted in an MLOS adjustment of +0.2 m into the net water level offset, which is large for Otaki. Thus the Kapiti coast storm-tide simulation of September 1994 is conservatively high. The simulated storm-surge in November 1994 was very large at about 0.7 m, compared with the largest recorded storm surge of 0.57 m at Kapiti Island (1999–2012).
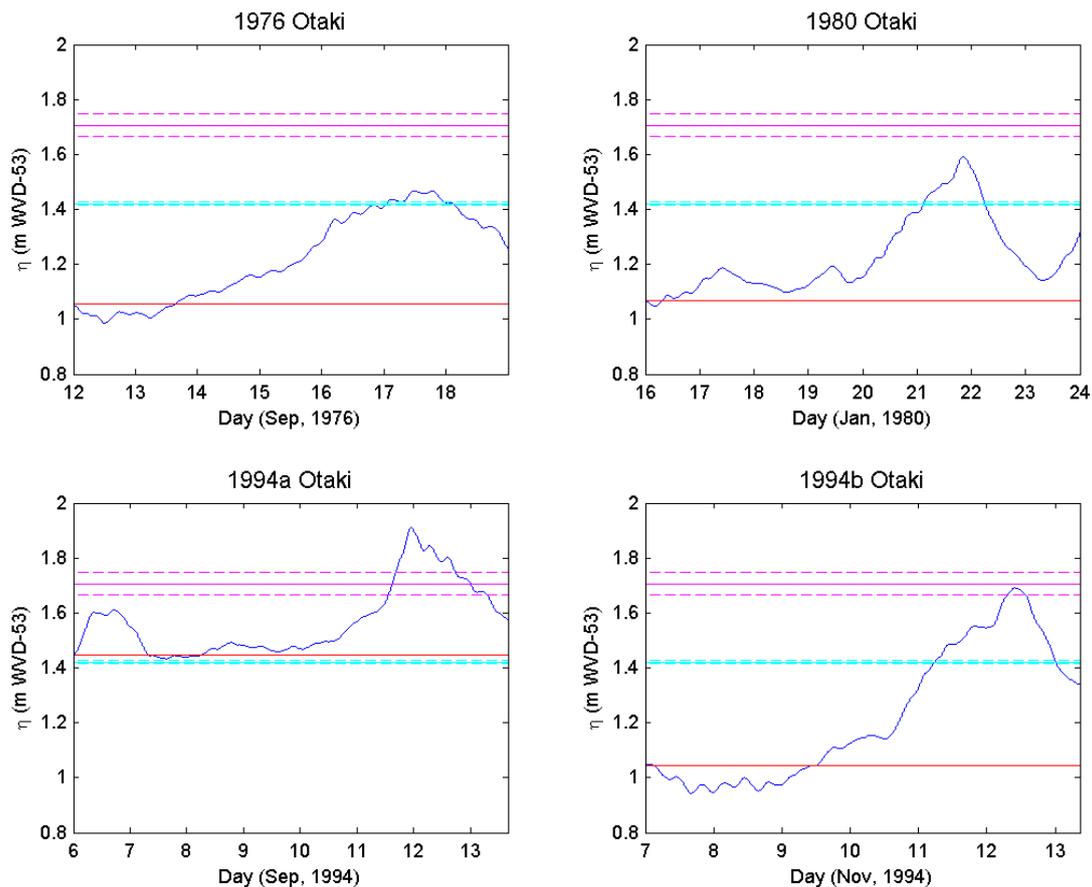
Figure A-7: Comparison of storm-tide simulations at Otaki against extreme-value analysis of Kapiti Island sea-level records. The net water level offset for the simulation was adjusted so that the joint-probability of the offshore storm-tide and wave height had a 1% annual exceedance probability (100-year ARI), as explained in Section 2.4.2 and Table 2 3. A mean-sea-level was unable to be determined for the Kapiti Island sea-level record because the gauge has not been surveyed to datum; therefore the Wellington MSL05–11 = 0.196 m (WVD-53) was added to both the extreme-values and the simulated tide offsets. Magenta = 1% AEP (100-year ARI) storm tide level (with dashed 95% confidence intervals); light blue = 63% AEP (1-year ARI) storm tide level (with dashed 95% confidence intervals); red = net water level offset for storm-tide simulation; blue = simulated storm-tide. Wave setup has not been added to the plotted simulated storm tide.

Comparison of storm events
Water level time series – Wellington

Time series of modelled water levels were recorded at selected locations around the Wellington Harbour (Figure A-8). These time series are taken slightly offshore outside of the surf zone and thus do not include wave setup due to near-shore breaking.

An example of water levels in the middle of Wellington Harbour is shown in Figure A-9. The total simulated water level at Port Wellington is plotted against sea-level measurements in Figure A-6. The simulations were run holding the tidal depth equal to the highest tide on the day of the storm as explained in Section 2.5. The astronomical tides, as calculated from constituents, are shown for reference. The simulations show that the tide has the largest effect on water levels, followed by storm surge caused by wind and pressure. Time series for the other points shown in Figure A-8 are given in Appendix F.
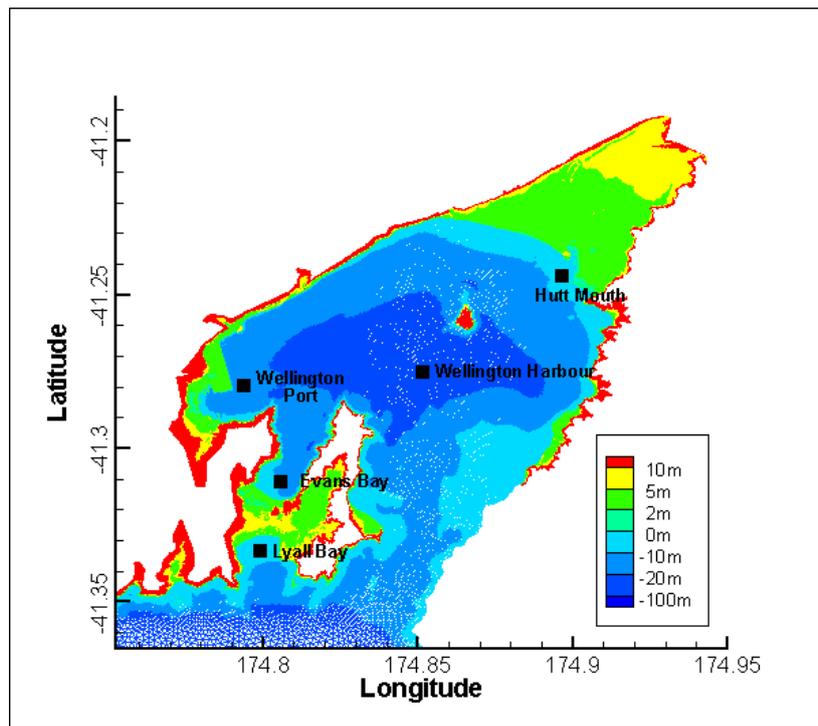

Figure A-8: Locations in the Wellington Harbour grid where water level time-series were recorded during the simulations. Colours show water depth and land elevation.
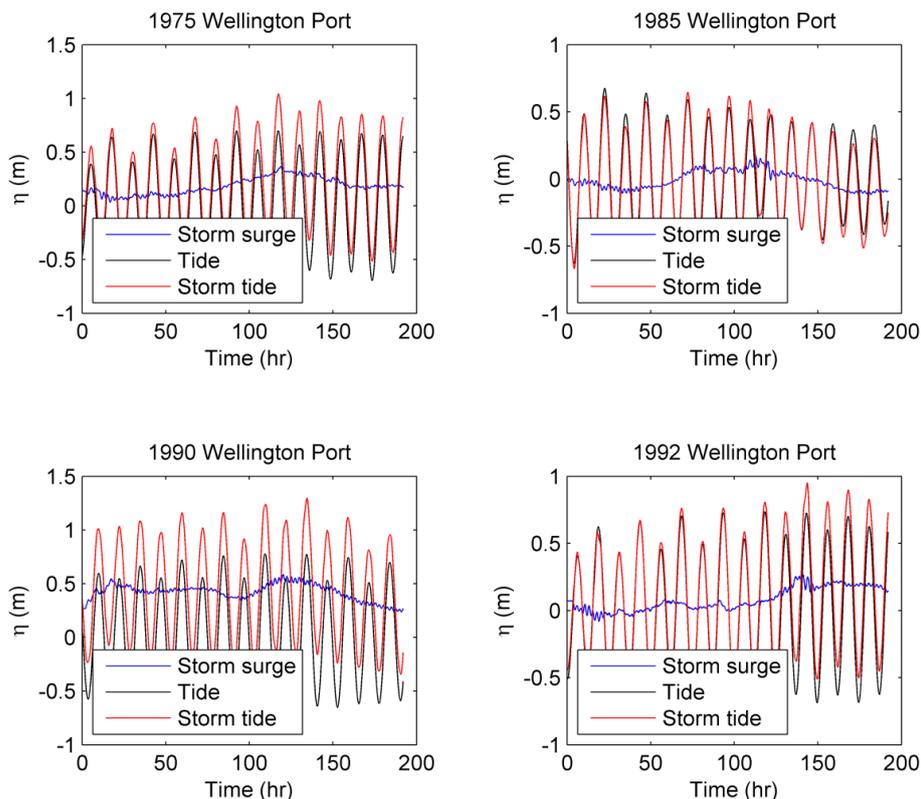
Figure A-9: Time series of simulated water levels in Wellington harbour during the four selected storm events (Table 2-3). The blue lines show the storm surge water level; black lines show astronomic tides and the red lines show the combined storm-tide. The day of the storm of interest starts at 120 hr. Storm surge simulations were run with a fixed tide level equal to the highest tide on the day of the storm as explained in Section 2.5. All water levels are relative to WVD-53.

Water level time-series – Kapiti

Locations where time-series data were recorded in the simulations run on the Kapiti Coast grid are shown in Figure A-10. Time series for Otaki are given in Figure A-11 and time series for the other sites are shown in Appendix G. The largest simulated storm surge at Otaki, Waikanae and Porirua occurred during the 7 November 1994 storm. The maximum simulated storm surge at these sites was 0.71 m, 0.69 m and 0.65 m respectively. However, the combination of higher astronomical tides and greater MLOS adjustment for the 6 September 1994 storm resulted in this event having the greatest storm-tide (tide + storm surge + MLOS). Additionally the tidal amplitude increases toward the north along the Kapiti Coast. In the inundation mapping (Figure 3-6 through Figure 3-8), we adjust the water level for the difference between local high tide at Otaki, Waikanae, Porirua and the reference location at Kapiti Island. The water level is adjusted by +0.09m, -0.02m and -0.28m for Otaki, Waikanae and Porirua respectively. After adjusting for the difference in tidal amplitudes along the coast, the storm-tide reached 1.89 m, 1.78 m and 1.55 m above WVD-53 at Otaki, Waikanae and Porirua respectively.
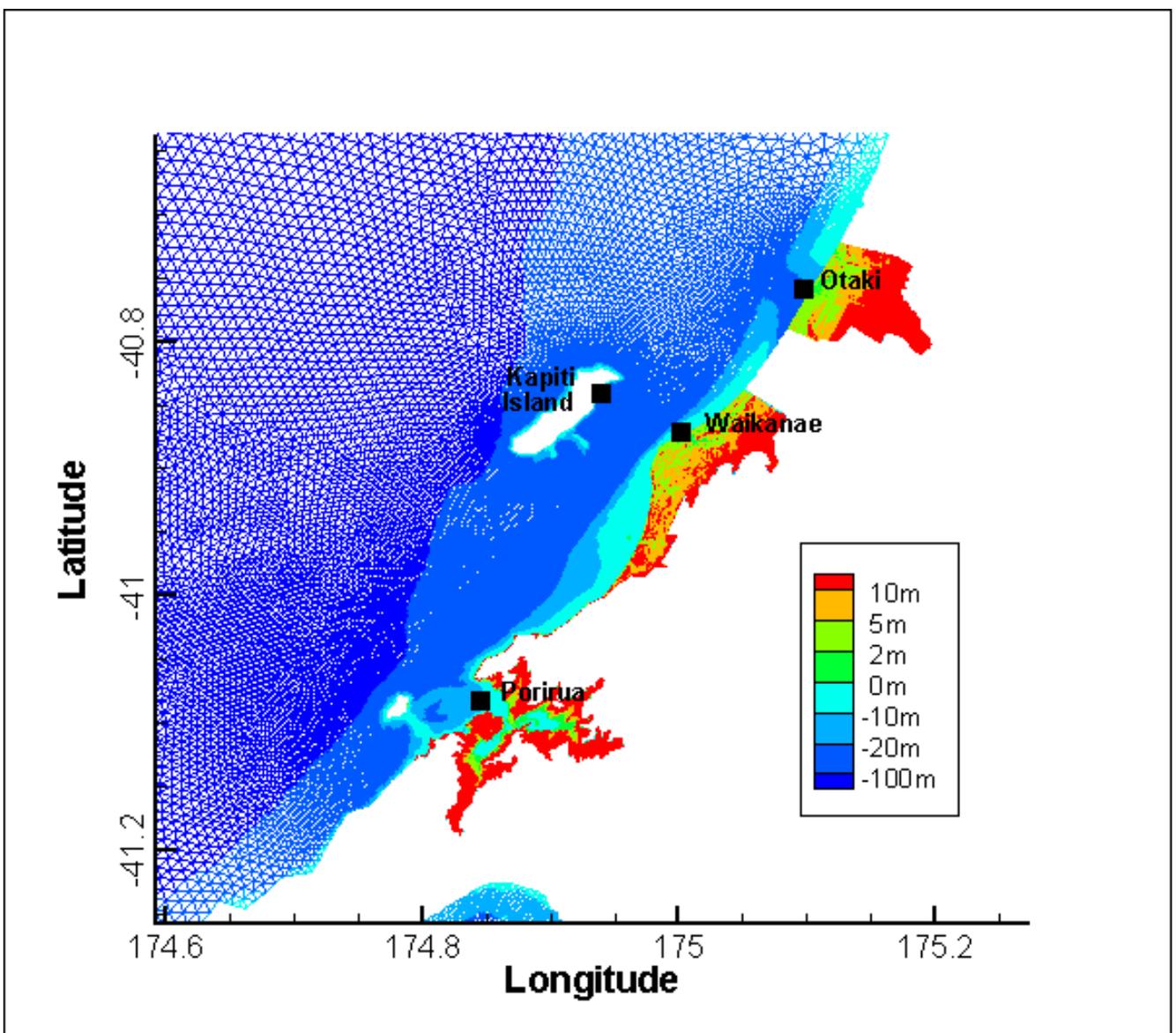
Figure A-10: **Locations on the Kapiti Coast grid where water level time series data were recorded during the simulations.** Colours show land elevation and water depth.

Storm-tide predictions along coast

Storm surge and storm-tide along the entire coastline of the Greater Wellington Region were simulated for the eight storm events (four for the Kapiti coast and four for the south Wellington and east coasts). We used the maximum recorded water levels at points along the coastline, and subtract the constant tide offset added to each simulation. This provided the distribution of storm surge for each event along the coastline. We then calculated the high tide on the day of each event at each location and added this to each point. It was necessary to calculate the high tide at each location because of the substantial variation in tidal range along the Greater Wellington Region coastline, particularly the difference between the east and west coasts. Figure A-12 shows the storm-tide levels along the coast for each of the present-day 1% AEP joint probability scenarios.
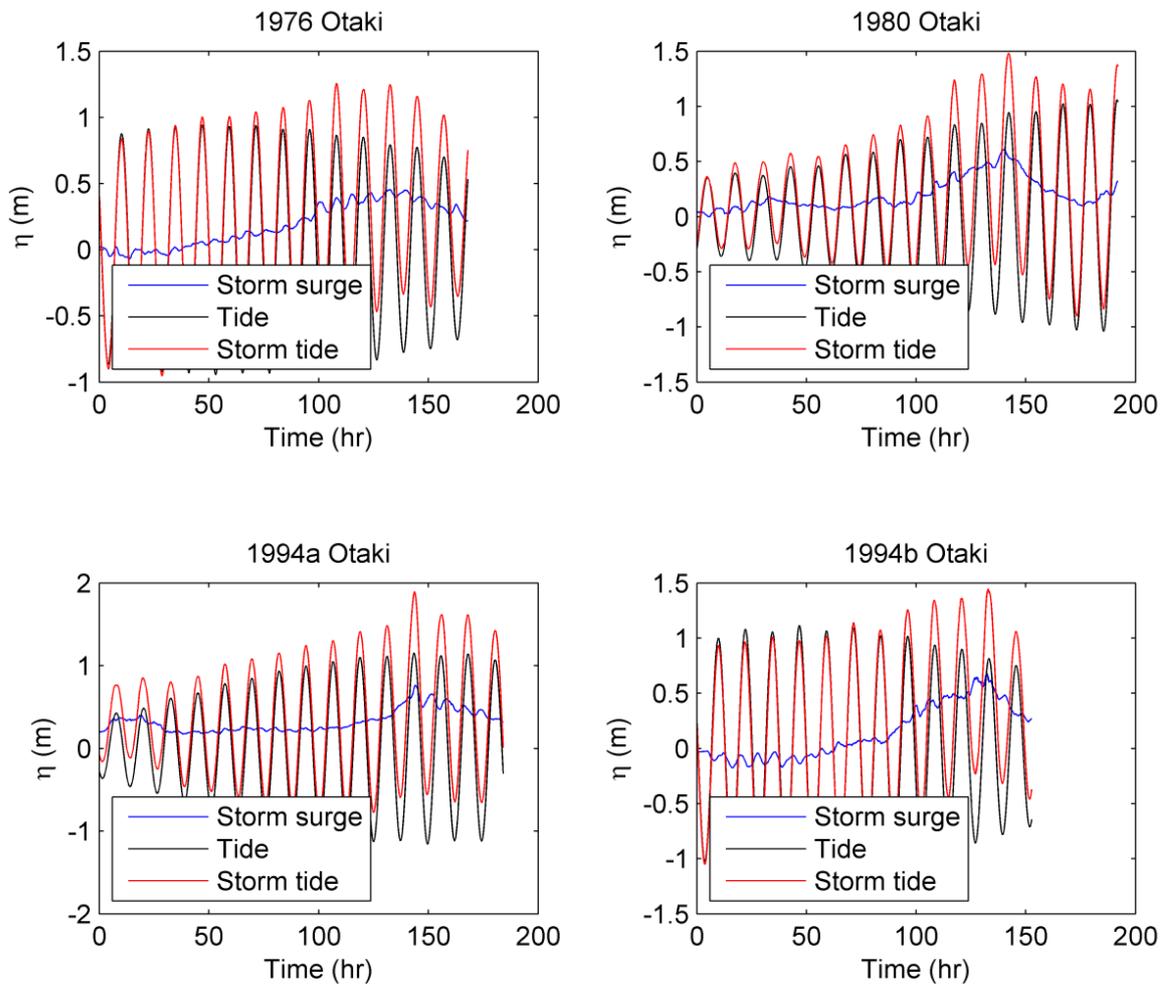
Figure A-11: Time series of simulated water levels at Otaki during the four selected storm events. The blue lines show the storm surge water level; black lines show astronomic tides and the red lines show the combined storm-tide. The day of the storm of interest starts at 120 hr. All water levels are relative to WVD-53. Note that because these time series are taken slightly offshore they do not include wave setup from near-shore breaking.
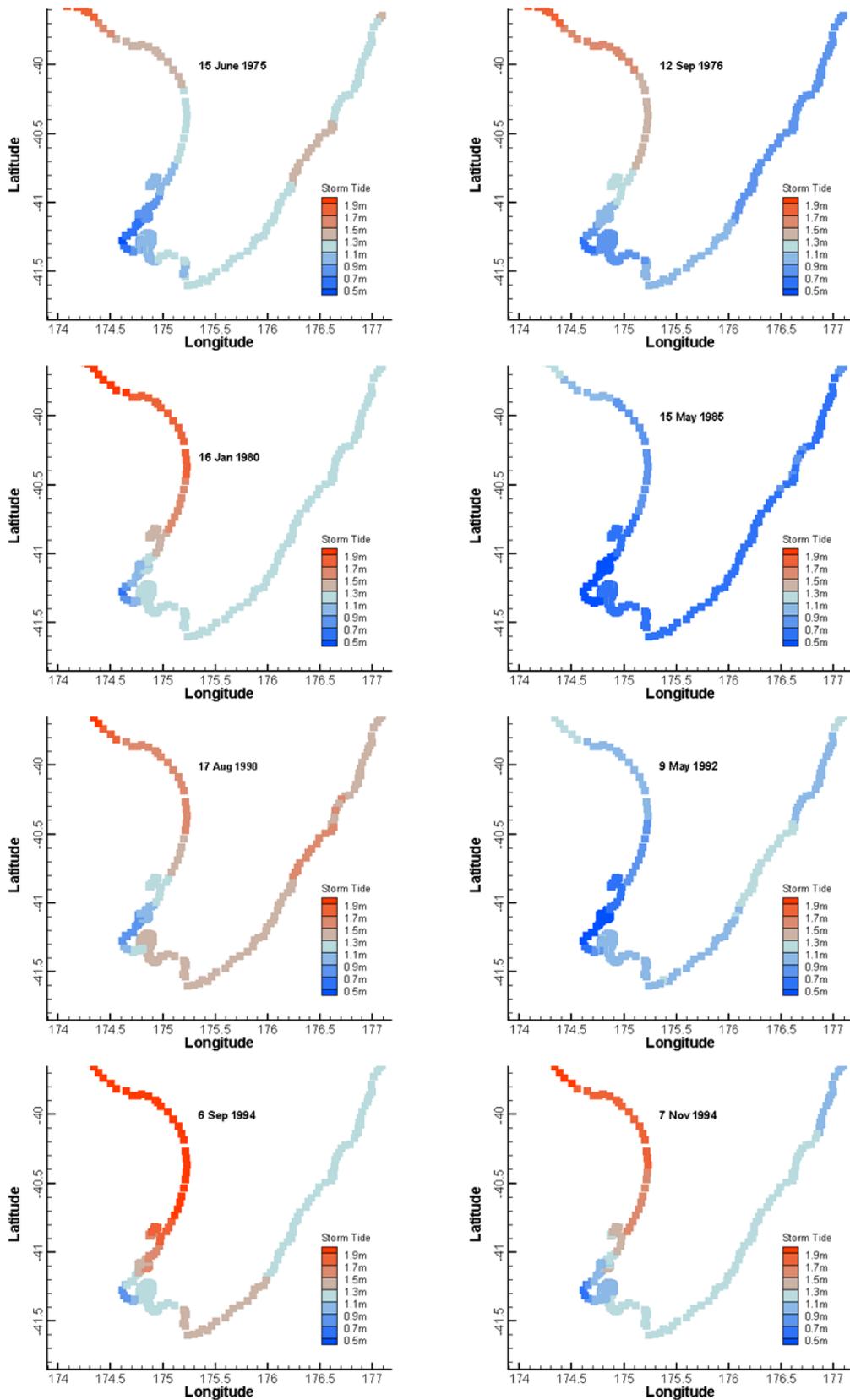
Figure A-12: **Storm-tide levels along the coast for each of the present day 1% AEP joint probability scenarios.**

Appendix B Wave model and wave setup calculation

Wave conditions in the Wellington region were simulated using the SWAN model (Booij et al. 1999; Ris et al. 1999). This is a spectral model in that it describes the sea state in terms of the amount of energy in each band of wave frequency and propagation direction. The model computes the evolution of this wave spectrum by accounting for the input, transfer and loss of energy through the various physical processes. The model accommodates the processes of generation by wind stress, propagation with refraction by the seabed and/or currents, transfer of energy between interacting waves of different frequencies and directions (a nonlinear effect), and dissipation by white-capping, bottom friction and depth-induced breaking. The model can incorporate boundary conditions representing waves arriving from outside the model domain.

As an alternative to the original formulation for rectangular grids, SWAN can now also be implemented on unstructured meshes (Zijlema 2010), and it is this implementation that was used in this project.
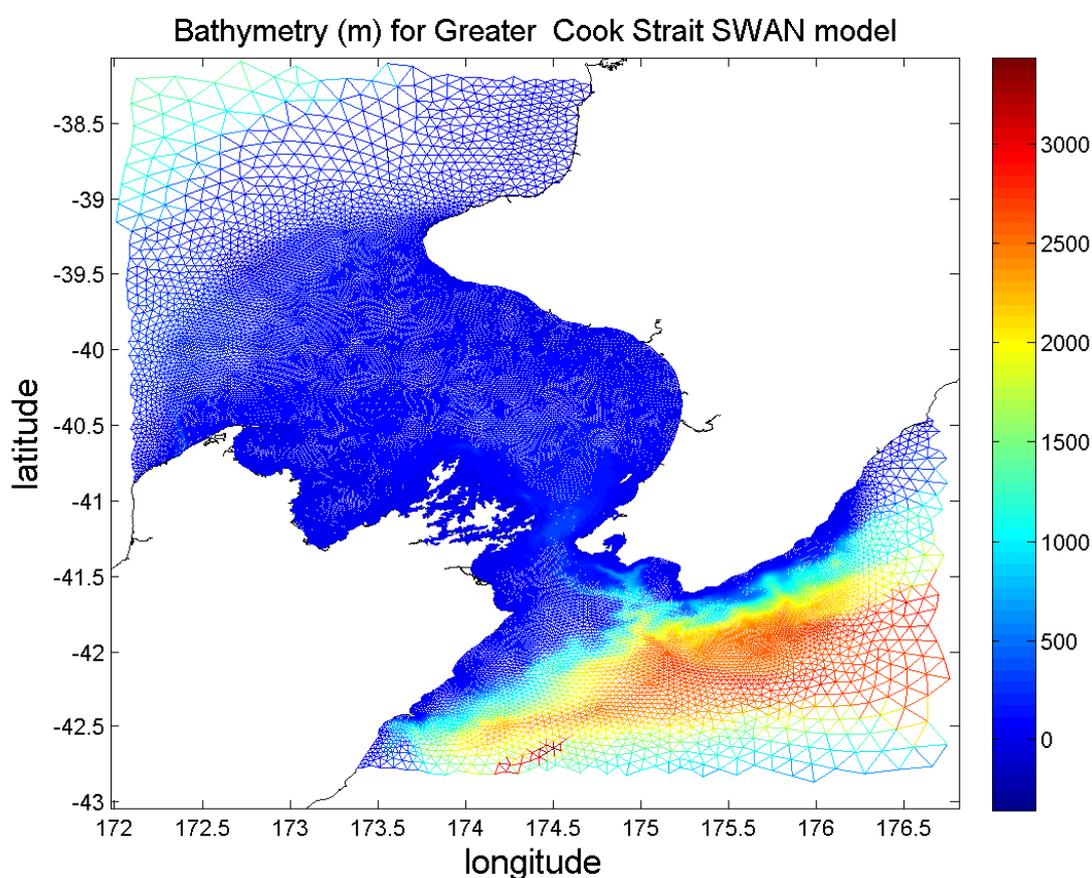
Figure B-1: Computational mesh used for SWAN wave model simulations in the Greater Cook Strait region.

Wave model grid

For consistency, an unstructured mesh was used (Figure B-1) based on a mesh developed for tidal modelling of the New Zealand region using RiCOM as described in Appendix A but with several modifications.

Firstly, the extent of the model domain was reduced to cover only longitudes between 172.125°E and 176.625°E, and latitudes between 42.750°S and 38.250°S. In simulating the sea state in the Greater Cook Strait region it is necessary to include swell arriving from more distant waters,

including in principal very large areas of the Pacific Ocean, Tasman Sea and Southern Ocean. NIWA has a suite of deep-water wave prediction models from global to regional scales that can provide this swell information accurately on an outer domain boundary placed just outside the region of interest. While for the present work higher spatial resolution is needed within the Greater Cook Strait region, there is no advantage for wave simulations in running SWAN on the full domain used in the RiCOM simulations.

The bathymetry in some offshore regions which had been based on relatively sparse data was also updated using the depths interpolated from the ETOPO1 global bathymetry dataset (Amante and Eakins 2009). This had the benefit of reducing some large depth gradients, to which the SWAN model numeric can be sensitive. Some smoothing was also applied to reduce unrealistically-large gradients in some shallow-water locations.

In each node of the spatial grid, the SWAN model solves for a 2-dimensional wave energy spectrum at a set of discrete wave frequencies and propagation directions. In this case 33 wave frequencies were used, from 0.042 Hz to 0.802 Hz, and 24 equally-spaced directions. These extra dimensions make spectral wave models computationally expensive (compared to a two dimensional hydrodynamic model on the same spatial mesh). This also gives a pragmatic reason for using a more limited spatial extent than the full RiCOM mesh, and also for not incorporating into the wave model mesh the increased resolution applied to the Hutt Valley and Kapiti Coast regions in the RiCOM grid for inundation studies (as described in Appendix A).

Boundary conditions

As part of the WASP project, NIWA carried out a hindcast of wave conditions for the period September 1957 through August 2002, forced by inputs from the ERA-40 reanalysis data set (A global re-analysis of the weather spanning the period mid-1957 to mid-2002 produced by the European Centre for Medium-Range Weather Forecasts (ECMWF), Uppala et al. 2005), which provides global six-hourly wind fields at 1.125⁰×1.125⁰ resolution. For the wave simulations, the Wavewatch III™ spectral wave model (Tolman 2009) was run on a global domain at the same resolution as the ERA-40 datasets. Directional wave spectra output from this hindcast were applied on the outer boundaries of the Greater Cook Strait grid to provide a representation of swell entering the region.

Wind forcing

Winds in the Cook Strait region are strongly influenced by topographic forcing as they pass through the gap in mountainous terrain, which causes winds to accelerate and to align in predominantly northerly or southerly directions. The spatial resolution of the ERA-40 data is too coarse to adequately represent these localised effects, which become evident when compared with measured winds, or with wind fields from higher-resolution weather models, such as the NZLAM-12 model used in NIWA's operational forecasting system since 2007.

When applied in a wave model, the inadequate (smooth) representation of wind fields on coarser grids results in significant under-prediction of the waves generated by these winds. Hence we applied a "trained interpolation" technique (described in Appendix D) to downscale the ERA-40 wind fields, using interpolation coefficients derived from regression between coarse-resolution wind fields (from the UK Met Office global model at 120 km resolution) and 12 km resolution NZLAM-12 winds over a one-year period. This trained interpolation was performed on a regular grid with longitudes from 172.125°E to 176.625°E and latitudes from 42.750°S to 38.250°S, both at 0.125° increments to provide input wind fields for the wave model. The SWAN model then internally interpolates input winds from this regular grid to the unstructured computational mesh.
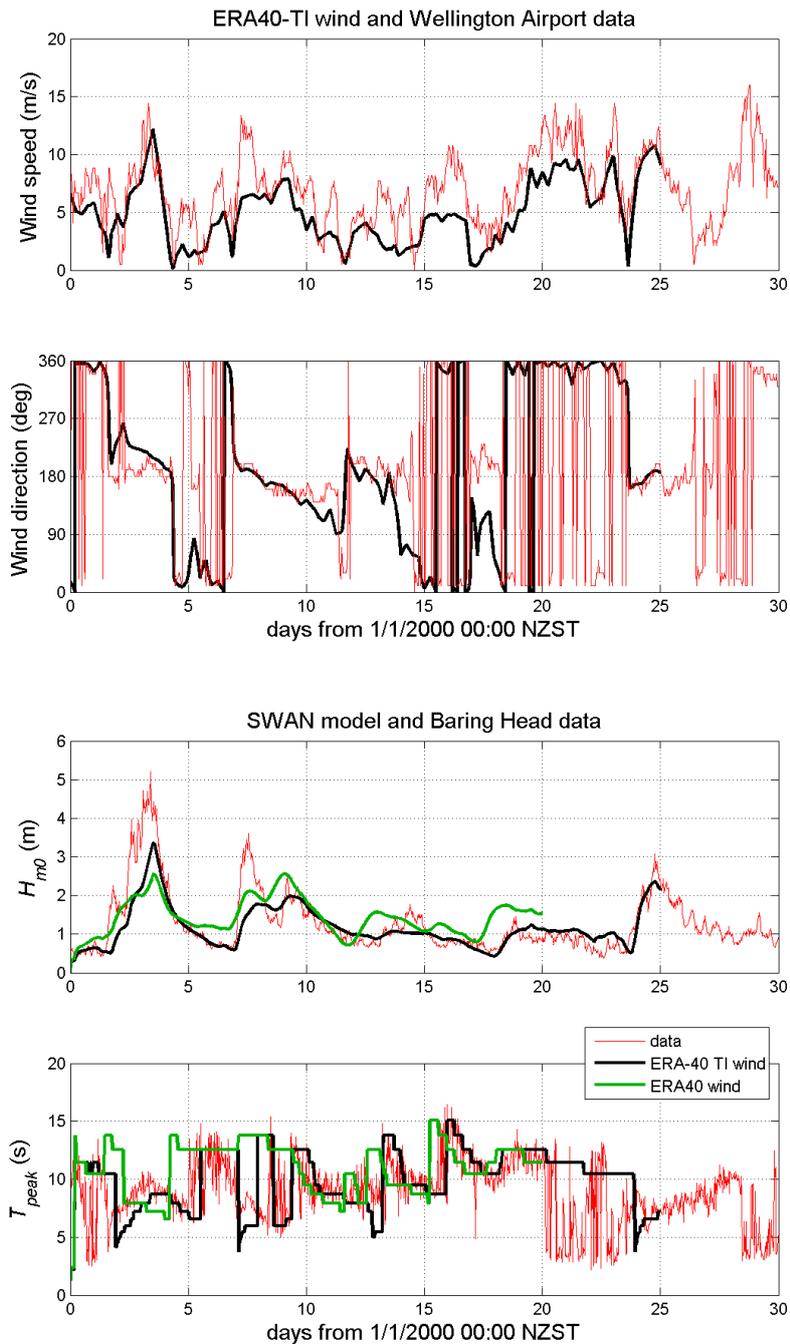
Figure B-2: Comparisons of simulated and measured values of wind and wave properties. (Top) wind speed and direction at Wellington Airport; (bottom) significant wave height and peak wave period at the location of the Baring Head wave buoy. Results of a simulation using input winds derived from ERA-40 wind fields by trained interpolation (black lines) and by standard bilinear interpolation (green lines) are shown.

Wave model verification

Using the inputs described above, the SWAN model was run for a 30-day verification simulation starting from 00:00 NZST on 1 January 2000. Wave model outputs were compared with measurements from NIWA's Baring Head wave buoy, located southeast of Wellington Harbour at (41.4022 ºS, 174.8467ºE). These are shown in Figure B-2 along with comparisons of winds at Wellington Airport.

The simulation period included four periods of northerlies, during which the wave model provided good agreement with the moderate wave heights, indicating a sound representation of swell entering through the southern model boundary. In the early stages of the first period of southerlies

(day 1.5 to 3.0), however, the model winds while of reasonably accurate strength, had a more SSW than southerly direction, and consequently wave heights at Baring Head were under predicted. When the direction of the model winds came into closer agreement with measured Airport winds from day 3.0 to 4.5, better agreement was obtained with the decreasing wave height in the weakening phase of this southerly, which continued into the following northerly period (day 4.5 to 7). In the second southerly period, wind direction was generally accurate but wind speed and hence wave height was initially under predicted (day 7.0 to 8.0), but better agreement in wave statistics was obtained later (day 8.0 on) when either the wind was northerly, or input wind speed matched measured values more closely.
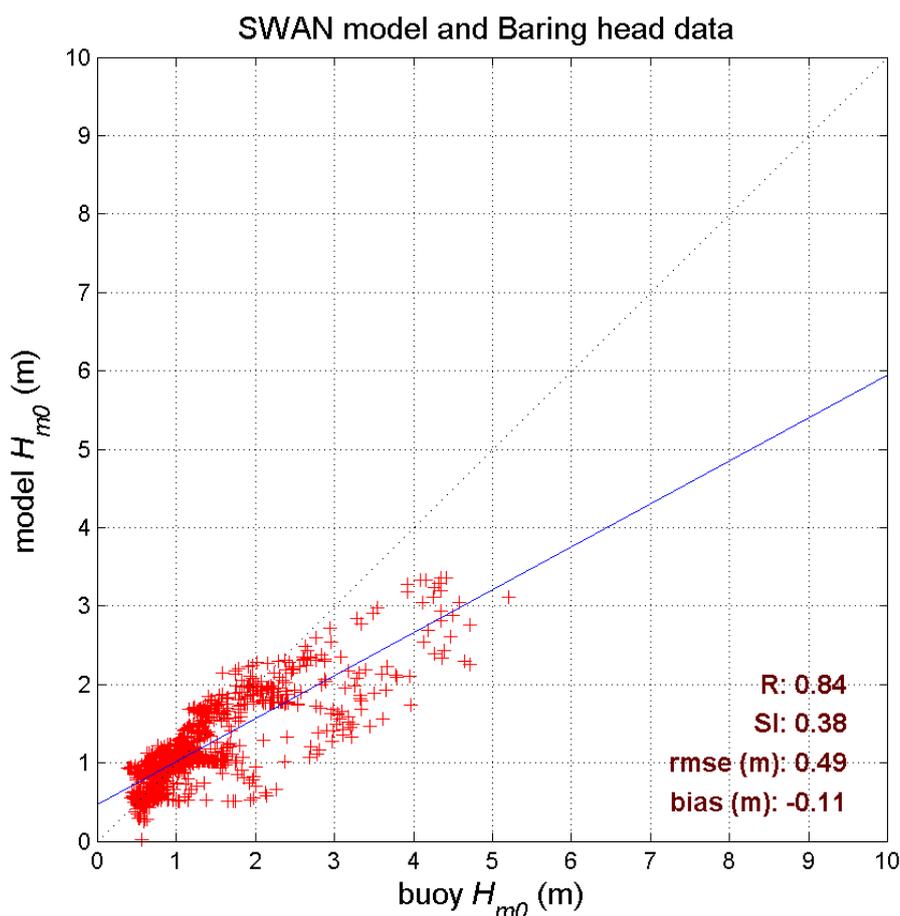
Figure B-3: Scatter plot between measured and simulated significant wave height at Baring Head during the January 2000 simulation.

A scatter plot (Figure B-3) of measured and simulated significant wave heights shows a large number of records, corresponding to moderate wave conditions, that lie close to the equivalence line, but also a significant population of under-predicted heights during more energetic conditions.

In summary, then, we find that the SWAN model simulation is able to give an accurate representation of wave conditions when input wind fields are well-represented, but can under-predict wave conditions during strong southerly events in which the wind is not well reproduced.

Storm event simulations

The SWAN wave model was then applied to simulate wave conditions during 13 historic storm events, with nominal storm peak dates listed in Table B-1. Simulations were set up to start 10 days before 00UT (12:00 NZST) on the day of the peak, to allow adequate spin-up, and were each run for 13 days. Similarly to the verification simulations, input wind fields were derived by trained

interpolation of ERA-40 data to a regular grid at 0.125° resolution, while boundary conditions were provided by directional wave spectra from NIWA's deep-water ERA-40 wave hindcast.

Outputs of wave statistics were produced every three hours over the full unstructured mesh, including significant wave height, mean and peak wave period, mean and peak wave direction, directional spreading, root mean square bed orbital velocity, radiation stress, and the wave-induced force acting on mean currents, for use as inputs to the inundation modelling.

All of the simulated storms occurred at times before the 1995 deployment of the Baring Head Waverider buoy, but four storms (Events 5-8 in Table B-1) overlap the availability of data from the Maui-A platform at (39.55 ºS, 173.45ºE) (Figure B-4). We see that wave height is over-predicted for some of these events, and under-predicted for others. The scatter plot (Figure B-5) shows quite a large scatter, but less consistent under-prediction that was the case for the Baring Head verification (Figure B-3).

The SWAN model simulation enabled near-shore wave conditions to be characterised. However it was found that the spatial resolution of the wave model mesh was insufficient to fully resolve the near-shore wave breaking in all areas where inundation modelling was required. Where the wave breaking is not resolved (often occurring within a single cell), the wave forces are under-represented in the input to the RiCOM model. When this occurred the wave setup was not properly accounted for. To overcome this difficulty, an alternative approach to derive wave setup from the SWAN simulations was used, as described below.

Table B-1: Event numbers and dates of storm events selected for further analysis or modelling.
Blue letters indicate those used for modelling on the Kapiti Grid and red letters indicate those used for modelling on the Wellington grid.

Event No.	storm peak date
1	13/9/1958
2	6/8/1964
3	31/7/1965
4	15/6/1975
5	12/9/1976
6	19/7/1978
7	16/1/1980
8	15/5/1985
9	17/8/1990
10	9/5/1992
11	26/8/1992
12	6/9/1994
13	7/11/1994
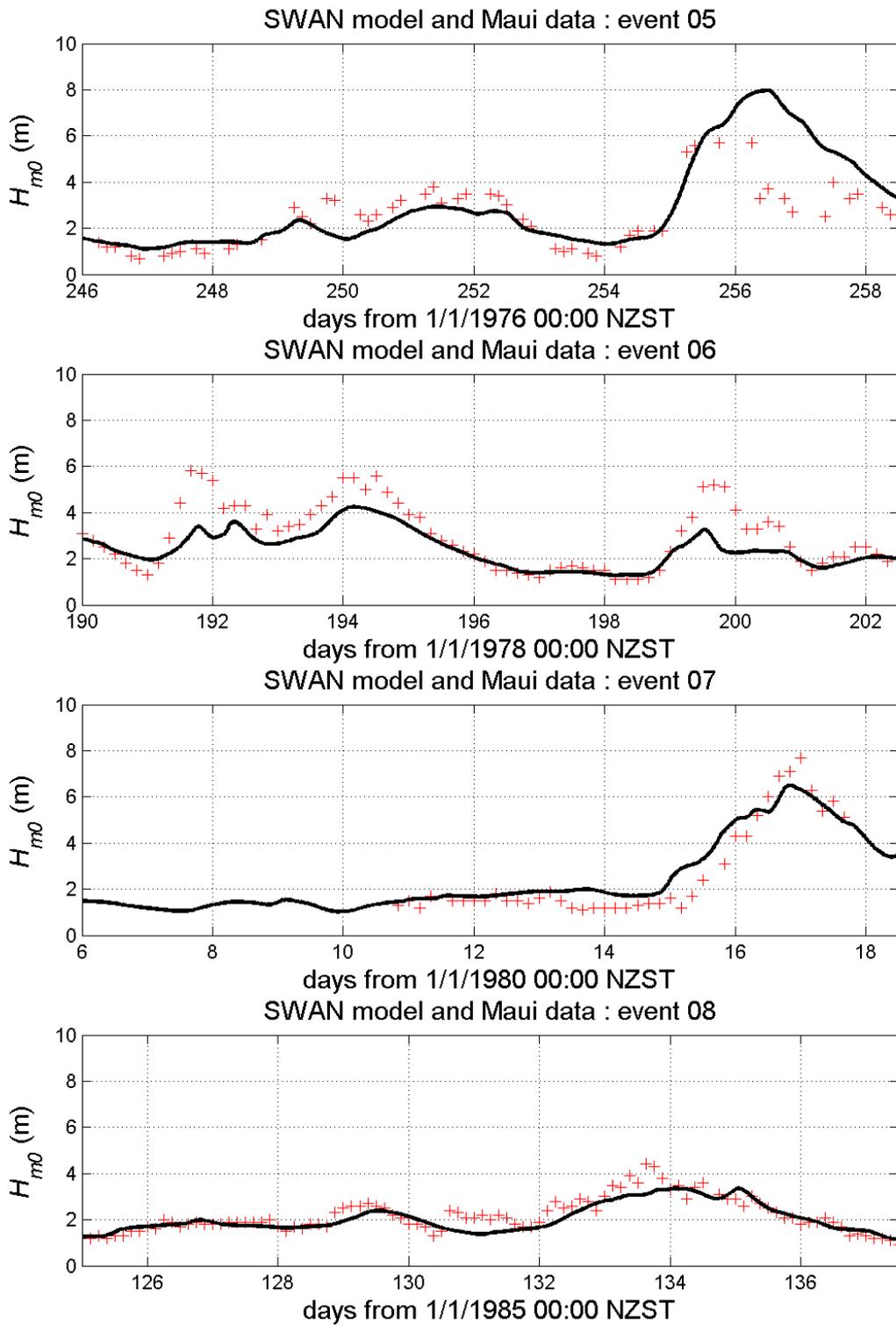
Figure B-4: Comparisons of simulated (black lines) and measured (red crosses) values of significant wave height at the Maui-A platform during four storm events.
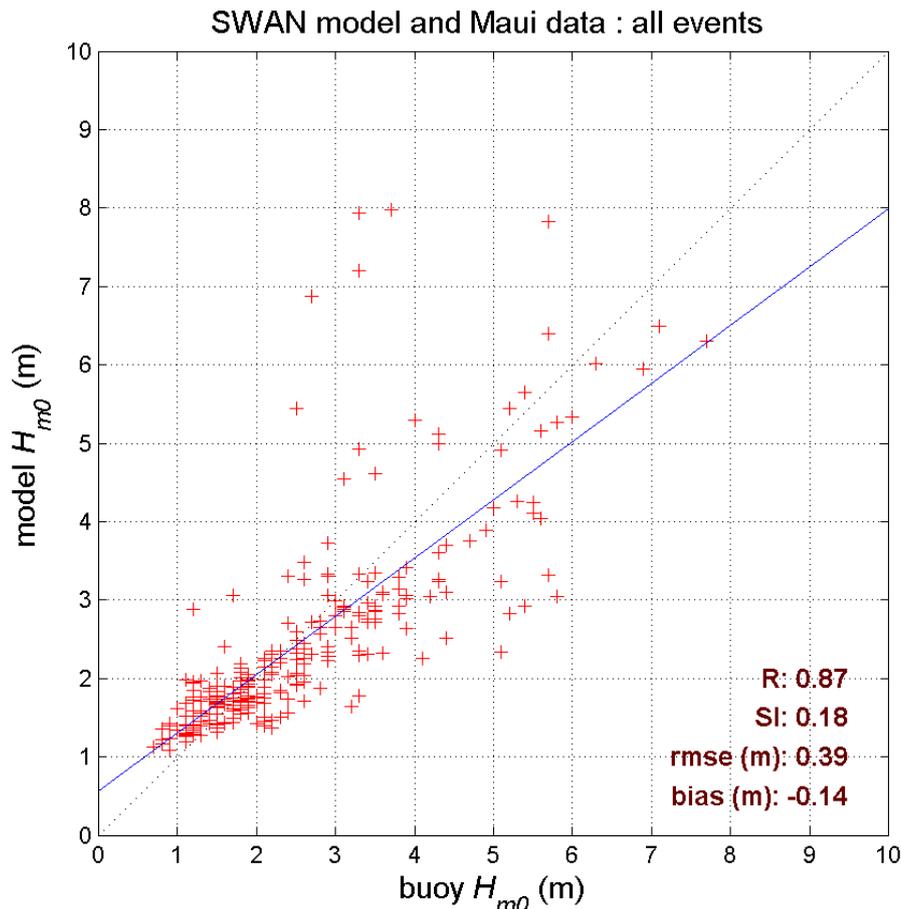
Figure B-5: Scatter plot comparing simulated and measured values of significant wave height at the Maui-A platform during four storm events. The solid blue line shows the linear best fit.

Wave setup and runup

Wave setup is a general rise in the water level near the beach that occurs over periods of several minutes or more due to waves transferring energy and momentum to water in the near-shore surf zone. Wave setup is included in the inundation modelling in this report. Wave runup is the motion of water up and down a beach (also known as "swash") in response to incident waves. Wave runup is transient and usually involves small water volumes so was not included as part of the total storm inundation level.

Wave setup and runup are strongly dependent on foreshore beach slope, for which information is not available at all points along the Wellington region's coast. Where beach slopes β are available, along with the offshore (deep water) significant wave height H_0 and wavelength L_0, wave runup R can be estimated using the relationship {Stockdon et al. 2006}:

$$R = 0.55[H_0 L_0 (0.563\beta^2 + 0.004)]^{1/2} \qquad (B-1)$$

which Stockdon et al. (2006) found to provide the best universal fit to a compilation of runup data from ten separate beach experiments with beach slopes covering a range from $\beta = 0.01$ to 0.11. Note that Equation (B-1) does not include the wave setup which is directly accounted for in the inundation modelling.

Beach slope was estimated for a set of 18 locations on the Greater Wellington coast at which beach profiles were available. Using only locations seaward of the maximum elevation, a linear fit was made to the section of each profile between elevations of 0.0 and +2.0 m above datum

(Wellington Vertical Datum–1953, henceforth referred to as WVD-53); except for some profiles where the elevation range was extended to ensure at least one point above and below +1.0m elevation.

For the purposes of estimating H_0 and L_0, wave statistics in water outside the wave breaking zone are required, at a depth of order 10 m or more. From the unstructured mesh used in the SWAN model, the (positive depth) vertex nearest to the seaward end of each profile was first located. This often corresponded to a depth of less than 10 m. So a second vertex was sought by selecting the vertex of greatest depth neighbouring the first vertex, and, if necessary, repeating until a neighbour with depth greater than 10 m was located.

The highest value of significant wave height H within each modelled event, and the corresponding value of peak period (T_p) were extracted at the two vertices described above and linearly interpolated to 10 m depth (with no extrapolation, i.e. using the vertex closest to 10 m depth where necessary). The corresponding significant wave height H_0 and wavelength L_0 at infinite depth were then calculated, using conservation of energy:

$$H_0^2 c_g(\infty, T_p) = H^2(d)c_g(d, T_p) \qquad\qquad \text{(B-2)}$$

where $c_g(d, T)$ is the group velocity for waves of period T at depth d.

The maximum wave runup during each of the thirteen simulated storm events was estimated for each of the profile locations.

As mentioned above, setup is a change in mean water level that arises as waves shoal and break, exerting a force on the ambient water level. The resulting force can accelerate a current (most likely when the force has a longshore component) or be balanced by a slope in the water surface (most likely for a shoreward-directed force), resulting in the piling up of water (setup) against the beach as well as a lowering of the mean water level (setdown) around the breakpoint. Ideally, all these processes might be simulated by including the wave-induced forces as calculated in the SWAN wave model into inundation modelling carried out with RiCOM. Accurate results will, however, depend on the near-shore breaking zone (typically restricted to tens to hundreds of metres) being well resolved within the model. This was not always found to be the case in the present study.

Where we have accurate detailed beach profiles, a supplementary estimate of wave setup can be made by solving a 1-dimensional version of the force balance problem, neglecting any longshore currents or sea level variation. In this case, the variation of the water level above its mean (still-water) value is a function $\eta(x)$ of the cross-shore distance x, and satisfies the equation

$$\frac{d\eta}{dx} = -\frac{3}{16}\frac{1}{h(x)+\eta(x)}\frac{d(H^2)}{dx} \qquad\qquad \text{(B-3)}$$

where $h(x)$ is the still-water depth, and $H(x)$ is the wave height. The variation of wave height with depth is given by Equation (B-2) above, modified by the further assumption that breaking causes the wave height to be limited to a fixed fraction of the water depth:

$$H(x) < \gamma h(x) \qquad\qquad \text{(B-4)}$$

where $\gamma \approx 0.8$ is a constant.

In order to estimate setup, we took the available profiles (linearly extrapolated offshore to 50 m depth) and, for each storm event, applied the values H_0 and T_p described above at the offshore limit, then numerically integrated the above equations shoreward to obtain the setup ($\bar{\eta}$) at the beach. A mean tidal level of 1 m above Chart Datum was used.

An example is shown in Figure B-6, which shows the cross-shore variation of wave height and setup as waves with an offshore height of 1.6 m progress shoreward. The waves shoal (increase in height) as they encounter shallow water. This results in a small set-down of the mean water level. When the waves start to break and lose height they exert a shoreward force on the surrounding water, creating setup.
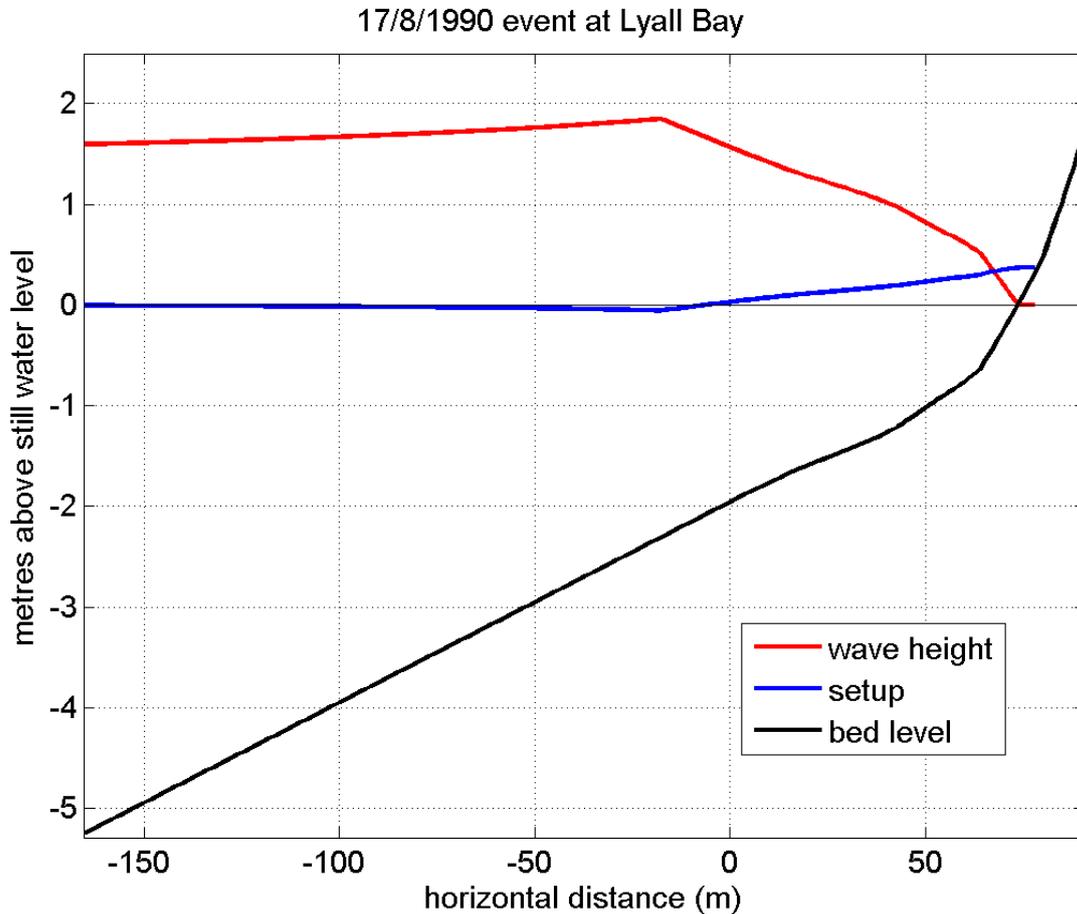

Figure B-6: Cross-shore variation of significant wave height and wave setup at the peak of the 17 August storm event at Lyall Bay. Setup is shown relative to mean still water level, which assumes a tidal sea level of 1.0 m above Chart Datum.

The method outlined above enabled estimates of setup to be made for the locations where beach profiles are available, but we would like to extend this information to other parts of the coast. In order to do this we note that empirical studies (Stockdon et al. 2006; Senechal et al. 2011) on beaches indicate that the scaling of wave setup R with offshore wave parameters can be well represented in the form

$$\bar{\eta} = K\sqrt{H_0 L_0} \tag{B-5}$$

Here *K* is a parameter that may depend on the properties of the beach, perhaps including a linear dependence on some measure of beach slope. We were able to estimate *K* at our profile sites from average values of $\bar{\eta}/\sqrt{H_0 L_0}$, then assuming this would vary slowly along the coast, interpolated K from the profile locations to the other coastal output sites. These values were then applied to estimate setup using Equation (B-5).
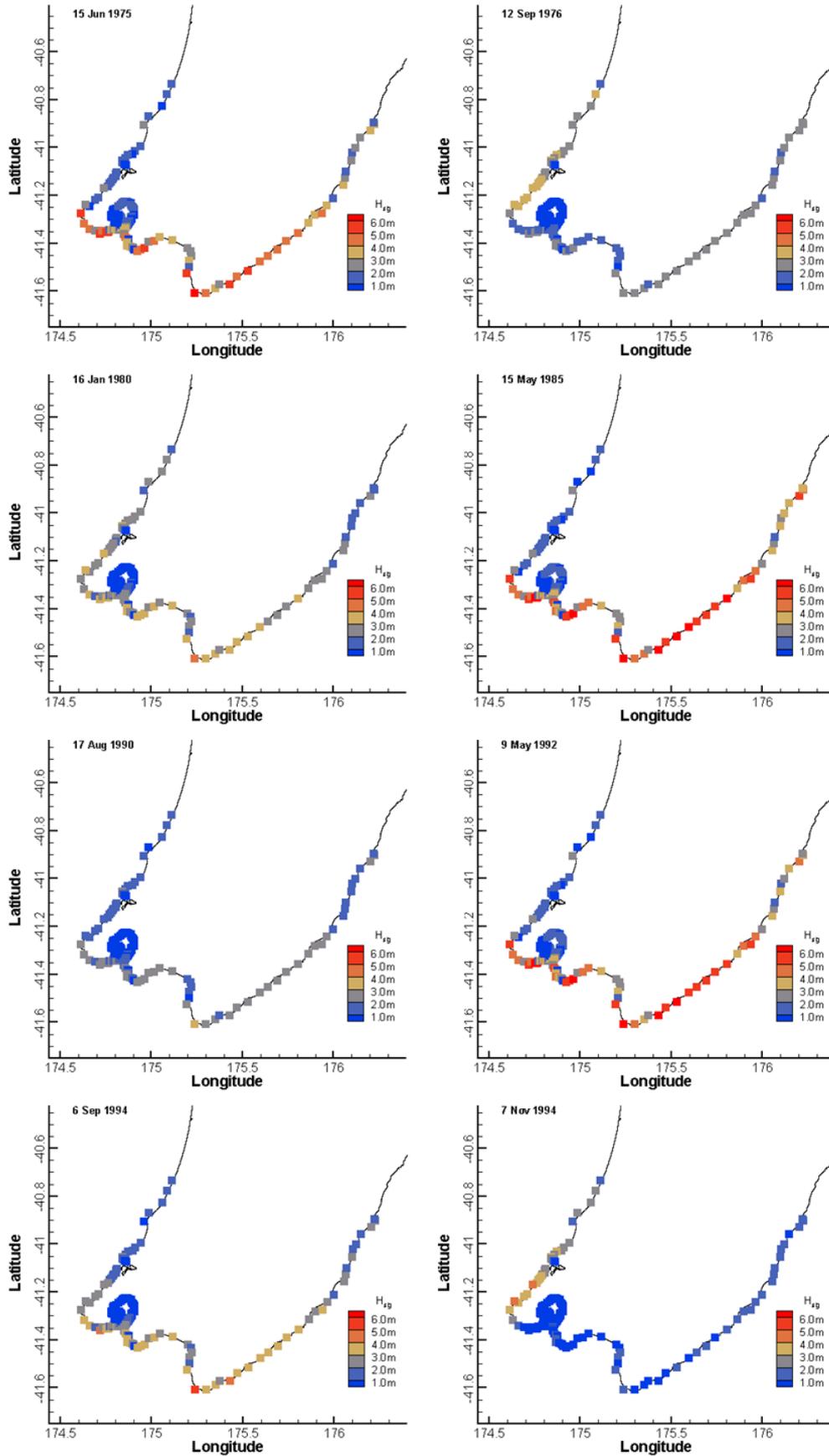
Figure B-7: Distributions of significant wave heights around the Greater Wellington Region coast line for several storm events. The maximum significant wave heights on the day of each storm are shown.

Wave heights along coast

The distributions of maximum significant wave heights around the Greater Wellington Region are shown for each of the eight storm events in Figure B-8. These maps show that the south-eastern coastline generally experiences the largest storm waves (>6 m) while the Kapiti Coast is generally sheltered in comparison. This is the opposite of the pattern for storm-tide that generally is higher along the Kapiti coast than the south-east coast.

A plot of the maximum significant wave height for each storm is plotted against distance along the coast in Figure B-8. East of Oteranga Bay, the 15 May 1985 and 8 May 1992 events produced the largest waves, with significant wave heights reaching close to 7 m in places. To the west and northward along the Kapiti Coast, the 7 November 1994 event produced the largest significant wave heights, closely followed by the 12 September 1976 and 16 January 1980 events. The storm events producing the largest significant wave heights along the Kapiti Coast generally produced similar sized waves along the southern and eastern coastline. The events producing large waves east of Oteranga Bay produce smaller waves (generally < 2 m) along the Kapiti Coast.

Wave runup and setup estimates

Wave runup estimates for the beach profile locations are provided in Figure B-9 and in Figure B-10. The runup estimates are provided for all thirteen events identified in the Joint Probability Analysis given in Table B-1. These include five additional storms that were not modelled for storm surge. We note, however, that several of the profiles (Eastbourne, Te Horo, Titahi Bay and Paraparaumu) have estimated slopes much steeper than the largest slope considered in the data set considered by Stockton et al. (2006). Hence estimates for those sites (shaded grey in **Error! Reference source not found.** and Table B-3) cannot be considered reliable. Two other locations (Evans Bay and Pukerua Bay) had estimated slopes slightly above the valid range, so must also be treated with some caution.

For sites in and near Wellington Harbour, the largest runups were produced during the 15 May 1985 storm, followed closely by the events of 31 July 1964 and 9 May 1992. For sites along the Kapiti Coast, the largest runups were produced by the 12 September 1976 event.

Maximum wave setup at the profile locations is listed for each storm event in Table B-3, while Figure B-9 shows both runup and setup values at the profile locations. Figure B-10 shows examples of the variation of offshore significant wave height and estimated wave setup through two storm events: the 15 May 1985 event at Raumati, and the 17 August 1990 event at Lyall Bay (the event causing the highest setup for that location).
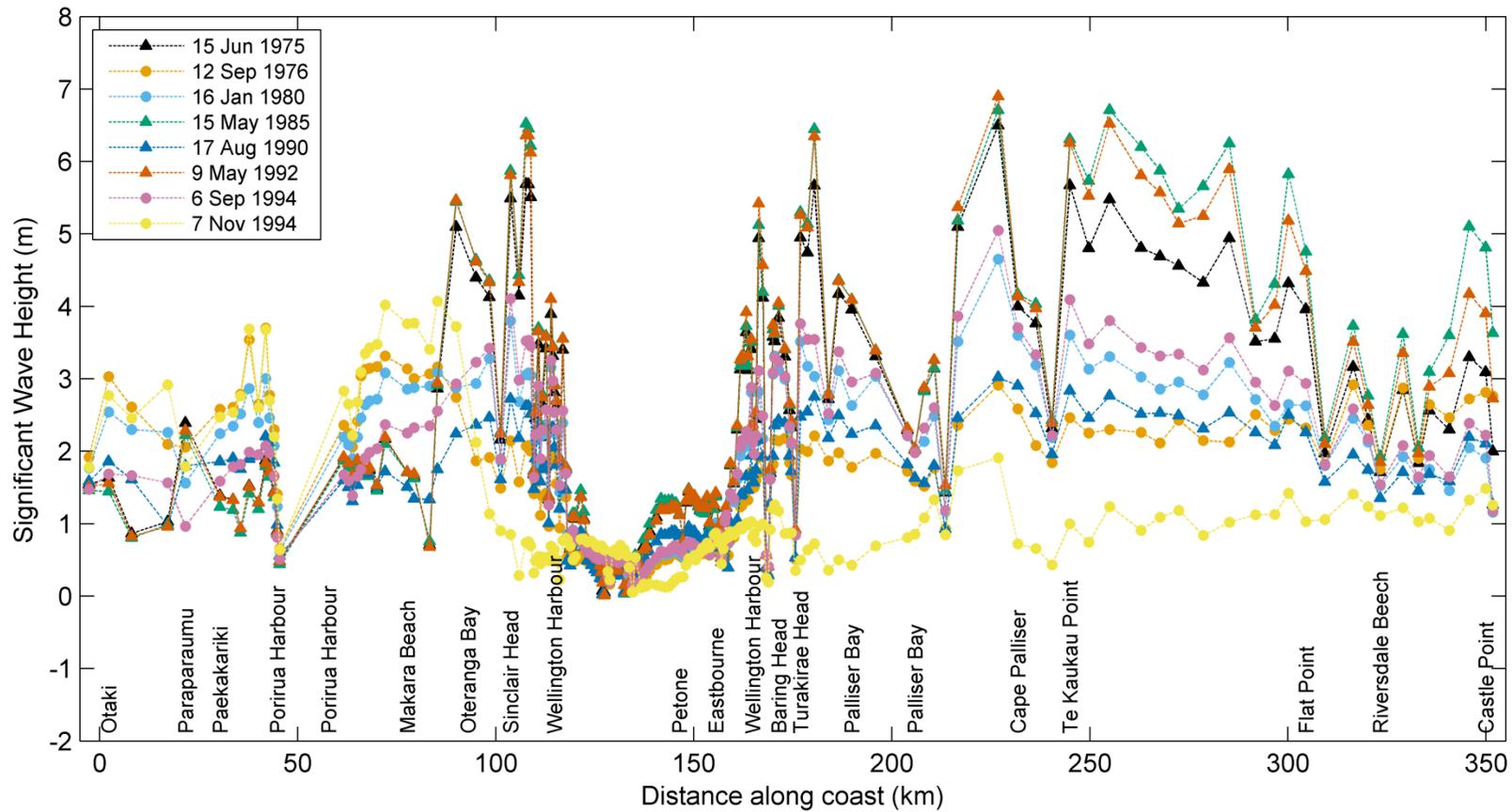
Figure B-8: Maximum significant wave heights along the Greater Wellington Region coastline for the eight historic storm scenarios. Distances along the coast are measured from Otaki (left) to Castle Point (right). Various locations along the coast are also plotted. The two entries for Porirua Harbour and Wellington Harbour mark the harbour entrances. Similarly the two entries for Palliser Bay indicate the extent of the opening to the bay Triangles are used for events selected for detailed modelling of the Wellington Harbour area, and circles for events selected for the Kapiti Coast.

Table B-2: Estimated maximum wave runup (m) during the simulated storm events at each of the beach profile locations. Data for locations with beach profiles much larger than the range considered by Stockdon et al. (2006) are shaded grey.

	profile location	slope	event												
No	Name	β	13-9-58	6-8-64	31-7-65	15-6-75	12-9-76	19-7-78	16-1-80	15-5-85	17-8-90	9-5-92	26-8-92	6-9-94	7-11-94
1	Lyall Bay	0.053	0.48	0.64	0.89	0.82	0.42	0.60	0.99	0.97	0.47	0.89	0.87	0.88	0.69
2	Island Bay	0.094	0.76	1.10	1.57	1.41	0.68	1.01	1.39	1.73	0.77	1.57	1.48	1.45	0.50
3	Owhiro Bay	0.095	0.74	1.10	1.60	1.44	0.66	1.01	1.38	1.77	0.75	1.60	1.51	1.45	0.49
4	Houghton Bay	0.099	0.70	0.97	1.50	1.33	0.63	0.88	1.26	1.65	0.69	1.49	1.36	1.30	0.47
5	Evans Bay	0.127	0.11	0.11	0.11	0.16	0.14	0.14	0.17	0.10	0.20	0.06	0.17	0.16	0.20
6	Eastbourne	0.238	0.46	0.42	1.67	1.53	0.42	0.97	0.62	1.68	0.67	1.67	1.22	1.40	0.39
7	Otaki Beach	0.023	0.67	0.50	0.73	0.50	1.09	0.81	0.63	0.53	0.75	0.48	0.72	0.44	0.68
8	Otaki River	0.038	0.72	0.54	1.04	0.49	1.14	0.87	0.68	0.53	0.81	0.45	0.76	0.59	0.76
9	Te Horo	0.384	3.06	2.31	4.37	1.98	5.23	3.64	3.03	1.79	3.55	1.63	3.16	2.05	3.30
10	Waikanae	0.060	0.76	0.61	1.01	0.51	1.35	0.89	0.81	0.59	0.87	0.31	0.49	0.54	0.88
11	Waikanae River	0.043	0.06	0.05	0.05	0.07	0.09	0.06	0.09	0.03	0.09	0.02	0.07	0.07	0.11
12	Raumati	0.100	0.24	0.14	0.36	0.36	0.65	0.22	0.36	0.43	0.26	0.36	0.28	0.28	0.47
13	Paekakariki	0.030	0.71	0.49	0.57	0.55	1.09	0.81	0.68	0.58	0.80	0.55	0.41	0.51	0.81
14	Karehana Bay	0.027	0.53	0.40	0.57	0.38	0.90	0.49	0.53	0.25	0.67	0.23	0.37	0.38	0.63
15	Titahi Bay	0.373	2.30	1.46	1.42	1.67	3.53	1.45	2.30	1.57	2.19	1.41	1.69	1.68	2.83
16	Titahi Bay Nth	0.011	0.66	0.42	0.45	0.44	0.99	0.63	0.62	0.47	0.76	0.44	0.32	0.40	0.70
17	Paraparaumu	0.411	0.25	0.24	0.21	0.32	0.38	0.25	0.40	0.12	0.39	0.10	0.32	0.30	0.49
18	Pukerua Bay	0.127	1.14	0.84	1.23	0.78	1.95	1.02	1.19	0.69	1.43	0.65	0.75	0.76	1.46

Table B-3: Estimated wave setup (m) during the simulated storm events at each of the beach profile locations. Data for locations with beach profiles much larger than the range considered by Stockdon et al. (2006) are shaded grey.

No.	Name	13-9-58	6-8-64	31-7-65	15-6-75	12-9-76	19-7-78	16-1-80	15-5-85	17-8-90	9-5-92	26-8-92	6-9-94	7-11-94
profile location							**event**							
1	Lyall Bay	0.37	0.37	0.56	0.55	0.30	0.42	0.46	0.57	0.37	0.56	0.53	0.48	0.25
2	Island Bay	0.56	0.61	0.99	0.95	0.46	0.70	0.70	1.02	0.57	0.99	0.89	0.75	0.35
3	Owhiro Bay	0.53	0.60	1.02	0.98	0.43	0.69	0.68	1.05	0.54	1.02	0.91	0.74	0.33
4	Houghton Bay	0.45	0.47	0.86	0.81	0.37	0.52	0.55	0.89	0.45	0.86	0.73	0.59	0.30
5	Evans Bay	0.07	0.06	0.07	0.10	0.08	0.09	0.11	0.05	0.13	0.03	0.10	0.10	0.13
6	Eastbourne	0.16	0.13	0.32	0.31	0.13	0.20	0.20	0.32	0.18	0.32	0.26	0.20	0.16
7	Otaki Beach	0.48	0.38	0.56	0.50	0.75	0.52	0.57	0.53	0.51	0.48	0.47	0.40	0.65
8	Otaki River	0.50	0.39	0.55	0.47	0.73	0.52	0.59	0.50	0.53	0.45	0.48	0.42	0.66
9	Te Horo	0.42	0.36	0.47	0.40	0.74	0.44	0.58	0.40	0.48	0.36	0.40	0.38	0.67
10	Waikanae	0.44	0.39	0.43	0.45	0.81	0.44	0.65	0.32	0.55	0.23	0.41	0.42	0.77
11	Waikanae River	0.08	0.07	0.07	0.11	0.13	0.08	0.14	0.07	0.14	0.06	0.11	0.10	0.18
12	Raumati	0.19	0.11	0.31	0.31	0.31	0.19	0.22	0.36	0.22	0.30	0.22	0.14	0.26
13	Paekakariki	0.50	0.34	0.62	0.59	0.71	0.49	0.54	0.64	0.54	0.57	0.46	0.37	0.64
14	Karehana Bay	0.32	0.30	0.32	0.35	0.54	0.33	0.48	0.26	0.42	0.23	0.33	0.35	0.57
15	Titahi Bay	0.29	0.25	0.28	0.33	0.48	0.25	0.45	0.29	0.41	0.26	0.34	0.34	0.57
16	Titahi Bay Nth	0.50	0.36	0.54	0.51	0.69	0.42	0.62	0.56	0.56	0.51	0.39	0.43	0.73
17	Paraparaumu	0.05	0.05	0.04	0.08	0.10	0.05	0.11	0.05	0.11	0.04	0.09	0.08	0.16
18	Pukerua Bay	0.47	0.40	0.46	0.48	0.79	0.44	0.66	0.38	0.60	0.35	0.46	0.46	0.82
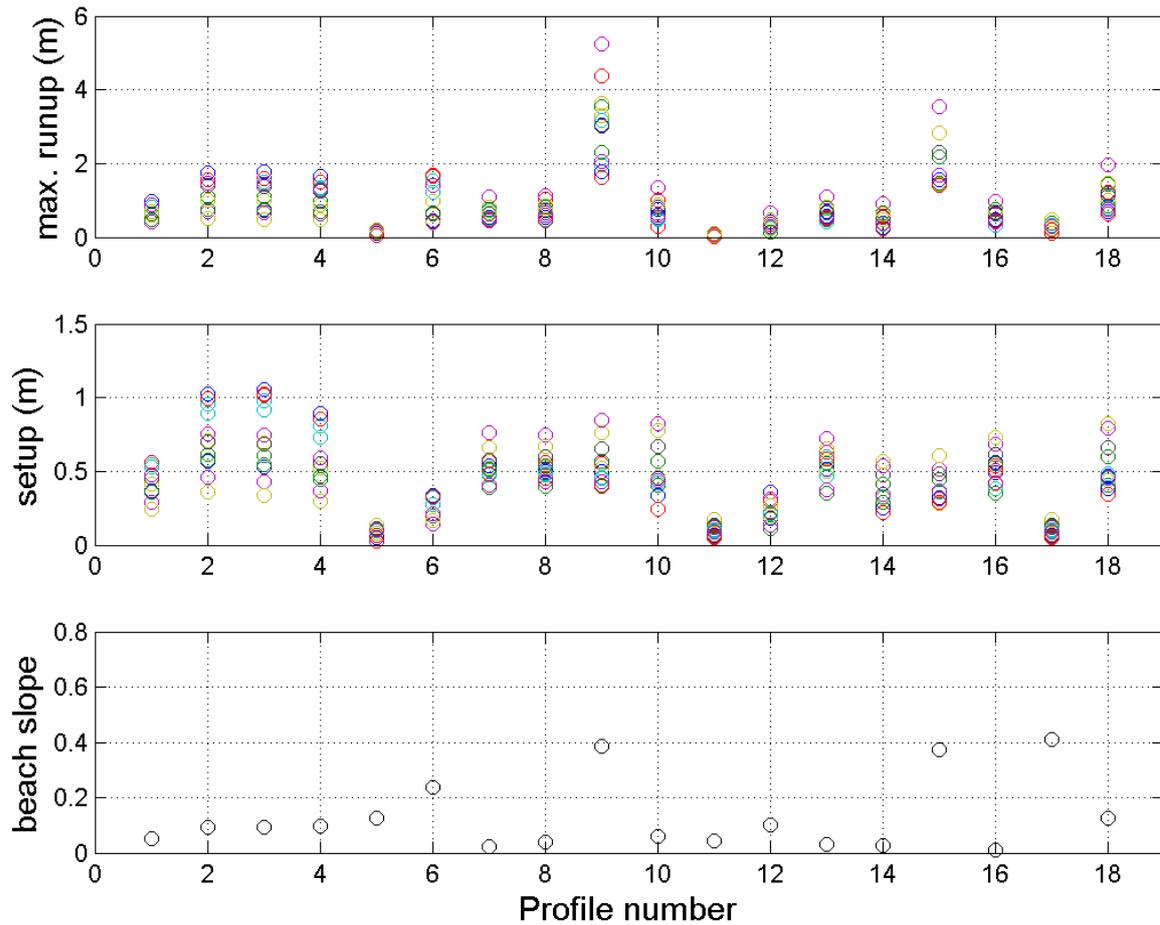
Figure B-9: Estimated wave runup and setup during thirteen simulated storm events at each of the eighteen locations for which beach profiles were available. Each colour represents a different storm event.
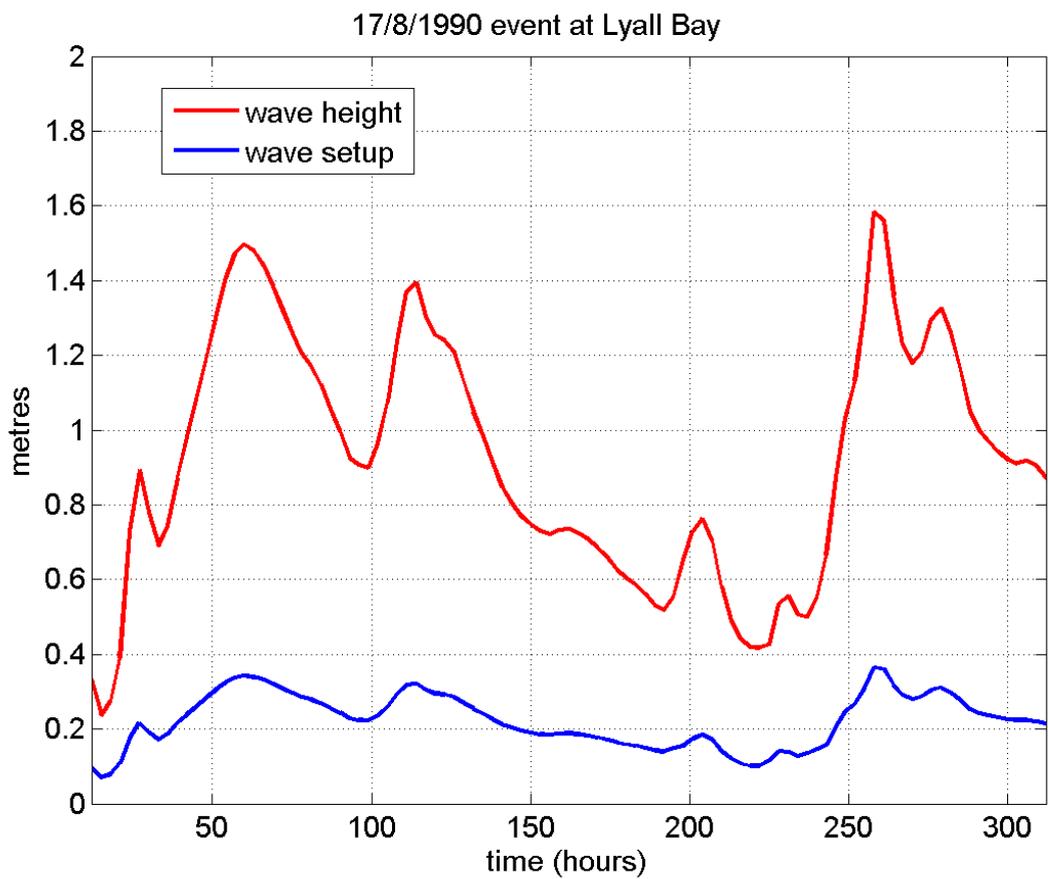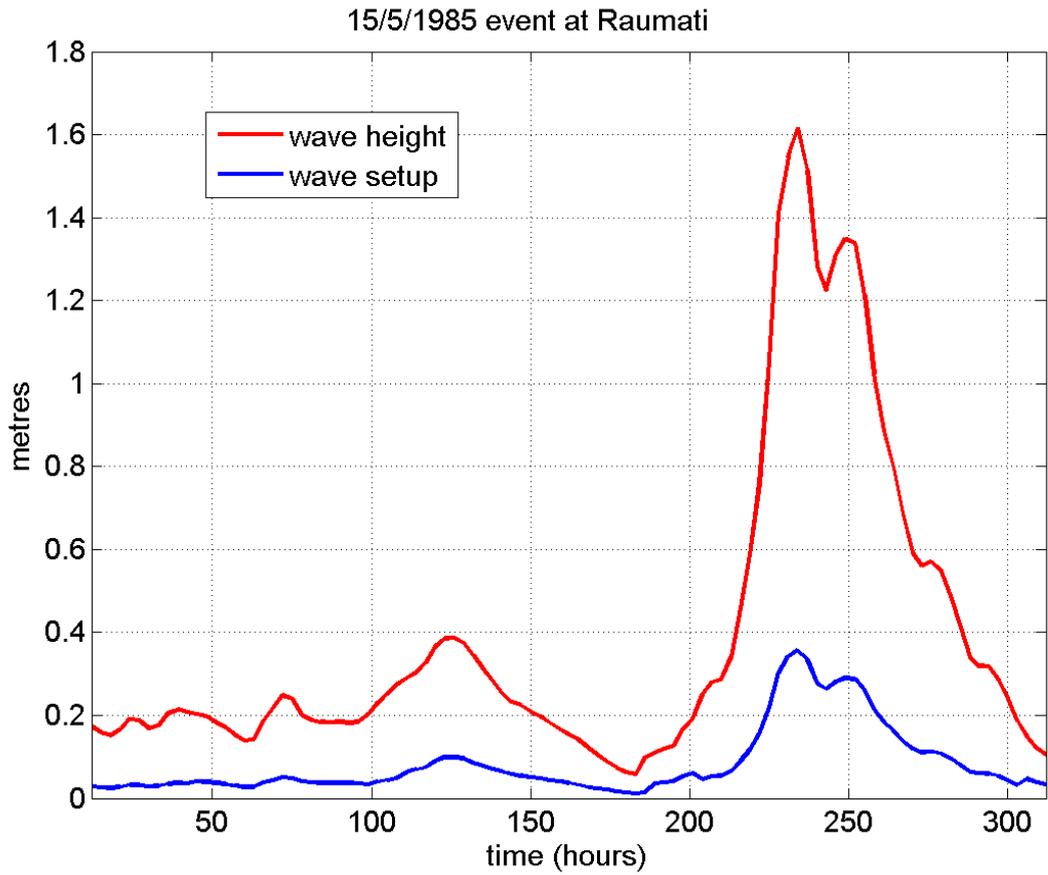
Figure B-10: Variation of significant wave height and estimated wave setup at the shore during two storm events.
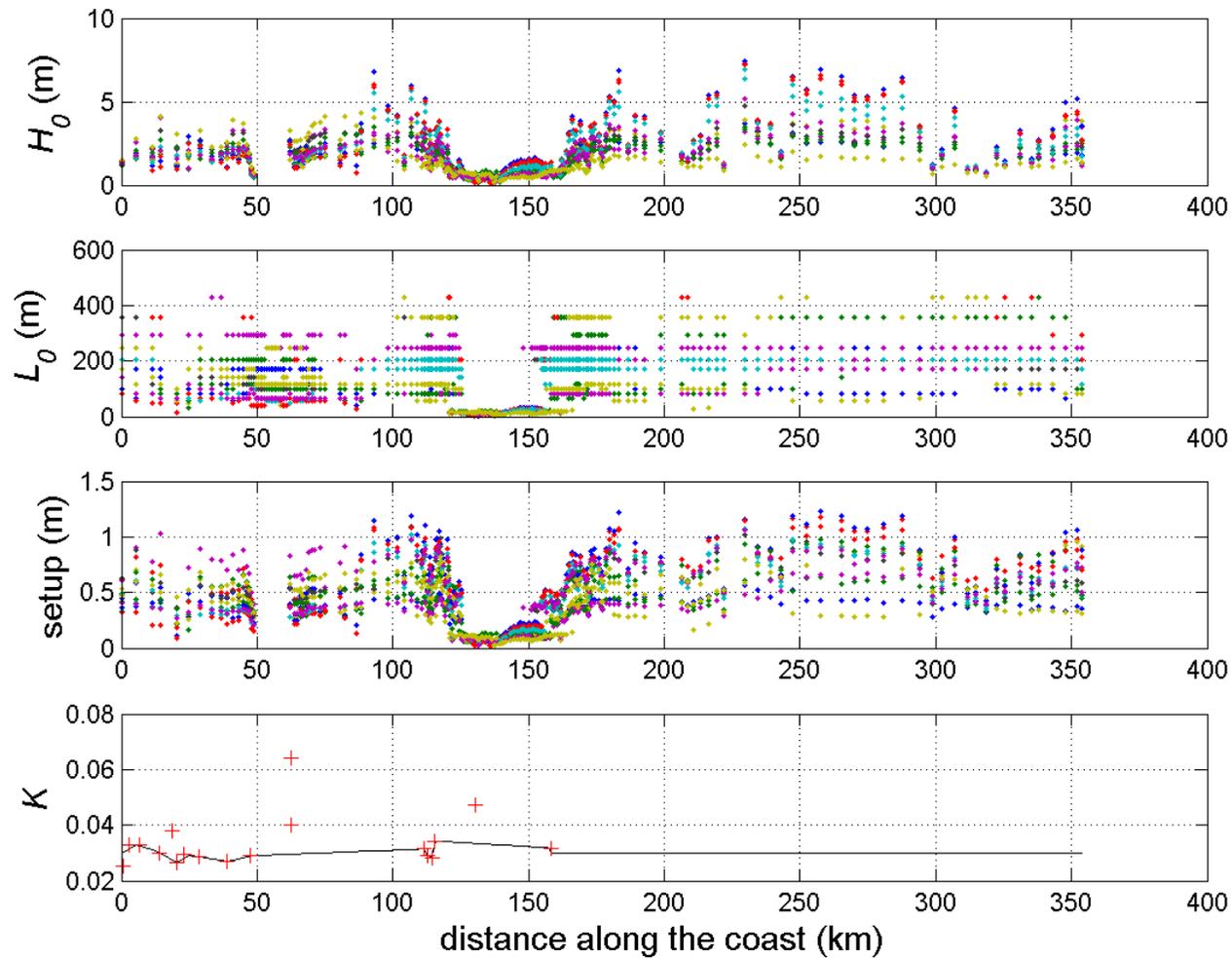
Figure B-11: **Simulated offshore wave height (H_0) and wavelength (L_0), and estimated wave setup during thirteen simulated storm events at coastal output locations.** The bottom panel shows the parameter K estimated at profile locations (crosses), and interpolated to other sites (line). The different colours represent different storm events.

Appendix C   Joint probability analyses plots

Plots of significant wave heights and storm-tide for the Joint Probability Analyses (October 1957-September 2002) are shown here for each of the sites indicated in Figure 2-3. The joint probability analysis for sites 3 and 4 are given in Figure 2-6 and Figure 2-5 respectively see the captions of Figure 2-5 and Figure 2-6 for further explanation.
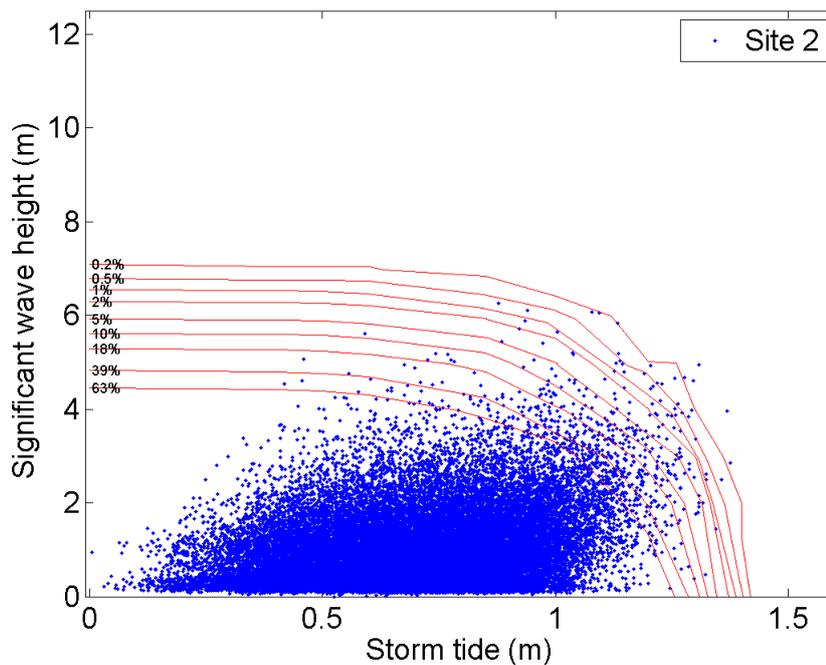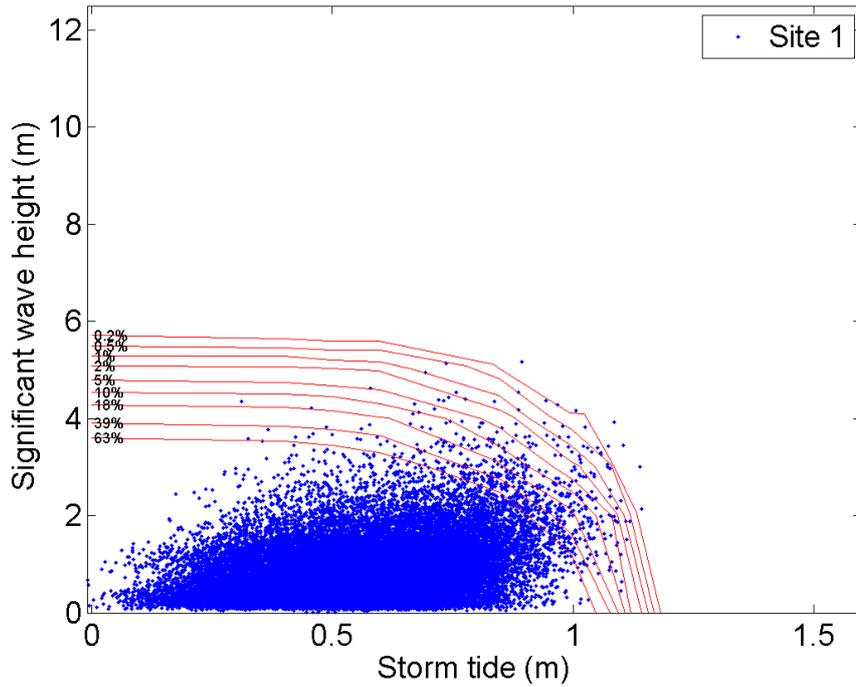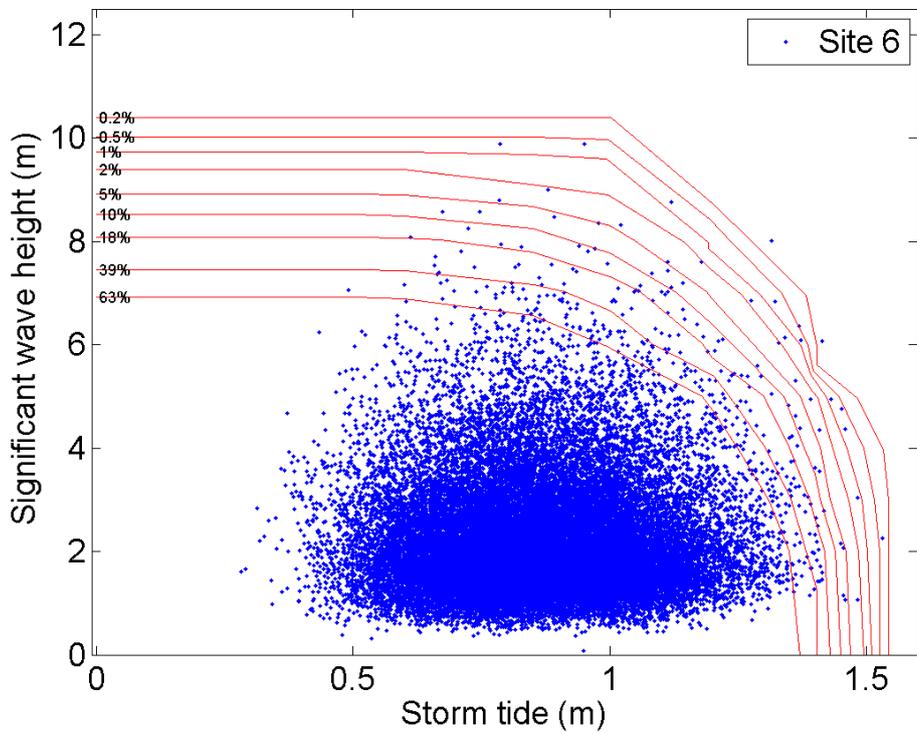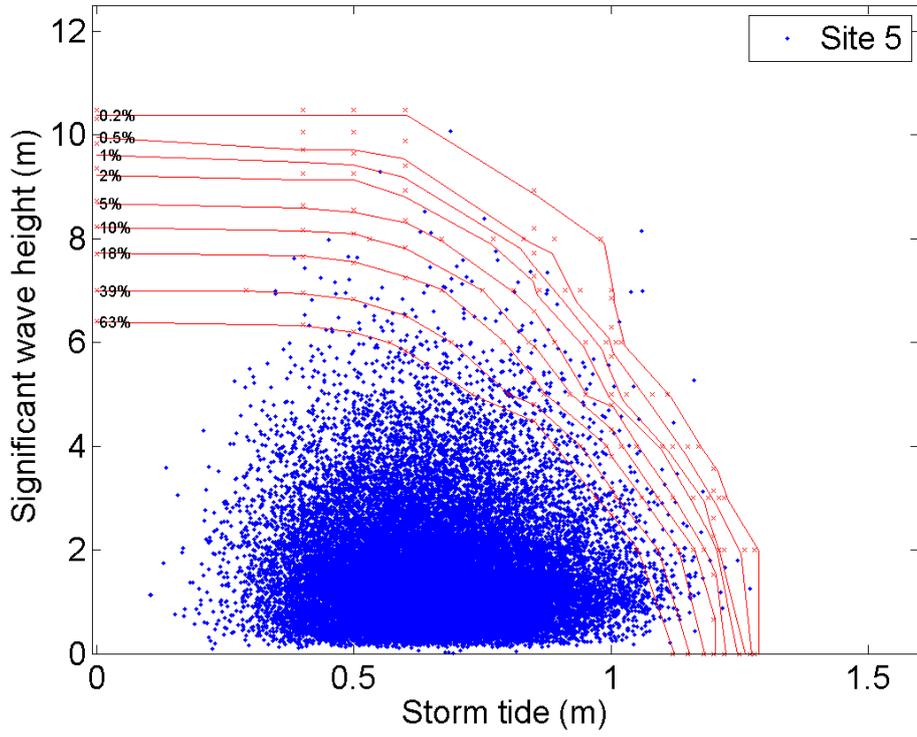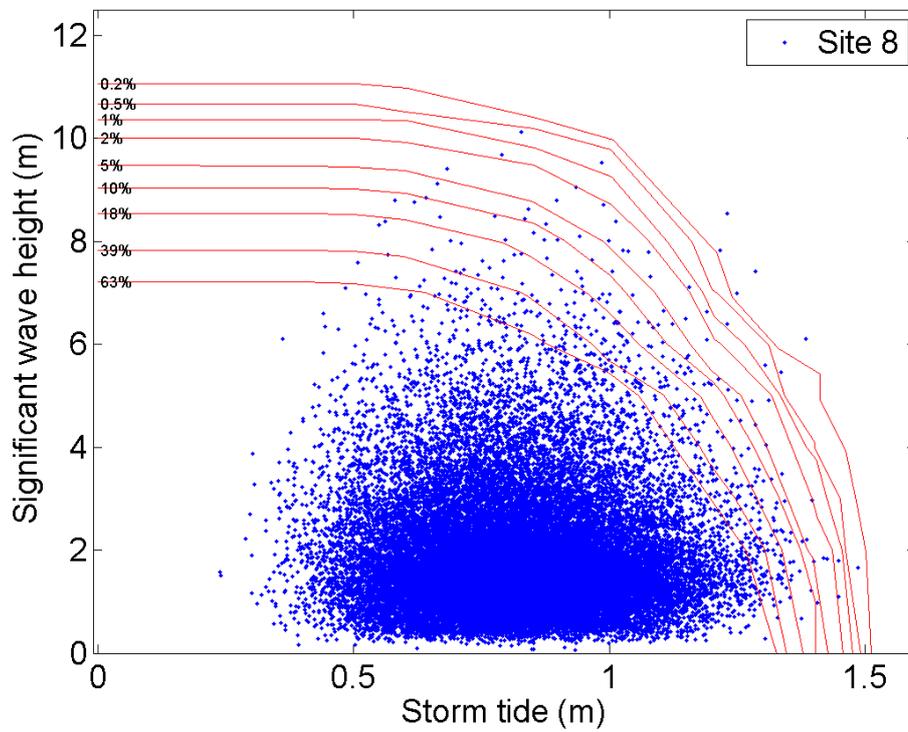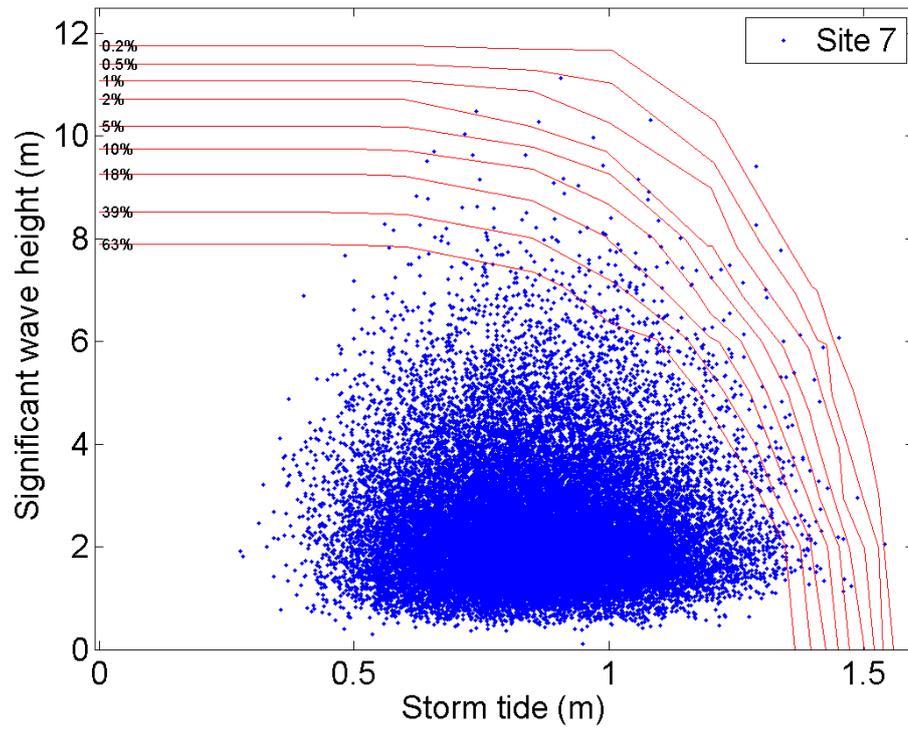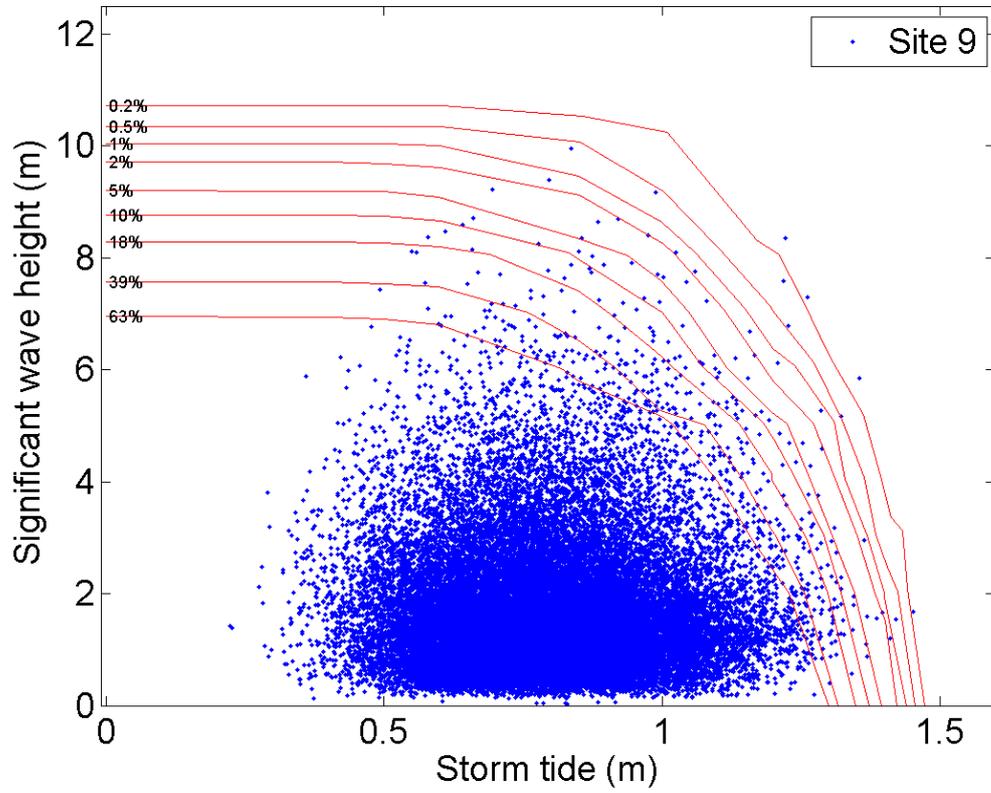
Appendix D Trained Interpolation

The aim is to derive wind fields $\left(U_f(\vec{x}_i), V_f(\vec{x}_i)\right)$ at all points $\{\vec{x}_i, i = 1, ..., N_f\}$ on a fine resolution grid, given the wind field $\left(U_c(\vec{x}_j), V_c(\vec{x}_j)\right)$ at all points $\{\vec{x}_j, j = 1, ..., N_c\}$ on a coarse grid. Writing *U* and *V* components in a single vector X, with $X_i = U(\vec{x}_i)$ and $X_{N+i} = V(\vec{x}_i)$ for $i = 1, ..., N$, we write the fine grid wind fields as a linearly-weighted sum of the coarse grid fields:

$$X_f = WX_c$$

Given a suitable training data set of coincident wind fields at multiple times (Uppala et al. 2005) on the two grids, we seek the set of weights W that minimises the mean square difference between the actual and interpolated fine grid fields:

$$\chi^2 = \sum_t (X_f(t) - WX_c(t))^2$$

This will be minimised for weights satisfying the linear system of equations

$$WC = D,$$

where

$$C_{i,j} = \sum_t X_{c,i} X_{c,j}$$

and

$$D_{i,j} = \sum_t X_{f,i} X_{c,j}$$

In effect, for each wind component on the fine grid, we find multiple linear correlations with wind components at each cell on the coarse grid.

As an example application for the Greater Cook Strait region, we wished to be able to interpolate from wind fields available from the ERA-40 data set on a coarse grid covering longitudes 172.125°E to 176.625°E, and latitudes 42.750°S to 38.250°S, both at 1.125° degree intervals, onto a fine grid covering the same ranges at 0.125° degree resolution.

For a training set, ideally we would use ERA-40 winds for the coarse grid data, and the best possible fine grid wind fields for some common time range. A suitable source for the fine grid winds is the NZLAM-12 model, on approximately 12 km resolution, available since 2007. There is, however, no time overlap with the ERA-40 data, which ends in 2002. Hence we instead picked a training period (eight months from 1/12/2010) for which NZLAM-12 winds were available, and for the coarse grid used concurrent winds from the UM global weather model, interpolated (with standard bilinear interpolation) to the Greater Cook Strait coarse grid.

The top row of Figure D-1 shows examples of concurrent NZLAM-12 and UKMO global winds from the training data set. On the coarse grid, the acceleration of wind through Cook Strait can only be represented in a very broad sense, while the finer scale allows the distinct area of acceleration south of Wellington to be captured, as well as allowing for much stronger gradients near the coastline.

After computing interpolation weights W from the training set, these were applied to estimate fine grid wind fields by interpolation from the original coarse grid wind fields. In the example shown in Figure D-1, we see that the interpolated winds are able to capture the spatial structure of topographically-steered winds through Cook Strait quite successfully.
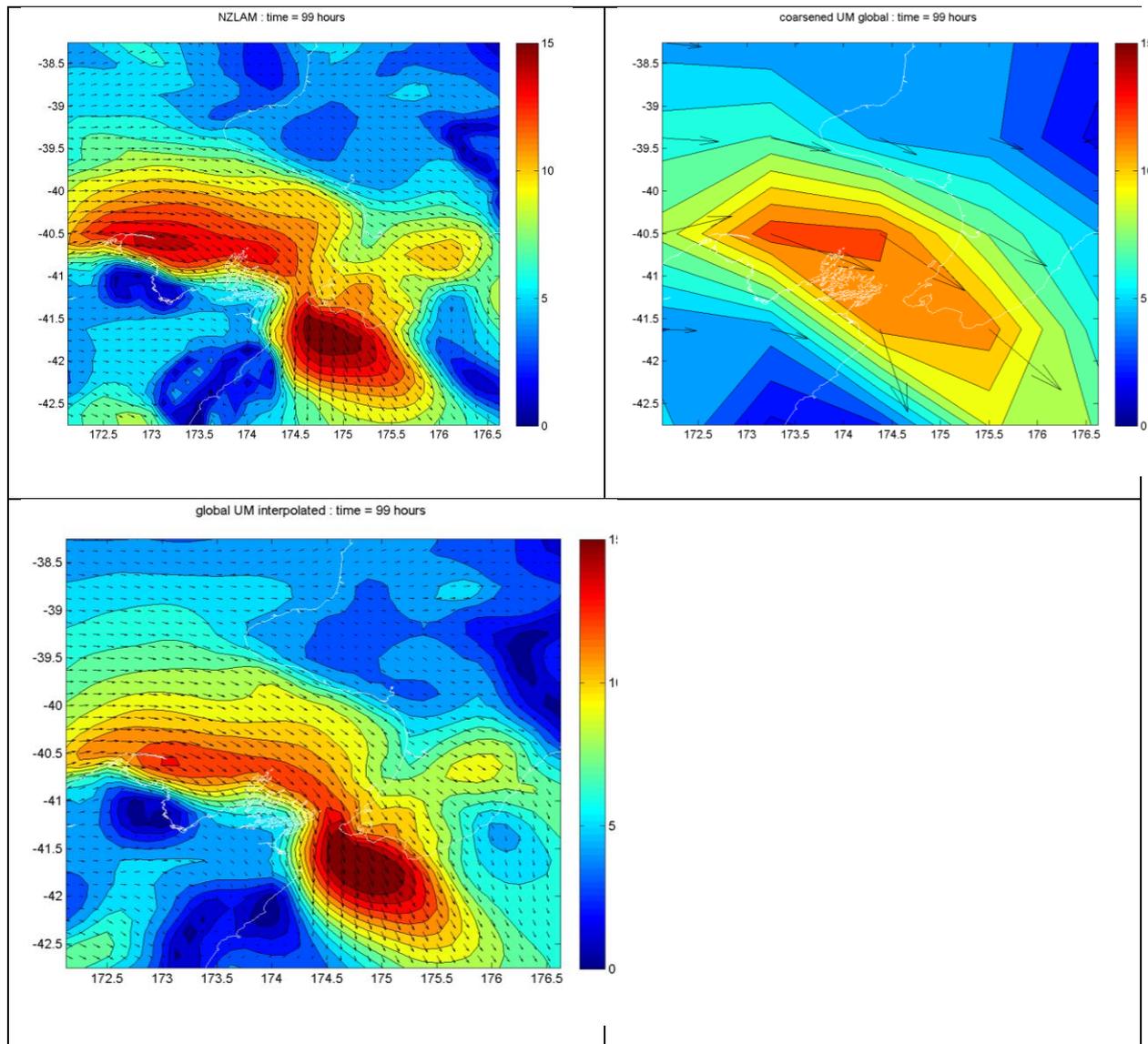
Figure D-1: Wind fields on the coarse and fine Greater Cook Strait grids, at 03:00UT on 1/12/2010. The colour scale shows wind speed, while arrows show wind velocity vectors. (top left) NZLAM-12 winds on the fine grid, (top right) UK Met Office global winds on the coarse grid, (bottom left) winds computed by trained interpolation on the fine grid.

Appendix E Climate change and storm intensity

While sea-level rise is the most well-known effect of climate change on storm-tide levels, changes to storm intensity and storm tracks could also influence storm surges and waves that are components of storm-tides. This Appendix addresses whether climate change is likely to cause additional changes to storm-tide over and above those caused by sea-level rise.

A study into the effect of climate change on extreme winds and storminess over all of New Zealand (Mullins et al. 2011) shows that extreme winds are likely to increase in winter and decrease in summer in general. These effects, however, are not large but a matter of a few percent. There is also likely to be an increase in cyclones (sub-tropical and mid-latitude low pressure systems rather than tropical cyclones) in the Tasman Sea over the summer.
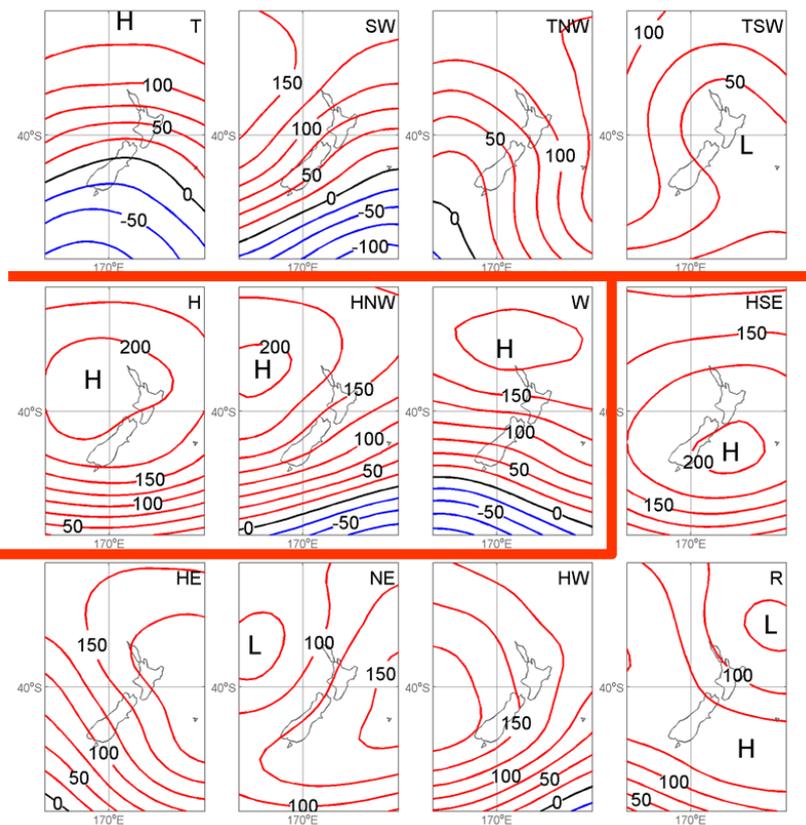
Figure E-1: Kidson circulation types (Kidson, 2000), in terms of 1000 hPa geopotential heights (m). The circulation types are given by the acronym in the top right hand corner. The types can also broadly be separated into three regimes: troughs (top four, T SW, TNW, TSW), zonal types (left, middle three; H, HNW, W) and blocking types (bottom, right five, HSE, HE, NE, HW, R).

Kidson typing is another method that can be used to look at changes to weather patterns due to climate change. Circulation types in New Zealand can generally be categorised into twelve distinct Kidson types (Kidson, 2000). Figure E-1 shows the 12 Kidson types which broadly fit into three regimes, troughs, zonal types and blocking types. The frequency of the different Kidson types can be used to gauge the changes in weather patterns due to climate change (Mullins et al. 2011). Data from the WASP New Zealand storm surge hindcast was used to investigate the relationship between the Kidson type and storm surge. As can be

seen in Figure E-2, Kidson types and storm surge are strongly linked. In the Greater Wellington Region storm surges occur in conjunction with trough Kidson types, especially types T (especially in the Kapiti Coast) and TSW (especially in the Wairarapa) and to some extent SW and TNW. Although there are no significant overall changes to occurrence rates of the different Kidson types at an annual level, seasonal changes can be observed (Mullins et al. 2011). In the Wellington region TSW is more frequent in summer and less in winter whereas T is more frequent in winter and less in summer. This suggests that storm surges could be expected to become more frequent in winter for Kapiti Coast and the Wellington region. This analysis does not give any indication as to the strength of the storm surge.

Changes in storm surge under climate change have also been modelled directly as part of the Wave and Storm Surge Projection project. Open coast storm surge over a thirty year period for four future climate scenarios was compared with the storm surge for the current climate. The four future scenarios were taken from the AR4 SRES Scenarios (Nakicenovic and Swart 2000). Three A2 scenarios were modelled with differing initial conditions and one B2 scenario. For each of these scenarios a General Circulation Model (GCM) over the entire earth was run with specified sea surface temperatures and atmospheric CO_2 content (either current day or as specified by the climate change scenario). In the vicinity of New Zealand these results were dynamically downscaled using a Regional Climate Model (Ackerley et al. 2012). The storm surge simulation was forced by pressure and 10 m winds taken from these models. For the nine points used in the joint probability analysis the upper quantiles of the storm surge peaks taken from the future scenarios were compared with those of the current climate to ascertain whether there were any significant changes in the storm surge due to climate change. For the 95 percentile there were no significant changes with the current 95th percentile lying within the confidence intervals of the future quantiles for almost all the scenarios (For one of the A2 scenarios there was a slight increase for the points in the Kapiti region however for the other two A2 scenarios and the B2 scenario there was no significant change). For the 99th percentile, however, there was a significant increase in storm surge in the Kapiti region of around 6% over all the future scenarios. No significant change was seen other areas. These results are consistent with those of Mullins et al. (2011) showing increased westerlies and increased occurrence of T in winter both of which contribute to storm surge on the Kapiti Coast. A 6% increase in storm surge, however, is equivalent to about a 0.03 m absolute increase in height. Compared to the effects of sea-level rise this is negligible. For clarity, therefore, this study uses the same storm-surge scenarios for the future runs as the present runs with the only difference being the sea-level rise.
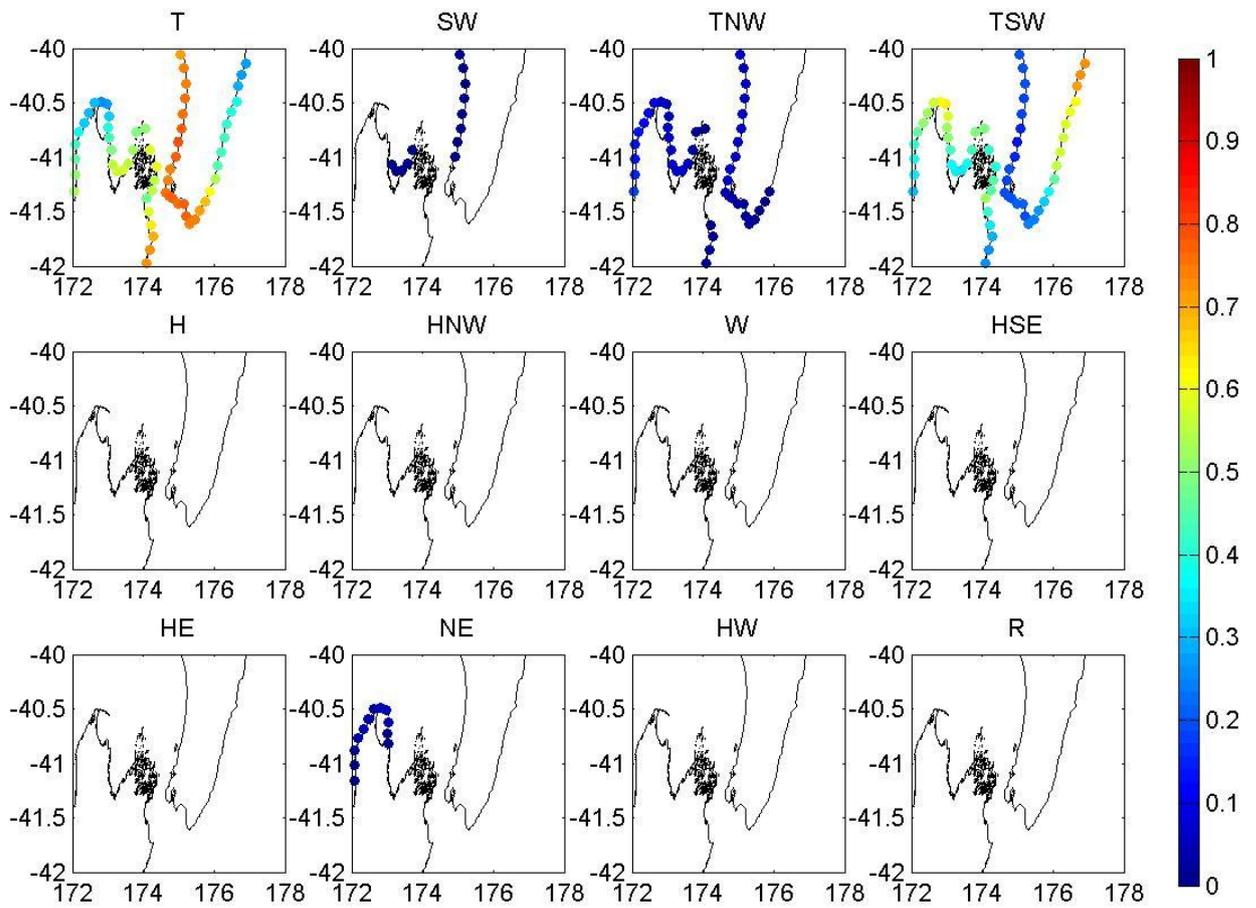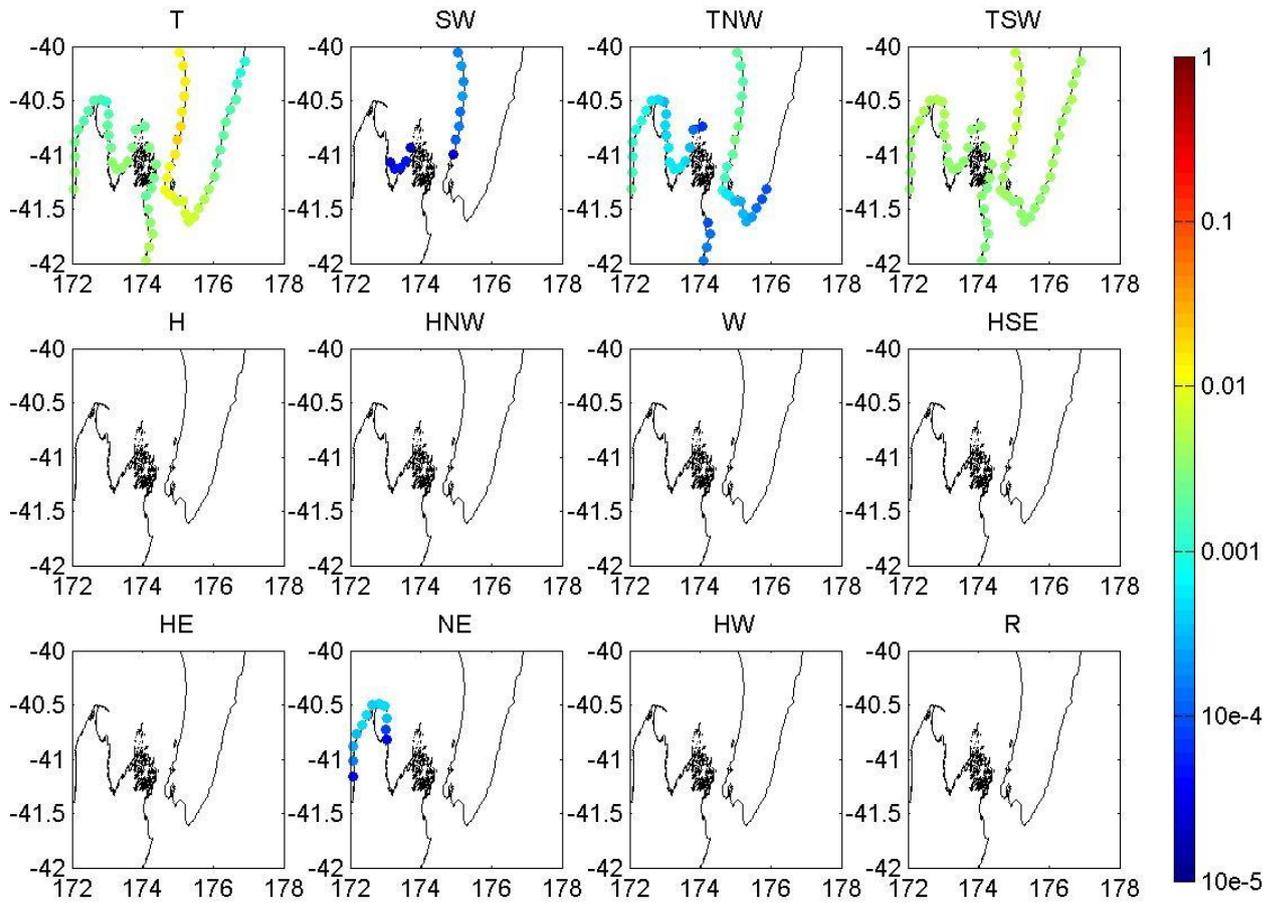
Figure E-2: Top: Probability of a given Kidson type given a storm surge over 30 cm; bottom: Probability of a storm surge over 30 cm given a certain Kidson type. Data points are only plotted where at least one instance of a storm surge for that Kidson type occurred in the 40 year period of the ERA-40 reanalysis.

Appendix F   Water level time series Wellington Grid

Times series of water surface level for the four storm events are plotted for each of the locations indicated in Figure A-8. The graphs show the Port of Wellington sea-level measurements and simulated net water level offset and simulated storm tide. Wave setup is not included in these graphs. See caption for Figure A-9 for further explanation.

1975 Wellington Harbour

1985 Wellington Harbour

1990 Wellington Harbour

1992 Wellington Harbour
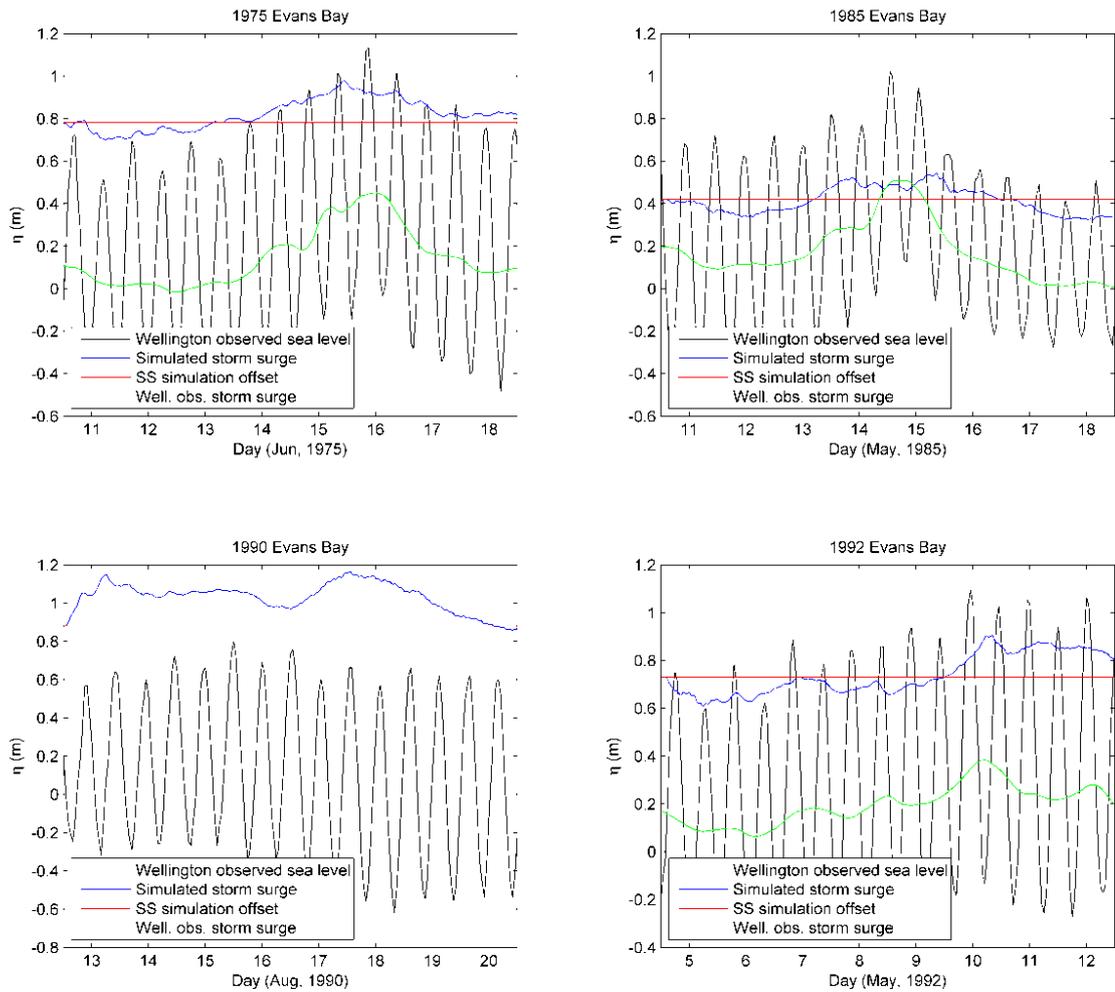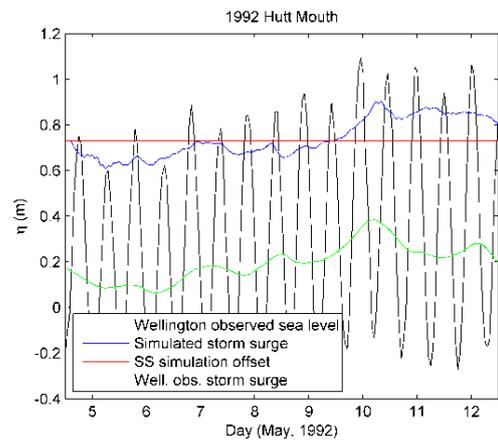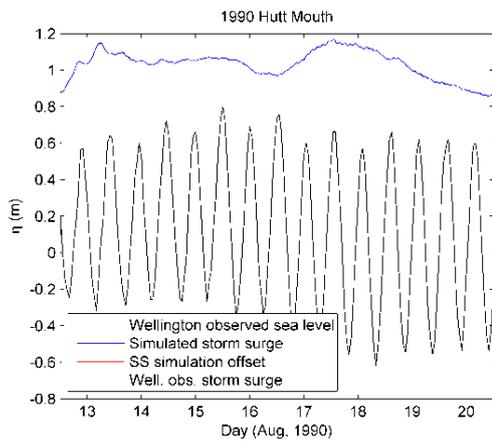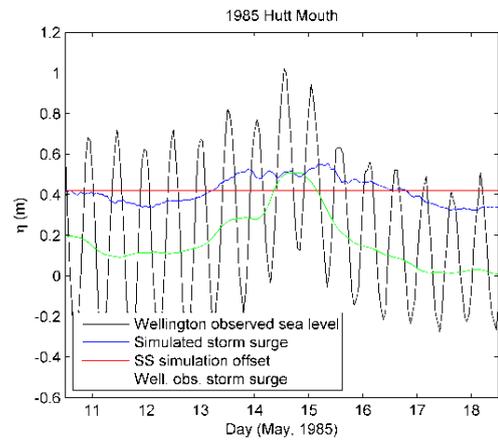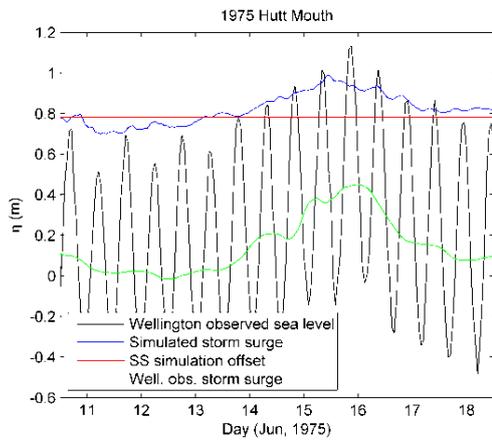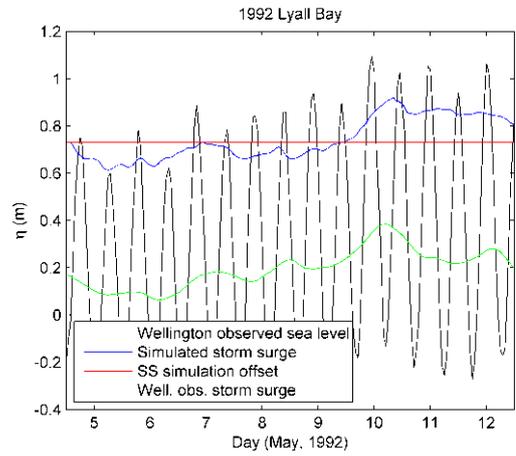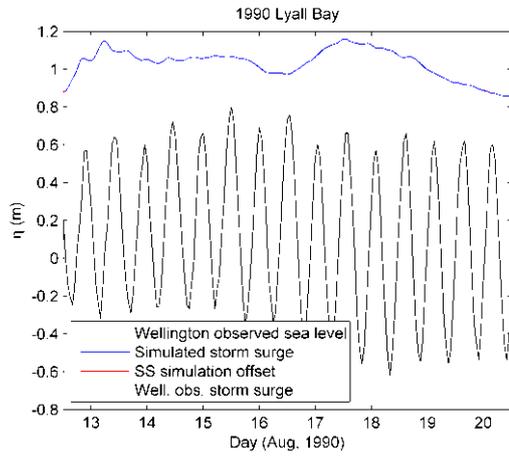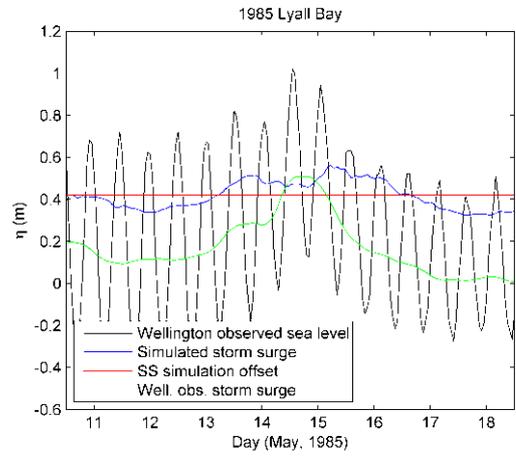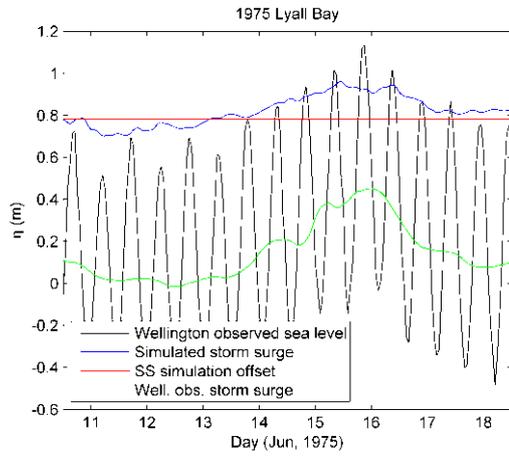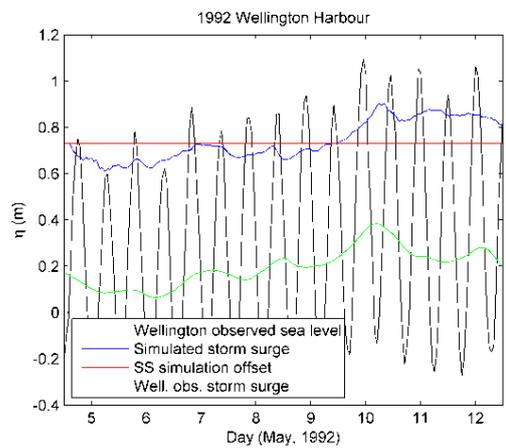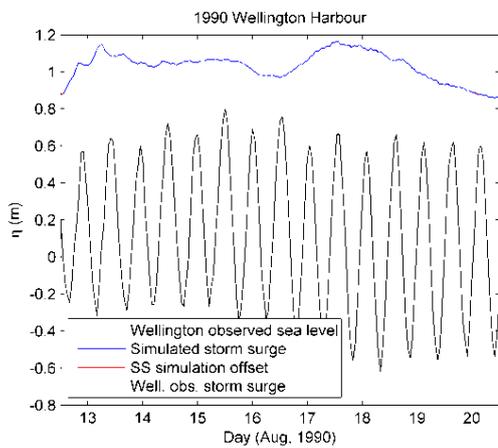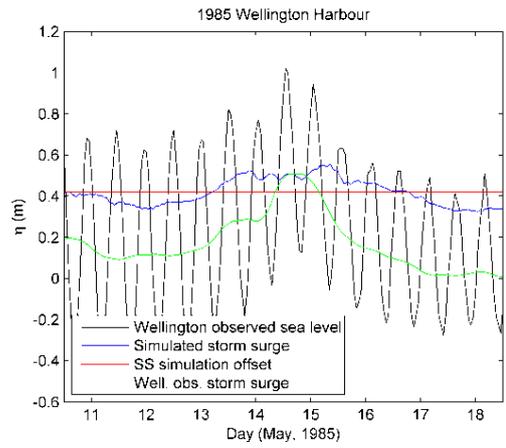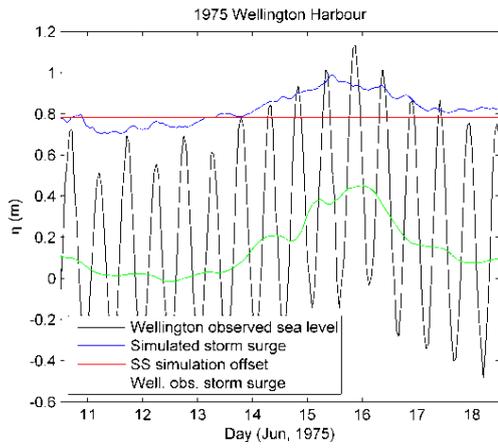
Appendix G Water level time series - Kapiti Grid

Times series of water surface level for the 4 storm events are plotted for each of the locations indicated in **Error! Reference source not found.**. The graphs show the net water level offset (red) and simulated storm tide (blue). The horizontal magenta line is the 1% AEP (100-year ARI) storm tide level (with dashed 95% confidence intervals); light blue is 63% AEP (1-year ARI) storm tide level (with dashed 95% confidence intervals). Wave setup has not been added to the plotted simulated storm-tide.

1976 Waikanae

1980 Waikanae

1994a Waikanae

1994b Waikanae
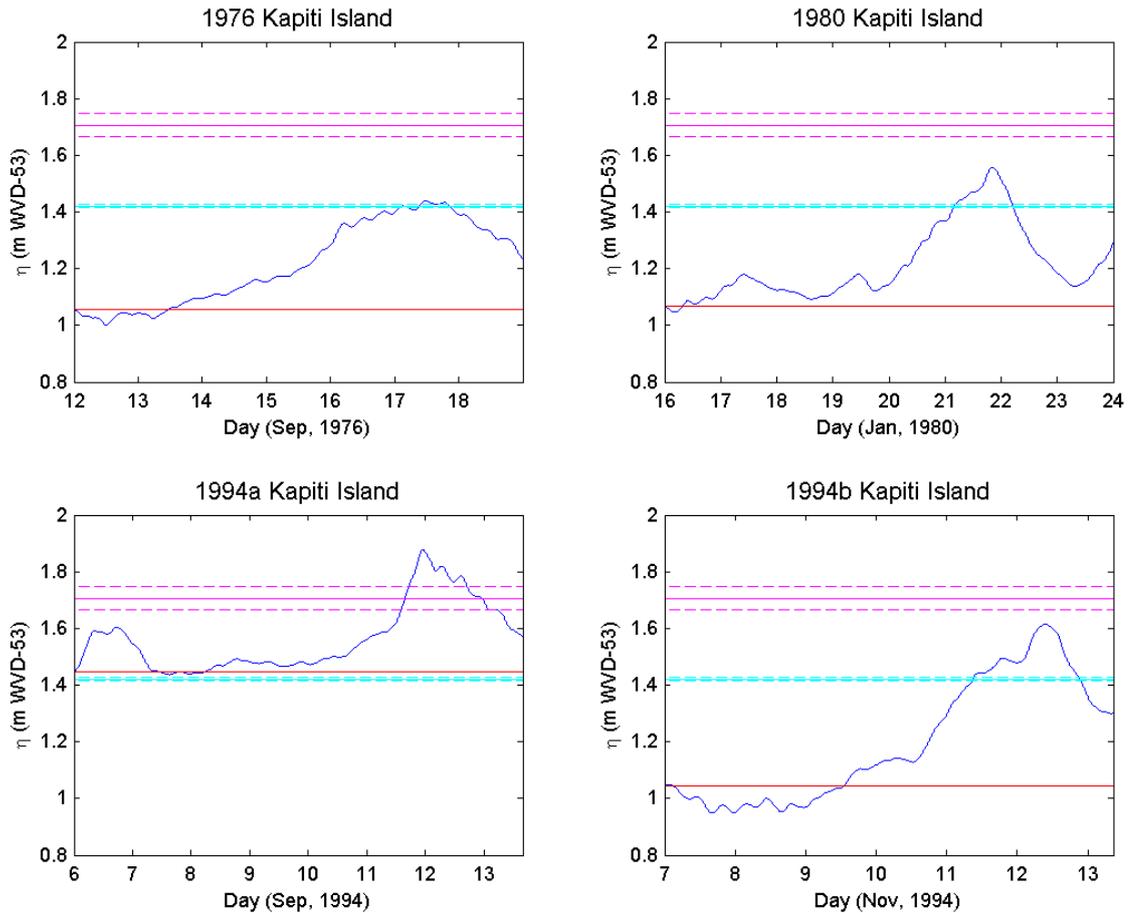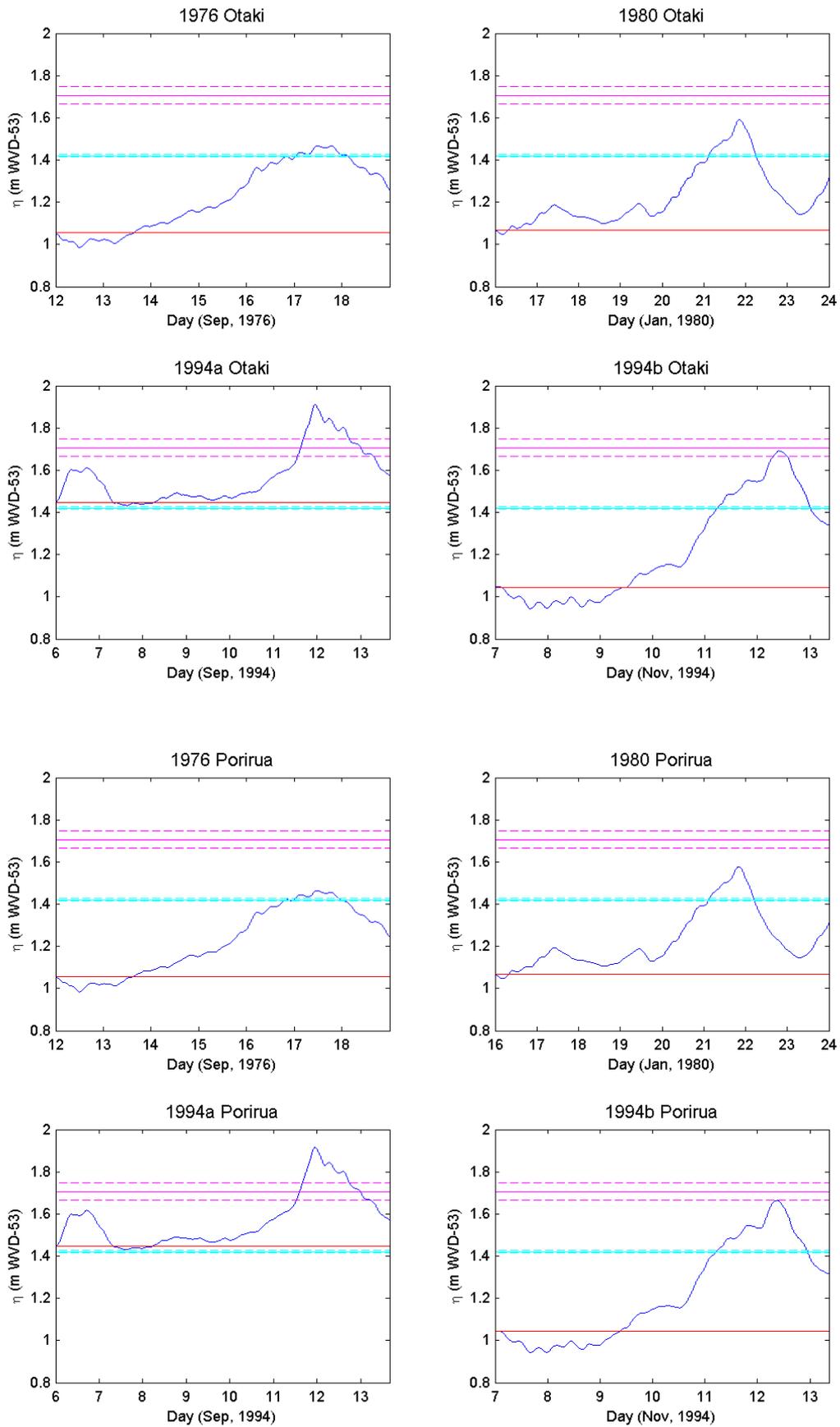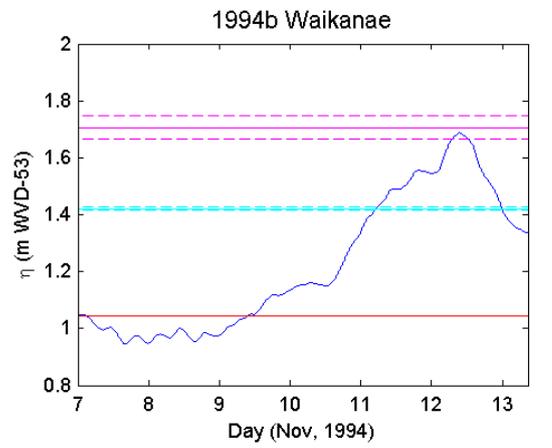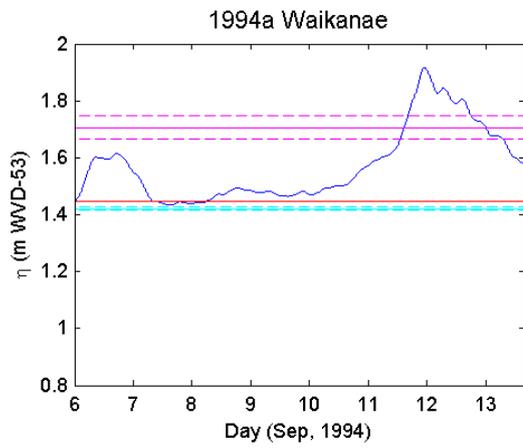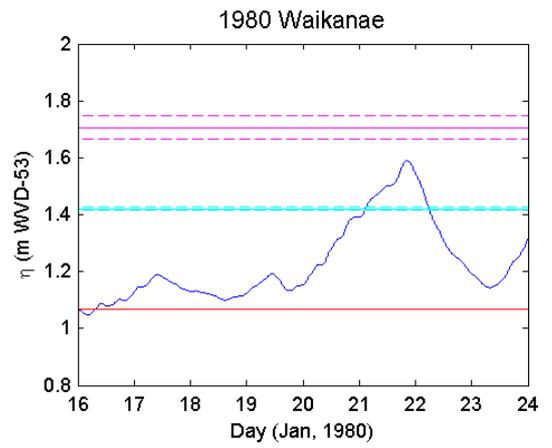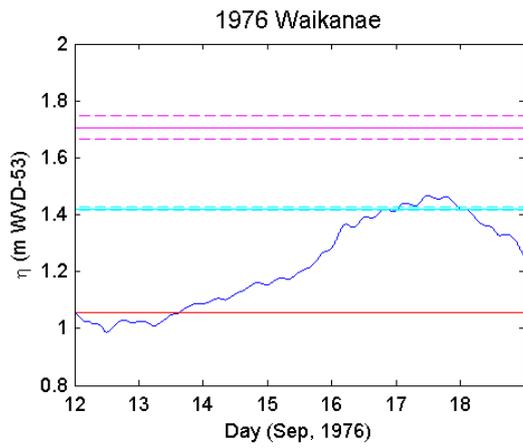
Appendix H Maps of maximum total water level
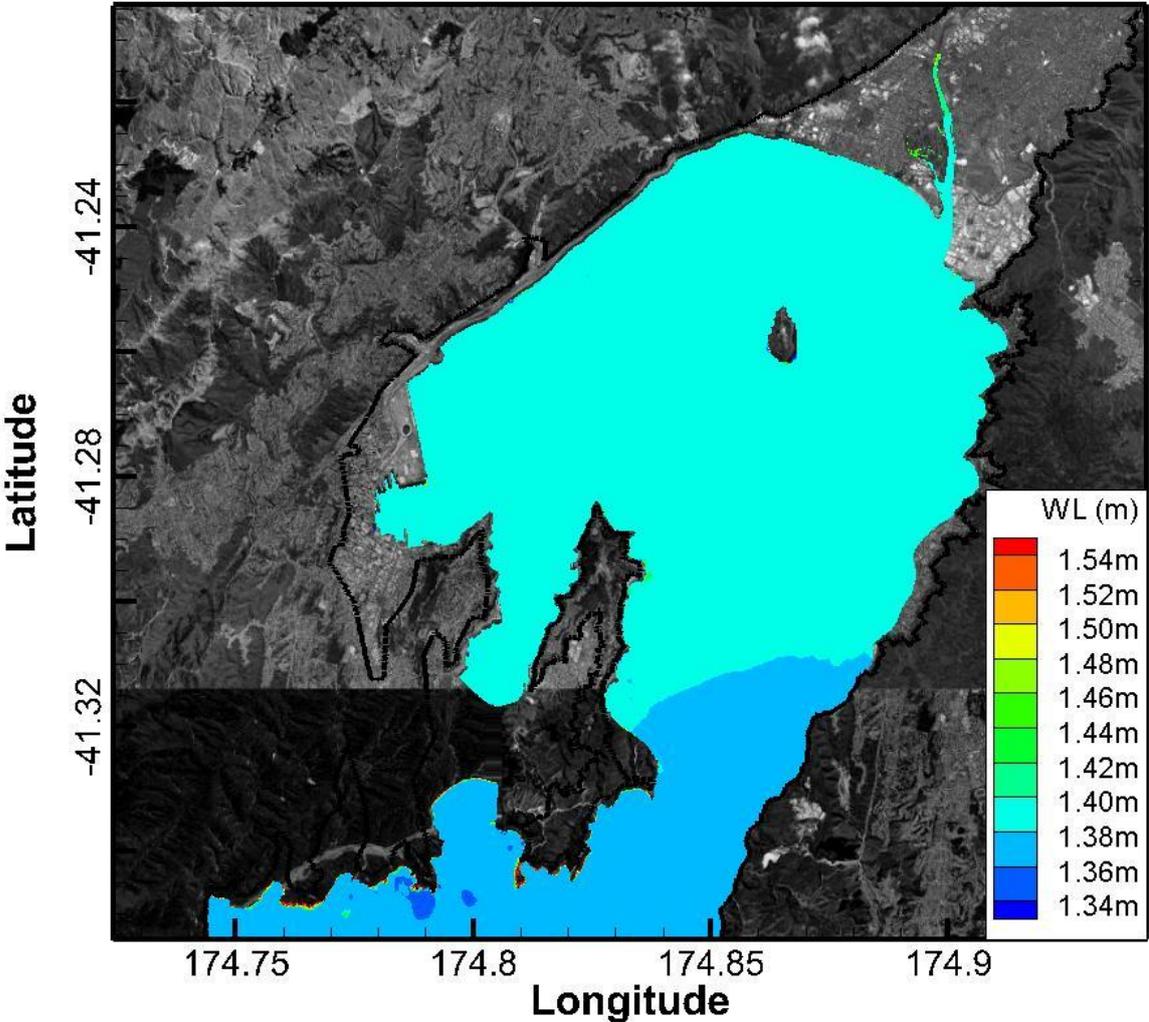
Figure H-1: Total inundation water levels in Wellington Harbour relative to WVD-53 for a 1% AEP storm event based on the August 1990 event at present day sea level. The colours show the maximum water level above WVD-53, over-laid on images from Google Earth (2012). The solid black line shows the extents of the land inundation grid.
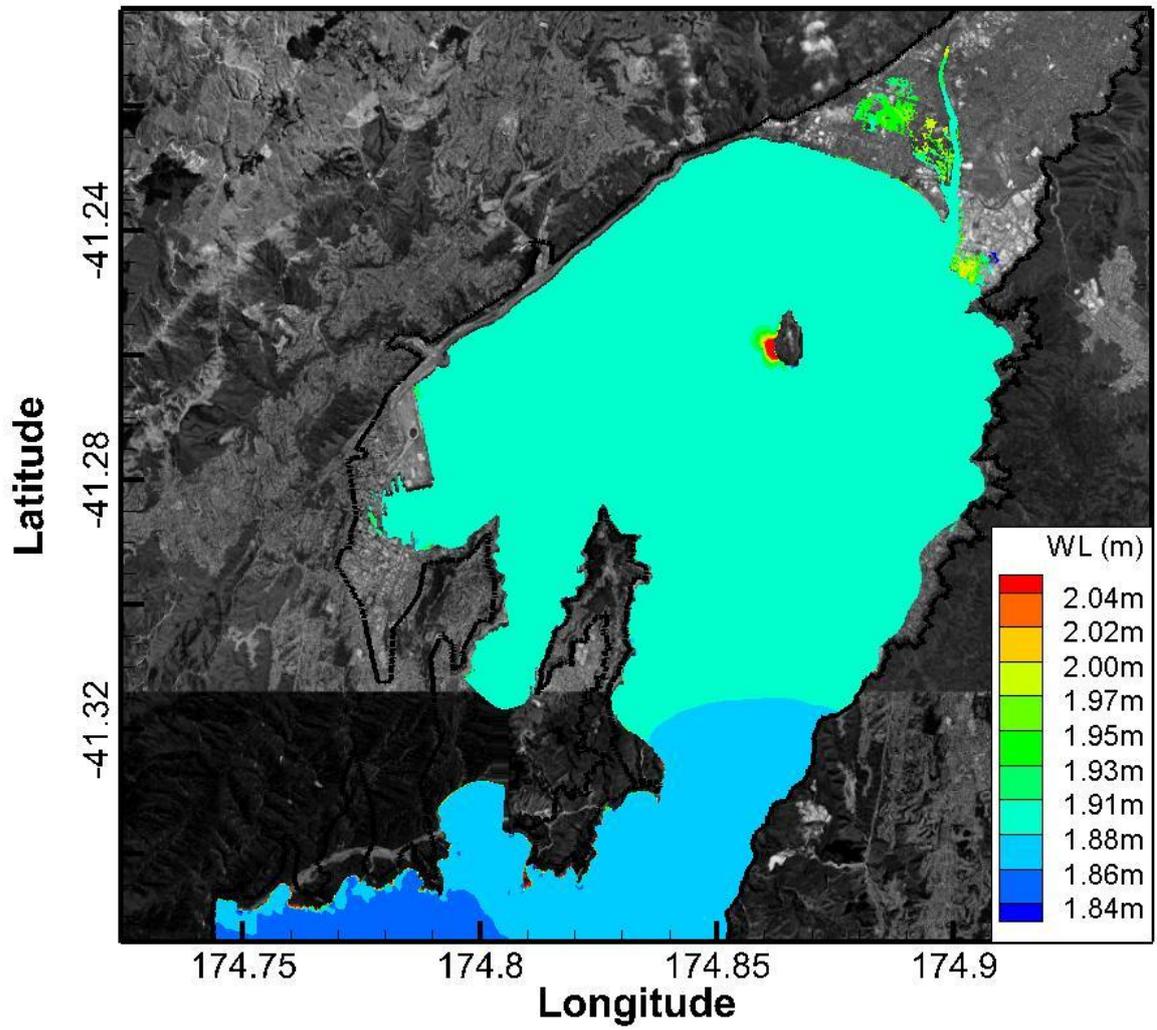
Figure H-2: Total inundation water levels in Wellington Harbour relative to WVD-53 for a 1% AEP storm event based on the August 1990 event with 0.5 m sea-level rise. The colours show the maximum water level above WVD-53, over-laid on images from Google Earth (2012). The solid black line shows the extents of the land inundation grid.
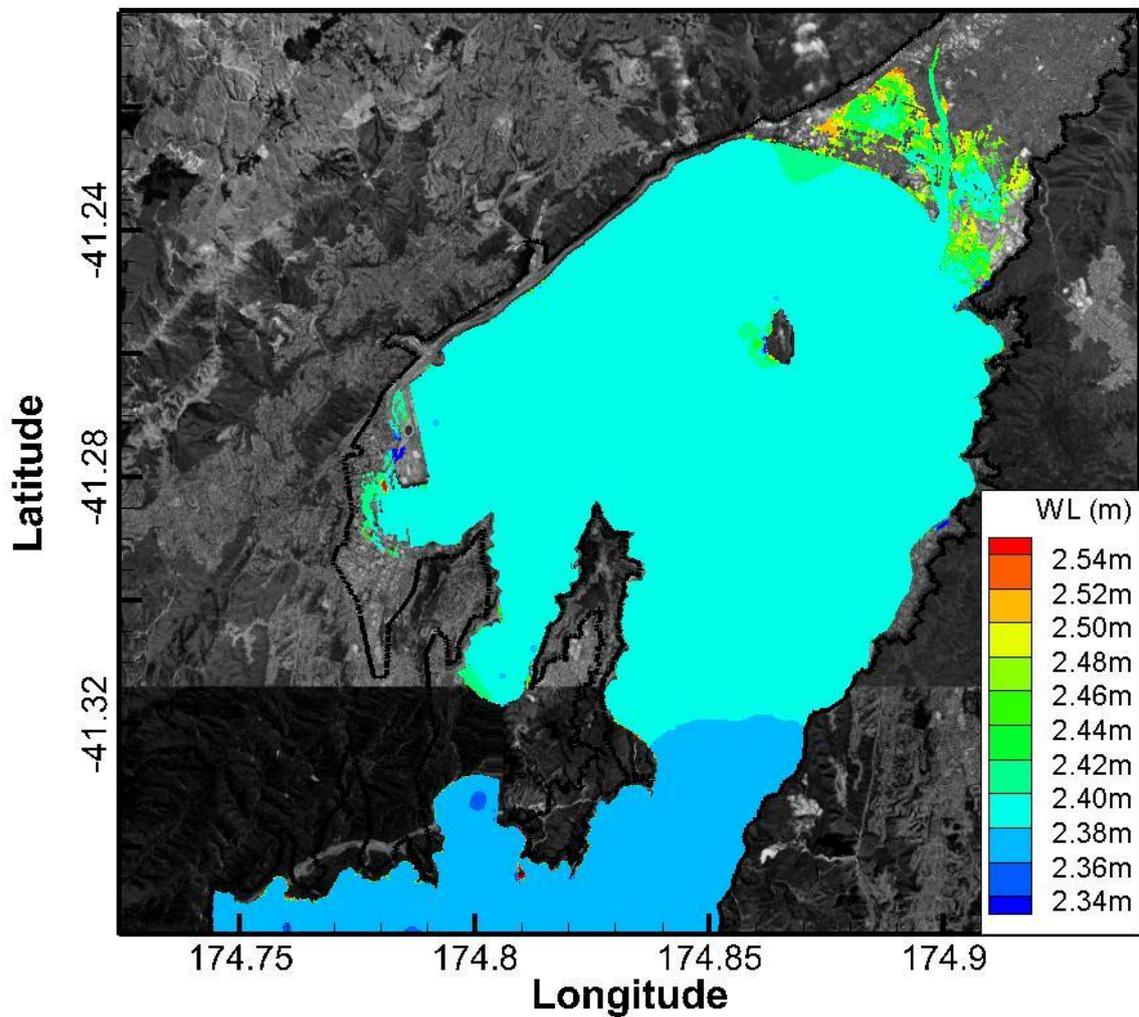
Figure H-3: Total inundation water levels relative to WVD-53 for a 1% AEP storm event based on the August 1990 event with 1.0 m sea-level rise. The colours show the maximum water level above WVD-53, over-laid on images from Google Earth (2012). The solid black line shows the extents of the land inundation grid.
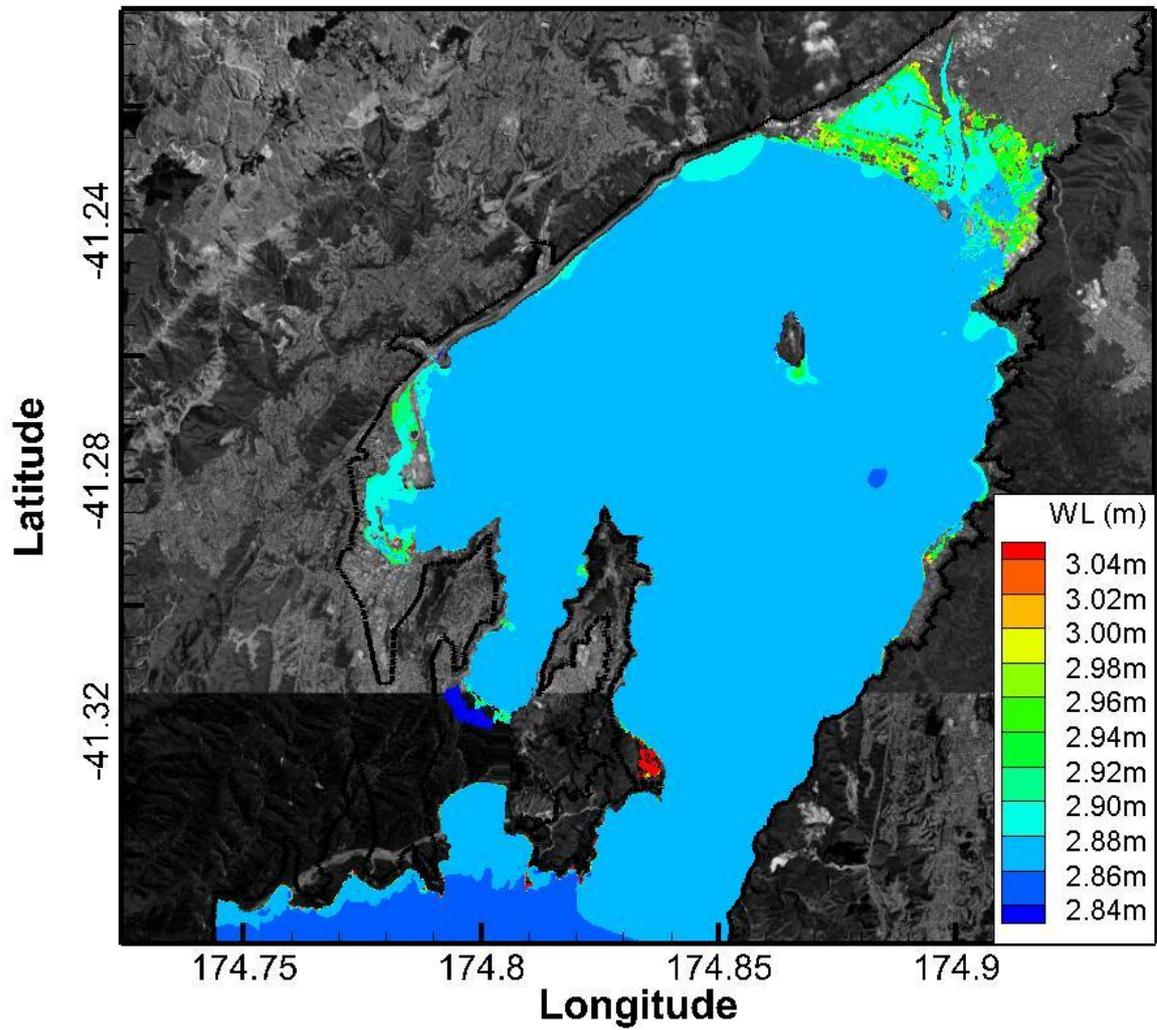
Figure H-4: Total inundation water levels relative to WVD-53 for a 1% AEP storm event based on the August 1990 event with 1.5 m sea-level rise. The colours show the maximum water level above WVD-53, over-laid on images from Google Earth (2012). The solid black line shows the extents of the land inundation grid.
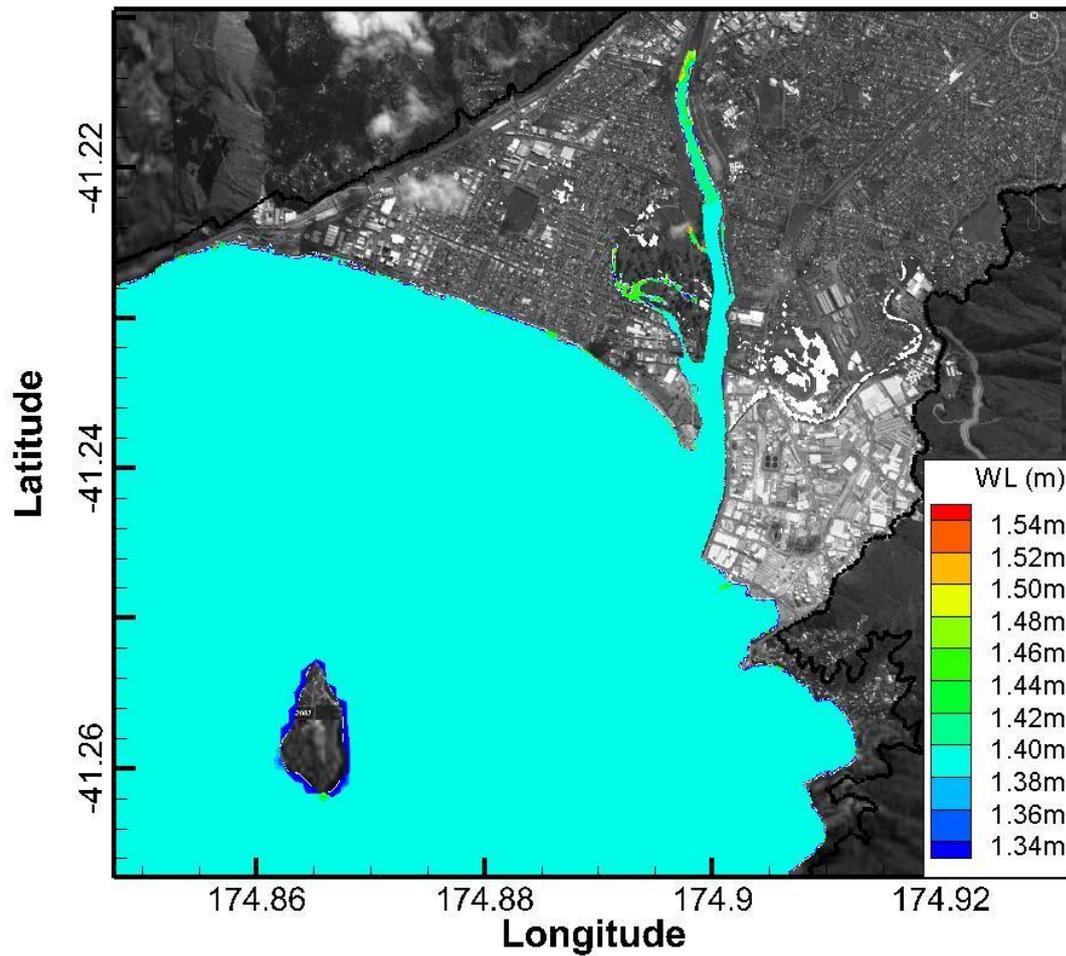
Figure H-5: Total inundation water levels relative to WVD-53 at Petone and Seaview for a 1% AEP storm event based on the August 1990 event. The colours show the maximum water level above WVD-53, over-laid on images from Google Earth (2012). The solid black line shows the extents of the land inundation grid.
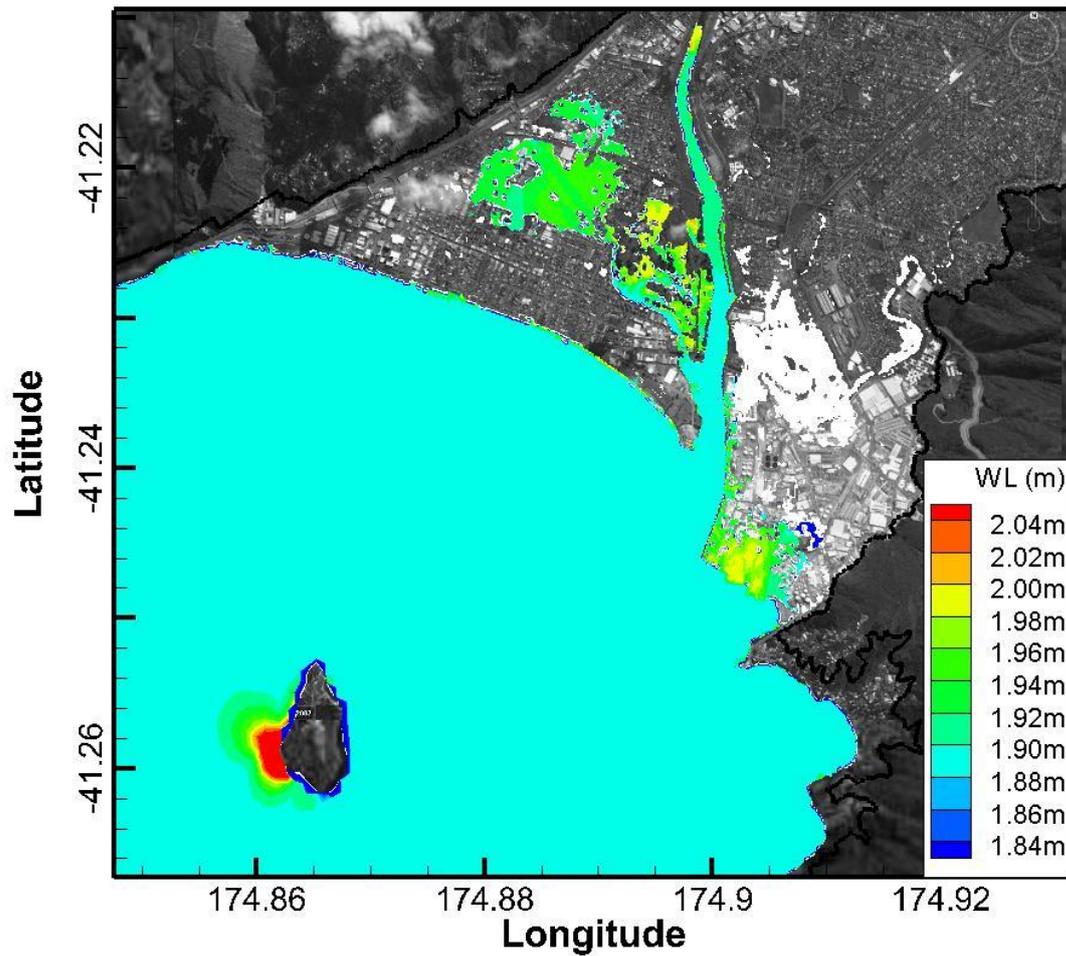
Figure H-6: Total inundation water levels relative to WVD-53 at Petone and Seaview for a 1% AEP storm event based on the August 1990 event with 0.5 m sea-level rise. The colours show the maximum water level above WVD-53, over-laid on images from Google Earth (2012). The solid black line shows the extents of the land inundation grid.
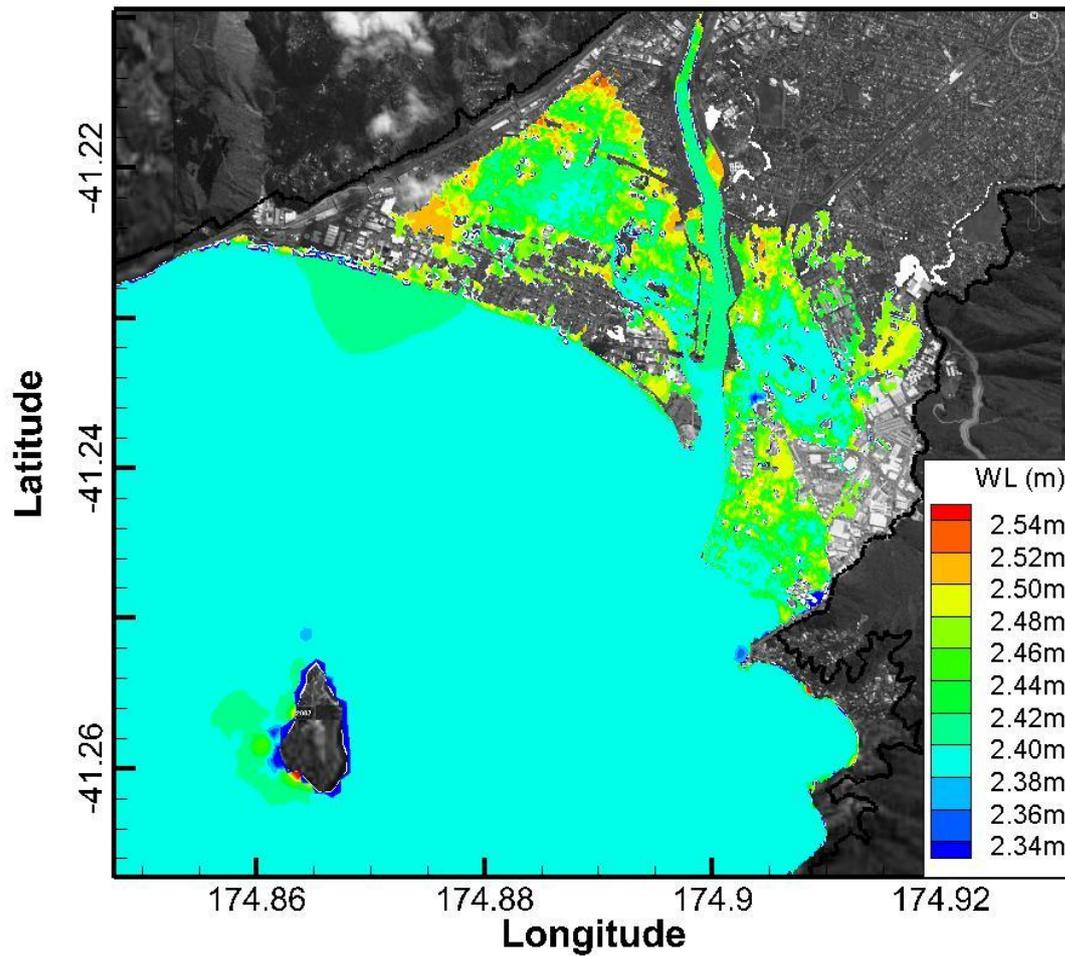
Figure H-7: Total inundation water levels relative to WVD-53 at Petone and Seaview for a 1% AEP storm event based on the August 1990 event with 1.0 m sea-level rise. The colours show the maximum water level above WVD-53, over-laid on images from Google Earth (2012). The solid black line shows the extents of the land inundation grid.
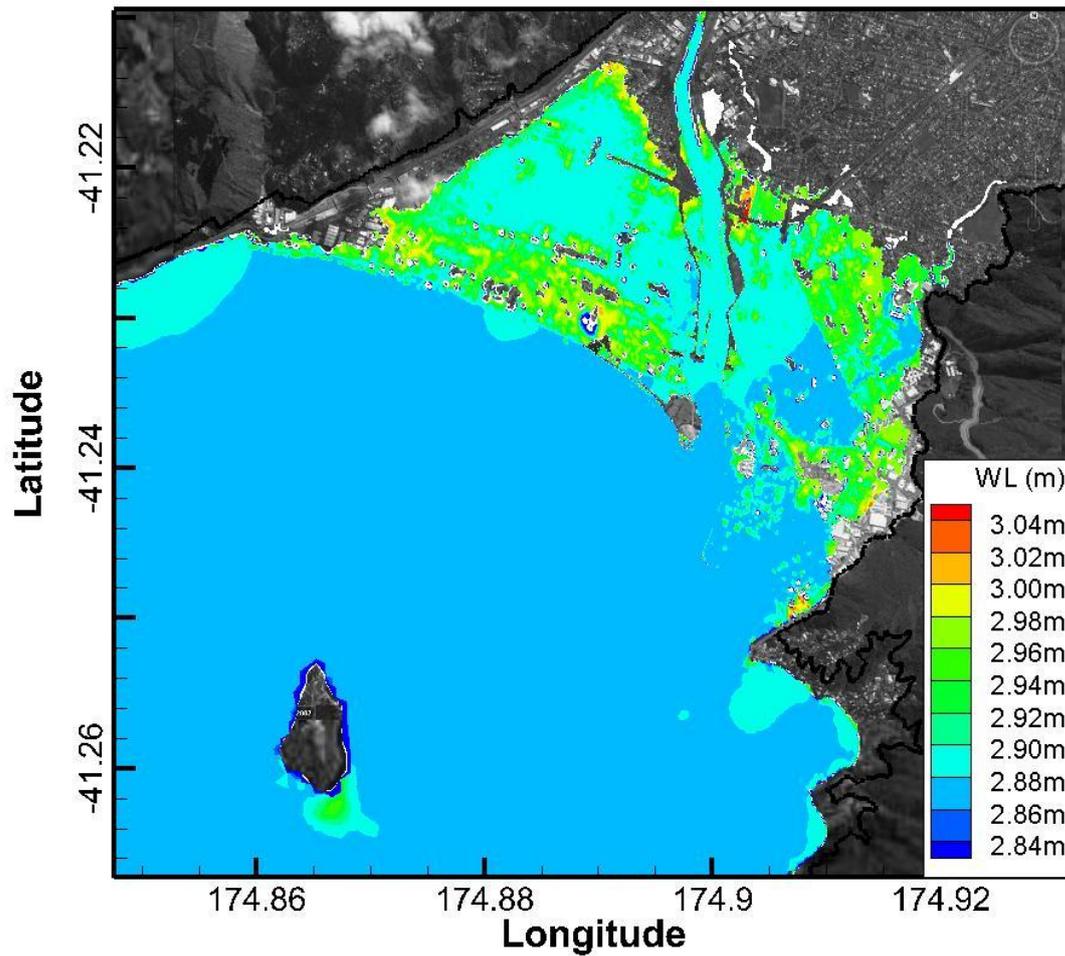
Figure H-8: Total inundation water levels relative to WVD-53 at Petone and Seaview for a 1% AEP storm event based on the August 1990 event with 1.5 m sea-level rise. The colours show the maximum water level above WVD-53, over-laid on images from Google Earth (2012). The solid black line shows the extents of the land inundation grid.
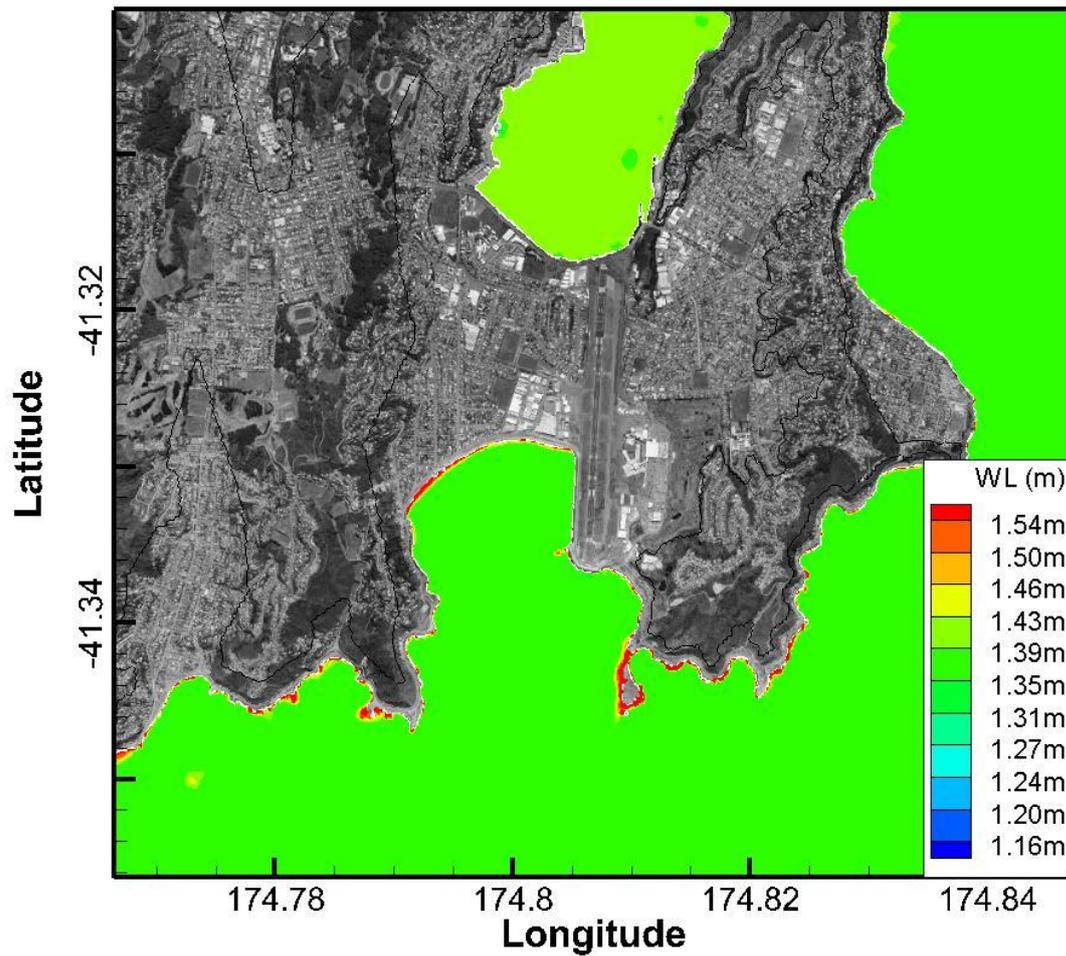
Figure H-9: Total water inundation levels relative to WVD-53 of Evans Bay and Lyall Bay with present day sea level. Simulations are based on the 17 August 1990 event and represent a 1% AEP joint probability wave and storm-tide producing the largest coastal water depths. White regions indicate areas that are below sea level at high tide but not inundated in the modelling.
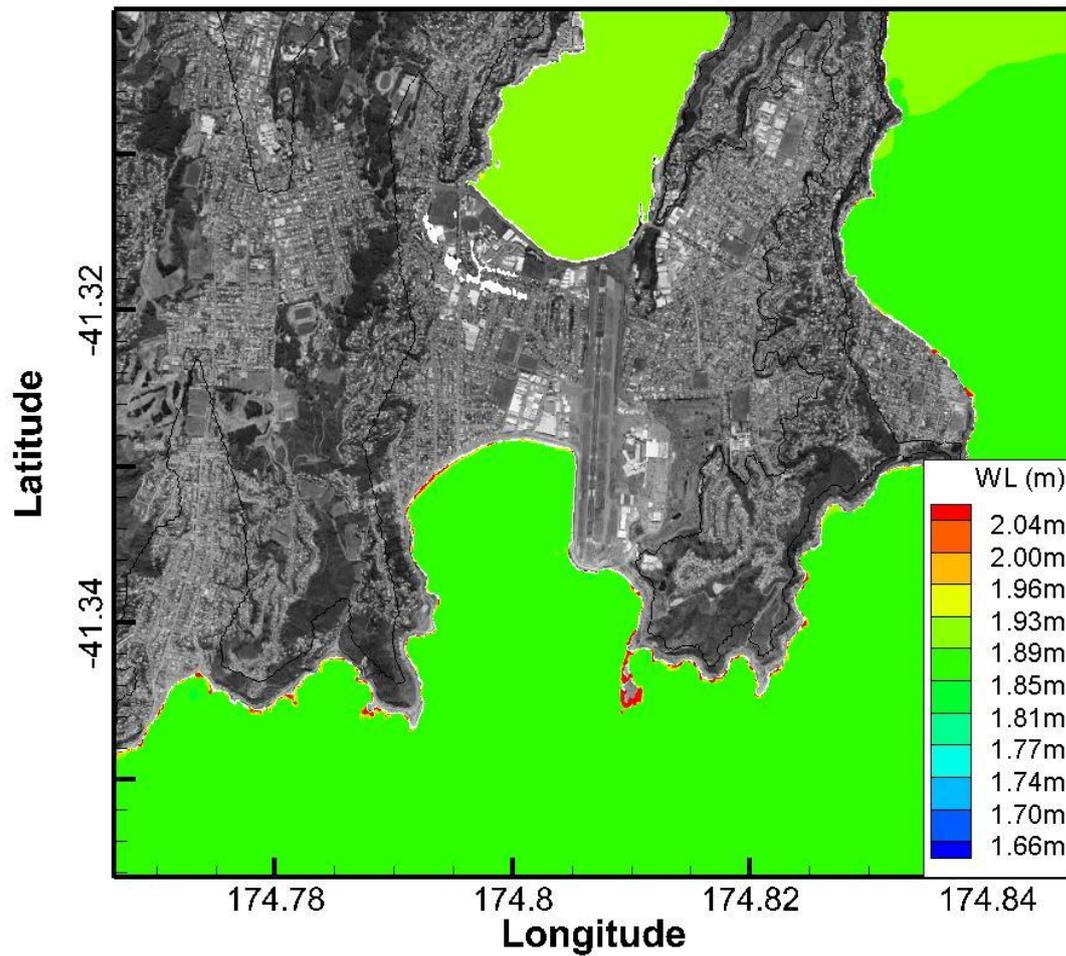
Figure H-10:   **Total inundation water levels relative to WVD-53 of Evans Bay and Lyall Bay with 0.5 m sea-level rise.**   Simulations are based on the 17 August 1990 event and represent a 1% AEP joint probability wave and storm-tide producing the largest coastal water depths. White regions indicate areas that are below sea level at high tide but not inundated in the modelling.
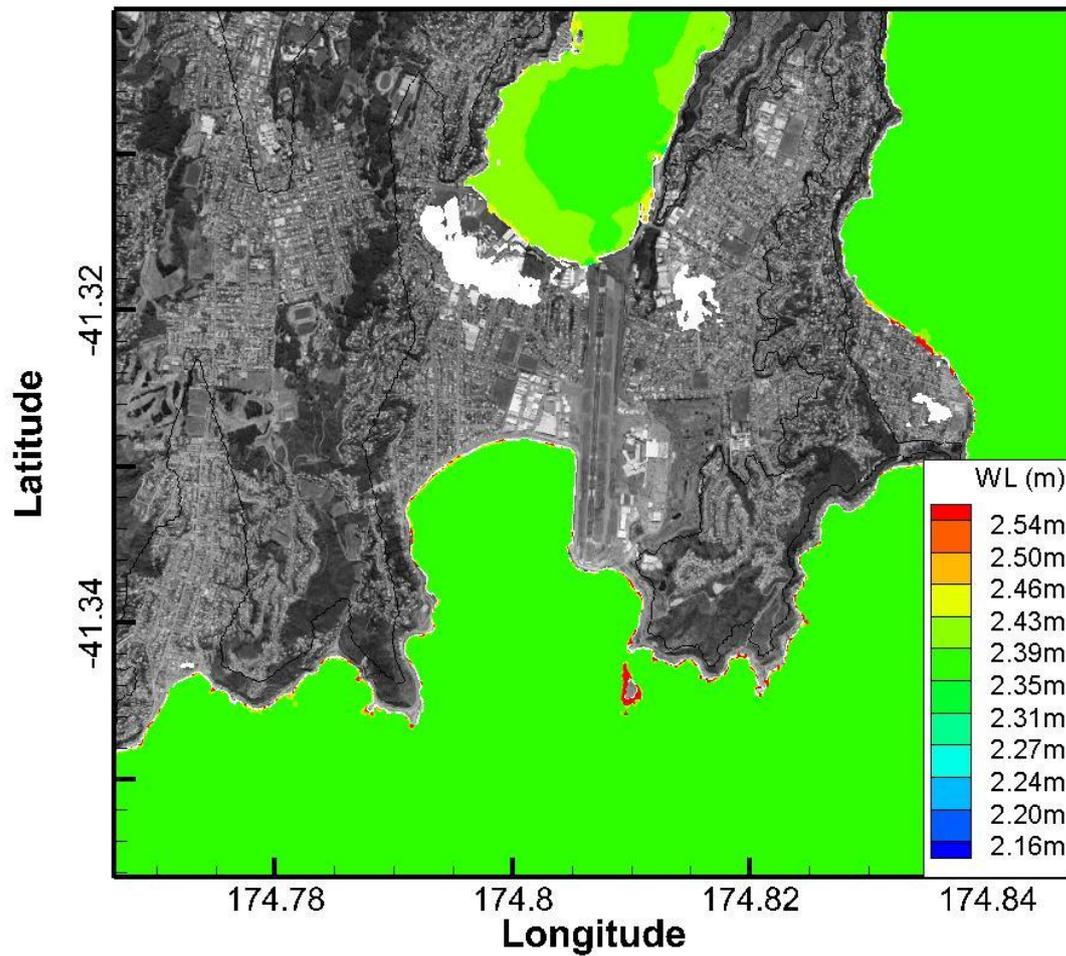
Figure H-11:   Total inundation water levels relative to WVD-53 of Evans Bay and Lyall Bay with 1.0 m sea-level rise.   Simulations are based on the 17 August 1990 event and represent a 1% AEP joint probability wave and storm-tide producing the largest coastal water depths. White regions indicate areas that are below sea level at high tide but not inundated in the modelling.
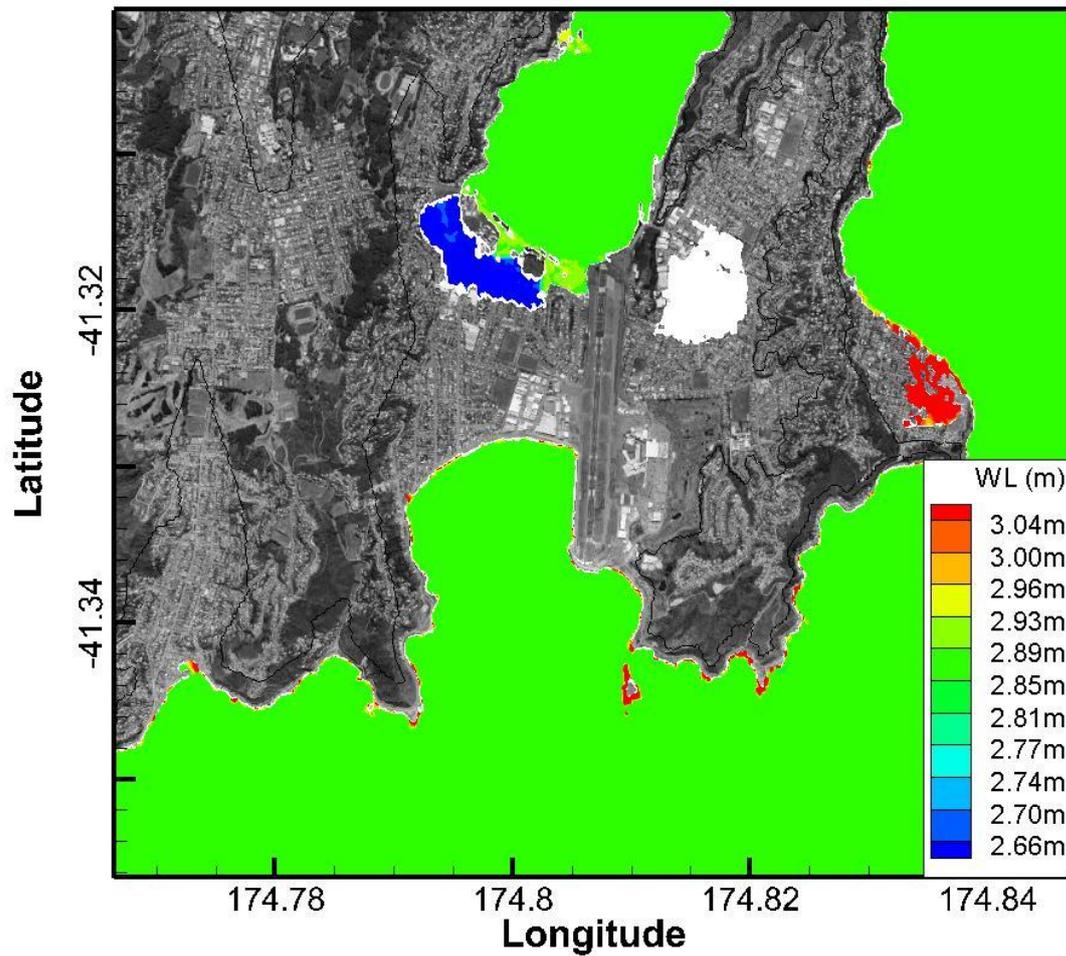
Figure H-12:   Total inundation water levels relative to WVD-53 of Evans Bay and Lyall Bay with 1.5 m sea-level rise.   Simulations are based on the 17 August 1990 event and represent a 1% AEP joint probability wave and storm-tide producing the largest coastal water depths. White regions indicate areas that are below sea level at high tide but are not inundated in the model.
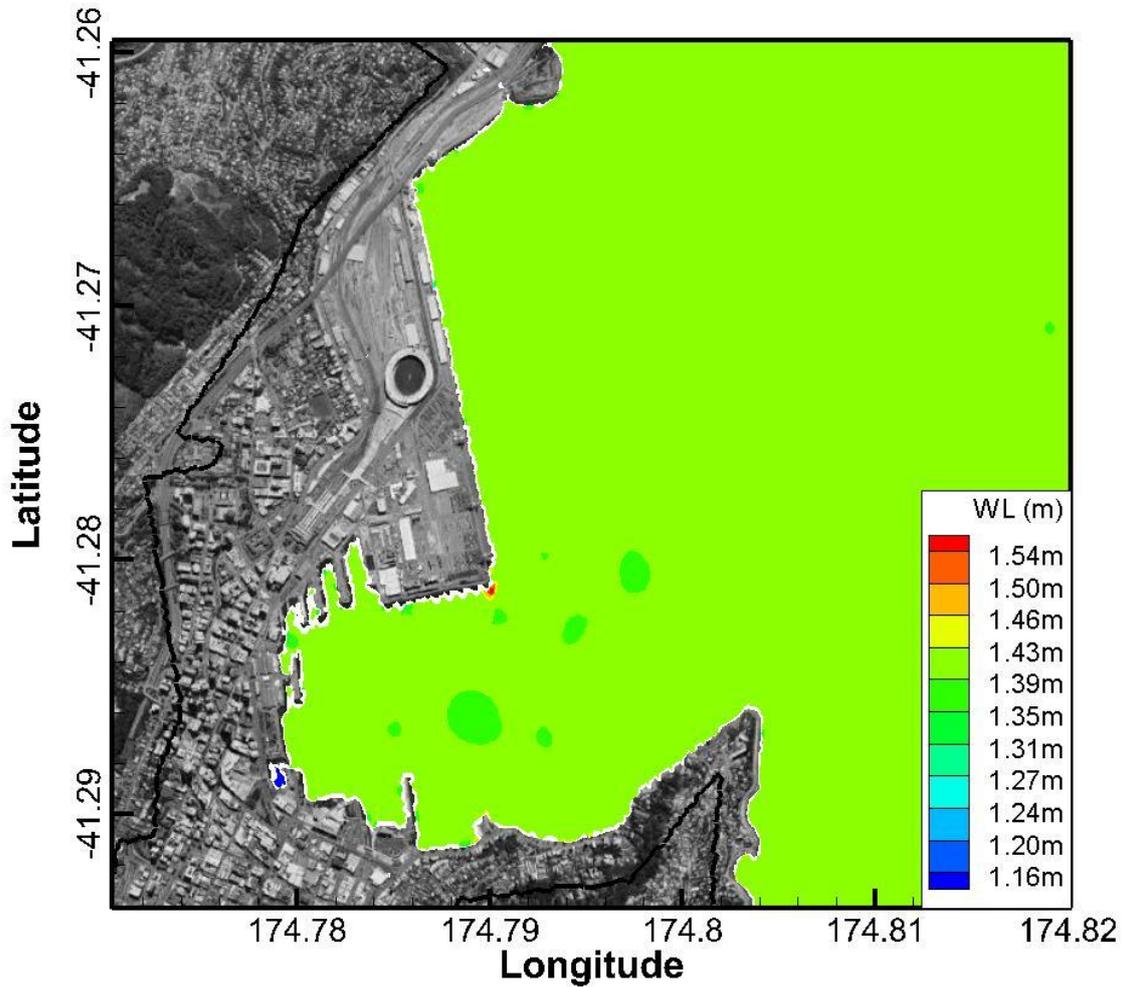
Figure H-13: Total inundation water levels relative to WVD-53 of Wellington central city at present day sea level. Simulations are based on the 17 August 1990 event and represent a 1% AEP joint probability wave and storm-tide producing the largest coastal water depths. White regions indicate areas that are below sea level at high tide but are not inundated in the model. The solid black line shows the extents of the land inundation grid.
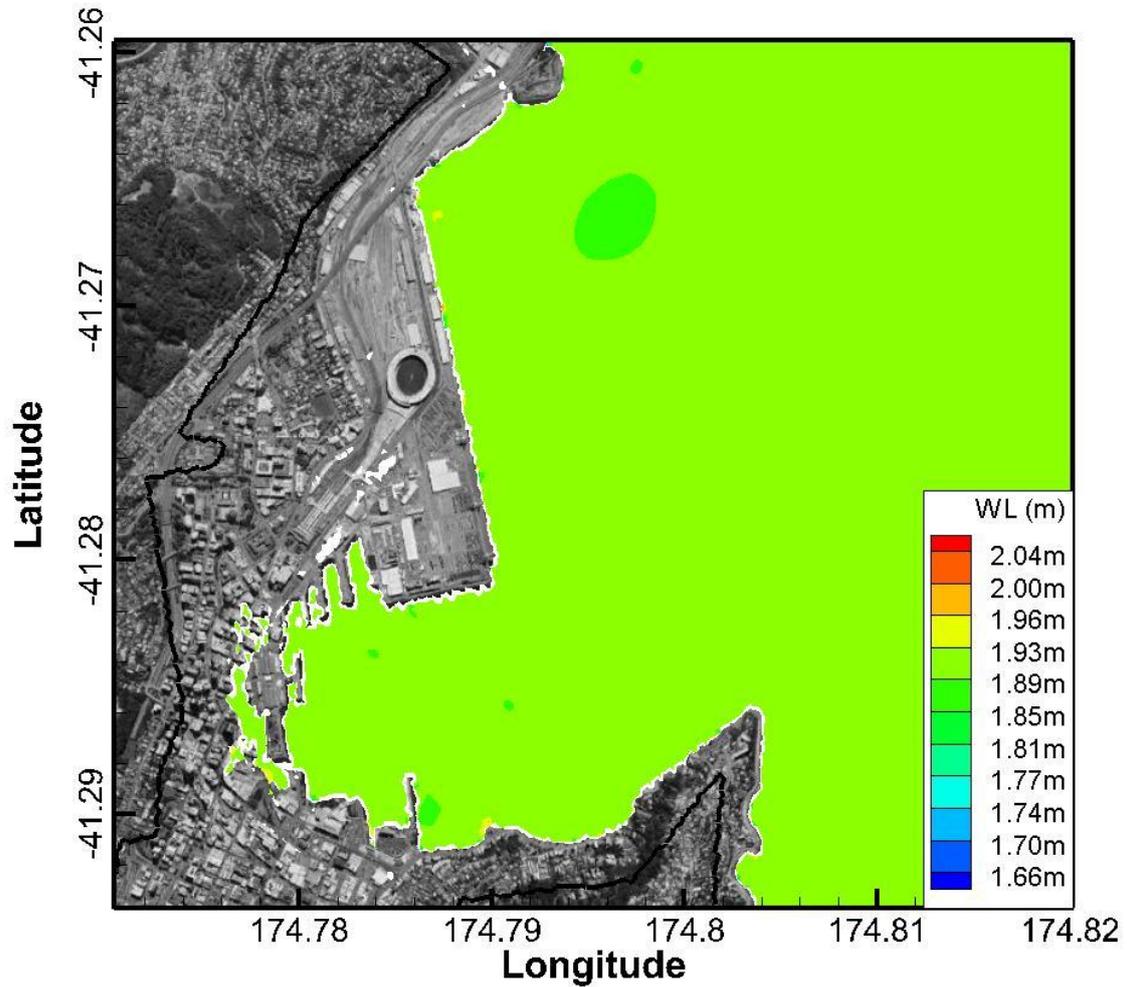
Figure H-14:   Total inundation water levels relative to WVD-53 of Wellington central city with 0.5 m sea-level rise.   Simulations are based on the 17 August 1990 event and represent a 1% AEP joint probability wave and storm-tide producing the largest coastal water depths. White regions indicate areas that are below sea level at high tide but are not inundated in the model. The solid black line shows the extents of the land inundation grid.
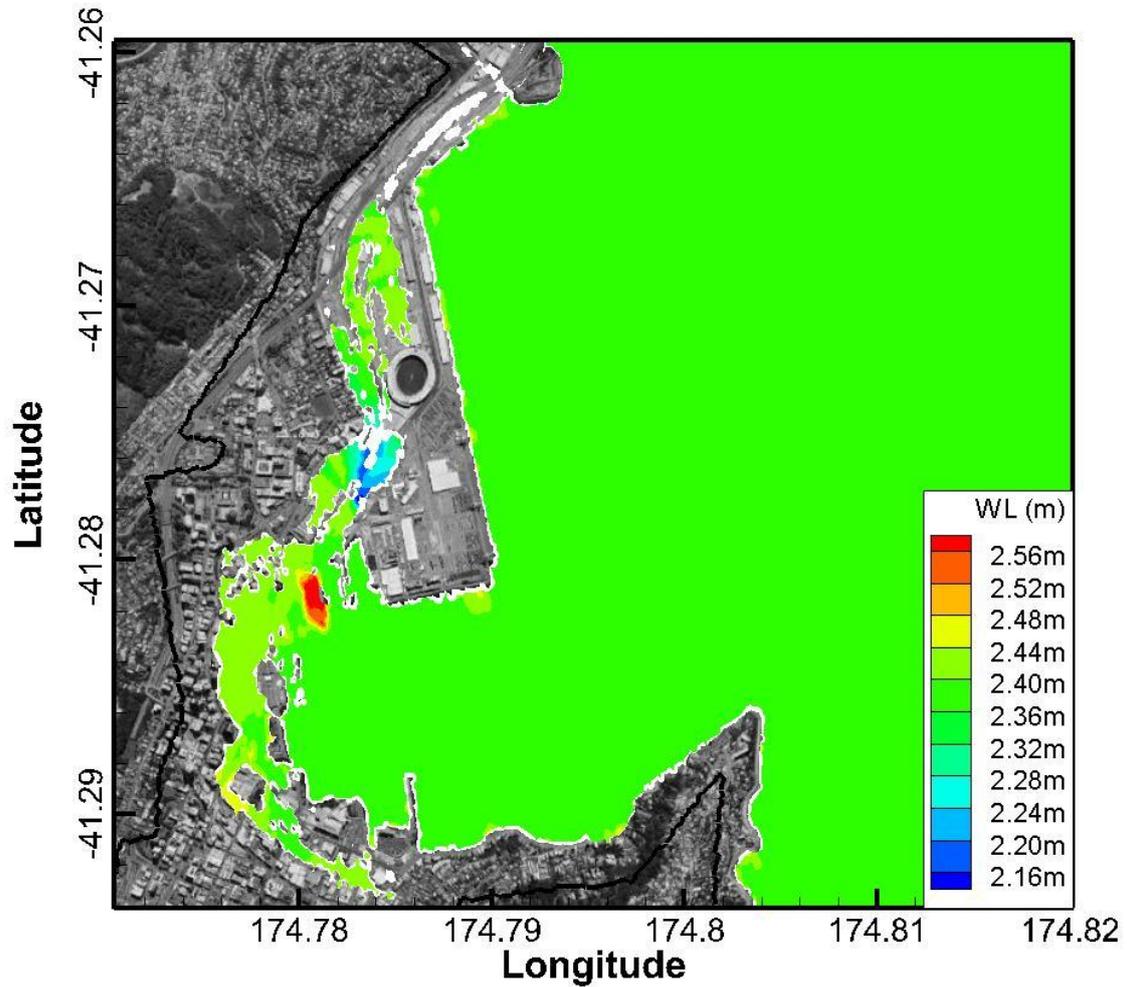
Figure H-15:   Total inundation water levels relative to WVD-53 of Wellington central city with 1.0 m sea-level rise.   Simulations are based on the 17 August 1990 event and represent a 1% AEP joint probability wave and storm-tide producing the largest coastal water depths. White regions indicate areas that are below sea level at high tide but are not inundated in the model. The solid black line shows the extents of the land inundation grid.
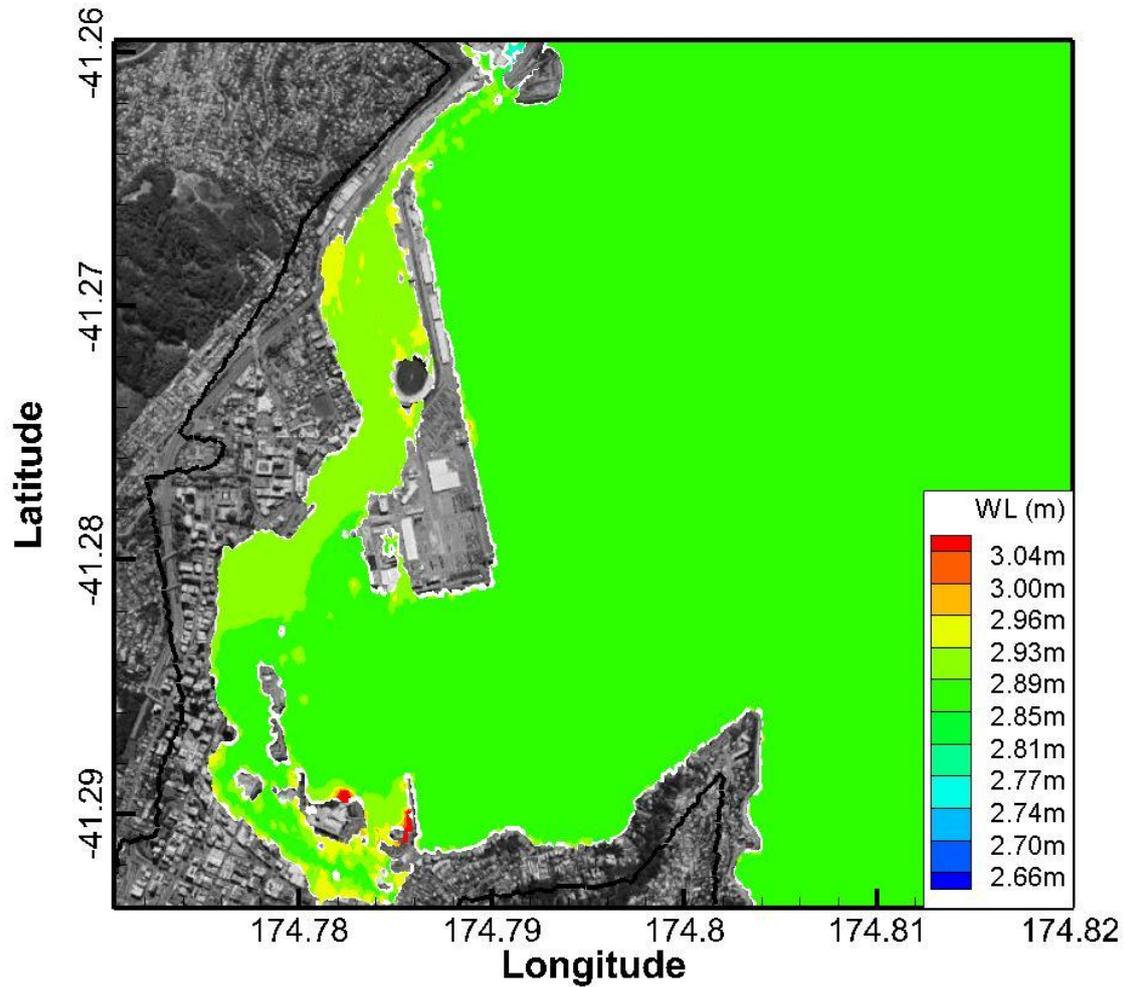
Figure H-16:   Total inundation water levels relative to WVD-53 of Wellington central city with 1.5 m sea-level rise.   Simulations are based on the 17 August 1990 event and represent a 1% AEP joint probability wave and storm-tide producing the largest coastal water depths. White regions indicate areas that are below sea level at high tide but are not inundated in the model. The solid black line shows the extents of the land inundation grid.
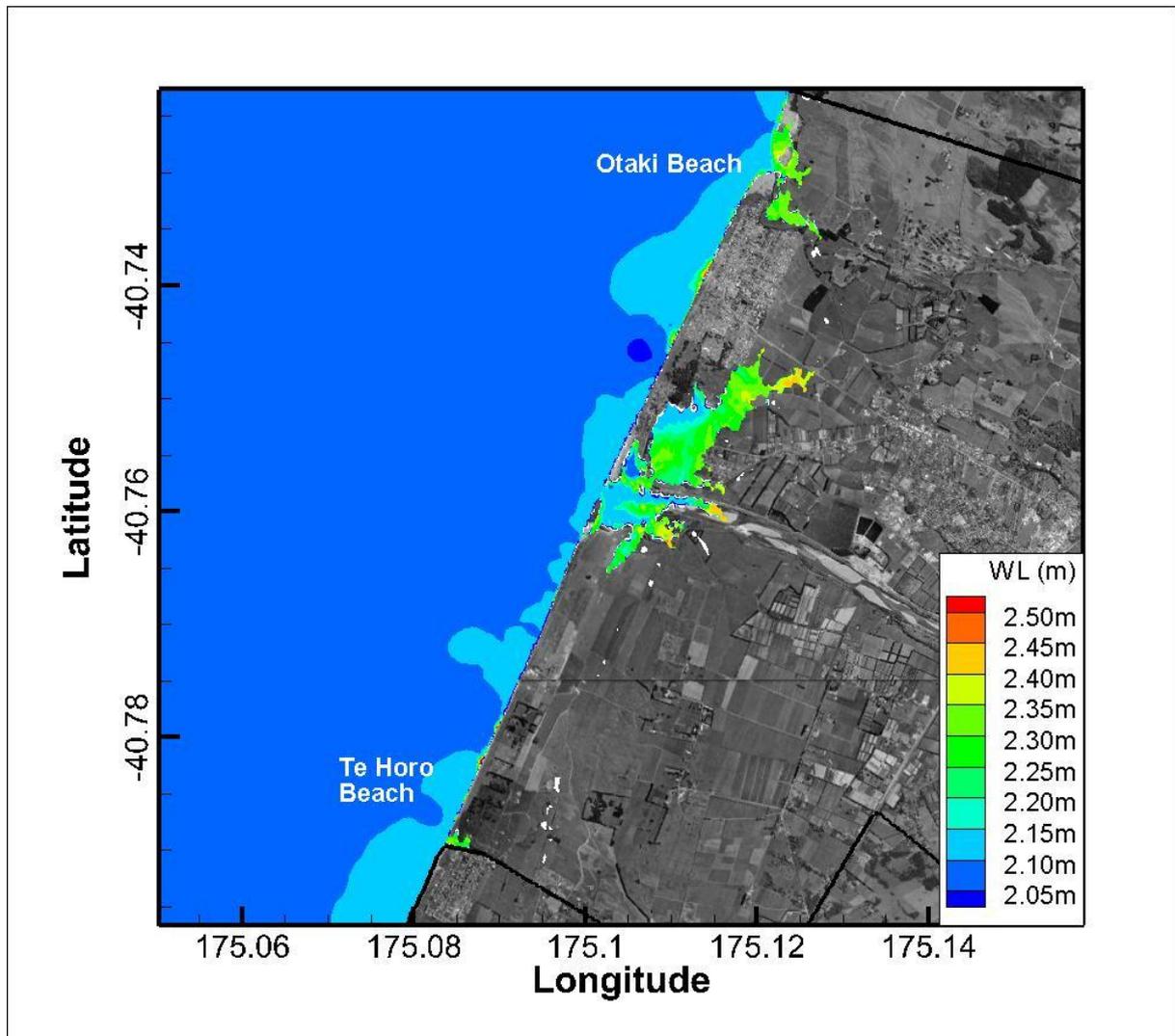
Figure H-17: **Total inundation water levels relative to WVD-53 for the area near Otaki for the 6 September 1994 event adjusted to present day sea level and 1% AEP.** The colours show the maximum water level above WVD-53, over-laid on images from Google Earth (2012). The solid black line shows the extents of the land inundation grid. White regions show where land elevations are lower than sea level at the coast but not inundated in the model.
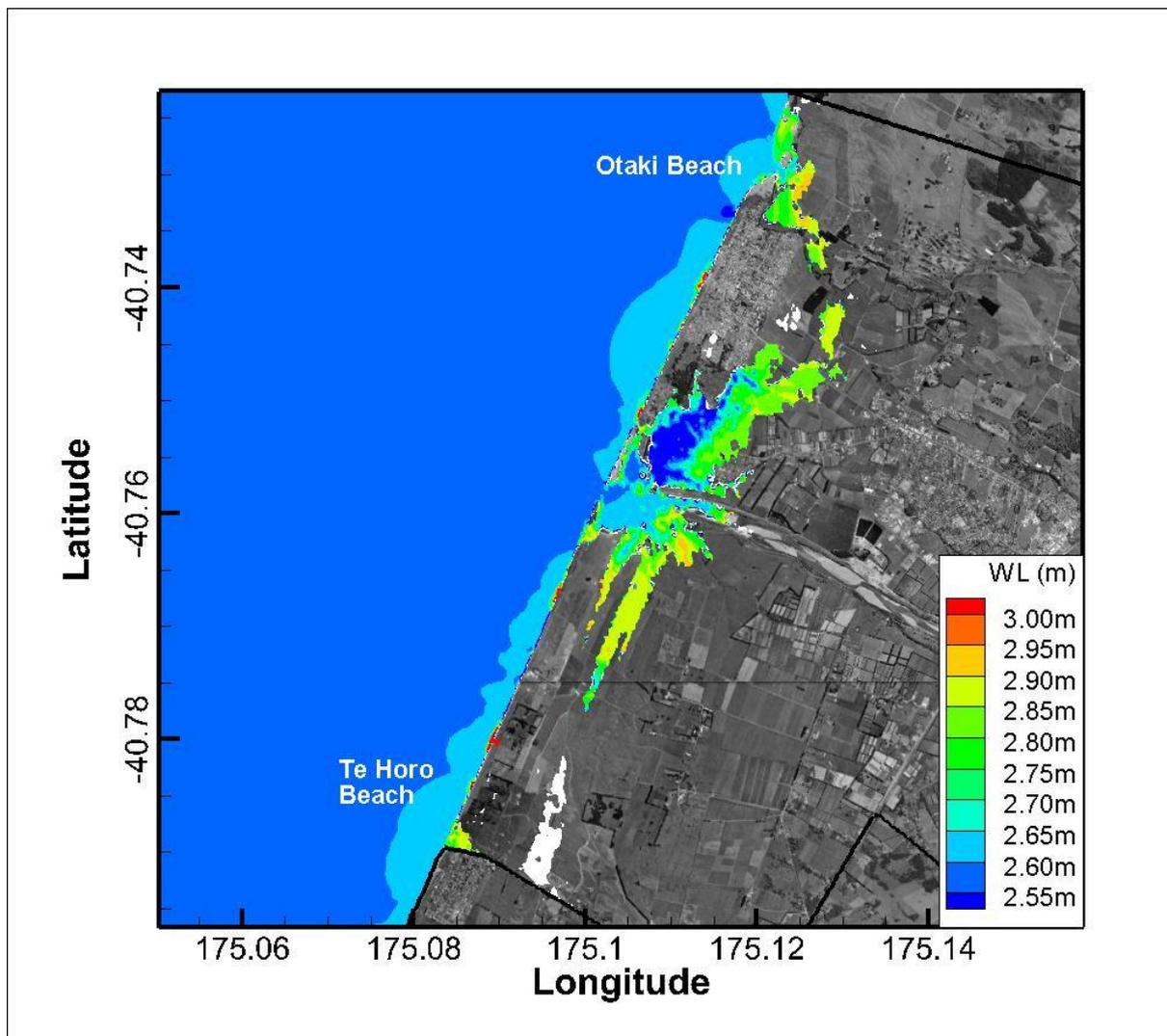
Figure H-18: Total inundation water levels relative to WVD-53 for area near Otaki with 0.5 m sea-level rise. The simulation is based on the 6 September 1994 event. The solid black line shows the extents of the land inundation grid. White regions indicate areas with topography below storm-tide level at the coast but not inundated in the simulation.
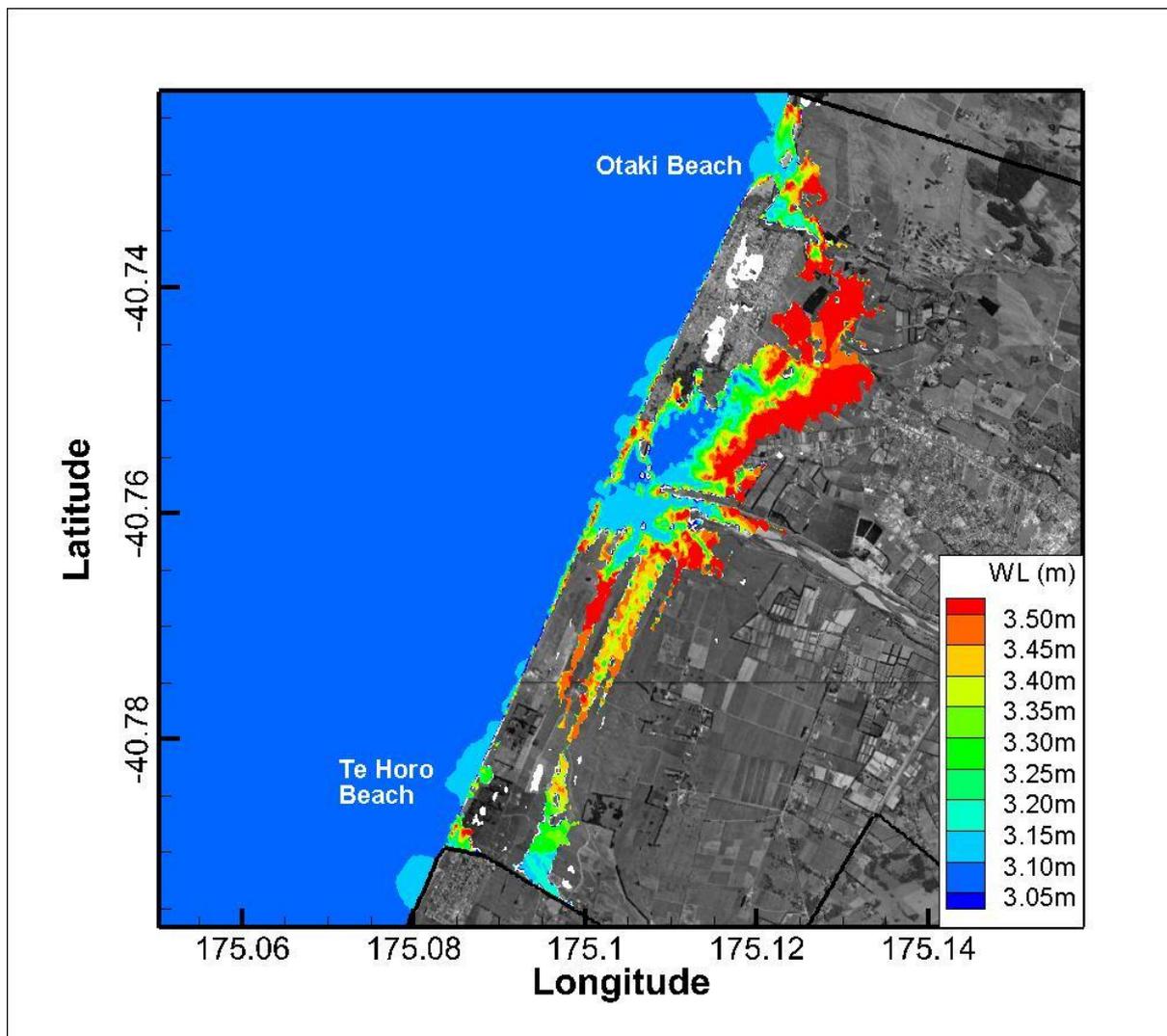
Figure H-19: **Total inundation water levels relative to WVD-53 for area near Otaki with 1.0 m sea-level rise.** The simulation is based on the 6 September 1994 event. The solid black line shows the extents of the land inundation grid. White regions indicate areas with topography below storm-tide level at the coast but not inundated in the simulation.
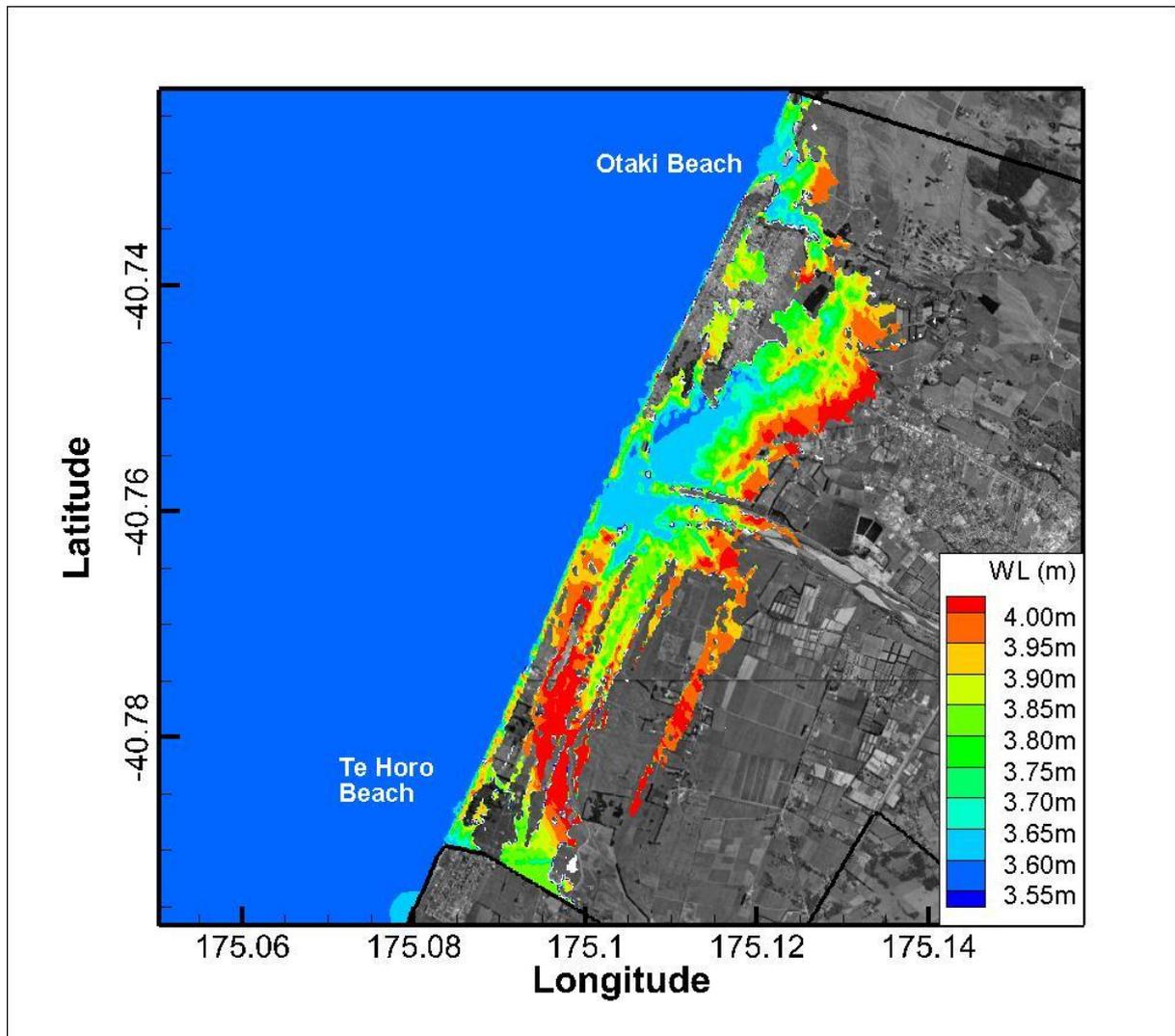
Figure H-20: Total inundation water levels relative to WVD-53 for area near Otaki with 1.5 m sea-level rise. The simulation is based on the 6 September 1994 event. The solid black line shows the extents of the land inundation grid. White regions indicate areas with topography below storm-tide level at the coast but not inundated in the simulation.
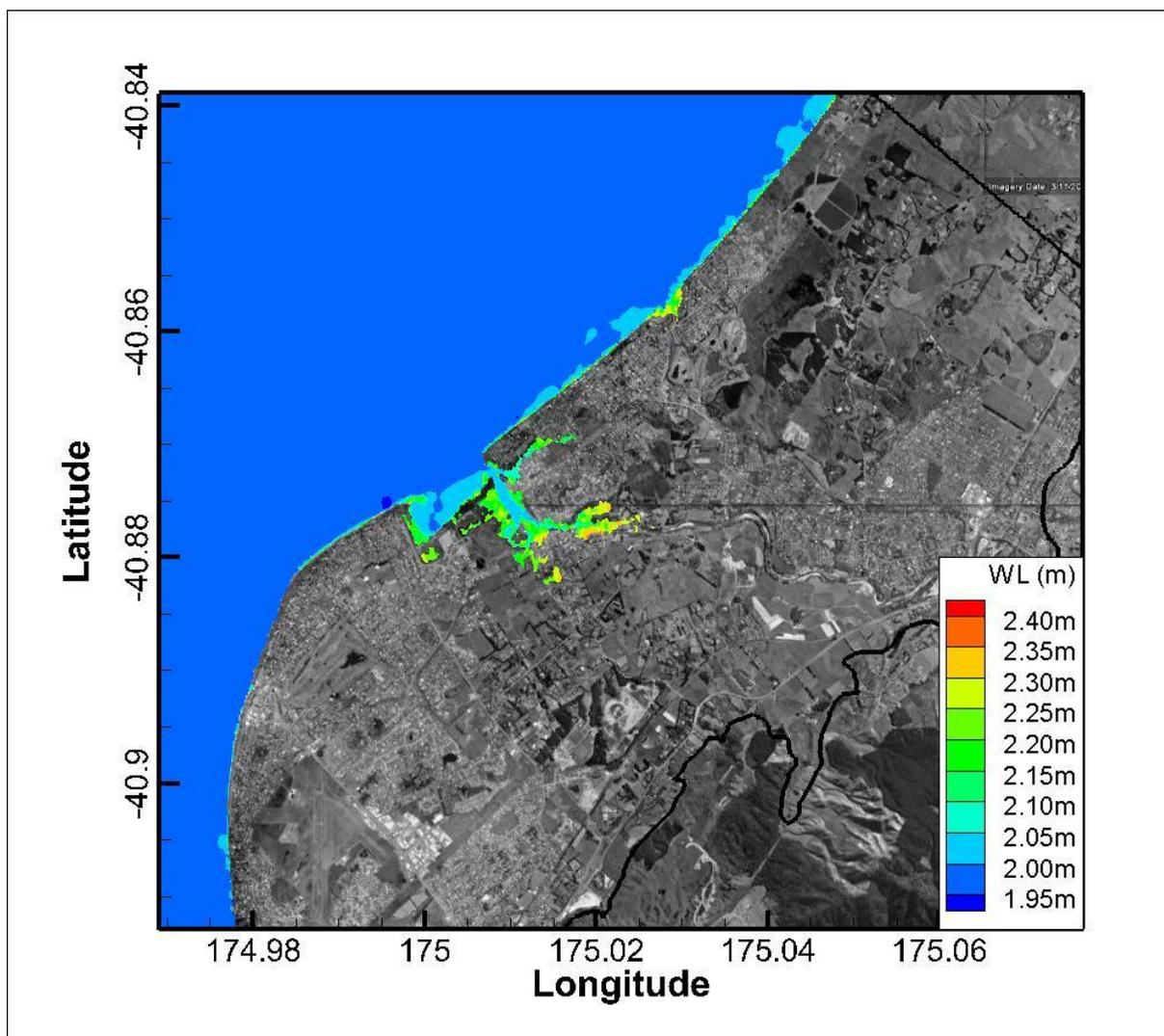
Figure H-21: Total inundation water levels relative to WVD-53 for Waikanae for the September 1994 event adjusted to present day sea level and 1% joint AEP. The colours show maximum water level above WVD-53, overlaid on images from Google Earth. The solid black line shows the extents of the land inundation grid. White regions show where land elevations are lower than the sea level at the coast but are not inundated in the model.
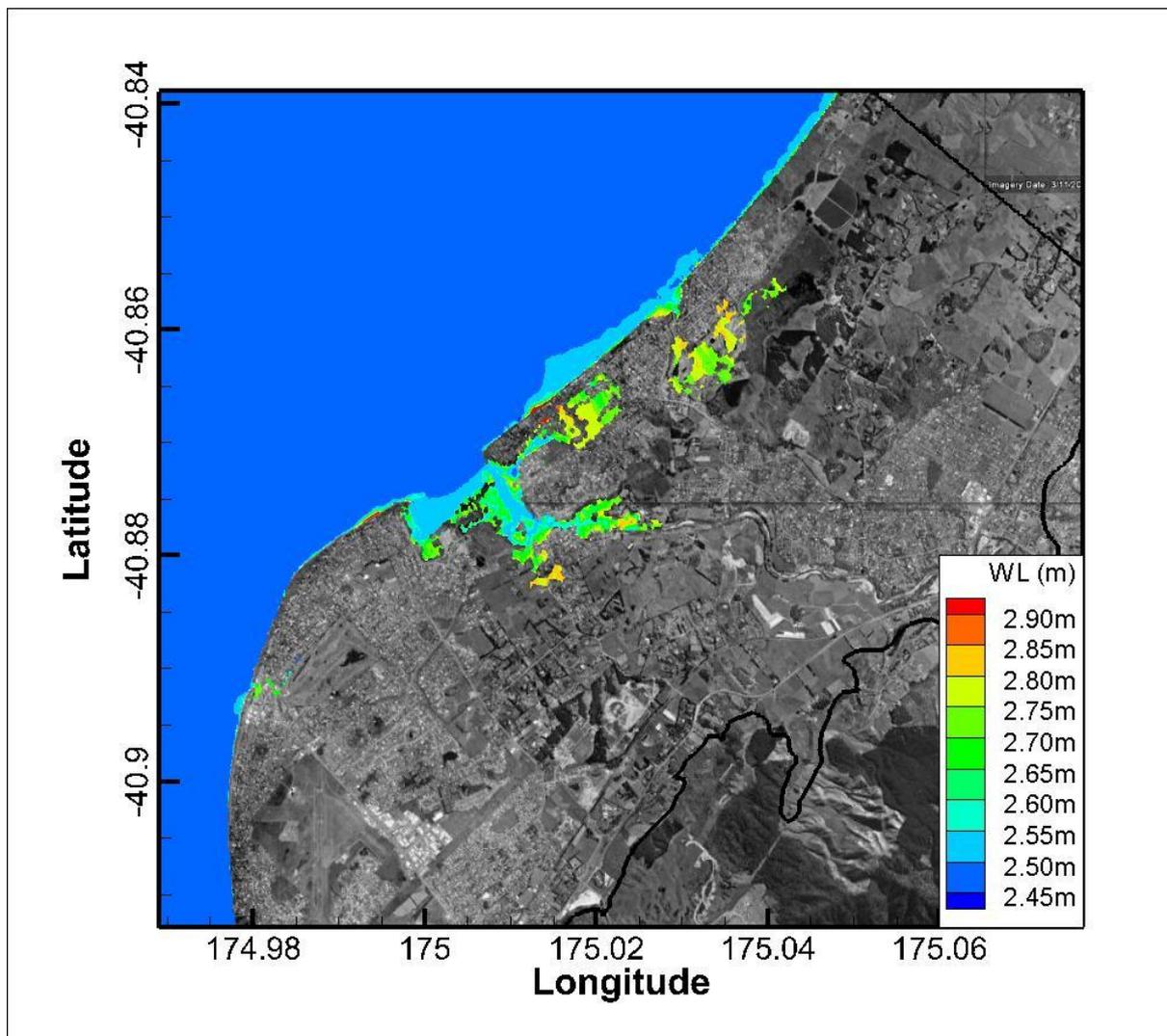
Figure H-22:   Total inundation water levels relative to WVD-53 at Waikanae with 0.5 m sea-level rise.   The simulation is based on the 6 September 1994 event. . The solid black line shows the extents of the land inundation grid. White regions show areas where the topography is below storm-tide sea level, but not inundated in the modelling.
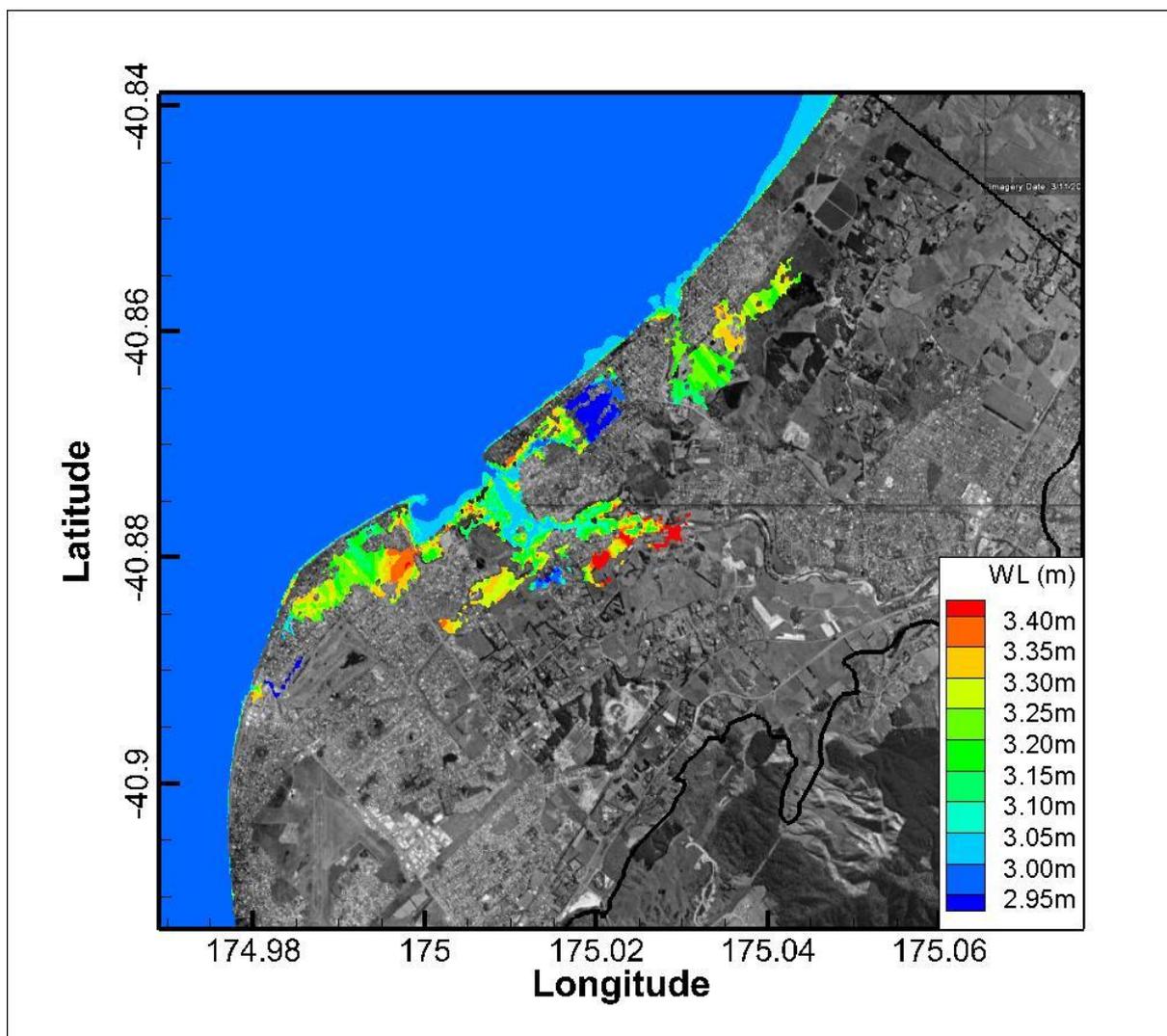
Figure H-23: **Total inundation water levels relative to WVD-53 at Waikanae with 1.0 m sea-level rise.** The simulation is based on the 6 September 1994 event. The solid black line shows the extents of the land inundation grid. White regions show areas where the topography is below storm-tide sea level, but not inundated in the modelling.
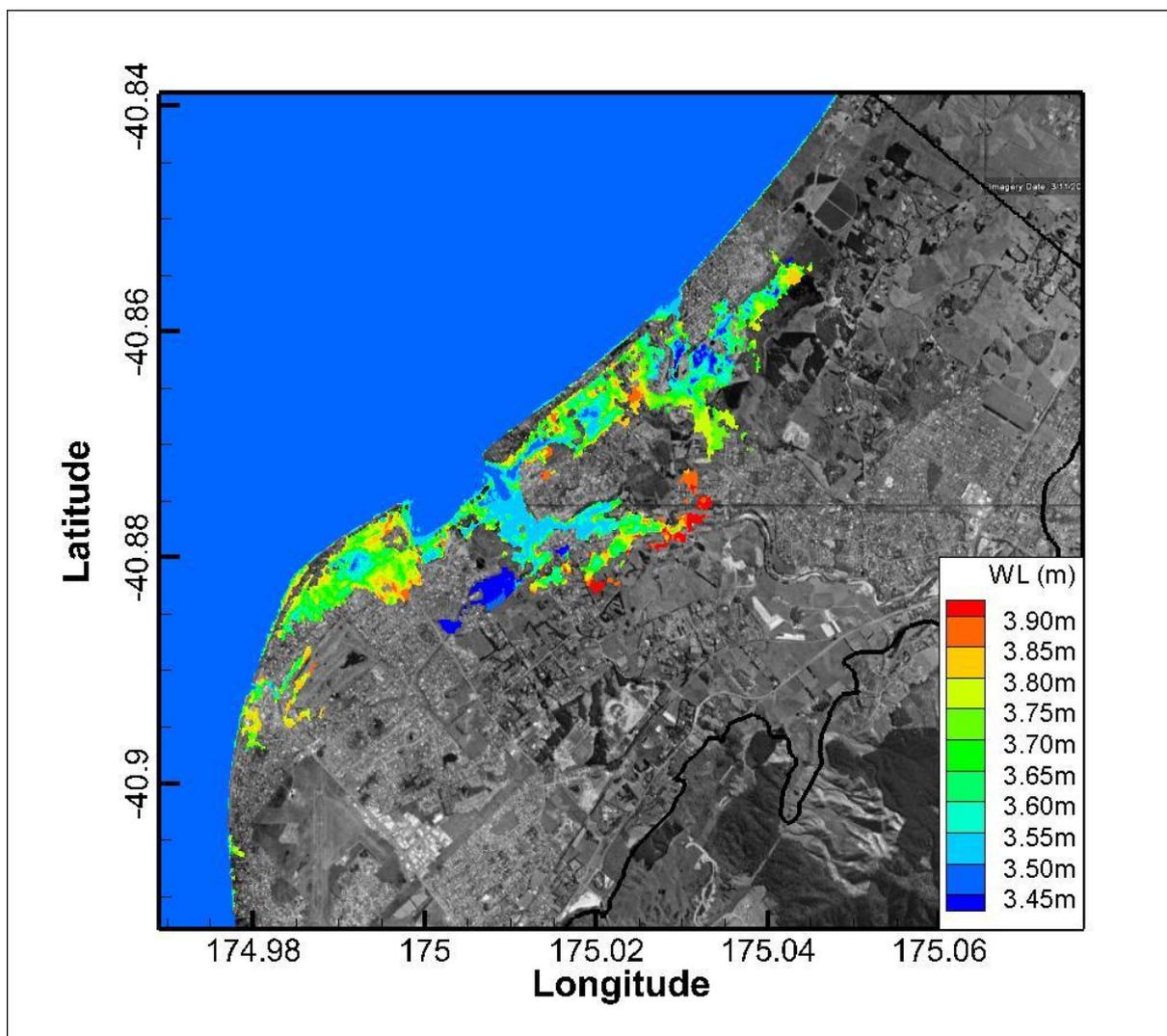
Figure H-24:   Total inundation water levels relative to WVD-53 at Waikanae with 1.5 m sea-level rise. The simulation is based on the 6 September 1994 event. The solid black line shows the extents of the land inundation grid. White regions show areas where the topography is below storm-tide sea level, but not inundated in the modelling.
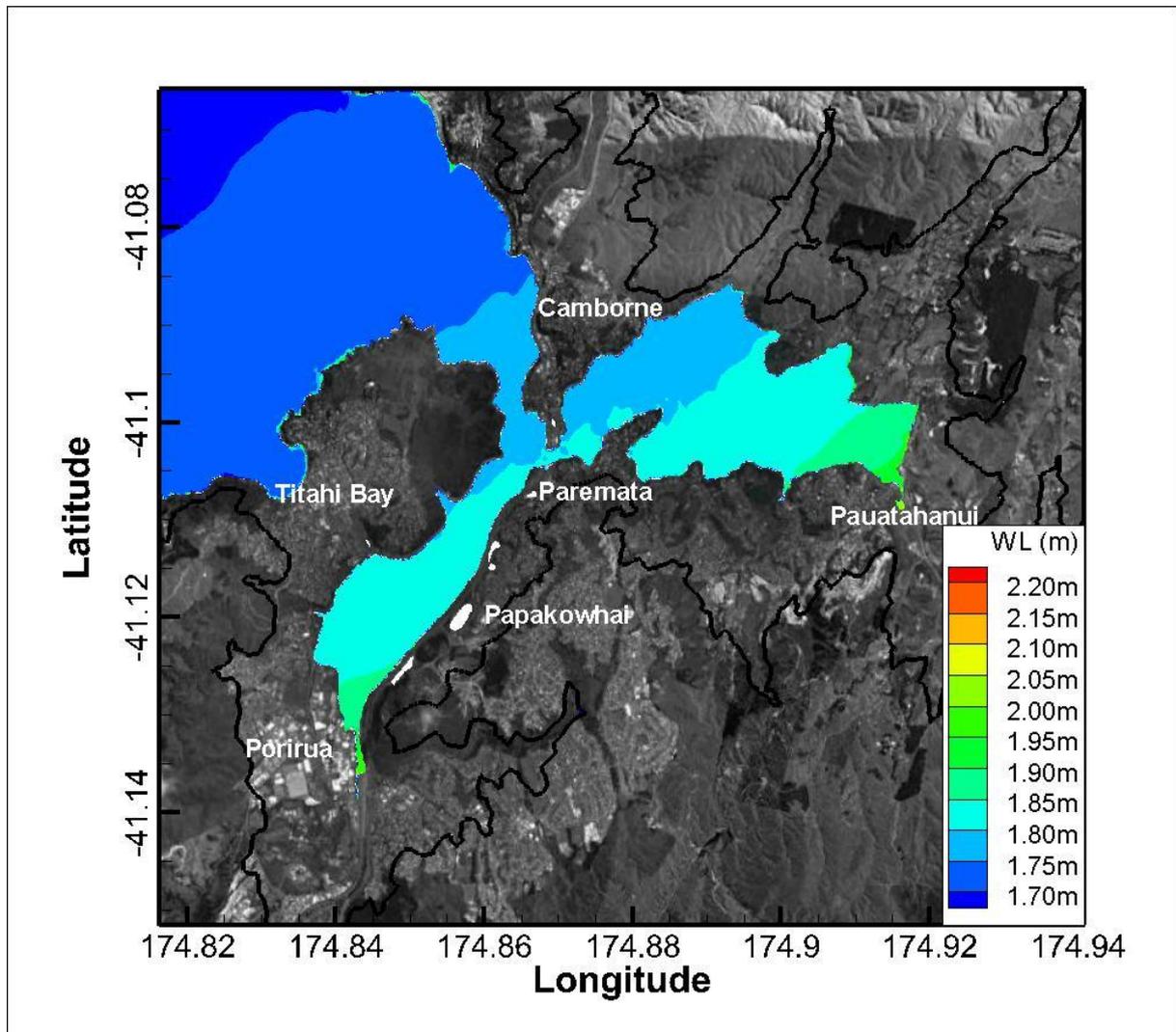
Figure H-25: Total inundation water levels relative to WVD-53 for Porirua Harbour for the 6 September 1994 event adjusted to present day sea level and 1% joint AEP. The colours show the maximum water level above WVD-53, overlaid on images from Google Earth. Highest astronomical tide (plus present day MLOS) is 0.952 m above WVD-53. White regions are areas with elevations lower than the sea level at the coast. The solid black line shows the extents of the land inundation grid.
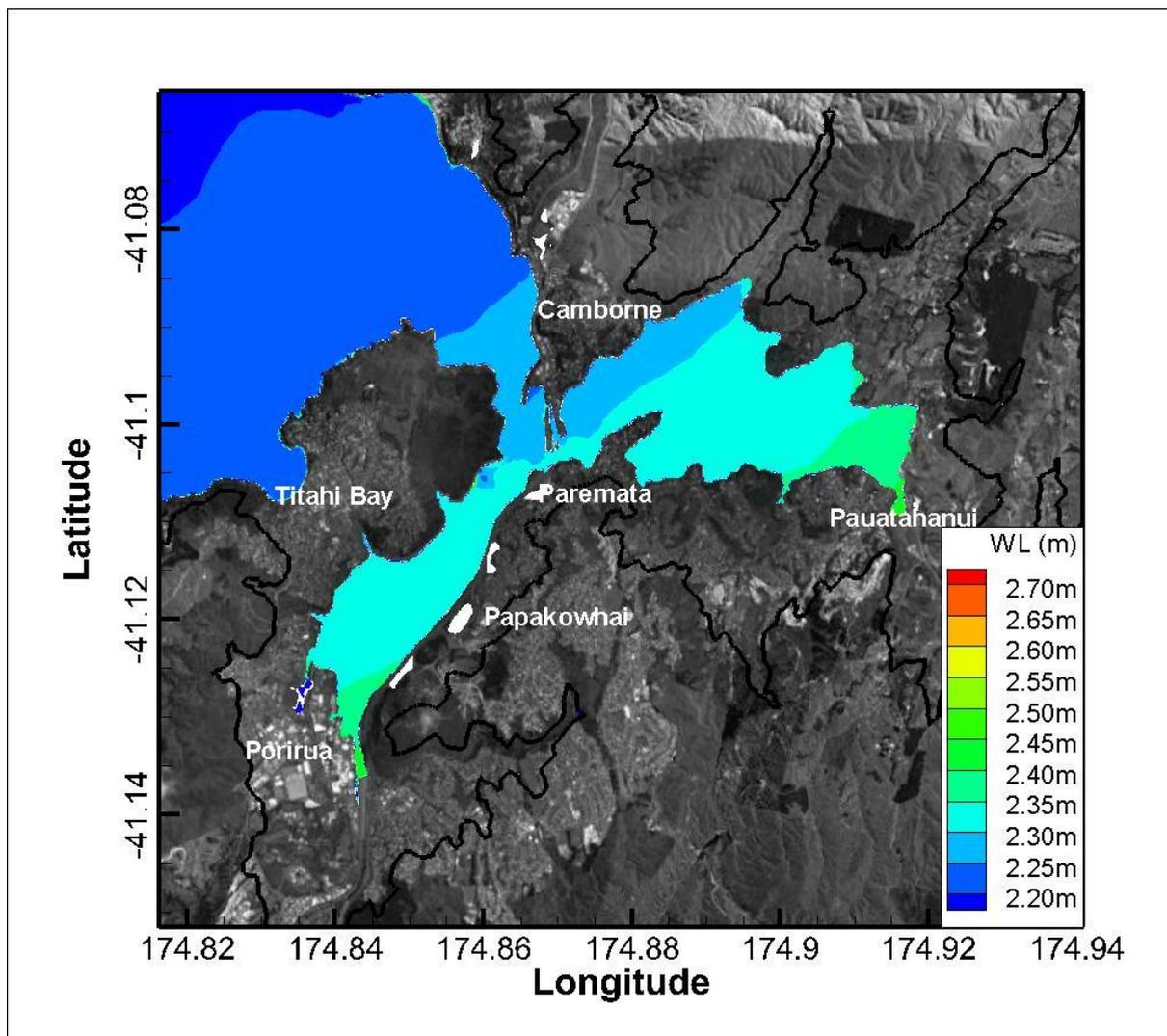
Figure H-26:   Total inundation water levels relative to WVD-53 at Porirua with 0.5 m sea-level rise. The simulation is based on the 6 September 1994 event. White regions show areas with elevations below storm-tide sea level but not inundated in the model. The solid black line shows the extents of the land inundation grid.
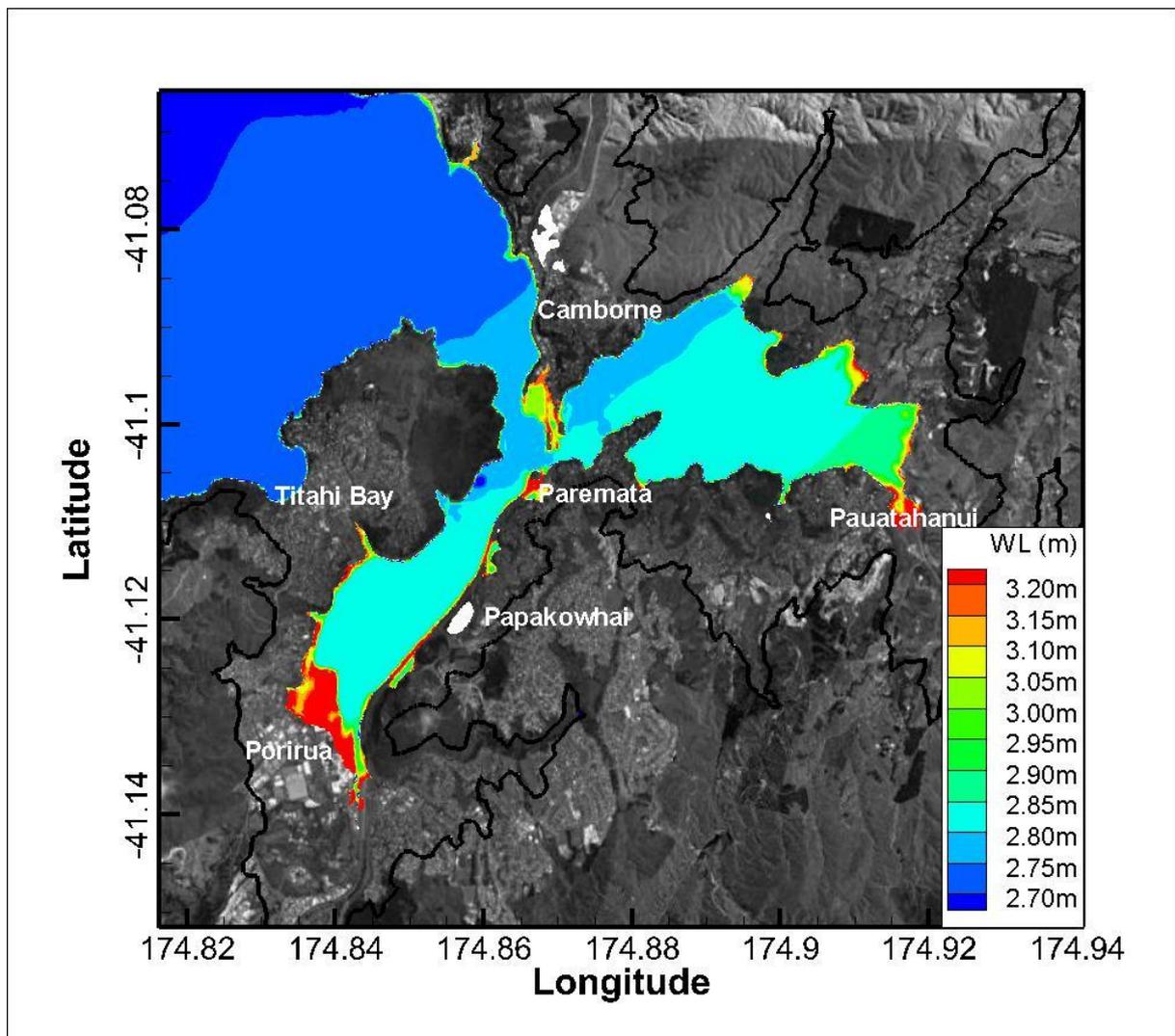
Figure H-27: **Total inundation water levels relative to WVD-53 at Porirua with 1.0 m sea-level rise.** The simulation is based on the 6 September 1994 event. White regions show areas with elevations below storm-tide sea level but not inundated in the model. The solid black line shows the extents of the land inundation grid.
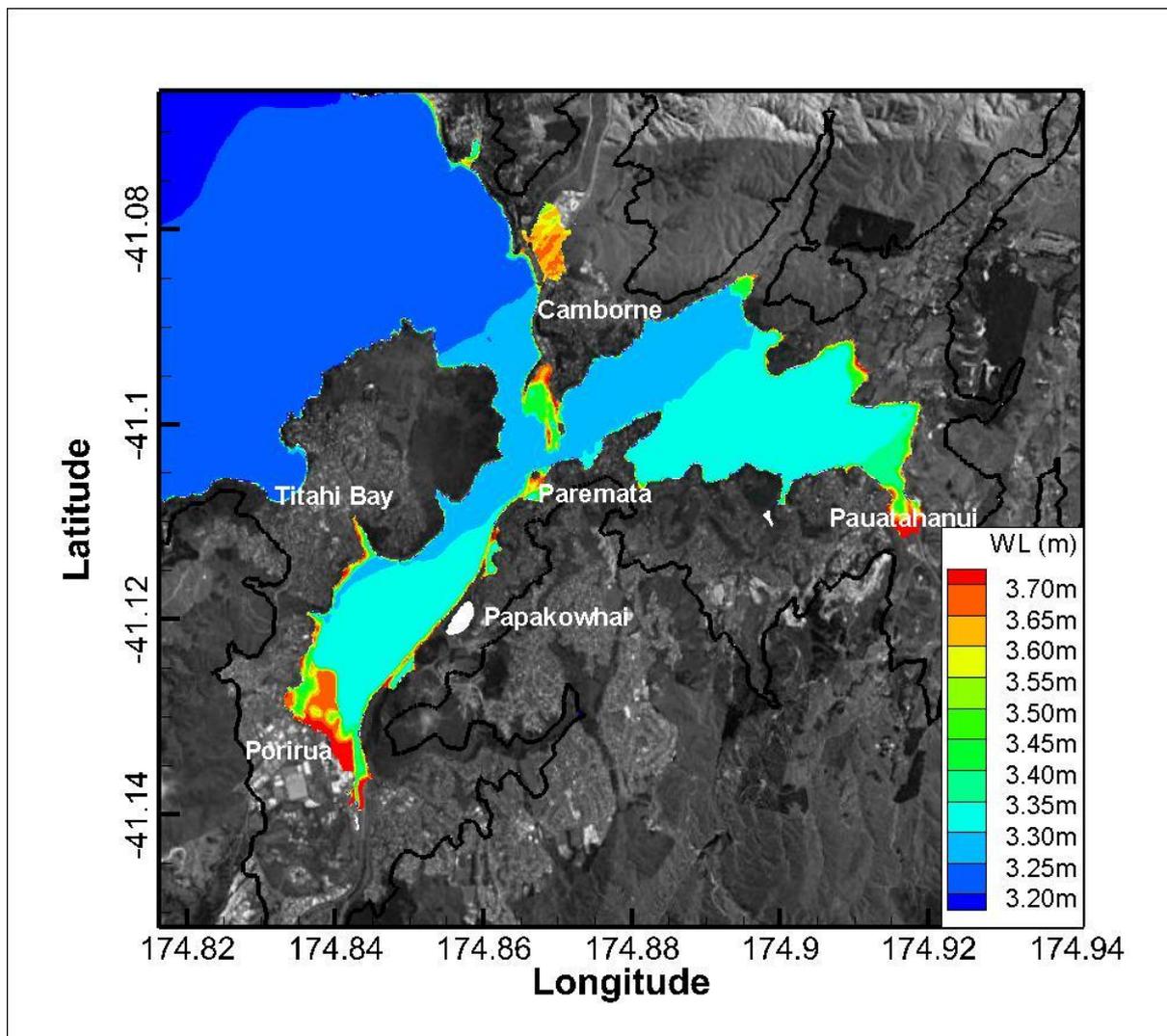
Figure H-28: **Total inundation water levels relative to WVD-53 at Porirua with 1.5 m sea-level rise.** The simulation is based on the 6 September 1994 event. White regions show areas with elevations below storm-tide sea level but not inundated in the model. The solid black line shows the extents of the land inundation grid.